

# Applied Drilling Engineering

**Adam T. Bourgoyne Jr.**

Professor of Petroleum Engineering  
Louisiana State U.

**Keith K. Millheim**

Manager—Critical Drilling Facility  
Amoco Production Co.

**Martin E. Chenevert**

Senior Lecturer of Petroleum Engineering  
U. of Texas

**F.S. Young Jr.**

President  
Woodway Energy Co.

**SPE Textbook Series, Volume 2**

**Henry L. Doherty Memorial Fund of AIME  
Society of Petroleum Engineers  
Richardson, TX USA**

## **Dedication**

This book is dedicated to the many students who were forced to study from the trial drafts of this work.

## **Disclaimer**

This book was prepared by members of the Society of Petroleum Engineers and their well-qualified colleagues from material published in the recognized technical literature and from their own individual experience and expertise. While the material presented is believed to be based on sound technical knowledge, neither the Society of Petroleum Engineers nor any of the authors or editors herein provide a warranty either expressed or implied in its application. Correspondingly, the discussion of materials, methods, or techniques that may be covered by letters patents implies no freedom to use such materials, methods, or techniques without permission through appropriate licensing. Nothing described within this book should be construed to lessen the need to apply sound engineering judgment nor to carefully apply accepted engineering practices in the design, implementation, or application of the techniques described herein.

© Copyright 1986 Society of Petroleum Engineers

All rights reserved. No portion of this book may be reproduced in any form or by any means, including electronic storage and retrieval systems, except by explicit, prior written permission of the publisher except for brief passages excerpted for review and critical purposes.

Manufactured in the United States of America.

ISBN 978-1-55563-001-0

ISBN 978-1-61399-159-6 (Digital)

Society of Petroleum Engineers  
222 Palisades Creek Drive  
Richardson, TX 75080-2040 USA  
<http://store.spe.org>  
[books@spe.org](mailto:books@spe.org)  
1.972.952.9393

# Chapter 8

## Directional Drilling and Deviation Control

### 8.1 Definitions and Reasons for Directional Drilling

Directional drilling is the process of directing the wellbore along some trajectory to a predetermined target. Deviation control is the process of keeping the wellbore contained within some prescribed limits relative to inclination angle, horizontal excursion from the vertical, or both. This chapter discusses the principles and mechanisms associated with directional drilling and deviation control.

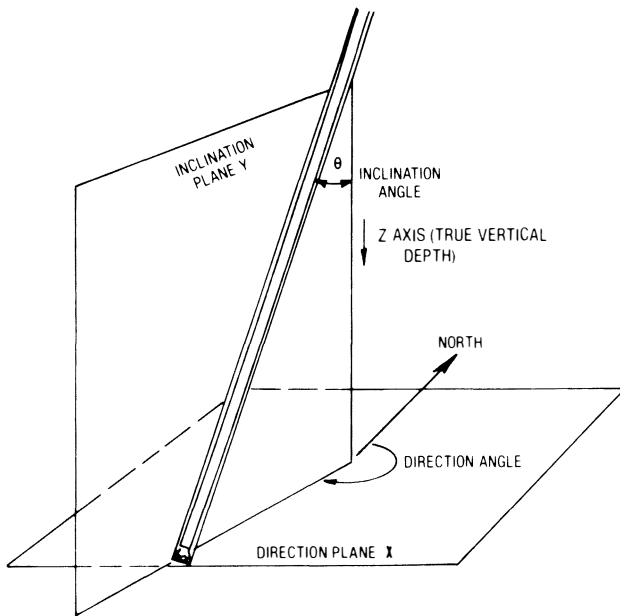
The preceding chapters deal with the one-dimensional process of penetrating the earth with the bit to some vertical depth. However, drilling is a three-dimensional process. The bit not only penetrates vertically but is either purposely or unintentionally deflected into the  $X$ - $Y$  planes (see Fig. 8.1) The  $X$  plane is defined as the direction plane and the  $Y$  plane is the inclination plane. The angles associated with the departures in the  $X$  and  $Y$  planes are called “direction” and “inclination” angles, respectively.

Fig. 8.2 presents a typical example of the trajectory-control situation. Here a structure is located almost entirely under a lake. Well 1, drilled on a part of the structure that is not under the lake, could be treated simply as a deviation-control well drilled on the shore. To develop the rest of the field, however, will necessitate drilling directional wells. The only way vertical wells could be drilled would be from a floating drilling vessel or platform, with the wells being completed on the lake bed (sub-lake completions), or from a floating or fixed production platform; and the economics of those approaches would be far less attractive than drilling directional wells from some convenient land-based site where a standard land rig can be used. In some situations, there is no alternative to drilling a directional well. For example, the lake may be the only source for drinking water in the area,

and thus there may be environmental restrictions that prohibit the use of power vessels and equipment such as offshore drilling rigs and production facilities.

The early drilling of directional wells was clearly motivated by economics. The oil fields offshore California were the spawning ground for directional drilling practices and equipment, and for a special group of people called “directional drillers.” Later discoveries of oil and gas in the Gulf of Mexico and in other countries promoted the expanded application of directional drilling. Offshore field development has accounted for the majority of directional drilling activities. Fig. 8.3 shows a typical offshore platform development. In a number of cases, fields have been discovered beneath population centers, and the only way to develop the fields economically has been to use a drilling pad and to drill directionally (see Fig. 8.4). Natural obstructions such as mountains or other severe topographical features frequently prohibit building a surface location and drilling a near-vertical well (Fig. 8.5). Sidetracking out of an existing wellbore is another application of directional drilling. This sidetracking may be done to bypass an obstruction (a “fish”) in the original wellbore (see Fig. 8.6) or to explore for additional producing horizons in adjacent sectors of the field (see Fig. 8.7).

Strong economic and environmental pressures have increased the use of directional drilling. In some areas it is no longer possible to develop a field by making roads to each surface location and drilling a near-vertical well. Instead, as in offshore installations, drilling pads must be built from which a number of wells can be drilled. Not only is directional drilling increasing, but trajectory programs are becoming more complicated and directional drilling is being applied in situations and areas where directional drilling has not been common. In hot-rock developments, for example, directional wells are being



**Fig. 8.1**—Inclination and direction planes as a wellbore proceeds in the depth plane.

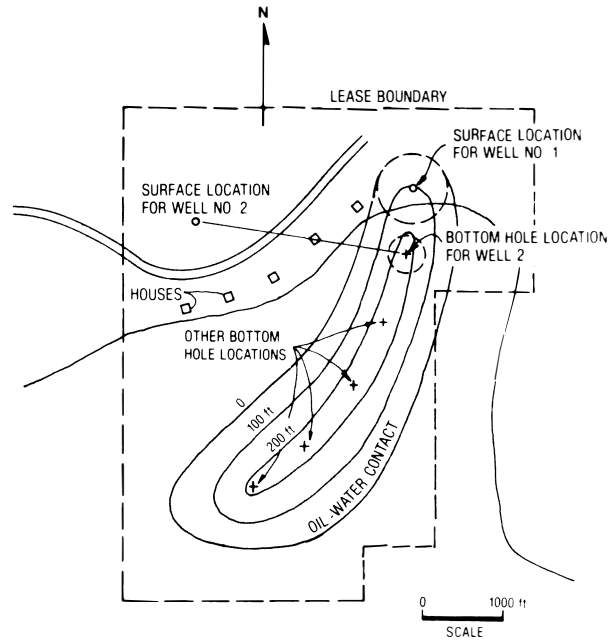


**Fig. 8.2**—Plan view of a typical oil and gas structure under a lake showing how directional wells could be used to develop it.

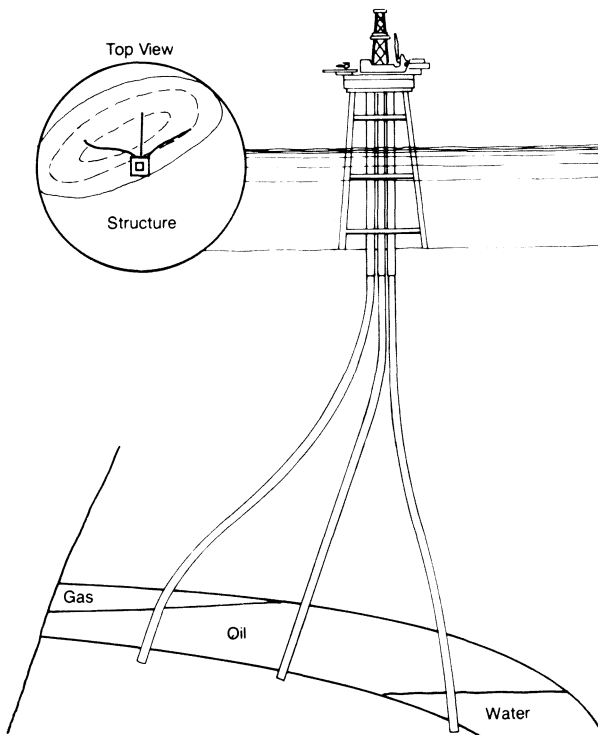


**Fig. 8.3**—Typical offshore development platform with directional wells.

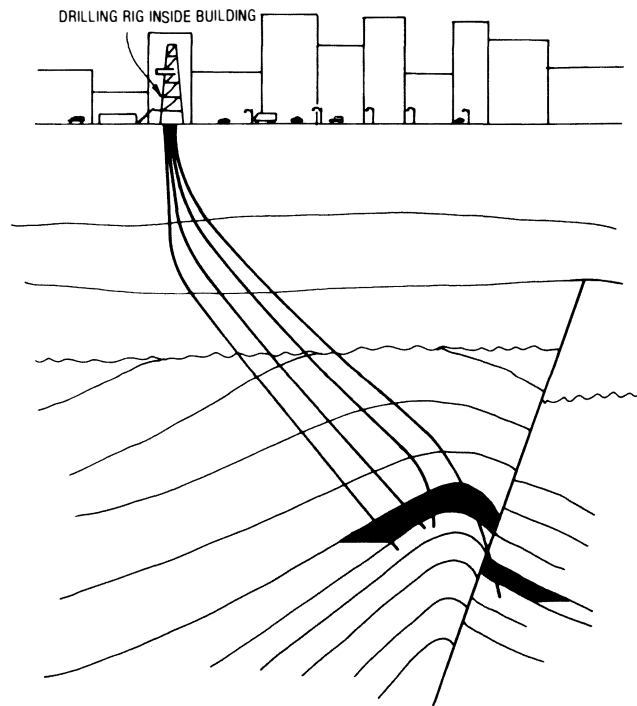


**Fig. 8.4**—Developing a field under a city using directionally drilled wells.



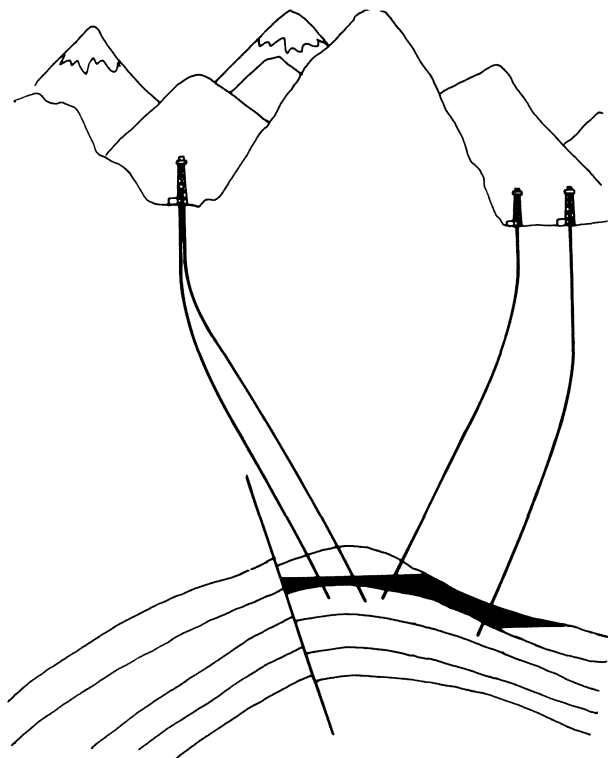


Fig. 8.5—Drilling of directional wells where the reservoir is beneath a major surface obstruction.

drilled in hard granites and other igneous and metamorphic rocks. Geothermal projects have been developed with directional wells. Wells with extended horizontal reaches of 14,000 ft are being drilled, with goals of going even farther. As the costs of field development increase—in deeper waters, remote locations, hostile environments, and deeper producing zones—the use of directional drilling will also increase.

## 8.2 Planning the Directional Well Trajectory

The first step in planning any directional well is to design the wellbore path, or trajectory, to intersect a given target. The initial design should propose the various types of paths that can be drilled economically. The second, or refined, plan should include the effects of geology on the bottomhole assemblies (BHA's) that will be used and other factors that could influence the final wellbore trajectory. This section explains how to plan the initial trajectory for most common directional wells.

Fig. 8.8 depicts three types of trajectories that could be drilled to hit the target. Path A is a build-and-hold trajectory: the wellbore penetrates the target at an angle equal to the maximum buildup angle. Path B is a "modified-S" and C is an "S" trajectory. With the S-shape trajectory the wellbore penetrates the target vertically, and with the modified-S trajectory the wellbore penetrates the target at some inclination angle less than the maximum inclination angle in the hold section. For Path D, a "continuous-build trajectory," the inclination keeps increasing right up to or through the target. The build-and-hold path requires the lowest inclination angle to hit the target; the modified-S requires more inclination; and the S-shape requires still more. The continuous-build path requires the highest inclination of all the trajectory types to hit the target.

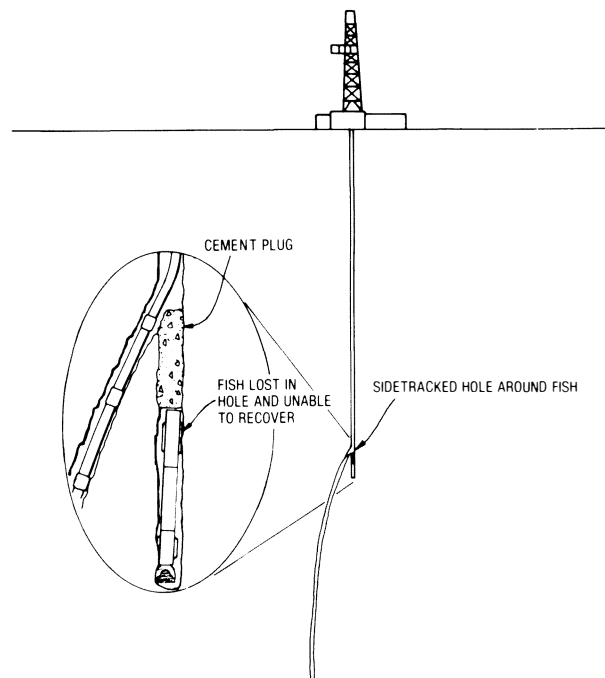


Fig. 8.6—Sidetracking around a fish.

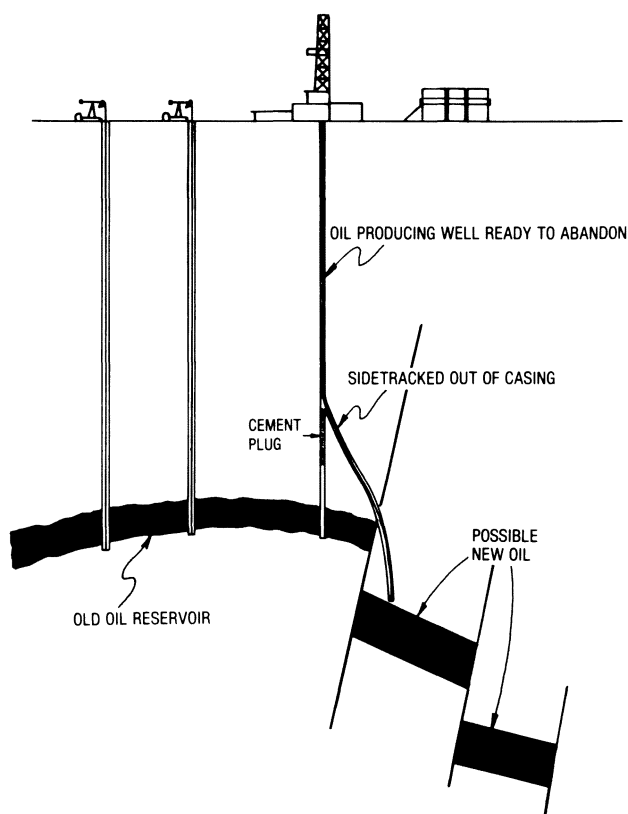


Fig. 8.7—Using an old well to explore for new oil by sidetracking out of the casing and drilling directionally.

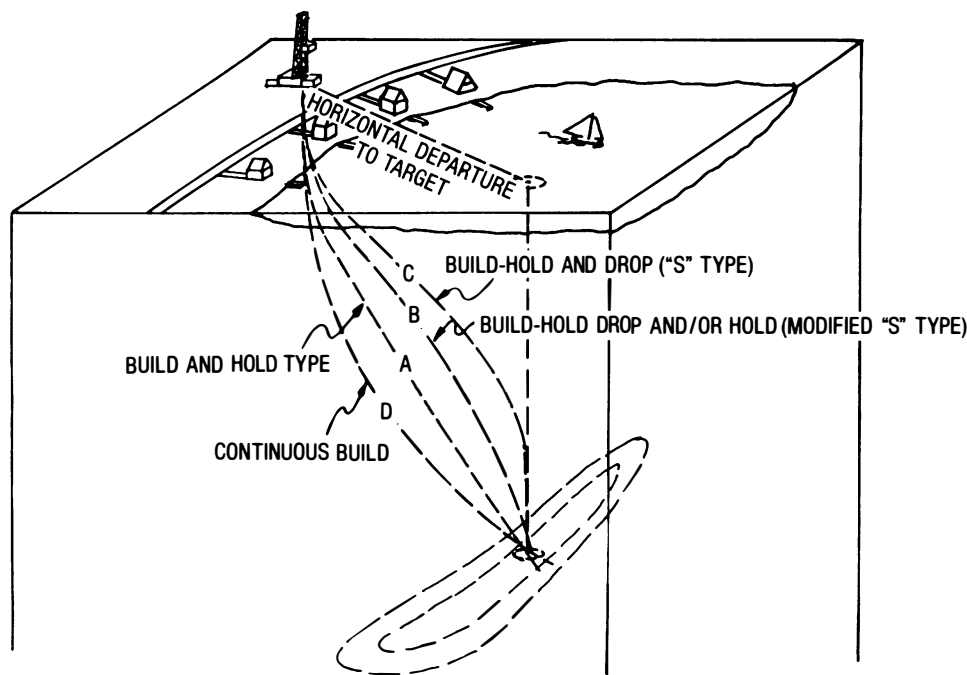


Fig. 8.8—Major types of wellbore trajectories.

### 8.2.1 Build-and-Hold Trajectory

Fig. 8.9 depicts a simple build-and-hold wellbore trajectory intersecting a target at a true vertical depth (TVD) of  $D_3$  and at a horizontal departure of  $X_3$  (Point B). The kickoff point is at a TVD of depth  $D_1$ , where the rate of inclination angle buildup is  $q$  in degrees per unit length.

The radius of curvature,  $r_1$ , is found thus:

$$r_1 = \frac{180}{\pi} \times \frac{1}{q} \quad (8.1)$$

To find the maximum inclination angle,  $\theta$ , consider in Fig. 8.9 that

$$90^\circ = \theta + (90 - \Omega) + \tau,$$

or

$$\theta = \Omega - \tau \quad (8.2)$$

The angle  $\tau$  can be found by considering Triangle OAB, where

$$\tan \tau = \frac{BA}{AO} = \frac{r_1 - X_3}{D_3 - D_1} \quad (8.3a)$$

and

$$\tau = \arctan \frac{r_1 - X_3}{D_3 - D_1} \quad (8.3b)$$

Angle  $\Omega$  can be found by considering Triangle OBC,

where

$$\sin \Omega = \frac{r_1}{OB} \quad (8.4)$$

and

$$L_{OB} = \sqrt{(r_1 - X_3)^2 + (D_3 - D_1)^2}.$$

Substituting OB into Eq. 8.4 gives

$$\sin \Omega = \frac{r_1}{\sqrt{(r_1 - X_3)^2 + (D_3 - D_1)^2}} \quad (8.5)$$

The maximum inclination angle,  $\theta$ , for the build-and-hold case, is not limited to  $X_3 < r_1$ . It is also valid for  $X_3 \geq r_1$ .

$$\theta = \arcsin \left[ \frac{r_1}{\sqrt{(r_1 - X_3)^2 + (D_3 - D_1)^2}} \right] - \arctan \left( \frac{r_1 - X_3}{D_3 - D_1} \right) \quad (8.6)$$

The length of the arc, Section DC, is

$$L_{DC} = \frac{\pi}{180} \times r_1 \times \theta,$$

or

$$L_{DC} = \frac{\theta}{q} \quad (8.7)$$

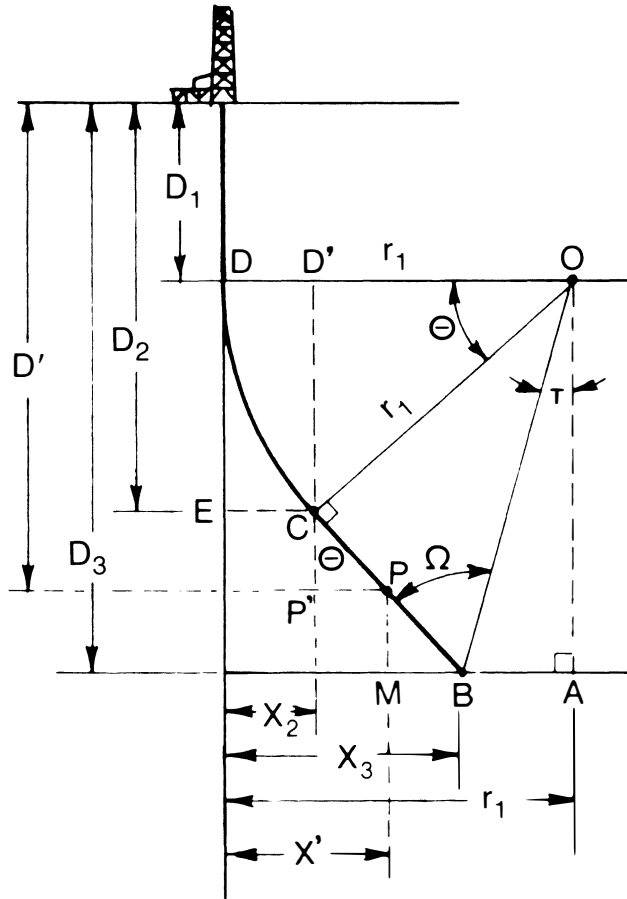


Fig. 8.9—Geometry of build-and-hold-type well path for  $X_3 < r_1$ .

The length of the trajectory path, CB, at a constant inclination angle can be determined from Triangle BCO as

$$\tan \Omega = \frac{CO}{L_{CB}} = \frac{r_1}{L_{CB}}$$

and

$$L_{CB} = \frac{r_1}{\tan \Omega}.$$

The total measured depth,  $D_M$ , for a TVD of  $D_3$  is

$$D_M = D_1 + \frac{\theta}{q} + \frac{r_1}{\tan \Omega}, \quad \text{..... (8.8)}$$

where  $D_M$  equals the vertical section to kickoff plus build section plus constant inclination section (Fig. 8.9).

The horizontal departure EC ( $X_2$ ) at the end of the build can be determined by considering Triangle D'OC, where

$$X_2 = r_1 - r_1 \cos \theta = r_1 (1 - \cos \theta). \quad \text{..... (8.9)}$$

To find the measured depth and horizontal departure along any part of the build before reaching maximum angle  $\theta$ , consider the intermediate inclination angle  $\theta'$ , the

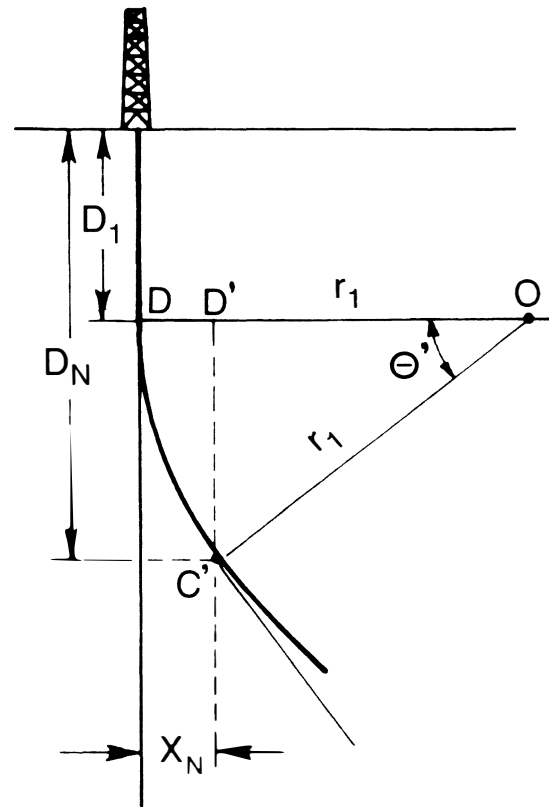


Fig. 8.10—Geometry for the build section.

inclination angle at  $C'$  (Fig. 8.10), which will yield a new horizontal departure,  $X_N$ . The distance  $d_N$  can be determined considering Triangle D'OC', where

$$D_N = D_1 + r_1 \sin \theta', \quad \text{..... (8.10)}$$

and the horizontal displacement,  $X_N$ , is

$$X_N = r_1 - r_1 \cos \theta' = r_1 (1 - \cos \theta'). \quad \text{..... (8.11)}$$

The TVD at the end of the build section is  $D_2$ , which can be derived from Triangle D'OC (Fig. 8.9):

$$D_2 = D_1 + r_1 \sin \theta. \quad \text{..... (8.12)}$$

The new measured depth for any part of the buildup is

$$D_{MN} = D_1 + \frac{\theta'}{q}. \quad \text{..... (8.13)}$$

The new measured depth at a TVD of  $D'$  can be determined from Triangle PP'C:

$$D_{MP} = D_1 + \frac{\theta}{q} + CP, \quad \text{..... (8.14)}$$

where

$$CP = \frac{CP'}{\cos \theta}$$

and

$$CP' = D' - D_2 = (D' - D_1 - r_1 \sin \theta).$$

Therefore,

$$CP = \frac{(D' - D_1 - r_1 \sin \theta)}{\cos \theta}. \quad \dots\dots\dots (8.15)$$

Substituting Eq. 8.15 into Eq. 8.14,

$$D_{MP} = D_1 + \frac{\theta}{q} + \frac{D' - D_1 - r_1 \sin \theta}{\cos \theta}. \quad \dots\dots\dots (8.16)$$

Eq. 8.16 also can be used instead of Eq. 8.14 to calculate the measured depth by making  $D' = D_3$ .

The horizontal departure at Point P is

$$X' = X_2 + P'P, \quad \dots\dots\dots (8.17)$$

where  $P'P = CP' \tan \theta$ .

Combining Eq. 8.17, Eq. 8.9, and  $CP'$  yields

$$X' = r_1(1 - \cos \theta) + (D' - D_1 - r_1 \sin \theta) \tan \theta. \quad \dots\dots\dots (8.18)$$

The preceding derivation is valid only when  $X_3 < r_1$ .

Another way of expressing the maximum inclination angle,  $\theta$ , in terms of  $r_1$ ,  $D_1$ ,  $D_3$ , and  $X_3$  for  $X_3 < r_1$  is

$$\begin{aligned} \theta = & \arctan \left( \frac{D_3 - D_1}{r_1 - X_3} \right) - \arccos \left\{ \left( \frac{r_1}{D_3 - D_1} \right) \right. \\ & \left. \times \sin \left[ \arctan \left( \frac{D_3 - D_1}{r_1 - X_3} \right) \right] \right\}. \quad \dots\dots\dots (8.19) \end{aligned}$$

**Example 8.1.** It is desired to drill under the lake to the location designated for Well 2. For this well, a build-and-hold trajectory will be used. Horizontal departure to the target is 2,655 ft at a TVD of 9,650 ft. The recommended rate of build is 2.0°/100 ft. The kickoff depth is 1,600 ft. Determine (1) the radius of curvature,  $R_1$ ; (2) the maximum inclination angle,  $\theta$ ; (3) the measured depth to the end of the build; (4) the total measured depth; (5) the horizontal departure to the end of the build; (6) the measured depth at a TVD of 1,915 ft; (7) the horizontal displacement at a TVD of 1,915 ft; (8) the measured depth at a TVD of 7,614 ft; and (9) the horizontal departure at a TVD of 7,614 ft.

**Solution.** From Eq. 8.1

$$r_1 = \frac{180}{\pi} \frac{1}{2^\circ/100 \text{ ft}} = 2,865 \text{ ft.}$$

Since  $X_3 < r_1$ ,  $\theta = \Omega - \tau$ . From Eq. 8.3a,

$$\tan \tau = \frac{r_1 - X_3}{D_3 - D_1} = \frac{210 \text{ ft}}{8,050 \text{ ft}} = 0.0261,$$

$$\tau = \arctan 0.0261 = 1.5^\circ.$$

From Eq. 8.5,

$$\sin \Omega = \frac{r_1}{\sqrt{(r_1 - X_3)^2 + (D_3 - D_1)^2}}$$

$$= \frac{2,865 \text{ ft}}{8,053 \text{ ft}} = 0.3558,$$

$$\Omega = \arcsin 0.3558 = 20.84^\circ.$$

The maximum inclination angle is

$$\theta = 20.84^\circ - 1.5^\circ = 19.34^\circ.$$

Using Eq. 8.19,

$$\begin{aligned} \theta = & \arctan \left( \frac{9,650 \text{ ft} - 1,600 \text{ ft}}{2,865 \text{ ft} - 2,655 \text{ ft}} \right) \\ & - \arccos \left( \frac{2,865 \text{ ft}}{9,650 \text{ ft} - 1,600 \text{ ft}} \right) \\ & \times \sin \left[ \arctan \left( \frac{9,650 \text{ ft} - 1,600 \text{ ft}}{2,865 \text{ ft} - 2,655 \text{ ft}} \right) \right] = 19.34^\circ. \end{aligned}$$

The measured depth to the end of the build at an inclination of 19.34° is

$$D_M = 1,600 \text{ ft} + \frac{19.34^\circ}{2^\circ} \times 100 \text{ ft} = 2,565 \text{ ft},$$

and the total measured depth to the target TVD of 9,650 ft, using Eq. 8.14, is

$$\begin{aligned} D_{tar} = & 2,565 \text{ ft} + \frac{R_1}{\tan \Omega} = 2,565 \text{ ft} + \frac{2,865 \text{ ft}}{\tan(20.84^\circ)} \\ = & 10,091 \text{ ft.} \end{aligned}$$

The horizontal departure to the end of the build, from Eq. 8.9, is

$$X_2 = r_1(1 - \cos \theta) = 2,865 \text{ ft} [1 - \cos(19.34^\circ)] = 161 \text{ ft.}$$

At a TVD of 1,915 ft, the measured depth at a rate of build of  $2^\circ/100$  ft can be determined by first calculating the inclination at 1,915 ft using Eq. 8.10:

$$1,915 \text{ ft} = 1,600 \text{ ft} + 2,865 \text{ ft} \sin \theta$$

$$\theta = \arcsin \left( \frac{315 \text{ ft}}{2,865 \text{ ft}} \right) = 6.31^\circ.$$

The arc length of the build to  $6.31^\circ$  can be calculated using Eq. 8.7:

$$L_{DC} = \frac{6.31^\circ}{2.0^\circ} \times 100 \text{ ft} = 315.5 \text{ ft}.$$

The measured depth for a TVD of 1,915 ft is

$$D_M = 315.5 \text{ ft} + 1,600 \text{ ft} = 1,915.5 \text{ ft},$$

which is only 0.5 ft more than the TVD.

The horizontal departure at a TVD of 1,915 ft is found from Eq. 8.11:

$$X_{1,915} = 2,865 \text{ ft} (1.0 - \cos 6.31) = 17.36 \text{ ft}.$$

The measured depth at a TVD of 7,614 ft is

$$\begin{aligned} D_M &= 1,600 \text{ ft} + \frac{19.34^\circ}{2^\circ} \times 100 \text{ ft} \\ &+ \frac{7,614 \text{ ft} - 1,600 \text{ ft} - 2,865 \text{ ft} \sin(19.34^\circ)}{\cos(19.34^\circ)} \\ &= 7,934 \text{ ft}. \end{aligned}$$

The horizontal departure at a TVD of 7,614 ft is calculated with Eq. 8.18:

$$\begin{aligned} X'_{7,614} &= 2,865 \text{ ft} (1 - \cos 19.34) \\ &+ (7,614 \text{ ft} - 1,600 \text{ ft} - 2,865 \text{ ft} \sin 19.34^\circ) \\ &\times \tan 19.34 = 1,935.5 \text{ ft}. \end{aligned}$$

The preceding derivation and example calculation is for the case where  $r_1 > X_3$  for a simple build-and-hold trajectory. For the case where  $r_1 < X_3$ , the maximum angle,  $\theta$ , can be calculated by

$$\begin{aligned} \theta &= 180 - \arcsin \left( \frac{D_3 - D_1}{X_3 - r_1} \right) - \arcsin \left\{ \left( \frac{r_1}{D_3 - D_1} \right) \right. \\ &\times \sin \left[ \arcsin \left( \frac{D_3 - D_1}{X_3 - r_1} \right) \right] \left. \right\}. \dots\dots\dots (8.20) \end{aligned}$$

### 8.2.2 Build-Hold-and-Drop (“S”) Trajectory

The second type of trajectory is the build, hold, and drop—or S-shape curve—which is depicted by Fig. 8.11 for the cases where  $r_1 < X_3$  and  $r_1 + r_2 > X_4$ , and in Fig. 8.12 for the cases where  $r_1 < X_3$  and  $r_1 + r_2 < X_4$ . In both cases, the maximum inclination is reduced to zero at  $D_4$  with drop radius  $r_2$ , which is derived in the same manner as the build radius,  $r_1$ . The following equations are used to calculate the maximum inclination angles for  $r_1 + r_2 > X_4$  and for  $r_1 + r_2 < X_4$ .

$$\begin{aligned} \theta &= \arcsin \left( \frac{D_4 - D_1}{r_1 + r_2 - X_4} \right) - \arcsin \left\{ \left( \frac{r_1 + r_2}{D_4 - D_1} \right) \right. \\ &\times \sin \left[ \arcsin \left( \frac{D_4 - D_1}{r_1 + r_2 - X_4} \right) \right] \left. \right\}. \dots\dots\dots (8.21) \end{aligned}$$

$$\begin{aligned} \theta &= 180^\circ - \arcsin \left[ \frac{D_4 - D_1}{X_4 - (r_1 + r_2)} \right] \\ &- \arcsin \left\{ \left( \frac{r_1 + r_2}{D_4 - D_1} \right) \right. \\ &\times \sin \left[ \arcsin \left[ \frac{D_4 - D_1}{X_4 - (r_1 + r_2)} \right] \right] \left. \right\}. \dots\dots\dots (8.22) \end{aligned}$$

### 8.2.3 Build, Hold, Partial Drop, and Hold (Modified “S”) Trajectory

The build, hold, partial drop, and hold (Fig. 8.13) is the modified S type of wellbore path. Consider that the arc length

$$L_{CA} = \frac{\theta'}{q}.$$

From the Right Triangle CO'B, the following relationships can be written.

$$L_{CB} = r_2 \sin \theta' \dots\dots\dots (8.23a)$$

and

$$s_{BA} = r_2 - r_2 \cos \theta' = r_2 (1 - \cos \theta'). \dots\dots\dots (8.23b)$$

Eqs. 8.21 and 8.22 can be rewritten by substituting  $D_5 + r_2 \sin \theta'$  for  $D_4$  and  $X_5 + r_2 (1 - \cos \theta')$  for  $X_4$ .

For any of the S-shape curves, the measured depths and horizontal departures can be calculated in the same way they are calculated for the build-and-hold trajectory by deriving the appropriate relationships for the various geometries.

### 8.2.4 Multiple Targets

When a directional well is being planned, the depth and horizontal departure of the target are given, as well as its dimensions. Targets may be rectangular, square, or circular. If the target is a circle, a radius is designated.

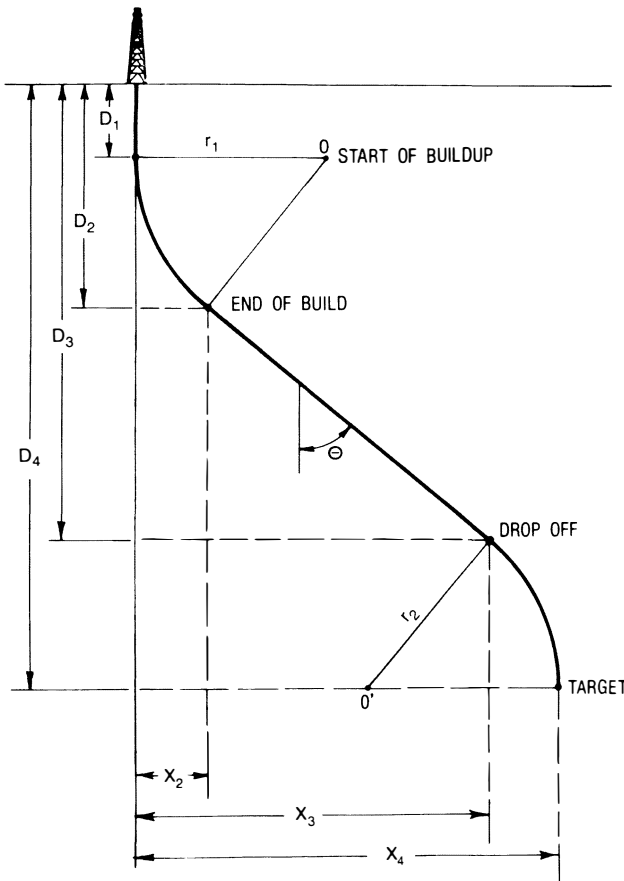


Fig. 8.11—Build-hold-and-drop for the case where  $r_1 < X_3$  and  $r_1 + r_2 < X_4$ .

Sometimes there are multiple targets, as shown by Figs. 8.14a and 8.14b. If they are favorably positioned, multiple targets can be economically penetrated with one of the aforementioned types of trajectories (Fig. 8.14a). Sometimes, however, they are unfavorably aligned (Fig. 8.14b) and expensive trajectory alterations are required. The trajectory in Fig. 8.14b could be difficult and expensive to drill even though the vertical section appears the same as that in Fig. 8.14a. The direction change to hit Target 3 would in most situations be extremely difficult to execute.

### 8.2.5 Direction Quadrant and Compass Schemes

In the previous discussions all the trajectory planning has been reduced to a two-dimensional problem, considering only depth and horizontal departure. All directional wells also have an  $X$  component that is associated with direction. For example, Well 2 in Fig. 8.2 has a target direction of  $100^\circ$  east of north by a normal compass reading. In directional drilling, a  $90^\circ$  quadrant scheme is used to cite directions and the degrees are always read from north to east or west, and from south to east or west. For example, the direction angle in Fig. 8.15a by compass (always read clockwise from due north) is  $18^\circ$ , and by the quadrant scheme it is N18E. The well in the second quadrant (Fig. 8.15b) at  $157^\circ$  is read S23E. In quadrant three (Fig. 8.15c), the well is S20W, for a measured angle of  $200^\circ$ . In quadrant four (Fig. 8.15d), the compass angle of  $305^\circ$  is read N55W.

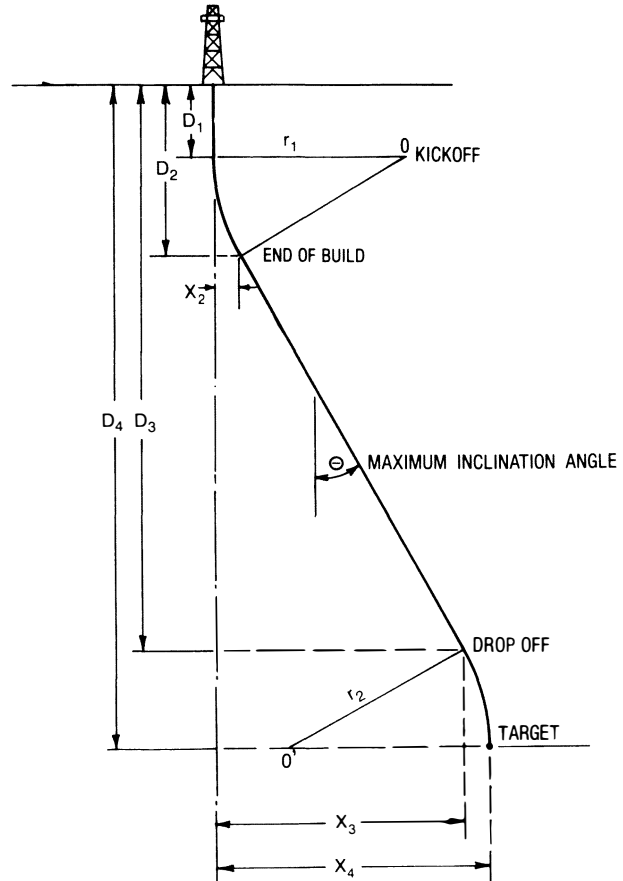


Fig. 8.12—Build-hold-and-drop for the case where  $r_1 < X_3$  and  $r_1 + r_2 > X_4$ .

**Example 8.2.** What are the directions, in the alternative format, of each of the following wells?

Well A	N15E
Well B	225°
Well C	N0E

**Solution.** Well A is in the first quadrant and is  $15^\circ$ ; Well B is in the third quadrant and should be read as S45W; and Well C represents  $0^\circ$  or north.

### 8.2.6 Planning the X-Y Trajectory

The first step in planning a well is to determine the two-dimensional  $Y$ - $Z$  trajectory (Fig. 8.1). The next step is to account for the  $X$  component of the trajectory that departs from the vertical plane section between the surface location and the bottomhole target. Fig. 8.16 is a plan view, looking down on the straight line projected path from Well 2's surface location to the bull's-eye of a target with a 100-ft radius. The dashed line indicates a possible path the bit could follow because of certain influences exerted by the bit, the BHA configuration, the geology, general hole conditions, and other factors that are covered later in this chapter.

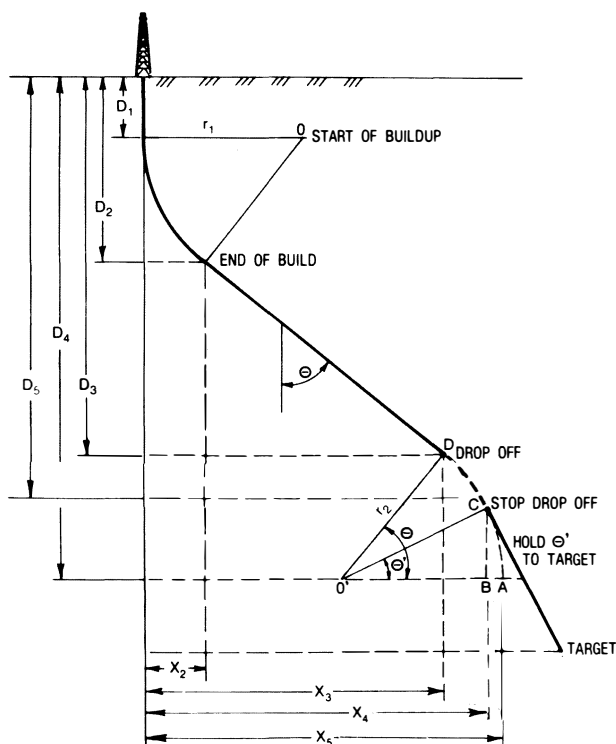


Fig. 8.13—Build-hold-and-drop and hold (modified-S) where  $r_1 < X_3$  and  $r_1 + r_2 < X_4$ .

The target area provides a zone of tolerance for the wellbore trajectory to pass through. The size and dimensions of the target are usually based on factors pertaining to the drainage of a reservoir, geological criteria, and lease boundary constraints.

When a well is kicked off, the practice is to orient the trajectory to some specific direction angle called "lead." This lead usually is to the left of the target departure line and ranges from 5 to 25°. The value used is generally based on local experience or some rule of thumb. More recent research on direction variation (or, to use an older term, "bit walk") indicates that the lead can be selected on the basis of analysis of offset wells and of factors that might cause bit walk.

As the drilling progresses after the lead is set, the trajectory varies in the  $X$  and  $Y$  planes as the bit penetrates in the  $Z$  plane. Figs. 8.17 and 8.18 are vertical and horizontal (elevation and plan) views of a typical trajectory path. Past the lead angle, the trajectory shows a clockwise, or right-hand, tendency or bit walk. A counter-clockwise curvature is called left-hand tendency or bit walk.

The initial trajectory design did not account for the excursion of the bit away from the vertical plane that goes through the surface location and the target's bull's-eye. There are many ways to calculate the three-dimensional path of the wellbore.<sup>1-3</sup> The most common method used in the field is "angle averaging," which can be performed on a hand calculator with trigonometric functions.

Consider the vertical section as depicted by Fig. 8.17. The distance from the surface to the kickoff point is  $D_1$ . At  $A_1$  the well is kicked off and drilled to  $A_2$ . The inclination angle at the kickoff is zero. Fig. 8.18 shows the

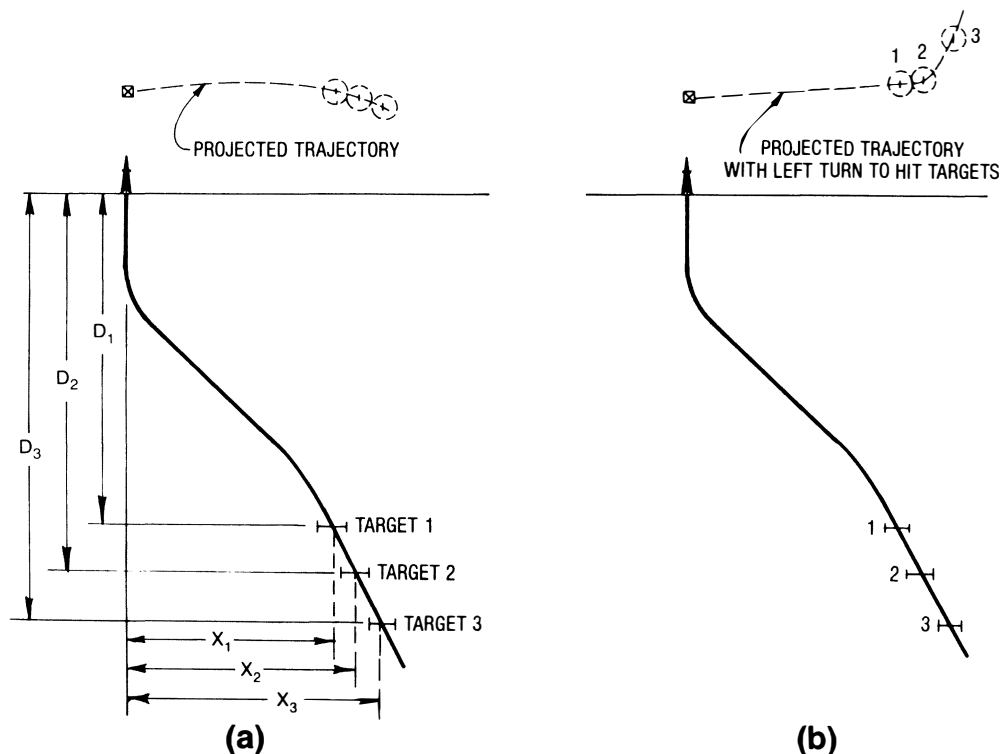


Fig. 8.14—Directional well used to intersect multiple targets.

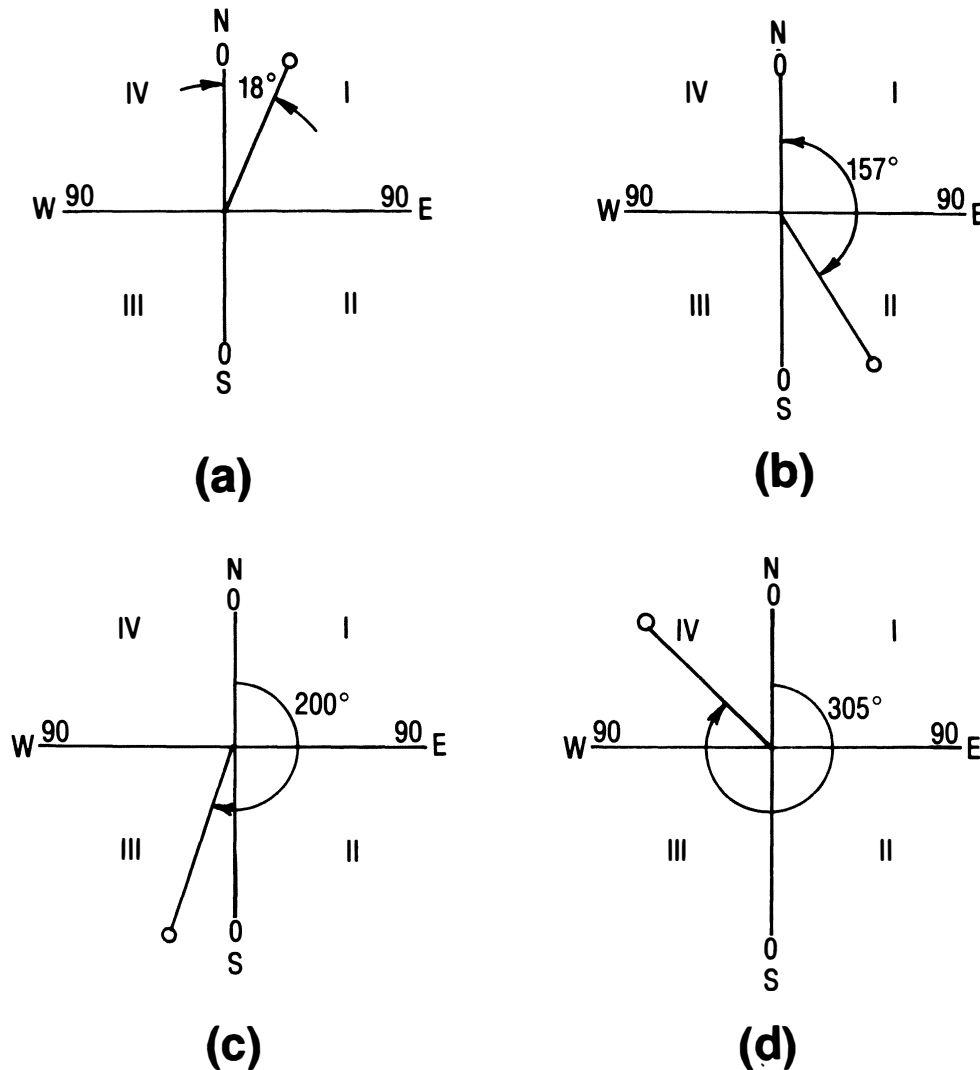


Fig. 8.15—Directional quadrants and compass measurements.

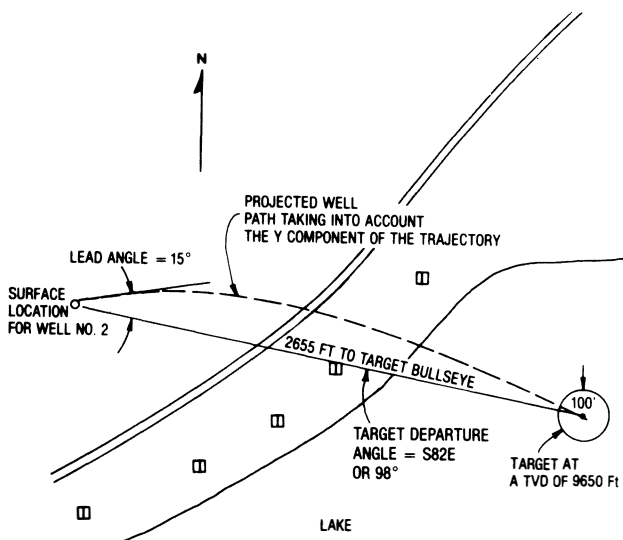


Fig. 8.16—Plan view.

top, or plan, view of the trajectory; Point  $A_1$  on the vertical section corresponds to the starting point,  $A_1$ , on the plan view. Using the angle-averaging method, the following equations can be derived for the north/south ( $L$ ) and east/west ( $M$ ) coordinates.

$$L = \Delta D_M \sin\left(\frac{\alpha_A + \alpha_{A-1}}{2}\right) \cos\left(\frac{\epsilon_A + \epsilon_{A-1}}{2}\right) \quad \dots\dots\dots (8.24)$$

and

$$M = \Delta D_M \sin\left(\frac{\alpha_A + \alpha_{A-1}}{2}\right) \sin\left(\frac{\epsilon_A + \epsilon_{A-1}}{2}\right) \quad \dots\dots\dots (8.25)$$

The TVD can be calculated by

$$D = \Delta D_M \cos\left(\frac{\alpha_A + \alpha_{A-1}}{2}\right), \quad \dots\dots\dots (8.26)$$

where  $\Delta D_M$  is the measured depth increment.



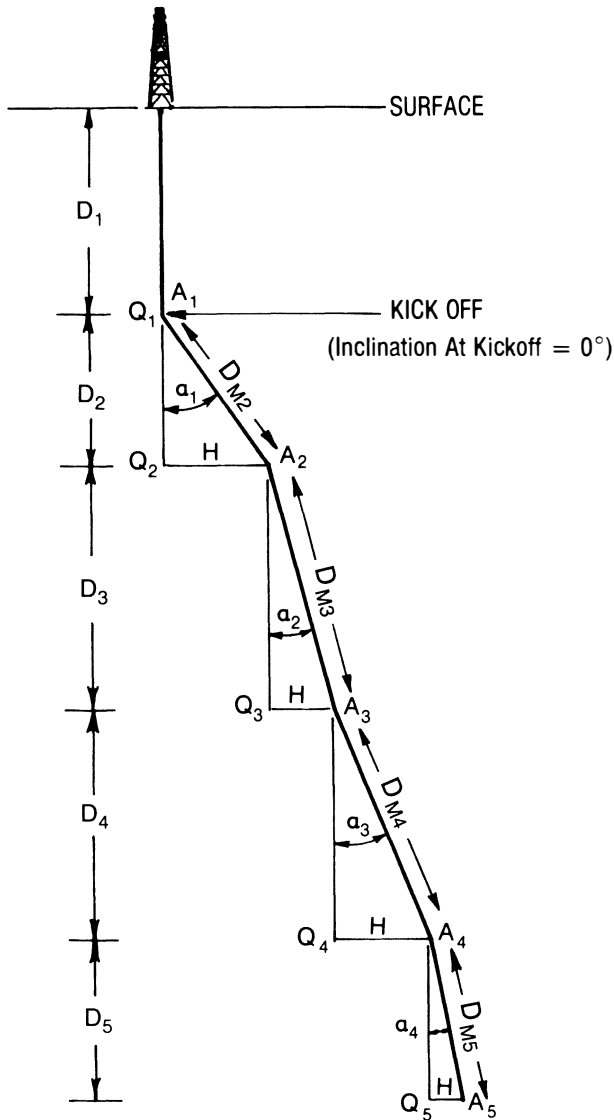


Fig. 8.17—Vertical calculation.

**Example 8.3.** Calculate the trajectory for the well from 8,000 to 8,400 ft, where the kickoff is at 8,000 ft and the rate of build is  $1^\circ/100$  ft, using a lead of  $10^\circ$  and a right-hand walk rate of  $1^\circ/100$  ft. Direction to the bull's-eye is N30E. Assume that the first 200 ft is to set the lead, where the direction is held constant to 8,200 ft and then turns right at a rate of  $1^\circ/100$  ft.

**Solution.** The north and east coordinates are calculated using Eqs. 8.24 and 8.25, and the TVD from 8,000 to 8,100 ft is calculated from Eq. 8.26.

$$L_2 = 100 \text{ ft} \sin\left(\frac{1^\circ + 0}{2}\right) \cos(20) = 0.82 \text{ ft},$$

$$M_2 = 100 \text{ ft} \sin\left(\frac{1^\circ + 0}{2}\right) \sin(20) = 0.30 \text{ ft},$$

\*For the first point the direction should not be averaged.

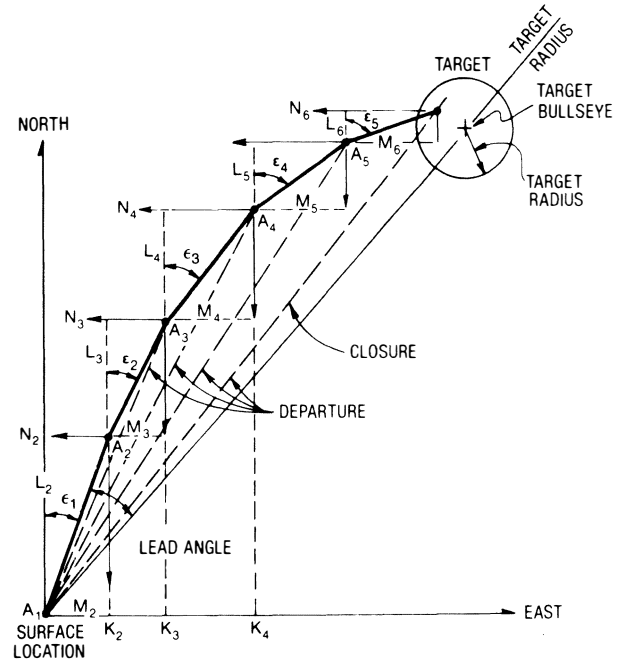


Fig. 8.18—Horizontal calculation.

and

$$D_2 = 100 \text{ ft} \cos\left(\frac{1+0}{2}\right) = 99.996 \text{ ft},$$

$$D = 8,000 \text{ ft} + 99.996 \text{ ft} = 8,099.996 \text{ ft}.$$

From 8,100 to 8,200 ft:

$$L_3 = 100 \text{ ft} \sin\left(\frac{1+2}{2}\right) \cos\left(\frac{20+20}{2}\right) = 2.46 \text{ ft}.$$

$$\text{Total north} = 0.82 + 2.46 = 3.28 \text{ ft}.$$

$$M_3 = 100 \text{ ft} \sin\left(\frac{1+2}{2}\right) \sin\left(\frac{20+20}{2}\right) = 0.90 \text{ ft}.$$

$$\text{Total east} = 0.30 + 0.90 = 1.20 \text{ ft}.$$

$$D_3 = 100 \text{ ft} \cos\left(\frac{1+2}{2}\right) = 99.966 \text{ ft}.$$

$$D = 8,099.996 + 99.966 = 8,199.962 \text{ ft}.$$

From 8,200 to 8,300 ft, the direction changes by  $1^\circ/100$  ft from N20E to N21E.

$$L_4 = 100 \text{ ft} \sin\left(\frac{2+3}{2}\right) \cos\left(\frac{20+21}{2}\right) = 4.09 \text{ ft}.$$

$$\text{Total north} = 3.28 + 4.09 = 7.37 \text{ ft}.$$

$$M_4 = 100 \text{ ft} \sin\left(\frac{2+3}{2}\right) \sin\left(\frac{20+21}{2}\right) = 1.53 \text{ ft.}$$

$$\text{Total east} = 1.20 + 1.53 = 2.73 \text{ ft.}$$

$$D_4 = 100 \text{ ft} \cos\left(\frac{2+3}{2}\right) = 99.90 \text{ ft.}$$

$$D = 8,199.962 + 99.90 = 8,299.862 \text{ ft.}$$

From 8,300 to 8,400 ft, the direction further changes to N22E.

$$L_5 = 100 \text{ ft} \sin\left(\frac{3+4}{2}\right) \cos\left(\frac{21+22}{2}\right) = 5.68 \text{ ft.}$$

$$\text{Total north} = 7.37 + 5.68 = 13.05 \text{ ft.}$$

$$M_5 = 100 \text{ ft} \sin\left(\frac{3+4}{2}\right) \sin\left(\frac{21+22}{2}\right) = 2.24 \text{ ft.}$$

$$\text{Total east} = 2.73 + 2.24 = 4.97 \text{ ft.}$$

$$D_5 = 100 \text{ ft} \cos\left(\frac{3+4}{2}\right) = 99.81 \text{ ft,}$$

$$D = 8,299.862 + 99.81 = 8,399.672 \text{ ft.}$$

The total departure at each depth can be calculated from each triangle— $A_1A_2K_2$ ,  $A_2A_3K_3$ ,  $A_3A_4K_4$ , and  $A_4A_5K_5$ —and the departure angle can be determined from the target of each triangle:

$$\text{total departure} = \sqrt{(\text{total north})^2 + (\text{total east})^2},$$

$$\text{departure angle} = \arctan\left(\frac{\text{total east}}{\text{total north}}\right).$$

Table 8.1 is a tabulation of the foregoing calculations.

Using the rate of build of  $1^\circ/100 \text{ ft}$ , calculate the TVD going from 0 to  $4^\circ$  inclination. Calculate first the radius of curvature,  $r_1$ , using Eq. 8.1:

$$r_1 = \frac{180^\circ}{\pi} \times \frac{100 \text{ ft}}{1} = 5,730 \text{ ft.}$$

Then find the TVD,  $D$ , using Eq. 8.26:

$$D = 8,000 \text{ ft} + 5,730 \text{ ft} \sin 4.0^\circ = 8,399.70 \text{ ft.}$$

Example 8.3 showed us how the trajectory variation in the direction plane is determined. The departure angle in Table 8.1 shows the effect of the  $1^\circ/100\text{-ft}$  rate of direction change, where the angle is increasing from the north to the east in a clockwise manner. These same calculations can be used in any of the quadrants as long as the

TABLE 8.1—DATA FOR EXAMPLE 8.3

$D_M$ (ft)	TVD (ft)	N North (ft)	N East (ft)	Departure (ft)	Departure Angle* (degrees)
8,000	8,000.00	0.00	0.00	0.00	—
8,100	8,099.99	0.82	0.30	0.87	20.1
8,200	8,199.96	3.28	1.20	3.49	20.1
8,300	8,299.86	7.37	2.73	7.86	20.33
8,400	8,399.67	13.05	4.97	13.97	20.85

\*Note that the statement of the problem requires the departure angle to be  $20^\circ$  to 8,200 ft. Roundoff error in the very small early-departure distances can cause the calculated departure angle to be different.

proper sign convention is observed. In planning a trajectory that is near  $0^\circ$  (first quadrant) and  $360^\circ$  (fourth quadrant), special care must be taken. For example, the average of  $359^\circ$  and  $1^\circ$  would be  $180^\circ$ , whereas  $358^\circ$  and  $360^\circ$  would be  $359^\circ$ . Logically, the way to handle this problem is to continue with the clockwise angle notation, so that  $359^\circ$  and  $1^\circ$  are  $359^\circ$  and  $361^\circ$ , which average  $360^\circ$ .

The steps to plan a trajectory are as follows.

1. From geological or other considerations, establish the target depth, number of targets, target radius, and horizontal departure to the target.

2. Select a kickoff point that seems appropriate and choose a type of trajectory such as a build and hold, an S-shape or a modified S-curve, or a continuous build. Make a two-dimensional plan.

3. Calculate the maximum inclination point and other trajectory information.

4. Determine the lead angle and estimate the rate of direction change.

5. Calculate the three-dimensional well path to hit the target by using the initial two-dimensional well plan as a guide. This reduces the number of trial-and-error calculations.

With this procedure a trajectory can be devised for most directional wells. The practical considerations in designing a directional well are covered later in this chapter.

### 8.3 Calculating the Trajectory of a Well

The normal method for determining the well path is to ascertain the coordinates by using some type of surveying instrument to measure the inclination and direction at various depths (stations) and then to calculate the trajectory. Sec. 8.5 discusses the various instruments in detail. All that must be known in this section is that values of inclination and direction can be obtained at preselected depths.

Fig. 8.19 depicts part of a trajectory path where surveys are taken at Stations  $A_2$ ,  $A_3$ , and  $A_4$ . At each station, inclination and direction angles are measured as well as the course length between stations. Each direction angle obtained by a magnetic type of survey must be corrected to true north, and each gyroscope must be corrected for drift. This is explained in Sec. 8.5. Assume in this section that all the direction readings are corrected for the declination void of magnetic interference, and that the drift conversion is performed for the gyroscopic surveys.

There are 18 or more calculation techniques for determining the trajectory of the wellbore. The main difference in all the techniques is that one group uses straight line approximations and the other assumes the wellbore

is more of a curve and is approximated with curved segments. It is beyond the scope of this chapter to derive every method. References at the end of the chapter cite sources for some of the more common ones.

### 8.3.1 Tangential Method

The simplest method used for years has been the *tangential method*. The original derivation or presentation to industry is unknown. The mathematics uses the inclination and direction at a survey station  $A_2$  (Fig. 8.19) and assumes the projected angles remain constant over the preceding course length  $D_{M2}$  to  $A_2$ . The Angles are  $A_1$  are not considered.

It can be shown that the latitude north/south coordinate,  $L$ , can be calculated using Eq. 8.27 for each course length  $D_M$ .

$$L_i = D_{Mi} \sin(\alpha_i) \cdot \cos(\epsilon_i). \quad (8.27)$$

Likewise, the east/west coordinate  $M$  is determined by Eq. 8.28:

$$M_i = D_{Mi} \sin(\alpha_i) \cdot \sin(\epsilon_i). \quad (8.28)$$

The TVD segment is calculated by Eq. 8.29:

$$D_i = D_{Mi} \cos \alpha_i. \quad (8.29)$$

To calculate the total north/south and east/west coordinates and the TVD,

$$L_n = \sum_{i=1}^n L_i, \quad (8.30)$$

$$M_n = \sum_{i=1}^n M_i, \quad (8.31)$$

and

$$D_n = \sum_{i=1}^n D_i. \quad (8.32)$$

### 8.3.2 Average Angle or Angle Averaging Method

It was recognized that the tangential method caused a sizable error by not considering the previous inclination and direction. The average angle and angle averaging method considers the average of the angles  $\alpha_1$ ,  $\epsilon_1$ , and  $\alpha_2$ ,  $\epsilon_2$  over a course length increment  $D_2$  to calculate  $L_2$ ,  $M_2$ , and  $D_2$ . Eqs. 8.24 through 8.26 are the angle averaging and average angle relationships:

$$L_i = D_{Mi} \sin\left(\frac{\alpha_i + \alpha_{i-1}}{2}\right) \cos\left(\frac{\epsilon_i + \epsilon_{i-1}}{2}\right),$$

$$M_i = D_{Mi} \sin\left(\frac{\alpha_i + \alpha_{i-1}}{2}\right) \sin\left(\frac{\epsilon_i + \epsilon_{i-1}}{2}\right),$$

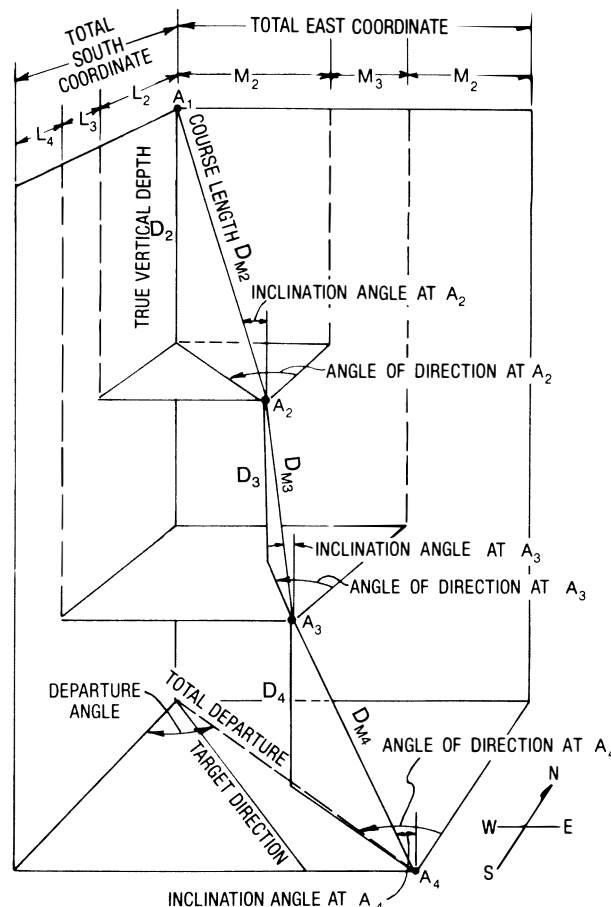


Fig. 8.19—Three-dimensional view of a wellbore showing components that comprise the X, Y, and Z parts of the trajectory.

and

$$D_i = D_{Mi} \cos\left(\frac{\alpha_i + \alpha_{i-1}}{2}\right),$$

and

$$L_n = \sum_{i=1}^n L_i,$$

$$M_n = \sum_{i=1}^n M_i, \text{ and}$$

$$D_n = \sum_{i=1}^n D_i.$$

On the basis of Eqs. 8.24 through 8.26, the trajectory calculation can easily be set in tabular form (Fig. 8.20) or set up as a program on a programmable hand calculator. Table 8.2 shows a sequence of steps used in the angle-averaging technique to determine the trajectory coordinates from measured values of inclination and direction.

SURVEY DATA			VERTICAL DEPTH CALCULATIONS							COURSE COORDINATES		TOTAL COORDINATES		TOTAL DEPARTURE	DEPARTURE ANGLE	
MEASURED DEPTH	INCL ANGLE	DIRECTION	COURSE LENGTH	AVERAGE INCLIN $\frac{\alpha_x + \alpha_{(x-1)}}{2}$	(D) COS (E)		T.V.D. $\Sigma (d)$	(D) SIN (E)	SURVEY AZIMUTH	AVERAGE AZIMUTH $\frac{\epsilon_x + \epsilon_{(x-1)}}{2}$	(H) COS (K) NORTH - SOUTH	(H) SIN (K) EAST - WEST	$\Sigma (L)$ NORTH - SOUTH	$\Sigma (M)$ EAST - WEST	$\sqrt{(N)^2 + (O)^2}$	ARCTAN $\frac{O}{N}$
X	(A)	$\alpha_x$	(C)	(D)	(E)	(d)	(G)	(H)	$\epsilon$	(K)	(L)	(M)	(N)	(O)	(P)	(Q)
* 1	7100	0	0	7100	0	7100 00	7100 00	0	0	0	0	0	0	0	0	0
** 2	7200	10.1	S68W	100	5.05	99 61	7199 61	8 80	248	248	- 3 30	- 8 16	- 3 30	- 8 16	8 80	S68W
3	7300	13.4	S65W	100	11.75	97 90	7297 51	20 36	245	246.5	- 8 12	- 18 67	- 11 42	- 26 83	29 16	S67W
4	7400	16.3	S57W	100	14.85	96 66	7394 17	25 63	237	241	- 12 43	- 22 42	23 85	- 49 25	54 72	S64W
5	7500	19.6	S61W	100	17.95	95 13	7489 3	30 82	241	239	- 15 87	- 26 42	- 39 72	- 75 67	85 46	S62W
6																
7																
8																
9																
10																
11																
12																
13																
14																
15																
16																
17																

\* AT POINT X1 (FOR KICK OFF POINT) ENTER VALUE OF ZERO FOR INCLINATION IN COLUMNS (B),(C),(E)  
COLUMNS (H) THROUGH (S) WILL ALSO BE ZERO.

\*\* AT POINT X2 (FIRST SURVEY STATION) ENTER AVERAGE VALUE FOR INCLINATION (E).  
USE ACTUAL SURVEY DIRECTION IN COLUMNS (J) AND (K).  
DO NOT USE AVERAGE AZIMUTH IN COLUMN (K) FOR CALCULATIONS AT POINT X2.

Fig. 8.20—Angle averaging method.

**Example 8.4.** Determine the trajectory coordinates for the corrected survey points given in Table 8.3.

**Solution.** Using the step-by-step procedure and the form depicted by Fig. 8.20, the solution is given as the filled-in values presented by Fig. 8.20.

### 8.3.3 Minimum Curvature Method

The minimum curvature method<sup>4</sup> uses the angles at  $A_1$  and  $A_2$  and assumes a curved wellbore over the course length  $D_2$  and not a straight line as shown by Fig. 8.21. Fig. 8.22 shows the curved course length and the two surveying stations  $A_1$  and  $A_2$ . This method includes the overall angle change of the drillpipe  $\beta$  between  $A_1$  and  $A_2$ . The overall angle, which is discussed and derived in Sec. 8.4, can be written for the minimum curvature method as

$$\cos \beta = \cos(\alpha_2 - \alpha_1) - \{\sin(\alpha_1) \sin(\alpha_2)[1 - \cos(\epsilon_2 - \epsilon_1)]\} \quad \dots (8.33)$$

As depicted in Fig. 8.21, the straight line segments  $A_1B + BA_2$  adjoin the curve segments  $A_1Q + QA_2$  at

Points  $A_1$  and  $A_2$ . It follows that

$$A_1Q = OA_1 \cdot \beta/2,$$

$$QA_2 = OA_2 \cdot \beta/2,$$

$$A_1B = OA_1 \cdot \tan(\beta/2),$$

$$BA_2 = OA_2 \cdot \tan(\beta/2),$$

and that

$$A_1B/A_1Q = \tan(\beta/2)/(\beta/2) = 2/\beta \tan(\beta/2)$$

and

$$BA_2/QA_2 = \tan(\beta/2)/(\beta/2) = 2/\beta \tan(\beta/2).$$

A factor of the straight line section vs. the curved section ratios is defined as  $F$ , where

$$F = 2/\beta_i \tan(\beta_i/2). \quad \dots (8.34)$$

If  $\beta$  is less than 0.25 radians, it is reasonable to set  $F = 1.0$ . Once  $F$  is known, the remaining north/south and

TABLE 8.2—TRAJECTORY COORDINATE DETERMINATION

Worksheet Letter	Value to be Obtained	Source or Equation for Obtaining Value
A	<i>Measured depth</i> : The actual length of the wellbore from its surface location to any specified station.	survey
$\alpha$	<i>Inclination angle</i> : The angle of the wellbore from the vertical.	survey
C	<i>Direction</i> : The direction of the course.	survey
D	<i>Course length</i> : The difference in measured depth from one station to another.	$A_x - A_{(x-1)}$
E	<i>Average inclination</i> : The arithmetic average of the inclination angles at the upper and lower ends of each course.	$\frac{\alpha_x + \alpha_{(x-1)}}{2}$
d	<i>Course vertical depth</i> : The difference in vertical depth of the course from one station to another.	(D) cos(E)
G	<i>True vertical depth</i> : The summation of the course vertical depths of an inclined wellbore.	$\Sigma(d)$
H	<i>Course departure</i> : The distance between two points that are projected onto a horizontal plane.	(D) sin(E)
$\epsilon$	<i>Survey azimuth</i> : The direction of a course measured in a clockwise direction from 0° to 360°; 0° is north.	survey, in degrees ( $\epsilon$ )
K	<i>Average azimuth</i> : The arithmetic average of the azimuths at the ends of the course.	$\frac{\epsilon_x + \epsilon_{(x-1)}}{2}$
L	<i>North/south course coordinate</i> : The course component displacement from one station to another; negative value = south.	(H) cos(K)
M	<i>East/west course coordinate</i> : The course component displacement from one station to another; negative value = west.	(H) sin(K)
N	<i>North/south total coordinate</i> : The summation of the course displacements in the north/south direction (south is negative).	$\Sigma(L)$
O	<i>East/west total coordinate</i> : The summation of the course displacements in the east/west direction (west is negative).	$\Sigma(M)$
P	<i>Total departure</i> : Shortest distance from vertical wellbore to each station point.	$\sqrt{(N)^2 + (O)^2}$
Q	<i>Departure direction</i> : The direction of vertical projection onto horizontal plane from station to surface location. Must take value calculated and put into proper quadrant. See sign convention below.	$\arctan \frac{(O)}{(N)}$

east/west coordinates and TVD can be calculated using the following equations.

$$M_i = (D_i/2)[\sin(\alpha_{i-1}) \cdot \sin(\epsilon_{i-1}) + \sin(\alpha_i) \cdot \sin(\epsilon_i)] \cdot F_i \quad (8.35)$$

$$L_i = D_i/2[\sin(\alpha_{i-1}) \cdot \cos(\epsilon_{i-1}) + \sin(\alpha_i) \cdot \cos(\epsilon_i)] \cdot F_i \quad (8.36)$$

$$D_i = D_i/2[\cos(\alpha_{i-1}) + \cos(\alpha_i)] \cdot F_i \quad (8.37)$$

The total departures and TVD are calculated using Eqs. 8.30 through 8.32.

Other calculation methods that have been commonly used are the balanced tangential method,<sup>2</sup> the radius of curvature method,<sup>3</sup> the mercury method,<sup>1</sup> acceleration method, trapezoidal method, and vector averaging method. It is interesting to note that the balanced tangential, trapezoidal, vector averaging, and acceleration methods, even though derived differently, yield the identical mathematical formulas for the north/south and east/west coordinates and TVD.

As to which method yields the most accurate results, Table 8.4 compares six of the different methods using data taken from a test hole. Note that the tangential method shows considerable error for M, L, and D. This is why the tangential method is no longer used. The differences among the average angle, the minimum curvature, and the balanced tangential methods are so small that any of the methods could be used for calculating the trajectory.

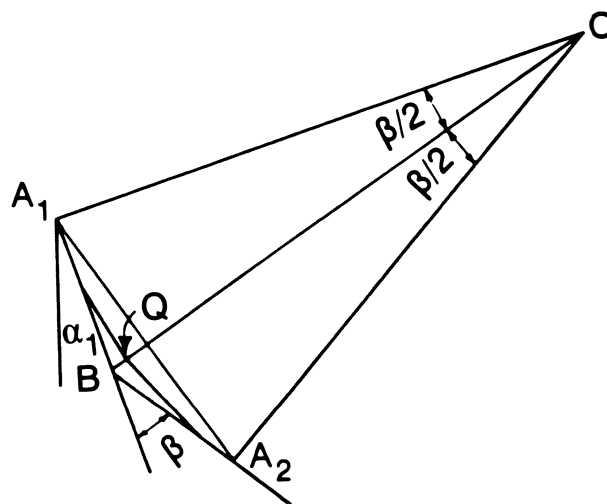


Fig. 8.21—Representation of minimum curvature ratio factor,  $F$ .

TABLE 8.3—DATA FOR EXAMPLE 8.4

$D_M$ (ft)	Inclination Angle (degrees)	Direction Angle
7,100	0	0
7,200	10.1	S68W
7,300	13.4	S65W
7,400	16.3	S57W
7,500	19.6	S61W

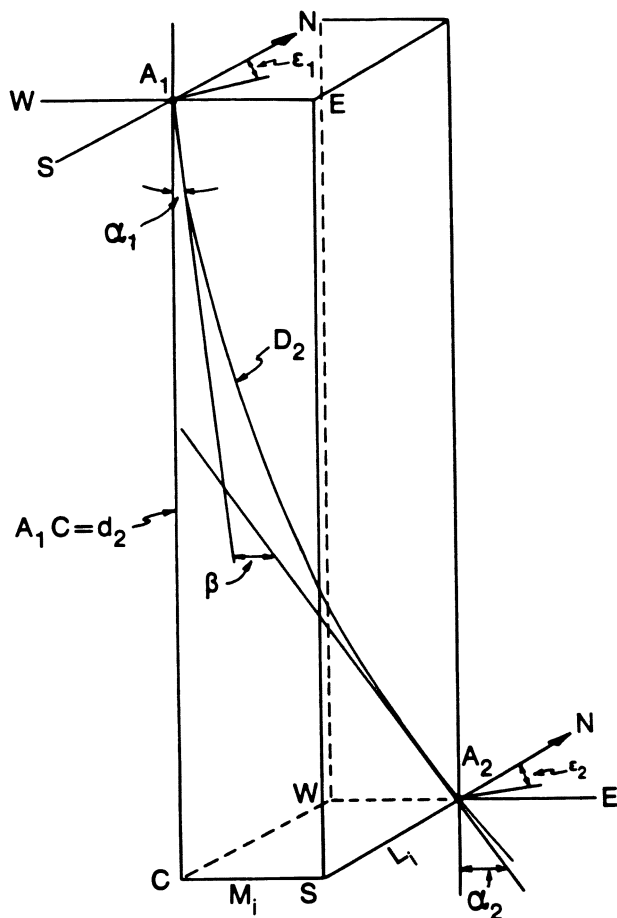


Fig. 8.22—A curve representing a wellbore between Survey Stations  $A_1$  and  $A_2$ .

It will be shown in Sec. 8.5 that the systematic errors overpower the variation in the survey calculation differences when comparing the multistation surveying methods.

With the advent of the programmable hand calculator, the minimum curvature method has become the most common.

## 8.4 Planning the Kickoff and Trajectory Change

In kicking off a well, setting the lead angle, or making a controlled trajectory change, some method must be used to force the bit in the desired direction. The first tool used to deflect the bit was a simple whipstock (Fig. 8.23a). Later, mud motors equipped with bent subs or bent housings were introduced (Fig. 8.23b), as well as jetting bits (Fig. 8.23c). These deflection tools are discussed in detail in Sec. 8.6. This section explains how to control a change in direction and inclination angle to achieve a change in trajectory.

All deflection methods depend on manipulating the drillpipe (rotation and downward motion) to cause a departure of the bit in either the direction plane or the inclination plane, or both. In Fig. 8.24, showing a drillstring with a deflection sub, an arrow indicates the direction the sub will cause the drillstem to face—the toolface direction. The magnitude of the deflection is controlled by the depar-

ture from the centerline of the deflecting tool. This includes the angle of the whipstock toe, bent sub, and the nozzle offset in a jetting bit.

### 8.4.1. Orientation of the Bit

For years the common ways to design a bit orientation were to refer to a “Ouija Board” (see Fig. 8.25) and to use tables of values relating the deflection-sub offset to a particular orientation. Later, Millheim *et al.*<sup>5</sup> demonstrated how to derive the equations necessary to design and analyze a kickoff and trajectory change.

Fig. 8.26 depicts the three-dimensional deflection of the course of a wellbore. At a measured depth (a), an inclination  $\alpha$  and direction  $\epsilon$  are measured. With a deflecting device, the course is to be deflected to a new inclination angle,  $\alpha_N$ , and a new direction,  $\epsilon_N$ . This will cause an overall angle change,  $\beta$ , which is directly related to what is called “dogleg severity.” If the wellbore in Fig. 8.26 were not deflected, it would continue on its present course to Point b. Deflected, the wellbore will follow the new desired course in Plane A to Point c or d.

### 8.4.2 Derivation of the Direction Change, $\Delta\epsilon$

The three-dimensional geometrical representation of the trajectory is presented in Fig. 8.27, where the wellbore is deflected at Point O. A vertical plane is projected through Points MOCEM' (see Fig. 8.28), normal to the horizontal plane O'A'B'E, and tending in a southeast direction. The plane cutting through DAB is parallel to the plane cutting MOCEM'. Lines AA', BB', and ODO' are vertical and parallel. If Line MOC is rotated 360°, it will transcribe a circle of radius  $r$ . Fig. 8.29 represents the circle cutting through Plane ACE with a rotation angle  $\gamma$  and normal to Planes OCE, OCA, etc.

The change in direction,  $\Delta\epsilon$ , shown by Fig. 8.27 is the angle of Triangle A'O'B', where

$$\tan \Delta\epsilon = \frac{A'B'}{O'B'} = \frac{AB}{O'E + EB'} \quad (8.38)$$

Fig. 8.29 shows the rotation of Line EA (radius  $r$ ) from Point A to Point B and transcribes an angle  $\gamma$ . It follows that

$$AB = r \sin \gamma.$$

TABLE 8.4—COMPARISON OF ACCURACY OF VARIOUS CALCULATION METHODS (after Craig and Randall<sup>1</sup>)

Direction:	Due north			
Survey interval:	100 ft			
Rate of build:	3°/100 ft			
Total inclination:	60° at 2,000 ft			
Calculation Method	Total Vertical Depth. Difference From Actual (ft)		North Displacement. Difference From Actual (ft)	
Tangential	1.628 61	- 25 38	998.02	+ 43.09
Balanced tangential	1.653 61	- 0.38	954.72	- 0.21
Angle-averaging	1.654 18	+ 0.19	955.04	+ 0.11
Radius of curvature	1.653.99	0.0	954.93	0.0
Minimum curvature	1.653.99	0.0	954.93	0.0
Mercury*	1.153 62	- 0 37	954.89	0.04

\* Fifteen-foot survey tool

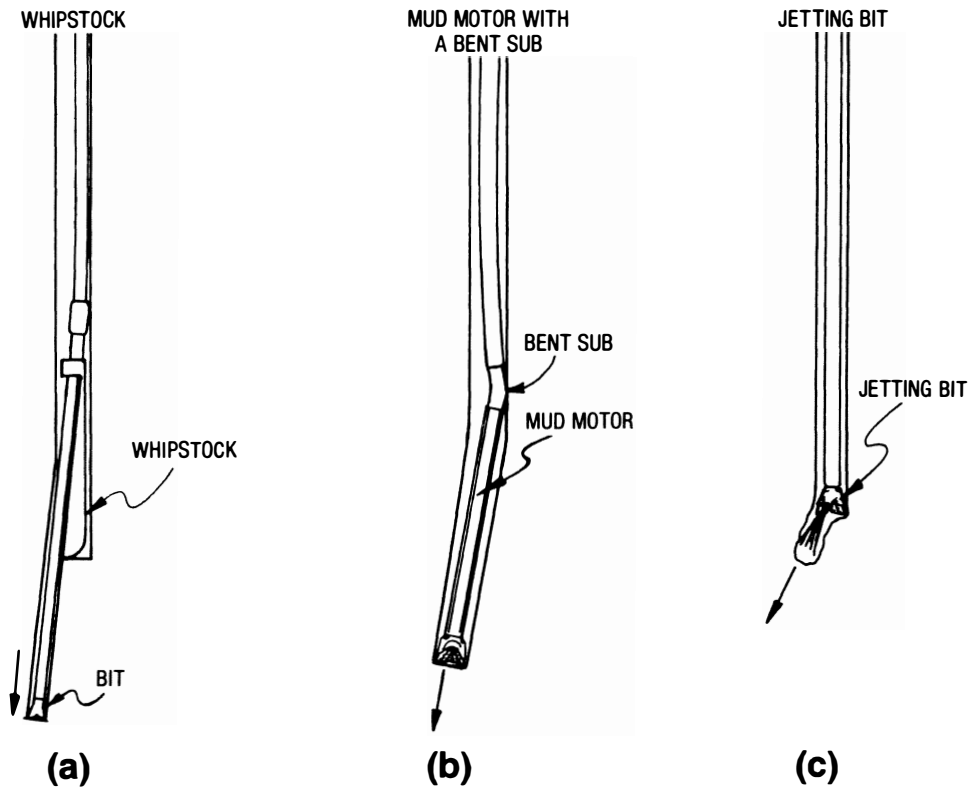


Fig. 8.23—Techniques for making a positive direction change.

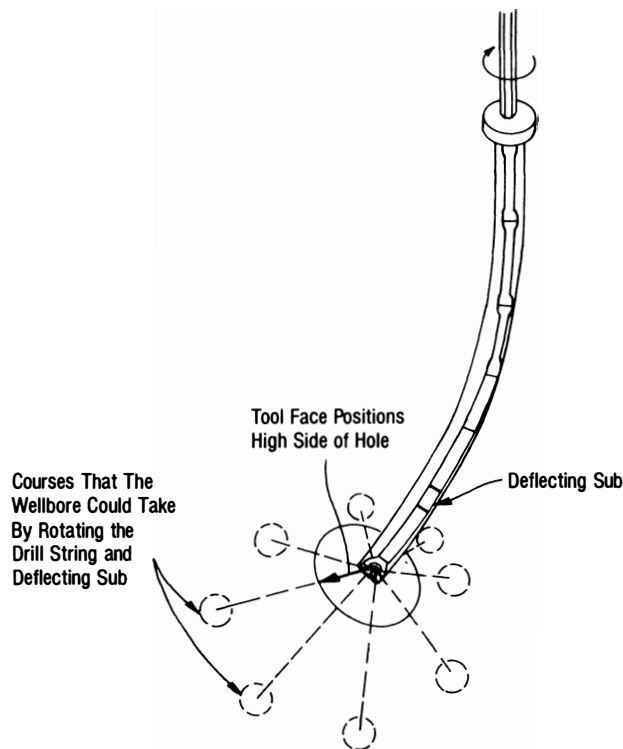


Fig. 8.24—System for deflecting the wellbore trajectory.

The next step is to determine relationships in terms of OE and EB. Triangle EBB' (Fig. 8.28) relates EB' to the angle  $\alpha$  as

$$EB' = EB \cos \alpha, \dots\dots\dots (8.39)$$

and from Triangle EAB (Fig. 8.29), EB is related to angle  $\gamma$ :

$$EB = r \cos \gamma.$$

Substituting EB in Eq. 8.39 forms Eq. 8.40:

$$EB' = r \cos \gamma \cos \alpha. \dots\dots\dots (8.40)$$

To determine O'E, consider Triangles OEC and OO'E, where

$$r = \ell \tan \beta \text{ (Fig. 8.28)}$$

and

$$O'E = \ell \sin \alpha.$$

Substituting these last two relationships for terms AB, O'E, and EB' into Eq. 8.38 and eliminating  $r$  yields

$$\tan \Delta\epsilon = \frac{\tan \beta \sin \gamma}{\sin \alpha + \tan \beta \cos \alpha \cos \gamma} \dots\dots\dots (8.41)$$

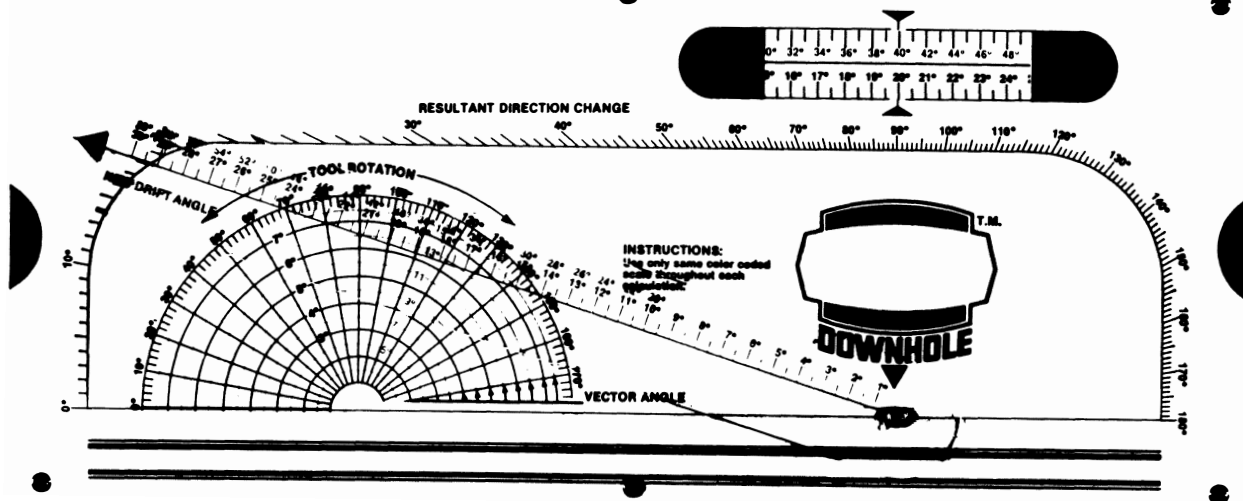


Fig. 8.25—Directional drilling Ouija Board.

and

$$\Delta\epsilon = \arctan \frac{\tan \beta \sin \gamma}{\sin \alpha + \tan \beta \cos \alpha \cos \gamma} \quad \dots \dots (8.42)$$

The overall angle change,  $\beta$ , is directly related to dogleg severity,  $\delta$ , by the following relationship.

$$\delta = \frac{\beta}{L_C}(i), \quad \dots \dots (8.43)$$

where  $L_C$  is the course length between the measured surveys and  $i$  is the index of angle change. For example, if  $i$  is 100,  $\delta$  could be degrees/100 meters if course length is reported in meters, or  $\delta$  could be degrees/100 ft if course length is in feet.

**Example 8.5.** Determine the new direction for a whipstock set at 705 m with a tool-face setting of  $45^\circ$  right of high side for a course length of 10 m. The inclination

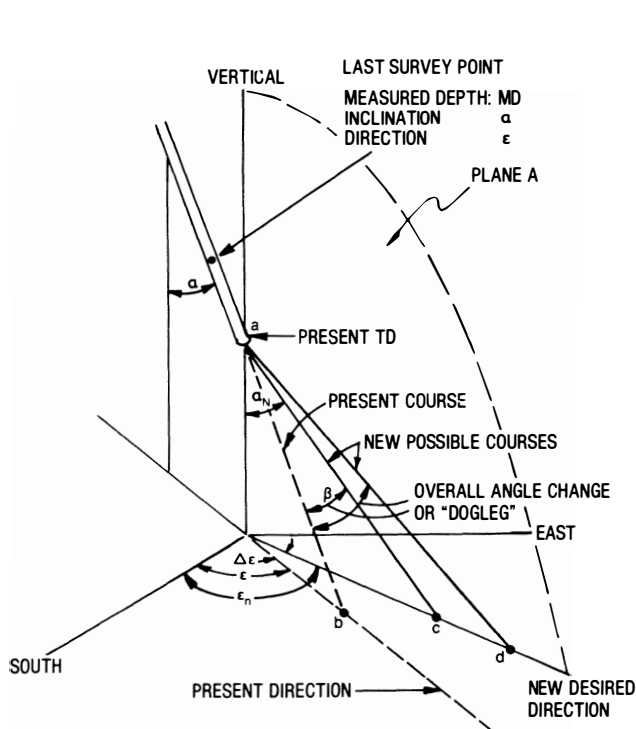


Fig. 8.26—Three-dimensional deflection of the course of a bore-hole (after Millheim et al. <sup>5</sup>).

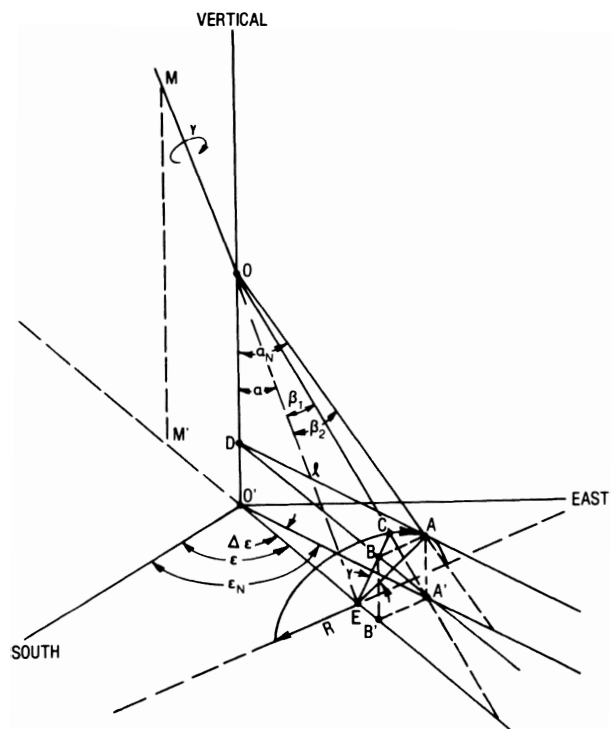


Fig. 8.27—Three-dimensional trajectory change model (after Millheim et al. <sup>5</sup>).



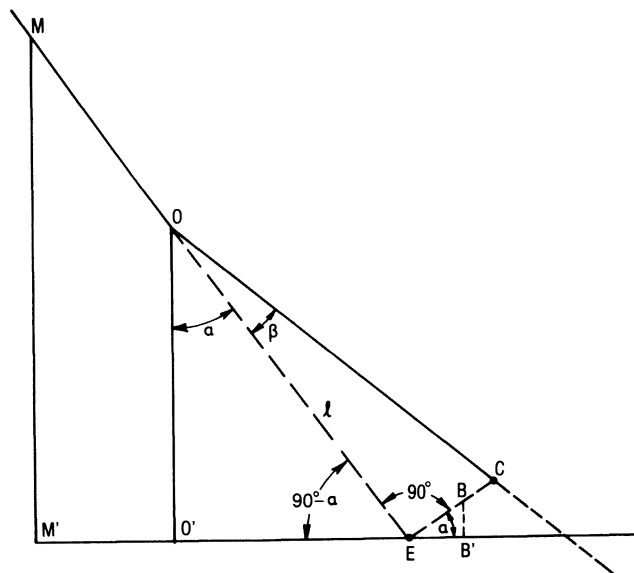


Fig. 8.28—Vertical plane through MOCEM' (after Millheim et al.<sup>5</sup>).

is  $7^\circ$  and the direction is N15W of 705 m. The curve of the whipstock will cause a total angle change of  $3^\circ/30$  m over a course length.

**Solution.** The overall angle change,  $\beta$ , can be determined from Eq. 8.43:

$$\beta = \frac{\delta L_C}{i} = \frac{3^\circ 10 \text{ m}}{30 \text{ m}} = 1^\circ,$$

and the direction change can be calculated using Eq. 8.42:

$$\begin{aligned} \Delta\epsilon &= \arctan \frac{\tan(1) \sin(45)}{\sin(7) + \tan(1) \cos(7) \cos(45)} \\ &= \arctan 0.09199 = 5.3^\circ. \end{aligned}$$

If  $\beta$  is right of high side of the hole, the new direction,  $\epsilon_N$ , is  $\epsilon + \Delta\epsilon$ ; and if the tool-face setting is left of high,  $\epsilon_N = \epsilon - \Delta\epsilon$ . Therefore, in this example, the new direction is

$$\epsilon_N = 345^\circ + 5.3^\circ = 350.3^\circ \text{ or } \text{N}9.7\text{W}.$$

#### 8.4.3 Derivation of the New Inclination Angle, $\alpha_N$

The new inclination angle,  $\alpha_N$ , can be derived by considering Triangle AOD in Plane OAA'O' (Fig. 8.27):

$$\begin{aligned} \cos \alpha_N &= \frac{OD}{OA} = \frac{OO' - O'D}{OA} = \frac{OO' - AA'}{OA} \\ &= \frac{OO' - BB'}{OA}. \end{aligned} \quad (8.44)$$

Using Triangles OO'E and EB'E (Fig. 8.28), the inclination angle,  $\alpha$ , can be obtained from

$$OO' = l \cos \alpha$$

and

$$BB' = EB \sin \alpha.$$

Substituting for EB in the above equation yields

$$BB' = r_l \cos \gamma \sin \alpha.$$

Triangles AOE and COE are equal, and AO equals OC. From Triangle AOE,

$$OA = OC = \frac{l}{\cos \beta}.$$

Substituting for OA, OO', and BB' in Eq. 8.44 yields

$$\cos \alpha_N = \cos \alpha \cos \beta - \sin \alpha \sin \beta \cos \gamma \quad (8.45)$$

and

$$\alpha_N = \arccos(\cos \alpha \cos \beta - \sin \alpha \sin \beta \cos \gamma), \quad (8.46)$$

where

$$\Delta\alpha = \alpha_N - \alpha. \quad (8.47)$$

#### 8.4.4 Derivation of the Tool-Face Angle, $\gamma$

The tool-face angle,  $\gamma$ , can be calculated by rearranging Eq. 8.45 if the initial and final inclination angles and the overall angles are known or set as desired values.

$$\gamma = \arccos \left( \frac{\cos \alpha \cos \beta - \cos \alpha_N}{\sin \alpha \sin \beta} \right). \quad (8.48)$$

The tool-face angle also can be calculated if the final inclination, direction change, and overall angle change are known or selected as desired values.

$$\gamma = \arcsin \left( \frac{\sin \alpha_N \sin \Delta\epsilon}{\sin \beta} \right). \quad (8.49)$$

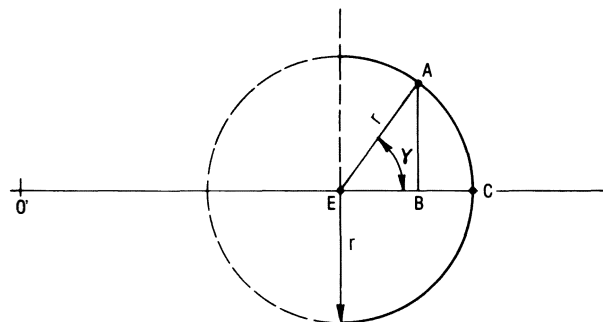


Fig. 8.29—Tool-face plane (after Millheim et al.<sup>5</sup>).

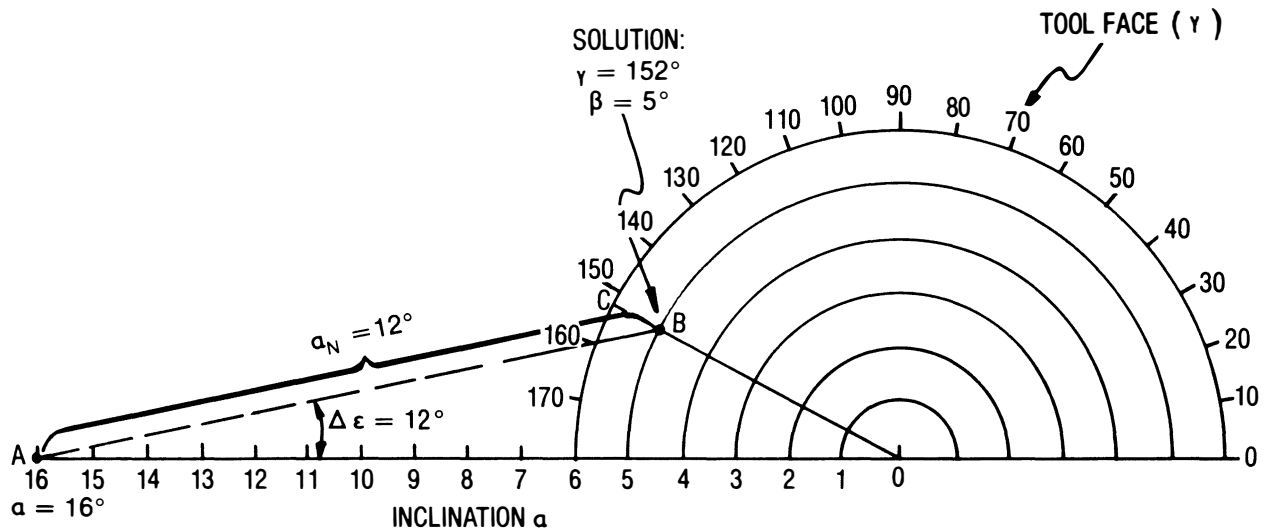


Fig. 8.30—Graphical Ouija analysis.

Eqs. 8.42, 8.46, 8.48, and 8.49 can be used to determine the direction change ( $\Delta\epsilon$ ), new inclination ( $\alpha_N$ ), overall angle change ( $\beta$ ), and tool-face angle ( $\delta$ ).

#### 8.4.5 Derivation of the Ouija Board Nomograph

A graphic technique that is the basis of the Ouija Board type of nomograph (Fig. 8.30) can be used to determine the same parameters as from the derived equations for  $\alpha_N$ ,  $\Delta\epsilon$ ,  $\beta$ , and  $\gamma$  for the condition where the value of the overall angle,  $\beta$ , is small—i.e., less than  $6^\circ$ . By specifying the small angle condition, the following identities can be written.

$$\cos \beta \approx 1,$$

$$\sin \beta \approx \beta \text{ (radians)},$$

and

$$\tan \beta \approx \beta \text{ (radians)}.$$

Substituting the identities into Eq. 8.42 and Eq. 8.45 yields the following relationships.

$$\Delta\epsilon = \arctan \frac{\beta \sin \gamma}{\sin \alpha + \beta \cos \alpha \cos \gamma}, \dots \dots \dots (8.50)$$

$$\beta = \frac{\cos \alpha - \cos \alpha_N}{\sin \alpha \cos \gamma}, \dots \dots \dots (8.51)$$

and

$$\gamma = \arcsin \left[ \frac{1 - \cos \alpha \cos \alpha_N}{\beta \sin \alpha} \tan(\Delta\epsilon) \right]. \dots \dots \dots (8.52)$$

In the nomograph (Fig. 8.30), the abscissa is the original inclination angle (except when  $\Delta\epsilon = 0$  and  $\beta = 0$ , in which case  $\alpha = \alpha_N$ ). The angle between the abscissa and

Line AB is  $\Delta\epsilon$ ; the point at which Line  $0^\circ B$  is projected through the outer semicircle at C is read as the tool-face angle,  $\gamma$ , left or right of high side. The number of degrees traversed by Line  $0^\circ B$  is the overall angle change,  $\beta$ . Line AB is the new inclination angle,  $\alpha_N$ .

The values in Fig. 8.30 are  $\alpha(0^\circ A) = 16^\circ$ ,  $\alpha_N(AB) = 12^\circ$ ,  $\gamma(C) = 152^\circ$ , and  $\beta(0^\circ B) = 5^\circ$ .

A nomograph like Fig. 8.30 can be created by drawing a scale of degrees (at increments of, say,  $\frac{1}{4}$  in. per degree) on the abscissa to represent the number of degrees in the original inclination angle, in this case  $16^\circ$ . The degrees decrease to zero from left to right. Placing the needle of the compass at  $0^\circ$ , draw enough  $1^\circ$  concentric semicircles to equal the degrees in  $\beta$  (in this case,  $6^\circ$ ). With a protractor, scale the outer semicircle from  $0^\circ$  (right) to  $180^\circ$  (left) in  $10^\circ$  increments.

**Example 8.6.** Determine where to set the tool face (the tool-face angle,  $\gamma$ ) for a jetting bit to go from a direction of  $10^\circ$  to  $30^\circ$  and from an inclination of  $3^\circ$  to  $5^\circ$ . Also calculate the dogleg severity,  $\delta$ , assuming that the trajectory change takes 60 ft.

**Solution.** Scale  $3^\circ$  on the abscissa. At the  $3^\circ$  mark (Point A), measure  $\Delta\epsilon$ , which is  $20^\circ$ ; from Point A, project the  $\alpha_N$  line 5° units of length. The end of the line is Point B. Draw a line from  $0^\circ$  to Point B (this line is equal to  $\beta$ ). Continue Line  $0^\circ B$  to C to find the tool-face setting:  $45^\circ$ . Fig. 8.31 depicts the graphical solution.

$$\delta = \frac{\beta}{L_c} i = \frac{2.4^\circ}{60 \text{ ft}} 100 \text{ ft} = 4.00^\circ / 100 \text{ ft}.$$

**Example 8.7.** Using the data of Example 8.6, calculate the tool-face setting and the dogleg severity.

**Solution.** Since Eq. 8.41 is in terms of  $\beta$ , which is an unknown, and Eqs. 8.48 and 8.49 are in terms of  $\gamma$ , it is necessary to rearrange the equations in terms of  $\alpha$ ,  $\alpha_N$ ,

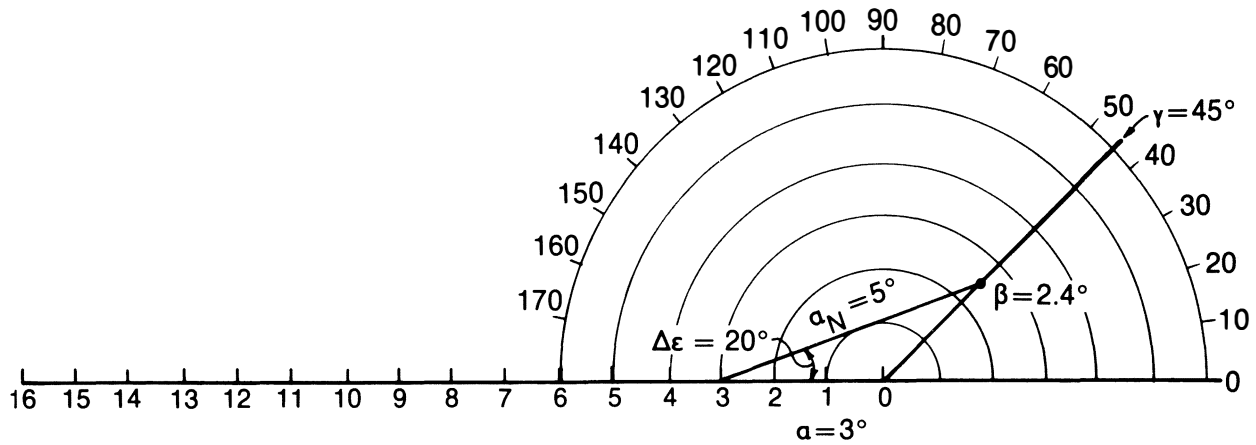


Fig. 8.31—Solution to Example 8.6.

and  $\Delta\epsilon$  only. By combining Eq. 8.41 with Eqs. 8.48 and 8.49 in terms of  $\sin \gamma$  and  $\cos \gamma$  and doing some manipulations, the total angle change,  $\beta$ , can be written in terms of only  $\Delta\epsilon$ , and  $\alpha$  and  $\alpha_N$ .

$$\beta = \arccos(\cos \Delta\epsilon \sin \alpha_N \sin \alpha + \cos \alpha \cos \alpha_N), \quad \dots \dots \dots (8.53)$$

or, in another form,

$$\cos \beta = \cos \Delta\epsilon \sin \alpha_N \sin \alpha + \cos \Delta\alpha - \sin \alpha \sin \alpha_N. \quad \dots \dots \dots (8.54)$$

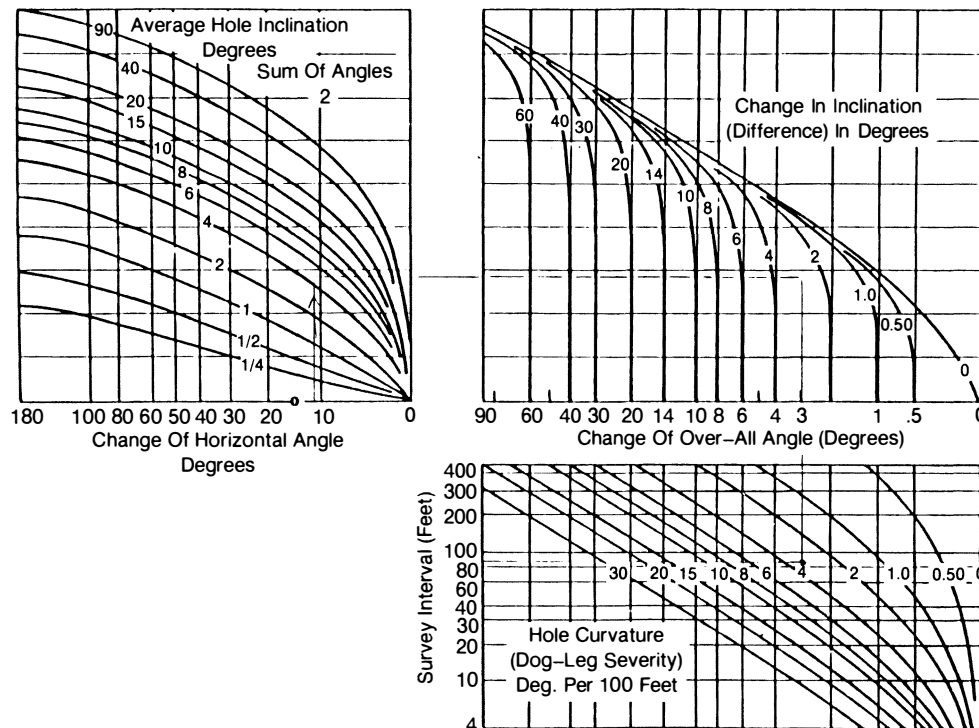
For Example 8.7,  $\Delta\epsilon = 20^\circ$ ,  $\alpha = 3^\circ$ ,  $\alpha_N = 5^\circ$ , and  $\Delta\alpha = 2^\circ$ .

$$\beta = \arccos[\cos(20) \sin(5) \sin(3) + \cos(3) \cos(5)] = 2.4^\circ.$$

#### 8.4.6 Overall Angle Change and Dogleg Severity

Eq. 8.55 derived by Lubinski<sup>6</sup> is used to construct Fig. 8.32, a nomograph for determining the total angle change,  $\beta$ , and the dogleg severity,  $\delta$ .

$$\beta = 2 \arcsin \sqrt{\sin^2 \left( \frac{\Delta\alpha}{2} \right) + \sin^2 \left( \frac{\Delta\epsilon}{2} \right) \sin^2 \left( \frac{\alpha + \alpha_N}{2} \right)}. \quad \dots \dots \dots (8.55)$$

Fig. 8.32—Chart for determining dogleg severity (after Lubinski<sup>6</sup>).

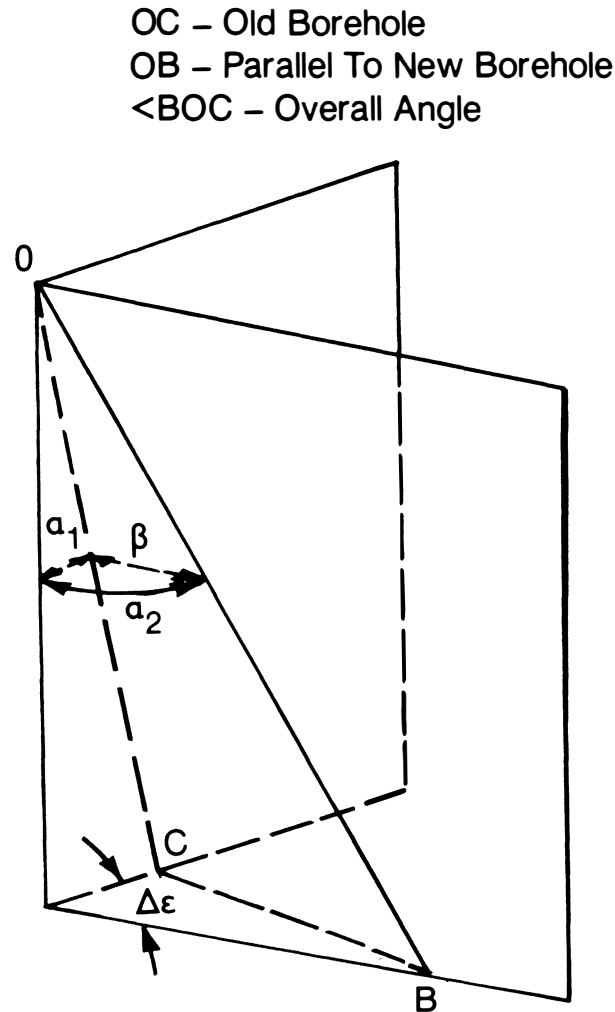


Fig. 8.33—Basis of chart construction is a trigonometric relationship illustrated by two intersecting planes (after Lubinski<sup>6</sup>).

The overall angle,  $\beta$ , calculated by Eq. 8.51, is the same as calculated by Eq. 8.50. However, Lubinski originally derived Eq. 8.51, which is based on measuring two consecutive sets of inclination and direction and is not concerned with the tool-face setting. Fig. 8.33 depicts the geometric basis for the derivation of the total angle change,  $\beta$ .

**Example 8.8.** Determine the dogleg severity following a jetting run where the inclination was changed from  $4.3^\circ$  to  $7.1^\circ$  and the direction from N89E to S80E over a drilled interval of 85 ft.

**Solution.** Using Eq. 8.55, the total angle change is

$$\beta = 2 \arcsin \sqrt{\sin^2 \left( \frac{2.8}{2} \right) + \sin^2 \left( \frac{11}{2} \right) \sin^2 \left( \frac{7.1 + 4.3}{2} \right)}$$

$$= 3.0^\circ,$$

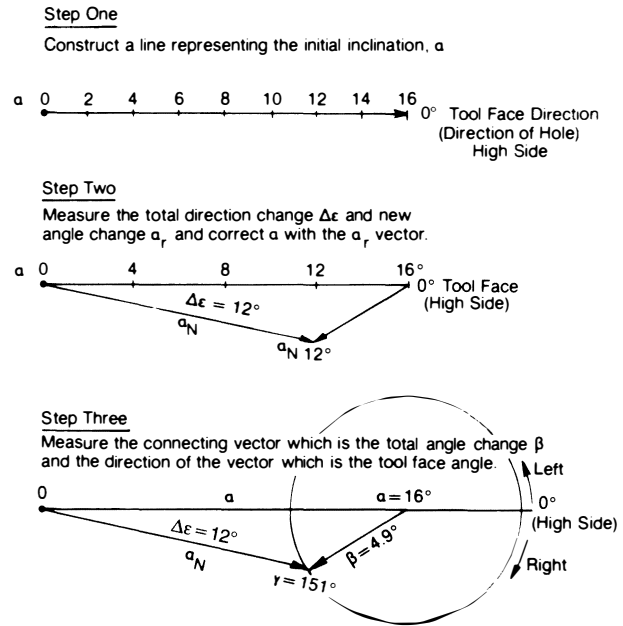


Fig. 8.34—Example solution using the Ragland diagram.

and using Eq. 8.53, the total angle change is

$$\beta = \arccos[\cos(11) \sin(7.1) \sin(4.3) + \cos(4.3) \cos(7.1)] = 2.99^\circ.$$

Using the nomograph given in Fig. 8.32, the change of horizontal angle is  $100^\circ - 89^\circ = 11^\circ$ , and the sum of the inclination divided by 2.0 is  $5.7^\circ$ . The change in inclination is  $2.8^\circ$ , yielding a total angle change,  $\beta$ , of  $3.0^\circ$  and a dogleg severity of  $3.5^\circ/100$  ft. Using Eq. 8.40, the dogleg severity calculates

$$\delta = \frac{2.99^\circ(100)}{85 \text{ ft}} = \frac{3.5^\circ}{100 \text{ ft}}.$$

#### 8.4.7 The Ragland Diagram

Another way of solving the trajectory change problem is by using what is called the Ragland diagram.<sup>7</sup> The method is essentially similar to the Ouija Board nomograph in that a graphical process is used to solve for the unknown parameters. Fig. 8.34 shows the steps using the Ragland diagram to solve for the same problem as presented by Fig. 8.30 using the Ouija Board solution.

The first step is to construct a vector that represents the length of the initial inclination,  $\alpha$ . This vector always represents the direction of the hole,  $\epsilon$ , and is the high side ( $0^\circ$  tool face) of the hole. For this particular case,  $\alpha_N$  and  $\Delta\epsilon$  are given as well as the initial inclination. The unknowns are the total angle change and tool-face setting. To find these unknowns, the new inclination vector  $\alpha_N$  is drawn from the  $0^\circ$  origin at a direction change of  $\Delta\epsilon = 12^\circ$ . The total angle change  $\beta$  is determined by connecting the  $\alpha$  and  $\alpha_N$  vectors and measuring the length of the  $\beta$  vector. In this example it is approximately  $4.9^\circ$ . The last step is to draw a circle around the origin point

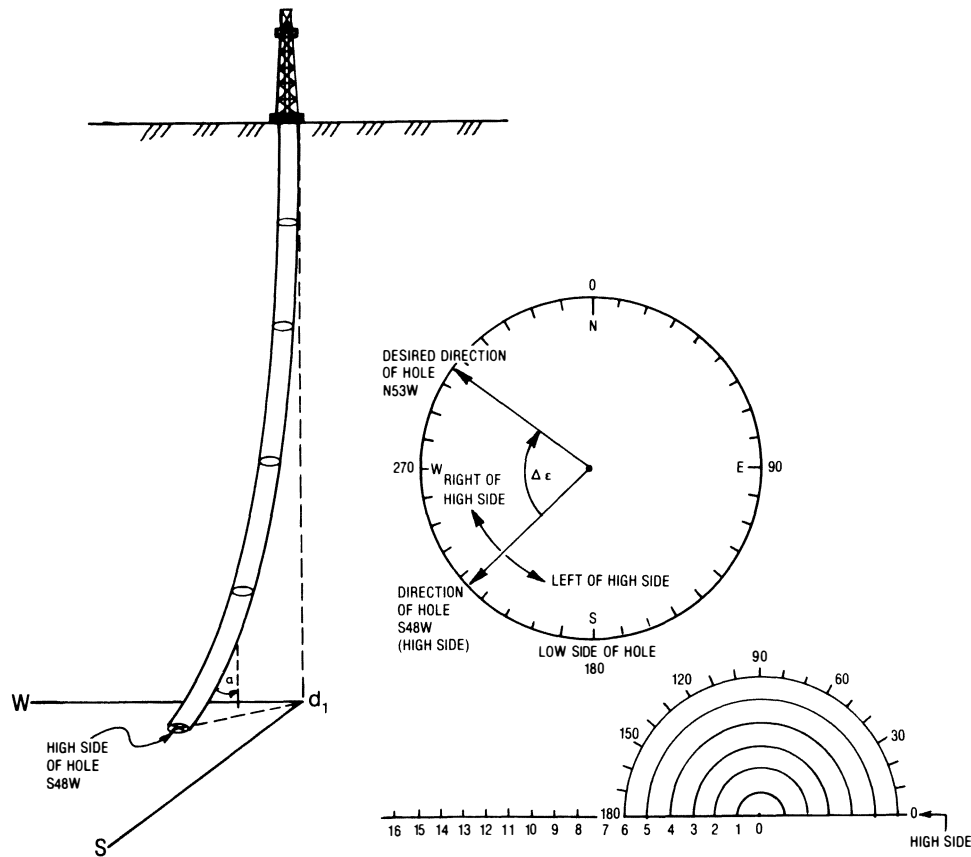


Fig. 8.35—Example of high side of wellbore showing how it corresponds to a Ouija diagram.

where  $\alpha = 16^\circ$ , and measure with a protractor the tool-face angle,  $\gamma$ . In the example,  $\gamma = 151^\circ$  and is right of the high side. For example, this case would represent a direction change from N40E to N52E where N40E is the original direction of the hole. However, if the direction change that is desired is N28E, the  $\alpha_N$  vector would be drawn above the  $\alpha$  vector, making the tool-face setting on the left of the high side.

Like the Ouija solution, the Ragland vector analysis uses any three knowns to solve for two unknowns. In Figs. 8.30 and 8.33,  $\alpha$ ,  $\alpha_{N1}$ , and  $\Delta\epsilon$  are knowns.  $\beta$  and  $\gamma$  are unknowns.

#### 8.4.8 Planning a Trajectory Change and Compensating for Reverse Torque of a Mud Motor

A kickoff or trajectory change is designed according to which of these plans is desired: (1) maximum build or drop without any direction change, (2) maximum direction change to the right or left of high side with no inclination change, (3) build with direction change to the right or left of high side, and (4) drop with direction change to the right or left of high side.

The design also depends on whether a jetting bit is used, or a mud motor with a bent sub or bent housing. Except in special circumstances, openhole whipstocks are seldom used to kick off or change a trajectory. They are mainly used now to kick off or sidetrack out of casing. This is discussed in Sec. 8.5.

Fig. 8.35 depicts a wellbore at a depth  $D_1$  where it is desired to build angle from  $\alpha$  to  $\alpha_N$  and to change the direction from S48W to N53W. The high side of the hole

at depth  $D_1$  is S48W. (The high side is defined as the direction of the wellbore and opposite the gravity side or low side of the wellbore.) Changing the direction of the wellbore will require some type of deflection technique whereby resetting the face of the deflecting tool will cause the wellbore to rotate to the right (clockwise) to a new direction of N53W. If a jetting bit is used to change direction, the tool-face angle can be calculated directly without any other corrections. However, if a bent sub or housing is used in combination with a mud motor, a correction must be made to compensate for reverse torque. When a mud motor in a borehole is activated and starts to drill, the tool face will always rotate to the left by some amount, depending on a number of factors that are discussed in Sec. 8.5. The left rotation, or reverse torque, must be compensated for by reorienting the tool face enough to offset the reverse torque effects.

The rotation of the drillstring because of the bit face torque can be estimated using Eq. 8.56:

$$\theta_M = \frac{ML_{\text{motor}}}{G_{\text{motor}}J_{\text{motor}}} + \frac{ML_{\text{BHA}}}{G_{\text{BHA}}J_{\text{BHA}}} + \frac{ML_{\text{drillstring}}}{G_{\text{drillstring}}J_{\text{drillstring}}} \dots \dots \dots (8.56)$$

and

$$J = \frac{\pi}{32}(\text{OD}^4 - \text{ID}^4)(\text{in.}^4),$$

where  $M$  is the torque generated at the bit and  $L$  is the length of any drillstring section ( $L_{\text{motor}}$  is length of motor and  $L_{\text{BHA}}$  is the length of the bottomhole assembly).  $G$  is the shear modulus of each drillstring element, and  $J$  is the polar moment of inertia.

Furthermore, the BHA and the drillstring could be subdivided according to different size drill collars, stabilizers, and drillpipe, and

$$\theta_M = M \sum \frac{L_i}{G_i J_i} \quad \dots \dots \dots (8.57)$$

**Example 8.9.** Calculate the total angle change of 3,650 ft of 4½-in. [3.826-in. ID] Grade E 16.60-lbm/ft drillpipe and 300 ft of 7-in. drill collars [2⅓-in. ID] for a bit-generated torque of 1,000 ft-lbf. Assume that the motor has the same properties as the 7-in. drill collars. Use the shear modulus of steel ( $G = 11.5 \times 10^6$  psi) for the BHA and drillstring. Calculate the total angle change if 7,300 ft of drillpipe was used.

**Solution.**

$$\begin{aligned} \theta &= \frac{M}{11.5 \times 10^6 \text{ psi}} \left( \frac{43,800 \text{ in.}}{19.2} + \frac{3,600 \text{ in.}}{229.6} \right) \\ &= 1.997 \times 10^{-4} M = 1.997 \times 10^{-4} \frac{1}{\text{in. lbm}} \\ &\times (1,000 \text{ ft-lbf}) \left( \frac{12 \text{ in.}}{\text{ft}} \right) = 2.396, \\ \theta_{1,000} &= \frac{2.396}{2\pi} 360^\circ = 137.3^\circ, \\ \theta_{(\text{long drillpipe})} &= 3.96 \times 10^{-4} \frac{1}{\text{in. lbm}} (1,000 \text{ ft-lbf}) \\ &\times \left( \frac{12 \text{ in.}}{\text{ft}} \right), \\ \theta &= \frac{4.772}{2\pi} (360) = 273.4^\circ. \end{aligned}$$

Example 8.9 shows that the longer the drillstring the more the bit face torque causes the drillstring to rotate. (In the case of drilling with a motor, the reactive torque is counterclockwise or to the left.)

Eq. 8.57 does not include the friction caused by the bent sub or any other part of the drillstring, especially at higher inclinations where drillstring friction can be considerable. However, at shallower depths (<3,000 ft) where the wellbore is at a low inclination (1 to 5°), Eq. 8.57 can give a first approximation for the amount of reverse torque

compensation that is needed. This calculation also requires a knowledge of bit face torque, which is discussed in Sec. 8.5.

The most foolproof way to compensate for the reverse torque problem is to run, right above the bent sub, a surface-indicating measuring tool that transmits the tool-face position frequently. Without relying on the calculational technique or guesswork, one can rotate the drillpipe dynamically to compensate for the reverse torque. If the surface recording system is not used, one must run a conventional single shot to orient the tool face making sure to correct for the reverse torque. For deeper kick-offs where it is difficult to estimate the amount of compensation for the reverse torque, for expensive drilling operations, and when in doubt, some type of surface-indicating tool-face monitor should be used.

**Example 8.10.** Plan a kickoff for the wellbore in Fig. 8.35 where the depth at kickoff is 2,560 ft, the direction at kickoff is S48W, the course length is 150 ft, and the inclination is 2°, and determine the dogleg severity. It is desired to set the direction at N53W to increase the inclination to 6°. Assume that the mud motor at this depth and inclination has 20° of reverse torque.

**Solution.** Using the graphic technique exemplified in Fig. 8.35, arrive at the following values:  $\Delta\epsilon = 79^\circ$ ,  $\alpha = 2^\circ$ ,  $\alpha_N = 6^\circ$ ,  $\gamma = 97^\circ$ , and  $\beta = 5.8^\circ$ . This is the calculation for the dogleg severity:

$$\delta = \frac{5.8}{150} \times 100 = 3.87^\circ/100 \text{ ft.}$$

Since it is desired to turn the well clockwise (right of high side) and the reverse torque will be 20° to the left, the actual tool-face setting must be  $97^\circ + 20^\circ$ , or  $117^\circ$  right of high side (N15W or 345°). If the correction for the reverse torque is not included, the dynamic tool face setting would be at  $97^\circ$  right of high side and the desired new direction and inclination would be incorrect. Fig. 8.36 shows the graphical solution and the correction for the reverse torque of the motor.

Example 8.10 shows one way to calculate the kickoff using a mud motor and bent sub or housing where the primary factors are the direction and inclination changes. The residual dogleg severity is a result of making the trajectory change. Changing the trajectory without regard for the dogleg severity can cause serious problems in running the BHA through the dogleg; it also can cause casing wear and later production problems. Better, by far, is to determine a maximum tolerable dogleg and to design the trajectory change accordingly. The easiest way to do this is to control the course length. If in Example 8.10 the course length is 50 ft, the dogleg severity is  $11.61^\circ/100$  ft, whereas if the course length were 200 ft, the dogleg severity would be only  $2.9^\circ/100$  ft. Once  $\beta$  is fixed, only a limited change in direction and inclination can be achieved for a given course length. If no direction change is desired, the tool face can be oriented to the high or low side of the hole and maximum inclination change can be made.

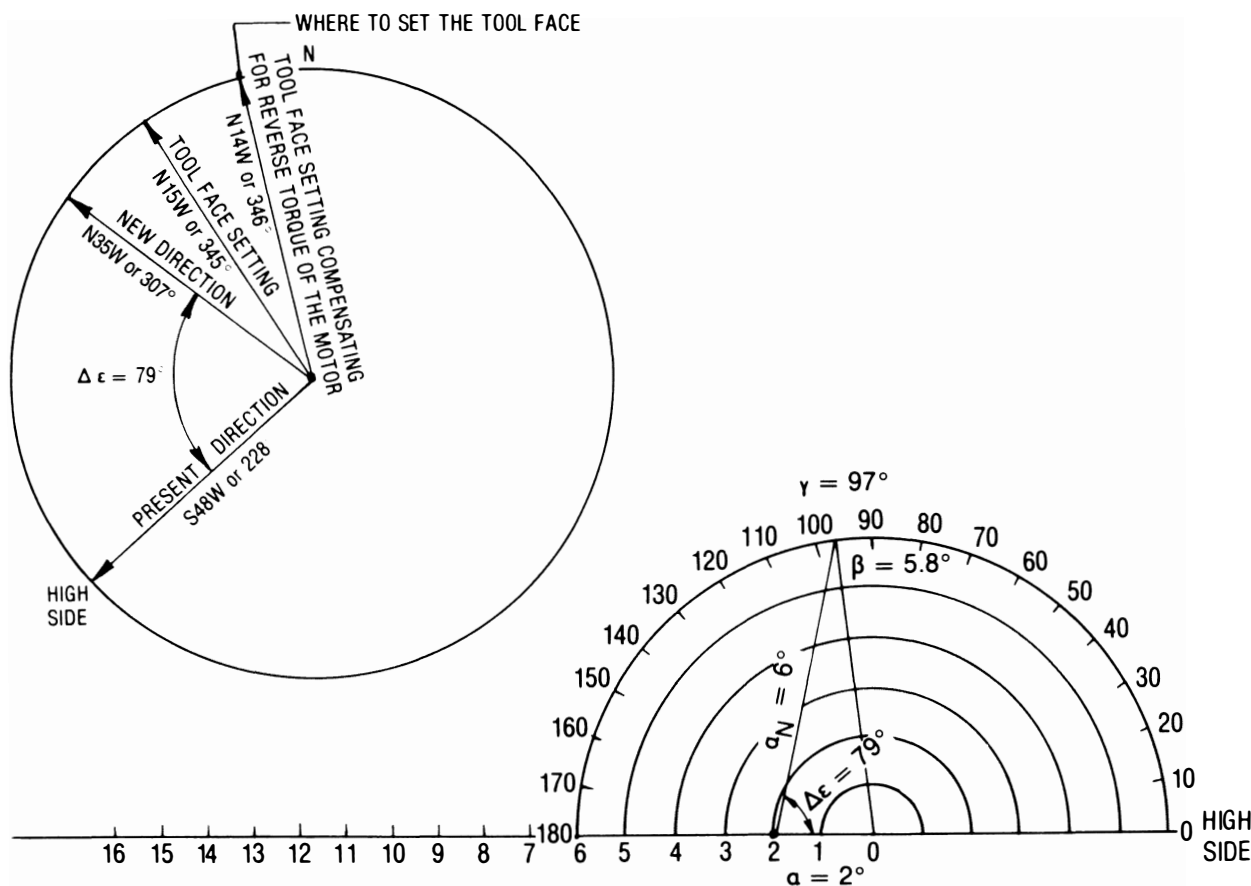


Fig. 8.36—Solution for Example 8.10.

The maximum direction change for a fixed value of  $\beta$  is illustrated by Fig. 8.37. Between 0 and  $1.5^\circ$  inclination, the maximum change is  $360^\circ$ ; at  $1.5^\circ$  the maximum change is  $90^\circ$ . Below  $\alpha = 1.5^\circ$  the maximum direction change is highly dependent on the inclination. At  $\alpha = 2^\circ$  the maximum change is  $50^\circ$  and at  $\alpha = 10^\circ$  the maximum change is  $10^\circ$ . Note that as the inclination increases, the tool-face setting for a maximum change reduces from  $180^\circ$  ( $\alpha = 1.5^\circ$ ) to approximately  $95^\circ$  ( $\alpha = 10^\circ$ ). Fig. 8.38 presents the same information for  $\beta = 1.5^\circ$  for inclinations between 10 and  $45^\circ$ . At  $\alpha = 45^\circ$  the maximum direction change is about  $3^\circ$ . Even though the maximum  $\Delta\epsilon$  for  $\alpha = 10$  to  $45^\circ$  occurs at one specific tool-face setting, the curves are so flat between  $\gamma = 80^\circ$  and  $\gamma = 120^\circ$  that an error in the tool-face setting between 80 and  $120^\circ$  would make very little difference in the resultant direction change.

Both figures show the importance of making the direction change at low inclinations. A design practice is to try to set the direction at an inclination between 1 and  $6^\circ$  and then build inclination only, holding the direction of the hole fairly constant. Too much curvature in direction will cause the BHA to respond in a direction opposite to the curvature, thus negating some of the benefits of the original trajectory change.

At higher inclinations where direction must be changed, the course length must be extended to minimize the dogleg severity.

In planning a trajectory change when a jetting bit is to be used, the type of jetting bit and nozzle size (which

should be large) must be selected. A mud motor with a bent sub or bent housing requires the selection of a bent sub with some amount of deflection. The total angle change  $\beta$  is not the bent sub angle, although the bent sub angle can approach  $\beta$  under certain circumstances. Fig. 8.39a shows a combination of bent sub and mud motor without the constraints of the borehole. Fig. 8.39b is the same bent sub assembly in the borehole. The effect of the bent sub depends on the geology, motor stiffness, bent sub angle, inclination, the BHA configuration above the bent sub, and the axial weight applied to the motor.

Manufacturers have published tables that present bent-sub angles in the rate of angle change in degrees per 100 ft. The effective bent sub angle can be derived from trajectory field data if all the necessary parameters are recorded. Example 8.11 presents how this can be done.

**Example 8.11.** Determine the effective bent sub response for a  $1\frac{1}{2}^\circ$  bent sub for a motor run where at 6,357 ft  $\alpha$  is  $1^\circ$  and  $\epsilon$  is S85E and at 6,382 ft  $\alpha_N$  is  $1^\circ$  and  $\epsilon_N$  is S20E; the tool face is  $160^\circ$  right of high side.

**Solution.** Using Eq. 8.53,  $\beta$  can be calculated as

$$\begin{aligned}\beta &= \arccos[\cos(65) \sin(1) \sin(1) + \cos(1) \cos(1)] \\ &= 1.07^\circ.\end{aligned}$$

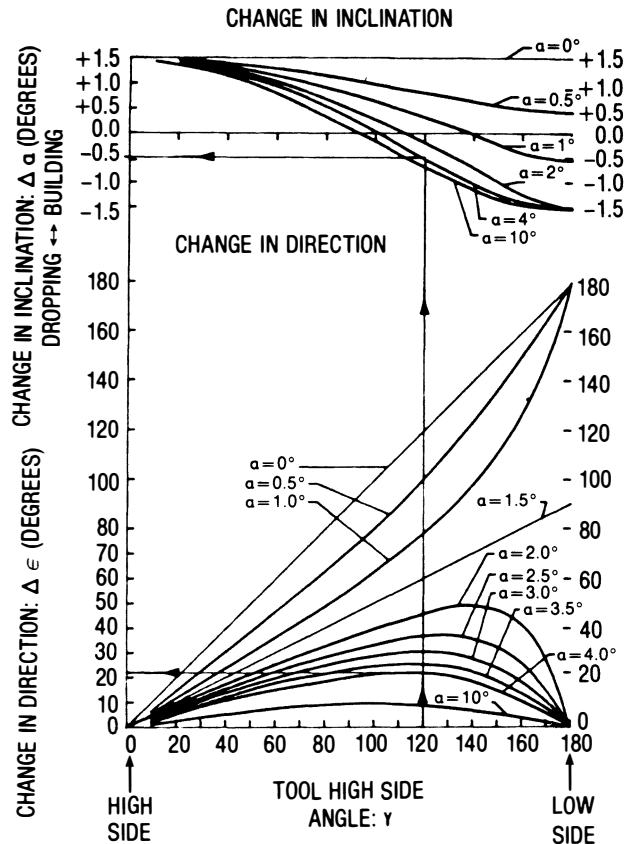


Fig. 8.37—Overall angle change ( $\beta = 1.5^\circ$ ); hole inclination from  $0.0^\circ$  to  $10.0^\circ$  (after Millheim et al.<sup>5</sup>).

The dogleg severity over the interval drilled is

$$\delta = 1.07^\circ \times \frac{100}{25 \text{ ft}} = 4.28^\circ/100 \text{ ft.}$$

If the mud motor length is 25 ft from the bit face to the bent sub, the maximum angle change that could be reached if the formation is soft enough to allow the bit to drill sideways without restriction is

$$\delta = 1.5^\circ \times \frac{100}{25 \text{ ft}} = 6.0^\circ/100 \text{ ft.}$$

The lower rate of build of  $4.3^\circ/100 \text{ ft}$  implies that the formation resisted the maximum rate of build by a factor of  $4.3^\circ/6.0^\circ = 0.72$ .

Another way of affecting the rate of angle change for this example is to move the bent sub farther from or closer to the bit. If the motor length is 30 ft instead of 25 ft, the unrestricted angle change is  $5^\circ/100 \text{ ft}$  instead of  $6^\circ/100 \text{ ft}$ . A positive displacement motor can also have a bent housing close to the bit. For a  $1.5^\circ$  bent housing 8 ft from the bit, the unrestricted angle change is  $18\frac{3}{4}^\circ/100 \text{ ft}$ .

Jetting bits have a fixed big jet direction which serves much the same purpose as the bent sub—to cause deflection. The effectiveness of the jetted pocket depends on

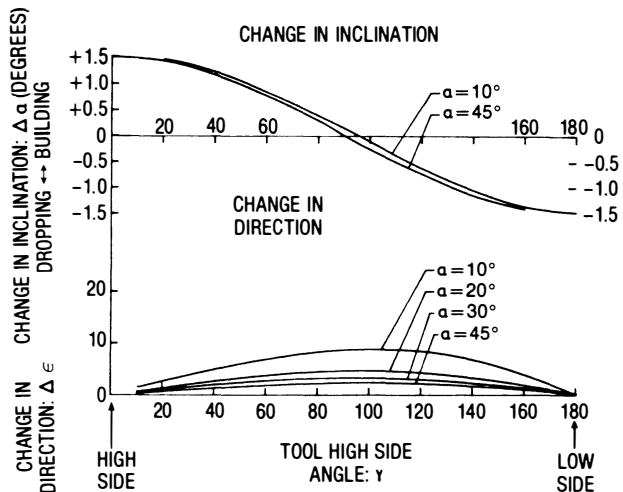


Fig. 8.38—Overall angle change ( $\beta = 1.5^\circ$ ); hole inclination from  $0.0^\circ$  to  $45.0^\circ$  (after Millheim et al.<sup>5</sup>).

the length of the jetting run, geology, hydraulics, and BHA configuration. A typical jetting run can be analyzed with the same techniques used for designing a trajectory change.

**Example 8.12.** A well has been jetted at three different depths: 1,745 to 1,752 ft, 1,850 to 1,862 ft, and 1,925 to 1,931 ft. At 1,722 ft the surveys were S32W at an inclination of  $2.25^\circ$ . The nozzle was oriented at S90E. The survey at 1,799 ft was S30E with an inclination of  $2.75^\circ$ . The second jetting run had a survey at 1,814 ft with the direction at S20E and the inclination at  $3.0^\circ$ . The nozzle orientation was N80E. At 1,877 ft the direction was S36E and the inclination was  $3.25^\circ$ . The last jetting station was at the last survey at 1,877 ft. Orientation of the nozzle was N70E. The direction and inclination at 1,940 ft was S66E and  $4.75^\circ$ . Normal drilling occurred between jetting runs. Determine the direction change  $\Delta\epsilon$ ,  $\beta$ , and  $\delta$  for each run.

**Solution.** If the beginning and ending inclinations and the tool-face setting are known, the total angle change, dogleg severity, and the change of direction can be determined using the graphical approach (see Figs. 8.40a, b, and c). This is done by drawing a line from  $\beta = 0^\circ$  to  $\gamma = 122^\circ$  and drawing a line from  $\alpha = 2.25^\circ$  that is  $2.75^\circ$  units long where it intercepts the other line.  $\Delta\epsilon$  is the angle ( $77^\circ$ ) between the two line segments at  $\alpha = 2.25^\circ$ . The total angle change ( $\beta = 3.1^\circ$ ) is the distance along the line from the origin ( $\beta = 0$  and  $\alpha = 0$ ) to the point of intersection with the other line ( $\alpha_N = 2.75^\circ$ ). The dogleg can be calculated by knowing  $\beta$  and the course length between surveys at 1,722 and 1,799 ft ( $L_C = 77 \text{ ft}$ ).

$$\delta = 3.1^\circ \times \frac{100 \text{ ft}}{71 \text{ ft}} = 4^\circ/100 \text{ ft.}$$

The measured change in direction from S32W to S30E is  $62^\circ$ . Using a similar approach, the other jetting runs can be analyzed. From 1,850 to 1,862 ft  $\Delta\epsilon = 14^\circ$ ,  $\beta = 1.0$ ,



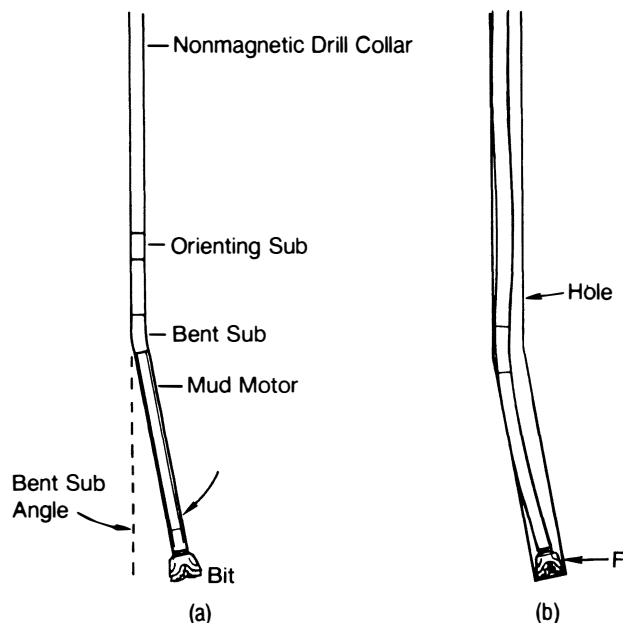


Fig. 8.39—Bent sub unconstrained and constrained in a wellbore.

and  $\delta = 1.58^\circ/100$  ft. The measured  $\Delta\epsilon$  is  $16^\circ$ . From 1,925 to 1,931 ft,  $\Delta\epsilon = 63^\circ$ ,  $\beta = 2.7^\circ$ , and  $\delta = 4.28^\circ/100$  ft. The measured  $\Delta\epsilon$  is  $33^\circ$ .

## 8.5 Directional Drilling Measurements

The trajectory of a wellbore is determined by the measurement of the inclination and direction at various depths and by one of the calculations presented in Sec. 8.3. A tool-face measurement is required to orient a whipstock, the large nozzle on a jetting bit, an eccentric stabilizer, a bent sub, or bent housing.

Inclination and direction can be measured with a magnetic single- or multishot and a gyroscopic single- or multishot. All these tools are self-contained and are powered

with batteries or from the surface. Magnetic tools are run on a slick line (steel wireline), on a sand line (braided steel cable), or in the drill collars while the hole is tripped, or they can be dropped (go-deviled) from the surface. Some gyroscope tools are run on conductor cable, permitting the reading of measurements at the surface and the supplying of power down the conductor cable. The battery-powered gyroscope tools are run on a wireline.

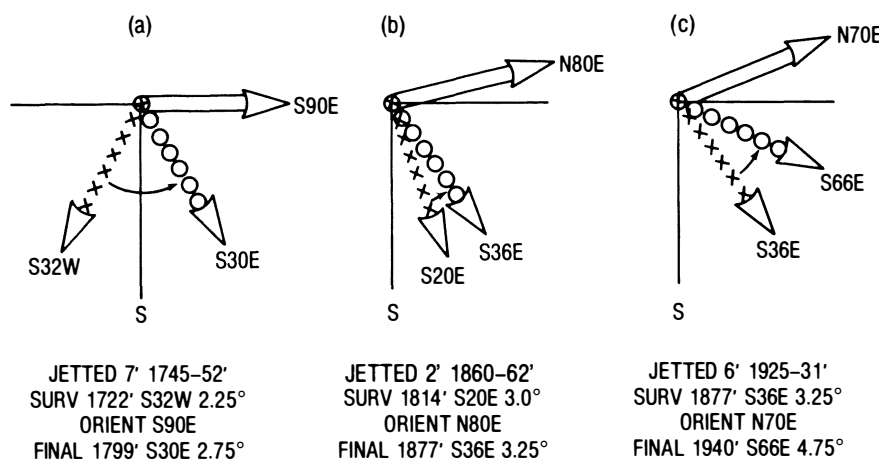
Another way to measure direction, inclination, and tool face is with an arrangement of magnetometers and accelerometers. Power can be supplied by batteries, a conductor cable, or a generator powered by the circulation of the drilling fluid. If the measurement tool is located in the BHA near the bit and the measurements are taken during drilling, it is called a measurement-while-drilling (MWD) tool.

This section presents the various measurement tools, the principles of operation, the factors that affect the measurements, and the necessary corrections.

### 8.5.1 Magnetic Single-Shot Instruments

The magnetic single-shot instrument records the inclination, direction, and tool face on either sensitized paper or photographic film. Fig. 8.41 shows a typical angle compass unit for  $0$  to  $20^\circ$  and  $0$  to  $70^\circ$  inclinations. In this arrangement, the direction and inclination indicator floats in a fluid, thereby minimizing the friction between the center post and the float. Fig. 8.42 shows some of the types of compass units for the various single-shot devices.

The angle inclination (AC) units range from  $0$  to  $3^\circ$  to  $0$  to  $70^\circ$  with a scribe line for tool-face orientation. The sample readings for the  $3$ ,  $20$ ,  $70$ , and  $80^\circ$  units are  $2.25^\circ$  inclination, S80E;  $6.5^\circ$  inclination, S65E;  $49^\circ$  inclination, S73E; and  $74^\circ$  inclination, S13E. The scribe lines indicate that the tool faces of the  $20^\circ$ , the  $70^\circ$ , and the  $70^\circ$  magnetic method of orientation (MMO) compasses are  $30^\circ$  right of high side,  $119^\circ$  right of high side, and  $40^\circ$  right of high side, respectively. A  $17$  to  $125^\circ$  unit shows the inclination as  $78^\circ$  and the direction as  $133^\circ$  or



NOTE: DRILLED BETWEEN JETTING RUNS

Fig. 8.40—Example of three jetting stops while trying to kick off and set the wellbore lead (after Millheim et al.<sup>5</sup>).

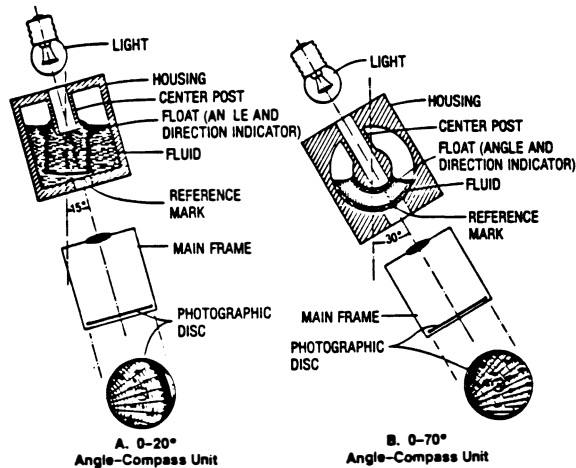
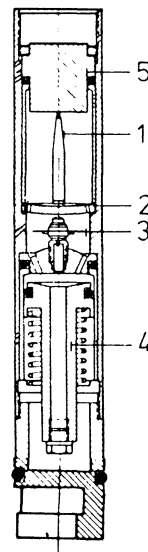


Fig. 8.41—Schematic diagrams of magnetic single-shot angle compass unit (courtesy Kuster Co.).



1. Pendulum
2. Circular glass
3. Compass
4. Pressure equalization
5. Cover glass

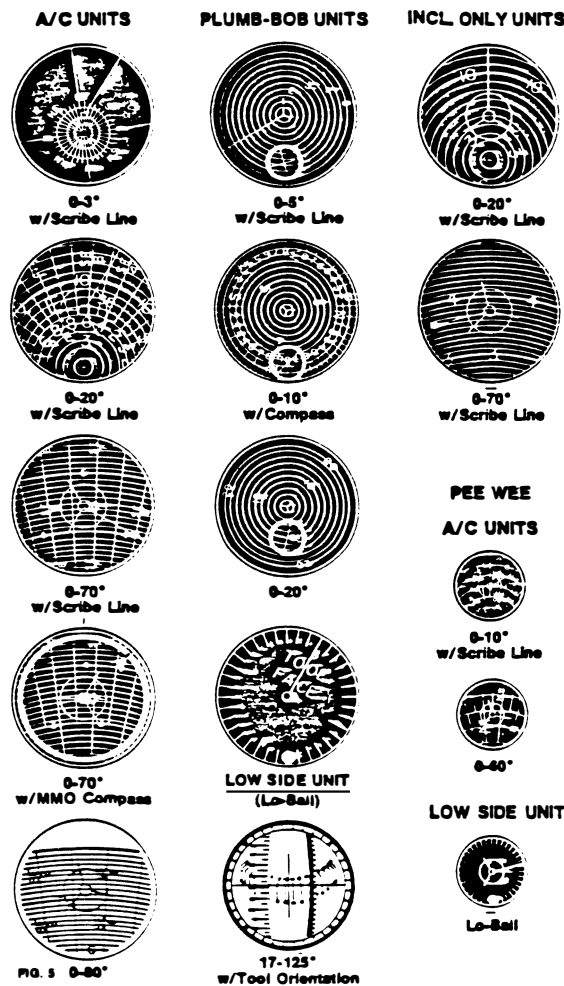
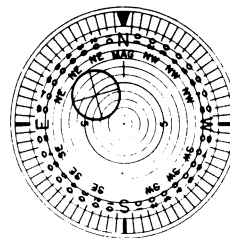


Fig. 8.42—Single-shot film disks (courtesy of Kuster Co.).



Indicated inclination  $5^{\circ} 0'$   
Direction of inclination  $N 45^{\circ} 0'$   
or azimuth  $45^{\circ}$

Fig. 8.43—Pendulum suspended inclinometer and compass unit for a 0 to  $17^{\circ}$  single-shot unit (after Eikelberg *et al.*<sup>8</sup>).

S47E. Other units show plumb bob units to measure only inclination (with and without scribe lines) and units to detect the low side of the borehole.

Fig. 8.43 shows a different type of compass unit that measures inclination by a Cardan-suspended pendulum that moves over a compass rose. The high-range units have a dual Cardan-suspended arrangement in which the compass moves on the main Cardan suspension and the inclinometer moves on an internal Cardan suspension (see Fig. 8.44).

Fig. 8.45 is a diagram of a typical single-shot unit with the bottom landing and orientation assembly. The unit is triggered either by a timer set for a period of time (up to 90 minutes) or by an inertial timer that does not activate until the unit comes to a complete stop. When the unit stops, the light comes on and a picture is taken.

Single-shot instruments are used to monitor the progress of a directional- or deviational-control well and to help orient the tool face for a trajectory change. The usual procedure is to load the film into the instrument, to activate the timer, to make up the tool, and to drop it down the drillpipe. When the timer is activated, a surface stopwatch is started, unless the motion timer is used. The surface stopwatch will indicate when the instrument has taken the picture. The tool is then retrieved with either a wire-line overshoot or the drillpipe. Fig. 8.46 shows a typical single-shot operation.

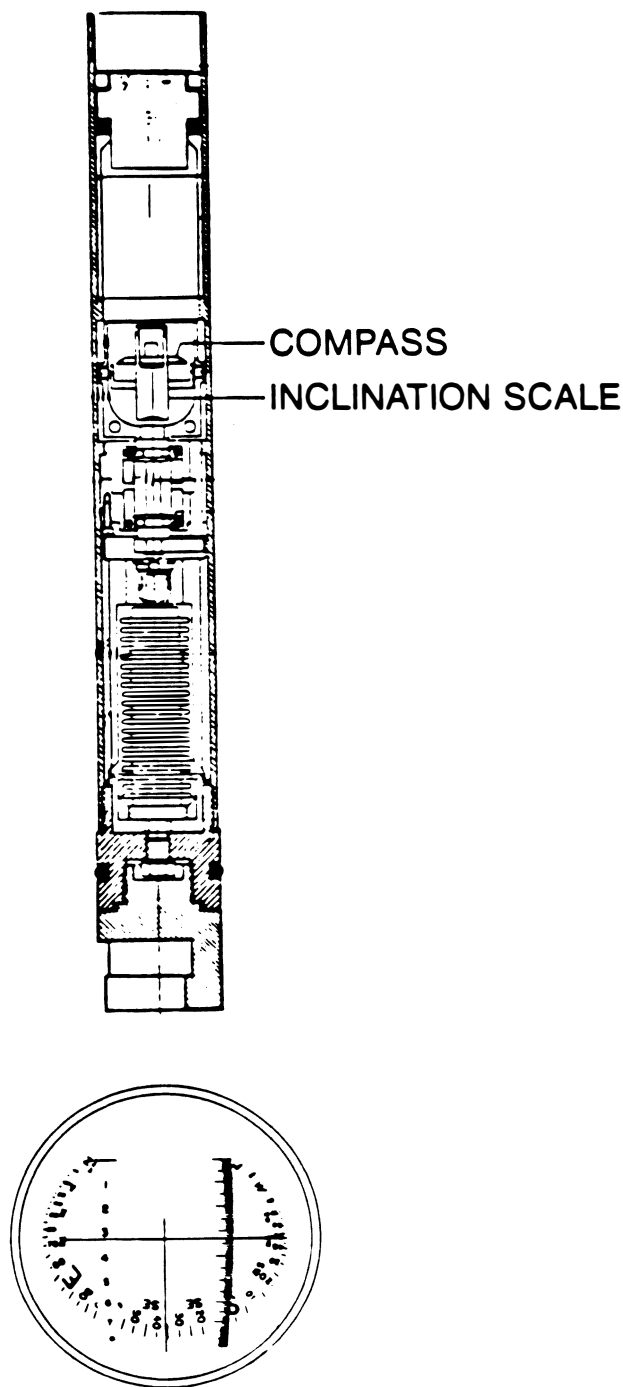


Fig. 8.44—Cardan suspended compass and inclinometer for a single-shot 5 to 90° unit (after Eikelberg *et al.*<sup>8</sup>).

Running a single-shot tool and interpreting data is simple. Valuable rig time, however, is consumed when a survey is run; depending on the depth of the well, the time used can range from a few minutes for shallow depths to more than an hour for a deep hole. Also, if the inclination becomes excessive, the tools must be pumped down. Another problem is the temperature in the area where the survey is taken. If the temperature is too high, the film will be completely exposed, yielding a black picture. To solve that problem, a special protective case is used to retard the temperature buildup in the film unit. The case fits over the single-shot tool and works like a vacuum flask, having a vacuum gap between the case and the tool. However, the tool still must be retrieved quickly because the case only slows the temperature rise.

Orientation of the tool face with a single-shot tool requires the use of either a mule-shoe mandrel and bottomhole-orienting sub or a nonmagnetic orienting collar. Fig. 8.47 shows a mule-shoe orienting arrangement. The mule-shoe orienting sleeve is positioned in the mule-shoe orienting sub to line up with the bent sub or bent housing knee, the large nozzle on a bit used for jetting, the undergauge blade of an eccentric stabilizer, or the whipstock wedge. The single-shot tool has a mule-shoe mandrel on the bottom that is shaped to go in the orienting sleeve only in the direction of the tool face.

If an MMO tool is used, the instrument is spaced so that a shadow graph compass in the single-shot instrument is opposite the magnets placed in the nonmagnetic collar. The location of the magnets is identified by a scribe line on the outside of the collar. When an orienting tool is made up, the positions of the orienting tool and of the scribe line on the nonmagnetic collar are observed and the make-up difference noted. An MMO single-shot picture will show a shadow graph, which indicates the direction of the scribe line on the drill collar; this graph is superimposed on a regular single-shot picture. When the makeup correction is considered, the true tool-face direction is obtained. This method of orientation is rarely used now.

### 8.5.2 Magnetic Multishot Instruments

The magnetic multishot instrument is capable of taking numerous survey records in one running. It either is dropped down the drillpipe or is run on a wireline in open hole.

Fig. 8.48 is a multishot instrument landed in such a way that the compass unit is spaced adjacent to the nonmagnetic collar. Fig. 8.49 is a depiction of a complete multishot instrument rigged for bottom landing, showing the component parts. Fig. 8.50 shows both sides of the watch and camera sections. The watch is spring wound and uses the power of the mainspring to operate a timer cam. The cam rotates, causing an electrical connection between the batteries and the motor and camera section. The motor drives a series of gears that finally drives the Geneva gear and the wheel assembly, which advances the film and turns on the light long enough for a picture to be taken.

A multishot tool is usually dropped down the drillpipe and landed in the nonmagnetic drill collar(s). During the trip out, a survey is taken approximately every 90 ft, the length of a stand. More closely spaced stations could be obtained, however, by stopping the pipe movement at a

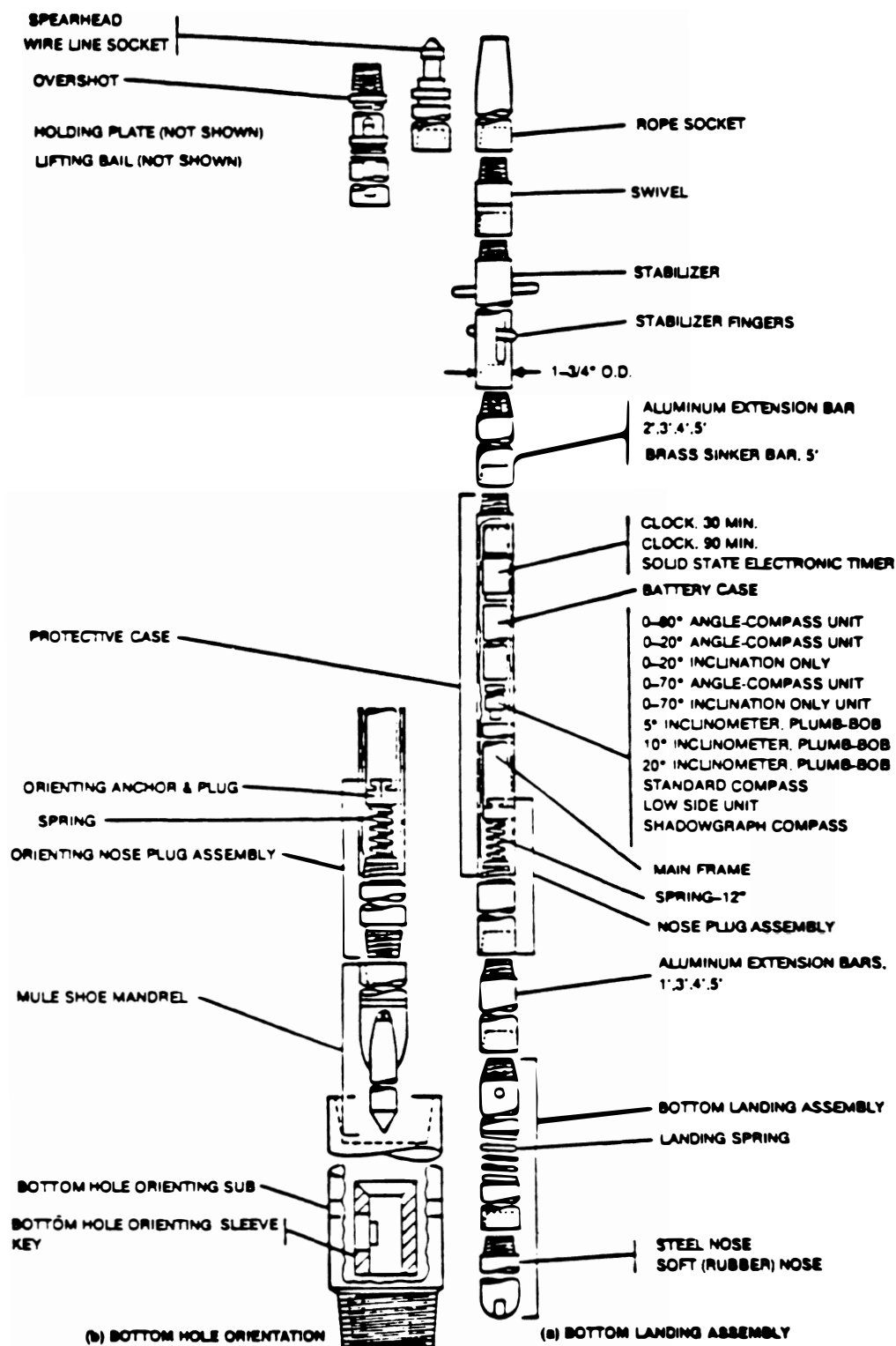


Fig. 8.45—Typical magnetic single-shot tool with landing sub (courtesy of Kuster Co.).

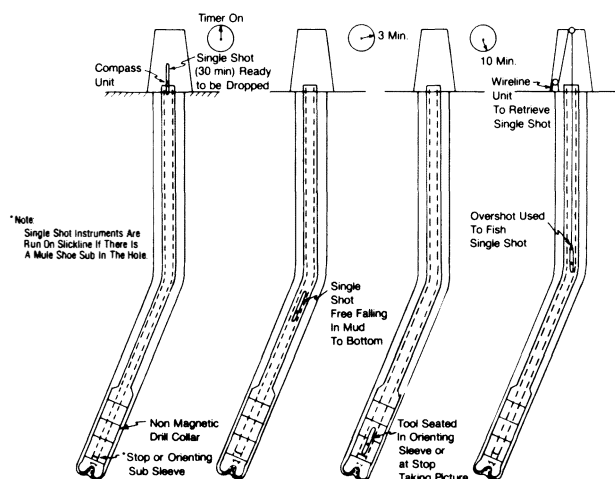


Fig. 8.46—Typical single-shot operation.

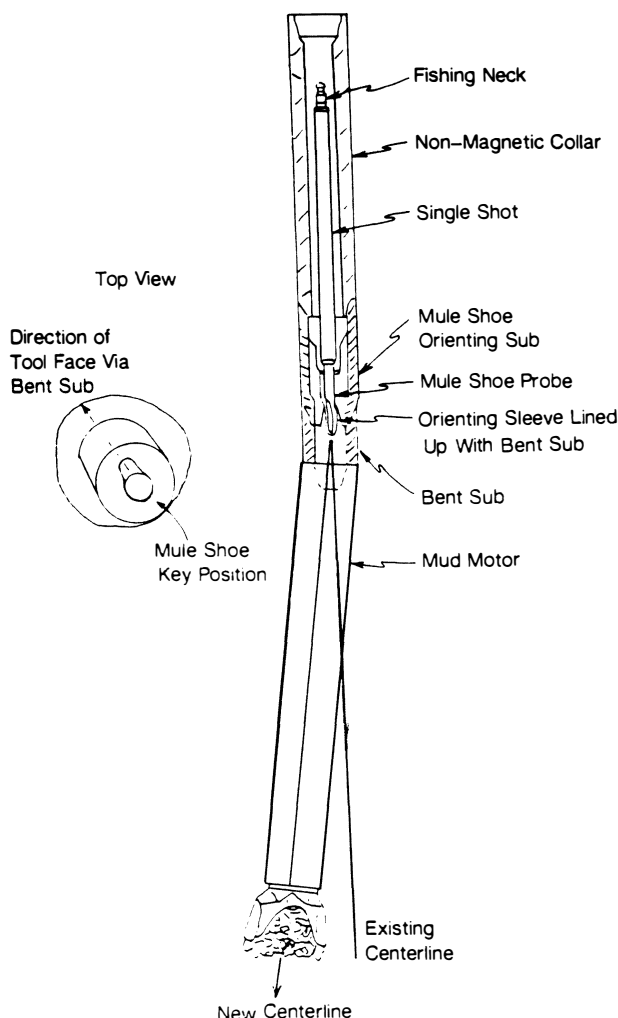


Fig. 8.47—Arrangement of the mule shoe for orienting a mud motor.

desired point and waiting for a picture. When the instrument is assembled at the surface and the timer is turned on, a stopwatch is also started. The watch is synchronized with the timer so that the operator knows exactly when a picture is being taken and how many frames were exposed. Fig. 8.51 illustrates how the stopwatch is used to take a picture. The upper dial records minutes and indicates the number of pictures taken; the lower dial indicates hours and records sets of 60 pictures.

Once a survey is completed, the tool is broken down, and the film is developed and read. Special readers that count the frames and project the picture onto a screen where it can be read easily are used (see Figs. 8.52A and B). Direction and inclination readings are identical to those of the single-shot units, except that there are no tool-face readings.

Multishot surveys typically are run at the end of a particular section of hole before casing is run. Because the surveys are usually closer together than the single-shot surveys and are run with the same instrument, multishot surveys are considered more representative of the trajectory of the borehole than a series of single-shot surveys. The accuracy of the multishot and single-shot surveys is affected by the inclination, the general trajectory direction, the position on the earth, and the magnetism of the wellbore and drillstring. All these factors will be covered later in this section.

### 8.5.3 Steering Tools

When a mud motor with a bent sub or housing is used, running a steering tool is sometimes wiser and more economical. Fig. 8.53 is a schematic of a typical operation with a steering tool. An instrument probe is lowered by a wireline unit and is seated in the mule-shoe orienting sleeve. The wireline can be passed through a circulating head mounted on the drillpipe. If this is done every 90 ft of drilled hole, the steering tool should be retrieved into the top stand. The top stand is set back and another stand is added. Then the stand with the steering tool is connected, and the steering tool instrument is run to the orienting sub and resealed. A way to overcome the need to pull the instrument every 90 ft is to insert a side-entry sub on the last drillpipe after tripping into the hole (Fig. 8.54). The stuffing box arrangement that prevents fluid leakage is built into the side of the sub. The steering tool is run conventionally and is seated in the orienting sleeve. The wireline is secured in the side-entry sub and let out the side, as illustrated in Fig. 8.55. As drilling continues, new joints of drillpipe can be added conventionally with the kelly. The wireline is clipped to the side of the drillpipe as more and more drillpipe is added. With care, this technique can be used to drill hundreds of feet without the need for tripping the instrument to the surface. Generally, drilling is continued until the side-entry sub reaches a point in the borehole where the inclination is so high that there is a risk of damaging the wireline. When this depth is reached, the drillpipe can be short tripped and the steering tool retrieved. The side-entry sub can be reset at the top of the string and the operation restarted.

The steering tool uses electronic means to measure direction and inclination. Direction is measured by flux-gate magnetometers that measure the earth's magnetic field in the  $x$ ,  $y$ , and  $z$  planes. From this measurement, the vector components can be summed up to determine

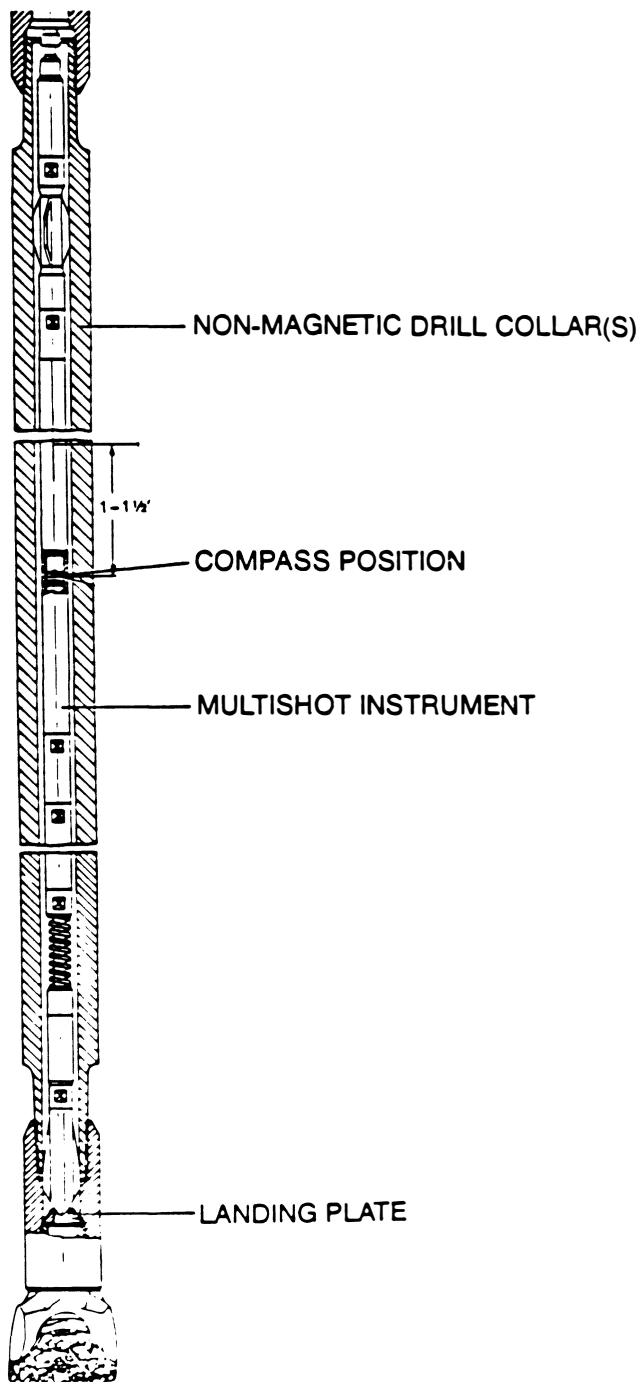


Fig. 8.48—Typical arrangement for landing a multishot instrument (after Eikelberg *et al.*<sup>8</sup>).

the wellbore direction. Inclination is measured by accelerometers that measure the gravity component along two axes. Fig. 8.56 shows the arrangement. The angle of the tool face below 3 to 7° can be determined by a computer with the magnetometer data. Above 3 to 7°, the angle of the tool face is referenced to the hole direction and is related to the gravity readings of the accelerometers.

Figs. 8.57A and B picture a typical steering-tool surface recorder and tool-face indicator mounted near the driller. Most steering tools constantly sense inclination, direction, and tool-face angle. Therefore, the steering tool

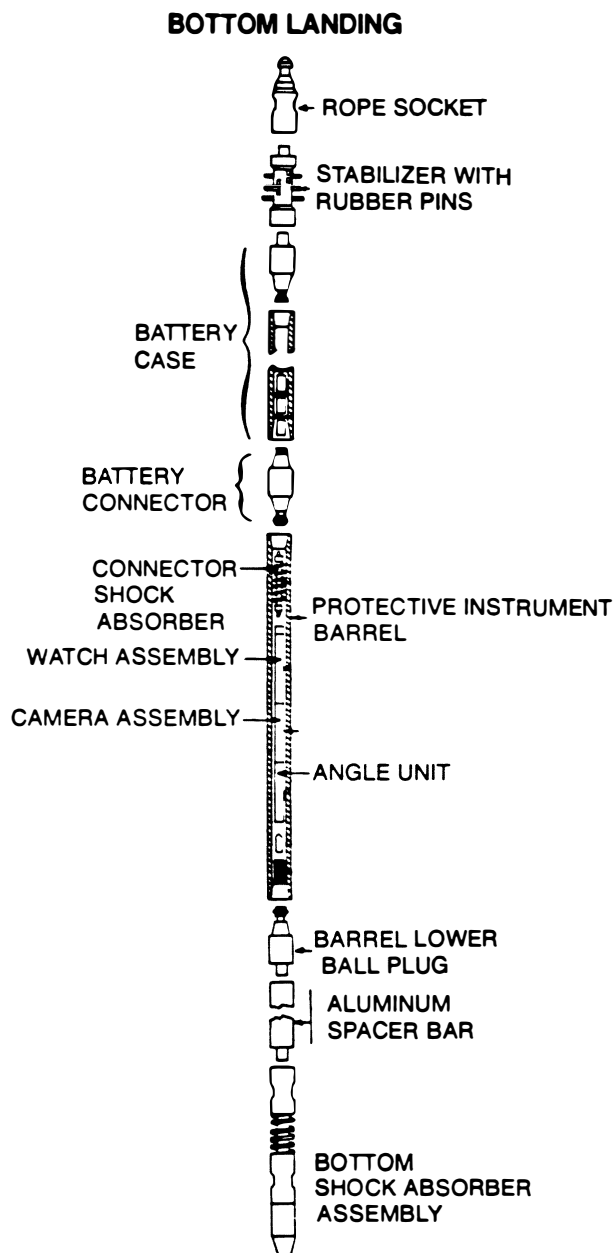


Fig. 8.49—Drop multishot survey instrument (courtesy of Kuster Co.).

gives the directional operator more information with which to adjust the tool face and to achieve better control of the mud motor. The steering tool takes the guesswork out of correcting the tool-face angle for the expected amount of reverse torque. Having a constant, continuous tool-face reading, the operator can make minor adjustments and even use the readings to slack off weight on the bit (WOB). As weight is applied, the reverse torque increases, and the tool face rotates back to the right as the bit drills off.

A steering tool is one of the most economical means of making a trajectory change when a mud motor and bent sub or bent housing are used for drilling, especially when rig costs are high and the trajectory change is below 3,000 to 4,000 ft. Table 8.5 sets out a typical steering-tool trajectory change.

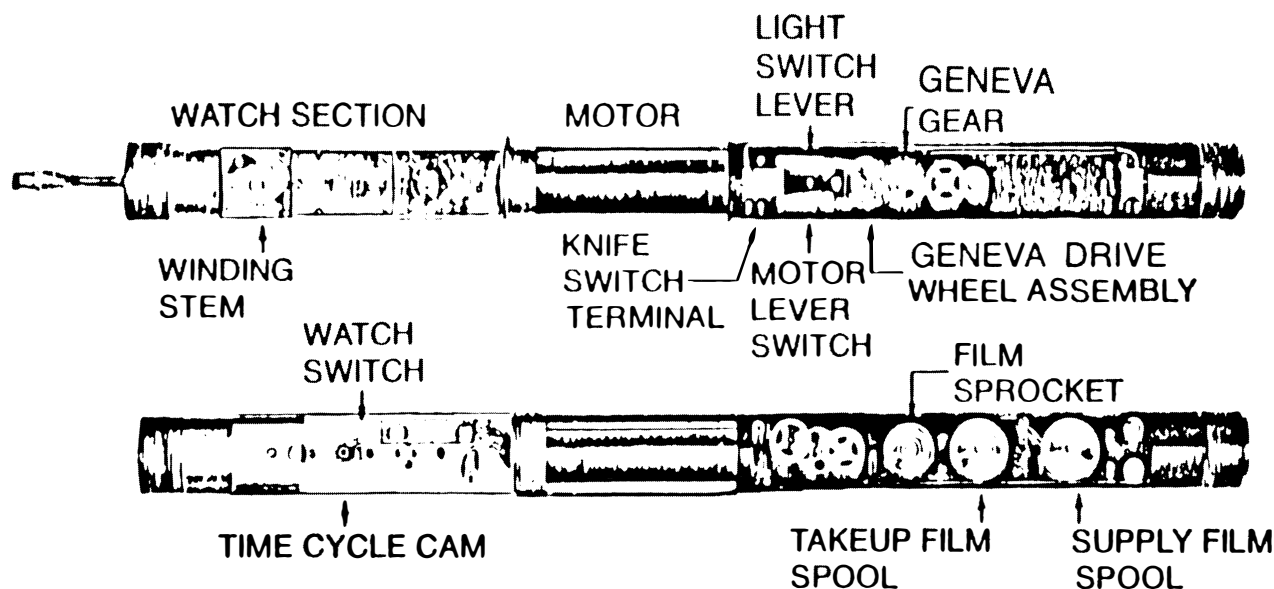


Fig. 8.50—Views of the watch and camera unit of a typical multishot tool (courtesy of Kuster Co.).

#### 8.5.4 Tools for Measuring Trajectory During Drilling

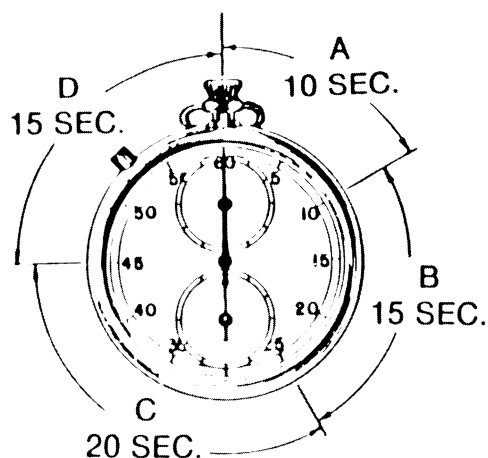
As early as the 1960's, companies were experimenting with ways to log formations during drilling, but, technologically, it was difficult to build tools that could withstand the harsh downhole environment and transmit reliable data. A spinoff of the effort to overcome the problem was a recognition that inclination, direction, and tool-face angle could be measured during drilling and the data could be transmitted to the surface.

Various transmission methods were used—such as electromagnetic, acoustic, pressure pulse, pressure-pulse

modulation, or cable and drillpipe. Of all the transmission methods, the pressure-pulse and pressure-pulse-modulation methods have evolved into commercial systems often used by the directional drilling community.

One of the earliest commercial systems offered to the industry was the Teledrift, which was designed as a sub that could be placed near the bit to record and to transmit the inclination of the wellbore to the surface. Fig. 8.58 depicts the teledrift tool at various transmission positions. An initial setting of the inclination range must be made before the tool is run into the hole. The range is for 2.5°,

#### SURFACE WATCH



SYNCHRONIZE WITH INSTRUMENT WATCH BY STARTING AT THE INSTANT CAMERA LIGHTS GO ON.

#### Time Intervals:

- A. 10 Seconds – Lights Are On, Exposing Film.
- B. 15 Seconds – Delay Before Moving. This Is An Allowance For Instrument Watch Lag During Survey.
- C. 20 Seconds – Instrument Is Idle Allowing Movement Of Drill String Without Affecting Picture. Most Moves Require Sufficient Time For Taking One or More Shots While Moving.
- D. 15 Seconds – Minimum Time For Plumb Bob and Compass To Settle For Good Picture, Plus Allowance For Instrument Gain During Survey

Fig. 8.51—Use of the surface watch while running a magnetic multishot operation (after Eikelberg *et al.*<sup>8</sup>).

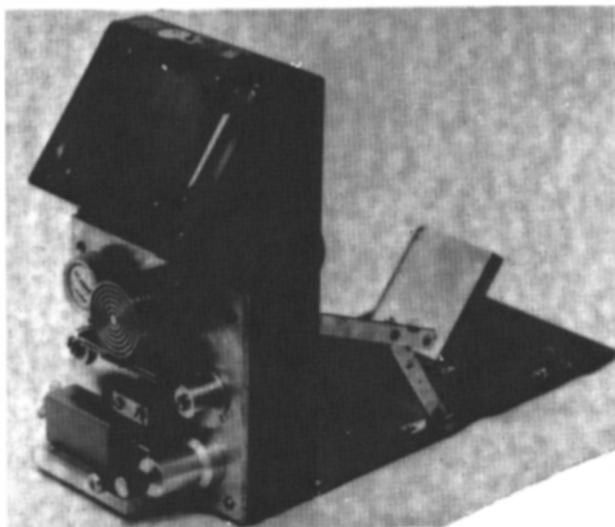


Fig. 8.52A—Typical multishot film reader (courtesy of NL Sperry Sun Co.).

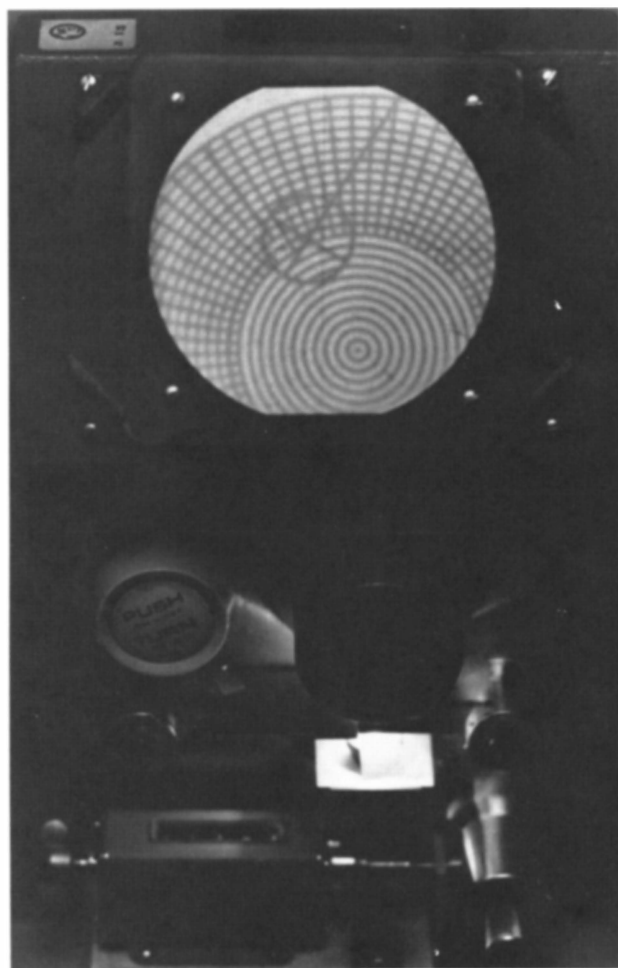


Fig. 8.52B—Projection of one survey frame for determining inclination and direction (courtesy NL Sperry Sun Co.).

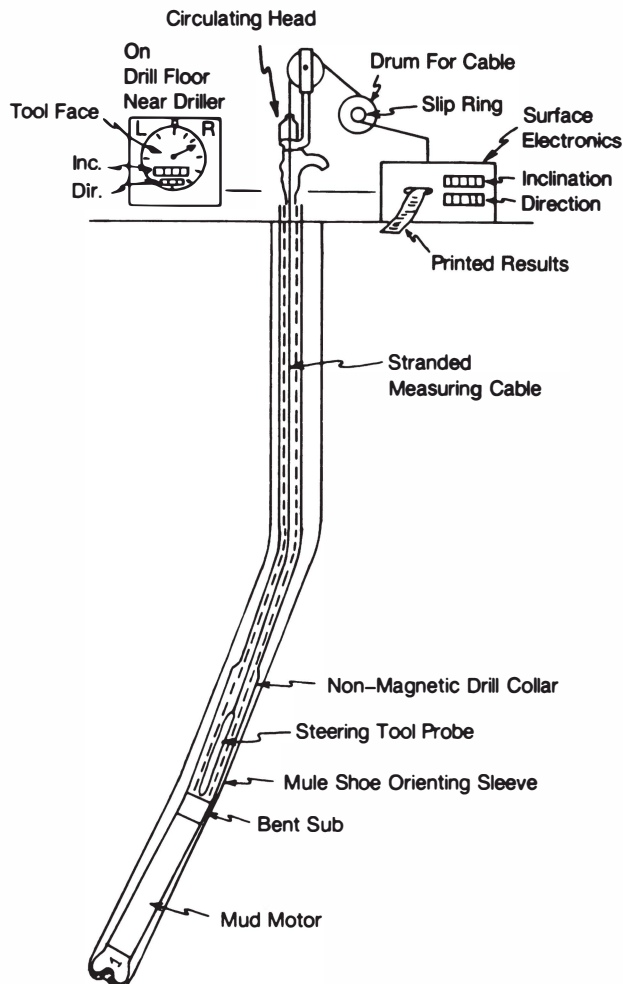


Fig. 8.53—Typical operation of a steering tool for orienting the bit.

in  $0.5^\circ$  increments between 0 and  $15^\circ$ . For example, an initial setting of 0 to  $2.5^\circ$  can be made. If the inclination exceeds  $2.5^\circ$ , the teledrift will report only  $2.5^\circ$ .

During drilling, the fluid velocity keeps the signal piston pressed down to its lowest position outside the pulse rings against the tension of the shaft spring. When a reading is needed, drilling is stopped, the bit is lifted off bottom, and circulation is terminated. The shaft spring forces the signal piston to the position that is proportional to the inclination or to the highest position if the inclination is greater than the maximum range setting. A pendulum controls the setting of the signal piston. As the inclination increases, the pendulum goes farther down the stop rings until it reaches the maximum inclination. The spring tension is released accordingly, allowing the signal piston to advance upward. When pumping begins, the signal piston is forced by each pulse ring, sending from one to seven pressure pulses up the drillstring to the surface, where the pulses are detected by a recorder that picks up the number of pulses and prints the data on a strip chart. Signal strength can vary from 60 to 150 psi and depends on the depth of the well and the condition of the mud. A problem arises if there is air or gas in the mud; either will reduce the signal transmission to a point at which the pulses are difficult to detect. Another problem is that materials in the drilling fluid may plug the tool. Properly



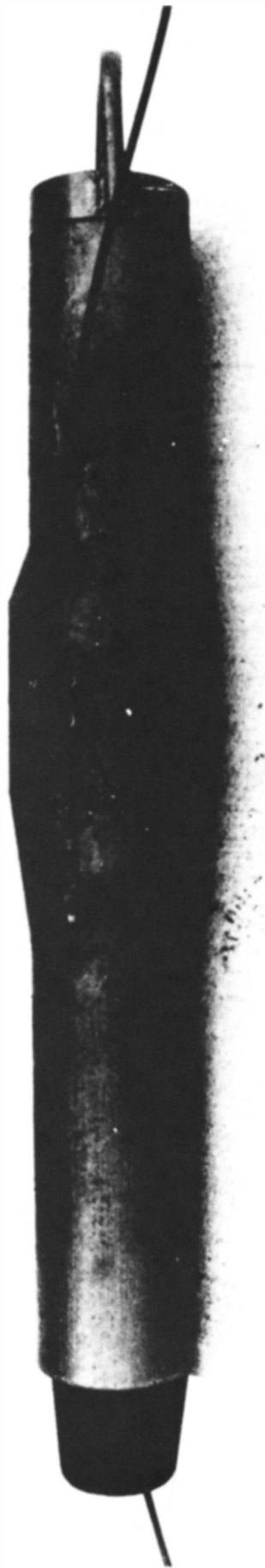


Fig. 8.54—Side-entry sub.

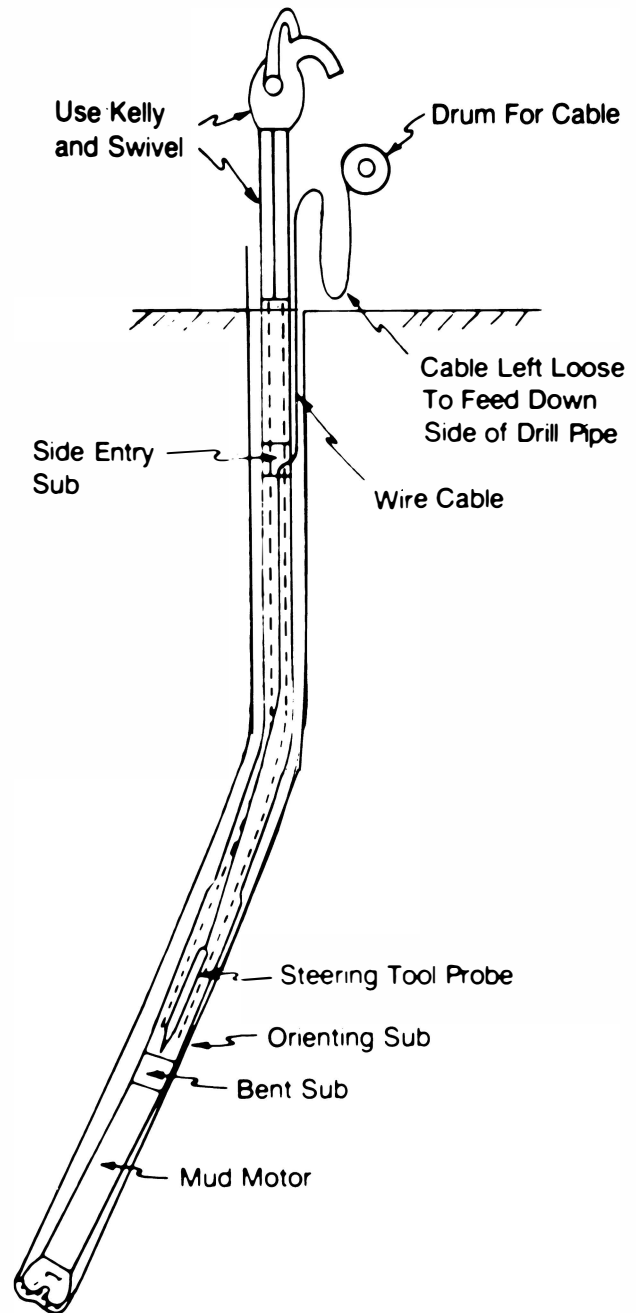


Fig. 8.55—Using a side-entry sub with a steering tool.

maintained and operated, however, the tool has application for deviation-control wells. As many inclination readings as desired can be obtained at any time when drilling and pumping are stopped. Thus decisions can be made before a well deviates to the point that drastic measures must be taken. Even though this tool is still available and is run periodically, its use has diminished with the advent of the various mud-pulse MWD tools that are now reliable and economical for a wide range of drilling situations.

The two most common MWD systems are the pressure-pulse and the modulated-pressure-pulse transmission systems. The pressure-pulse system can be subdivided further into positive- and negative-pressure-pulse systems.

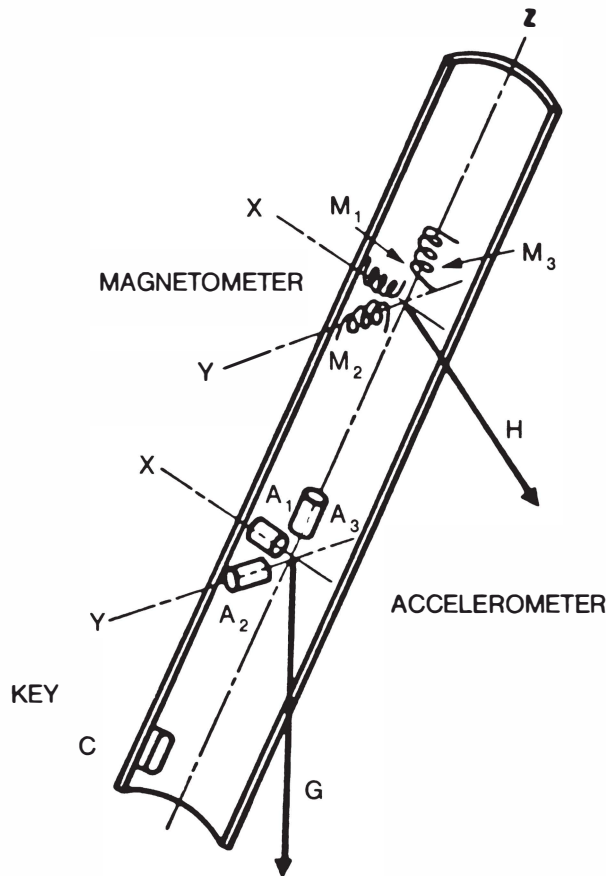


Fig. 8.56—Arrangement of sensors in a steering tool (after Eikelberg *et al.*<sup>8</sup>).

Fig. 8.59 depicts a typical MWD system with the downhole sensor unit, the sensor-to-signal unit, the pulser section, and the power section. At the surface, the signals are received by a pressure transducer and transmitted to a computer that processes and converts the data to inclination, direction, and tool-face angle. This information is transmitted to a terminal, which prints it, and to a rig-floor display similar to the steering-tool surface unit, which displays inclination, direction, and tool-face angle.

Most sensor packages used in an MWD tool consist of three inclinometers (accelerometers) and three flux-gate magnetometers. At low angles, inclination can be read with one of the gravity inclinometers. At higher angles—approaching 90°—another axis (hence another inclinometer) is needed to obtain correct values. Direction measurements are obtained from the three flux-gate magnetometers. The accelerometer readings are needed to correct the direction measurements for the inclination and the position of the magnetometers with the low side of the hole. Tool-face angle is derived from the relationship of hole direction to the low side of the hole, which is measured by the inclinometers.

Once the readings are measured, they are encoded through a downhole electronics package into (1) a series of binary signals that are transmitted by a series of pressure pulses or (2) a modulated signal that is phase shifted to indicate a logic 1 or 0. Fig. 8.60 shows a negative pulser, a positive pulser, and a mud siren that generates a continuous wave.

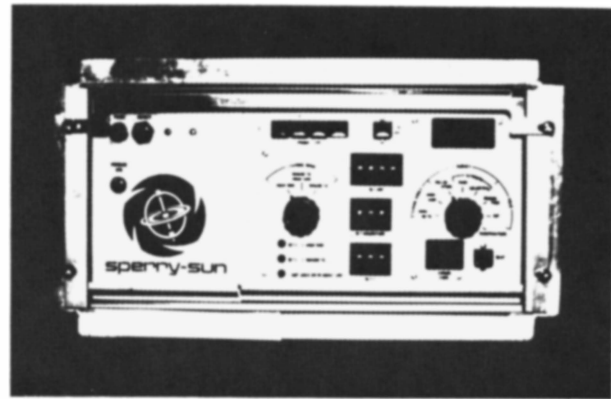


Fig. 8.57A—Steering-tool surface panel (courtesy of NL Sperry Sun Co.).



Fig. 8.57B—Tool-face indicator located on the drill floor (courtesy NL Sperry Sun Co.).

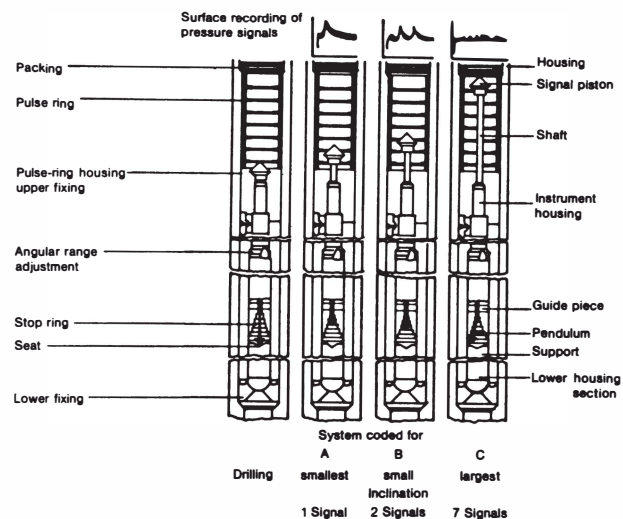


Fig. 8.58—Operation of a teledrift tool (after Eikelberg *et al.*<sup>8</sup>).

**TABLE 8.5—EXAMPLE OF STEERING TOOL DATA FOR A KICK OFF OF A GULF OF MEXICO DIRECTIONAL WELL**

Bit Depth		Magnetic Seat	High-Side Seat	Inclination (degrees)	Azimuth (degrees)	Dip	Magnitude (degrees)	Picture Inclination/Direction	Readout
Start (ft)	End (ft)								
820		105.4	333	7.4	122.1	62.2	50.3		
	910	133.5	356	13.0	122.1	59.6	50.3	11°5' S58E	3°L
910		137.3	359	12.8	122.4	59.7	50.6		0°
	950	83.8	309	16.3	115.0	69.6	49.4	16° S65E	50°L
950		62.9	289	16.7	113.5	59.7	49.4		50°L
	1,031	130.0	353	20.0	111.4	59.7	49.3	21°50' S68E	
1,031		135.0	355	22.7	111.5	59.3	49.4		5°L
	1,156	136.9	356	29.5	111.7	59.2	49.1	29° S67E	4°L
1,156		126.7	345.5	29.7	112.4	58.8	48.9		15°L
	1,212	119.0	337	32.7	111.7	58.8	48.8	32° S68E	30°L
1,212		112.0	330.1	37.3	111.7	58.7	48.9		30°L
	1,306	101.8	322.2	38.5	111.6	58.5	48.7	38° S67E	30°L
1,306		104.9	320.2	38.7	111.7	58.7	48.7		40°L
	1,398	129.3	342.5	44.0	117.3	58.6	48.9	44° S67E	15°L

The negative pulser works by an actuator that opens and closes a small valve that discharges a small amount of the drilling fluid to the annulus. The fluid causes a brief, small pressure decrease in the drillpipe (100 to 300 psi), causing a negative pressure pulse. The duration of the pressure pulse is related to how quickly the valve opens and shuts. Because both valve wear and power consumption must be considered, complex schemes are used to encode the sensor data and to transmit them with the fewest pulses in the shortest time. To transmit a set of data—including time for a turn-on sequence and for a parity check of inclination, direction, and tool-face angle—3 to 5 minutes typically are needed. Table 8.6 is an example of one reading of a negative pulse system for making a PDM motor trajectory change.

The positive pulser with a valve actuator works by restricting the flow of drilling fluid down the drillstring and creating a positive pressure pulse. The positive pressure pulse can be greater than the negative pulse and is easier to detect. The time required to transmit a set of data by the positive pulse system is about the same as that for a negative pulse system—3 to 5 minutes.

The mud siren is based on a mud-driven turbine that turns a generator that powers a motor whose speed varies between 200 and 300 cycles/sec. The motor drives a turbine rotor that, in conjunction with the stator, generates a carrier wave, which is modulated by the turbine rotor's speeding up or slowing down. The phase shift is detected at the surface and is interpreted as a logic 0 or 1.

All commercial MWD systems are powered either by batteries or by a mud-driven turbine. The lithium batteries limit the operating time, depending on the downhole temperature, to less than 300 hours. Because most bit runs last less than 100 hours, the battery pack can be replaced during a bit change. Battery-powered MWD systems have some advantages over a turbine-powered MWD system in that they permit almost full flow of the drilling fluid to the bit without a significant pressure loss. The turbine system is sensitive to the flow rate and to the type of fluid going through the turbine. Lost-circulation material or other debris that normally could be passed through the drill collars and bit is not tolerated as easily by the stator/rotor of a turbine.

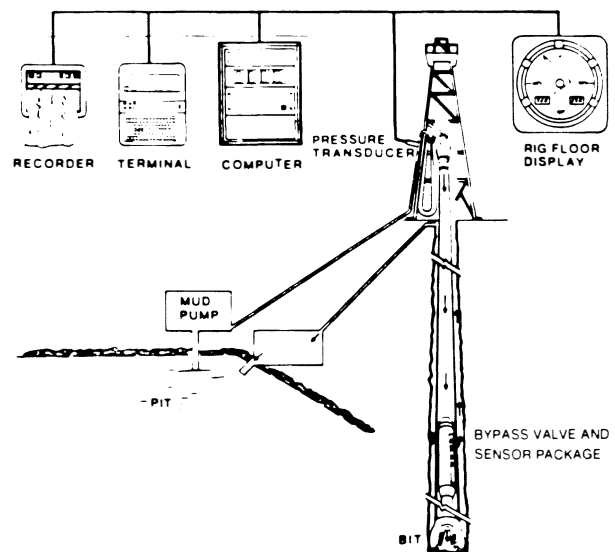
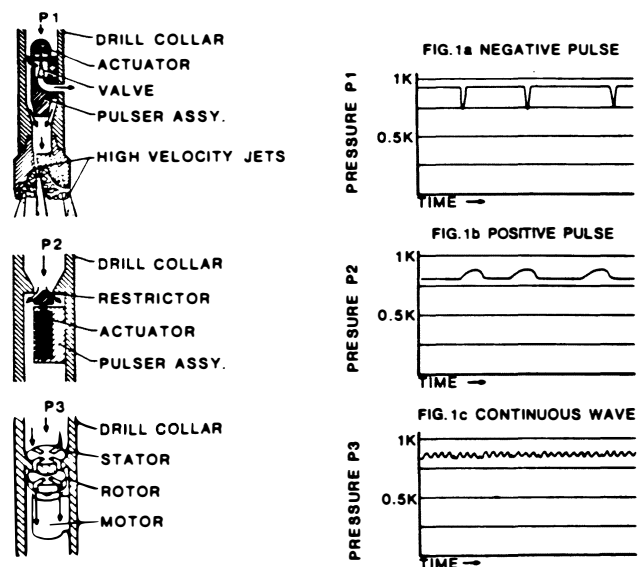
**Fig. 8.59—Typical MWD system (after Gearhart *et al.*<sup>9</sup>).****Fig. 8.60—Basic types of mud pulsers (after Gearhart *et al.*<sup>9</sup>).**

TABLE 8.6—TYPICAL OUTPUT OF A NEGATIVE PULSE SYSTEM

April 10, 1984 15:38 Amoco Production Anschutz Ranch Com #81										P.01 20:34:20 12-31-83			
Drift Angle 1115 MDIP = 67.7586				Tool Face 128 R TMF (X,Y,Z) = 1.1097				Direction 370:OE TGF (A,B) = 0.0239					
T	3,946	X	2,032	EA	0.019	EX	-0.306	V +	24.62	OTF	0.0	INC	1.37
A	2,602	Y	2,040	EB	-0.015	EY	-0.292	V -	-24.60	MDC	15.0	E	RDT 127.98
B	2,526	Z	4,308	EC	-1.001	EZ	1.226	TEMP	74.4			AZI	110.05
C	2,560			TMF (X,Y)			0.4229	DTMP	49.4				

MWDD, MWD, 0183.03.MSC

Field AFE-West Lobe Development  
Survey Method RC  
Elec Number 149  
Mag Number 302  
12-31-83 20:33:25

Well W-20-04  
Survey Number 130

Parameter	DGT 1	DGT 2	DGT 3	Counts
T	7	11	5	3,946
A	5	1	5	2,682
B	4	14	15	2,536
C	5	0	0	2,560
X	3	15	3	2,022
Y	3	15	13	2,040
Z	8	6	10	4,308
Depth				10397.00
Angle				1:15
Direction				S 70:0E
Tool Face				128P
				E 30 A 15
DAC				
DDO			S 70:	O E
DDC				
CL				4.100
TUD				10349.45
RCN/S				152.08 S
RCE/W				243.97 E
SECTION				287.32
DLS/CL				0.12
DLS/100 FT				0.30
PDD			S 60:	O E
TEMP				74.42
TMF				1.1097
TMF (X,Y)				.4229
DIP ANGLE				67.7586
ANG CORR				0: 0
DIR CORR				0: 0
MDC			15:	0 E
OTF				0:00

Courtesy of Gearhart Industries Inc.

Downloaded from http://onepetro.org/books/book/chapter-pdf/2794220/chapter08.pdf by Robert Durham on 26 January 2023

An advantage of the turbine-powered generator, on the other hand, is that it can supply more power to the downhole electronics and valve actuator and is more tolerant of high bottomhole temperatures.

Other developments related to MWD systems are still in the prototype stage: (1) electromagnetic systems, (2) electric cable, and (3) specially designed drill collars and drillpipe to be used in conjunction with electric cable. Advantages of the hard-wired systems are that they can transmit data very rapidly and can communicate with the downhole electronics. The disadvantage is that it is necessary to handle the signal-transmitting electric cables that are suspended in the drillpipe and the slip-ring arrangement on the kelly, which must be used to transmit the data from the rotating kelly to the surface instrumentation.

A new generation of MWD tools that can be run in hole and retrieved with a slick-line unit and overshoot is being developed. Also, other downhole sensors are being used to determine drilling parameters, such as torque and WOB; gamma ray and resistivity logging sensors are used for formation evaluation. Fig. 8.61A and B are typical outputs of an MWD system with drilling and logging sensors.

### 8.5.5 Magnetic Reference and Interference

Surveying instruments that are used to measure the wellbore direction on the basis of the earth's magnetic field must be corrected for the difference between true north and magnetic north. Fig. 8.62 depicts the earth's magnetic field, showing magnetic north and true north. The

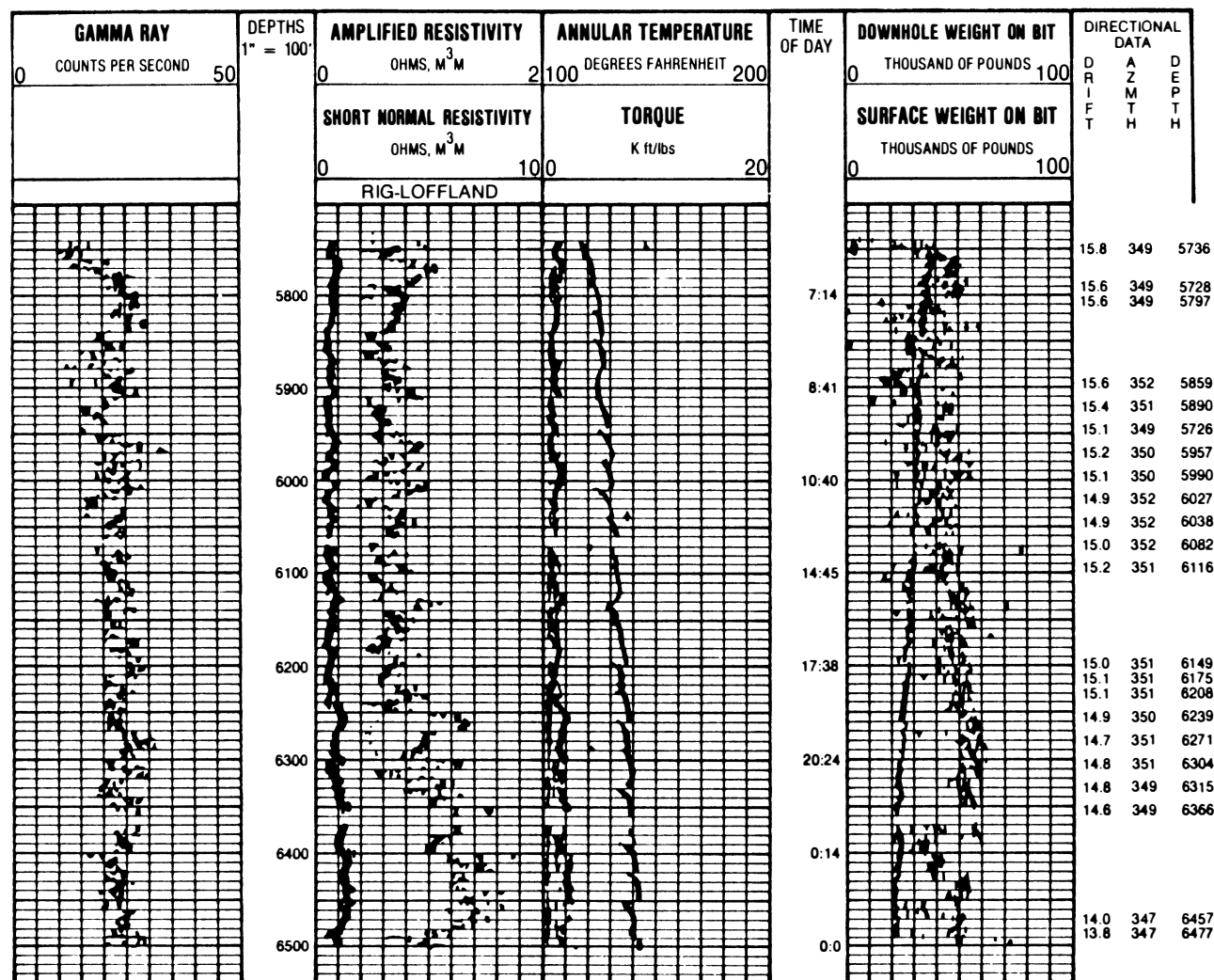


Fig. 8.61A—Typical multisensor MWD output.

compass reacts to the horizontal component of the magnetic field; the reaction decreases when the compass is moved northward. Declination is the angle between magnetic north and true north (see Fig. 8.63). The angle changes with time and depends on the position and surface features of the earth. Fig. 8.64 shows the declination angles for the U.S. The isogonal lines (lines of equal declination) indicate how much correction should be made, depending on where the survey is made (see Table 8.7).

**Example 8.13.** You are drilling a well near Corpus Christi, TX, and the directions are reading all in the SE quadrant. What is the correction for the direction readings?

**Solution.** The declination angle near Corpus Christi is 7.75E. Because it is an east declination, 7.75E must be subtracted from the direction readings.

Besides making a correction for true north, one must take special care when running a magnetic survey to prevent the effects of magnetic interference. Such interfer-

ence can be caused by a proximity to steel collars and by adjacent casing, hot spots in nonmagnetic collars, magnetic storms, and formations with diagenetic minerals.

Nonmagnetic drill collars are used to separate the compass from magnetic fields of magnetic steel above and below the compass and to prevent the distortion of the earth's magnetic field. The collars are of four basic compositions: (1) K Monel 500™, an alloy containing 30% copper and 65% nickel, (2) chrome/nickel steels (approximately 18% chrome and more than 13% nickel), (3) austenitic steels based on chromium and manganese (over 18% manganese, and (4) copper beryllium bronzes.

Currently, austenitic steels are used to make most nonmagnetic drill collars. The disadvantage of the austenitic steel is its susceptibility to stress corrosion in a salt-mud environment. The K Monel and copper beryllium steels are too expensive for most drilling operations; both, however, are considerably more resistant to mud corrosion than austenitic steels are. The chrome/nickel steel tends to gall, causing premature damage to the threads, especially for larger collars that require high makeup torques.

Fig. 8.65 shows the compass located in a nonmagnetic collar between the bit and the steel collars. The nonmagnetic collar does not distort the earth's magnetic field lines and isolates the interference field lines from the sections

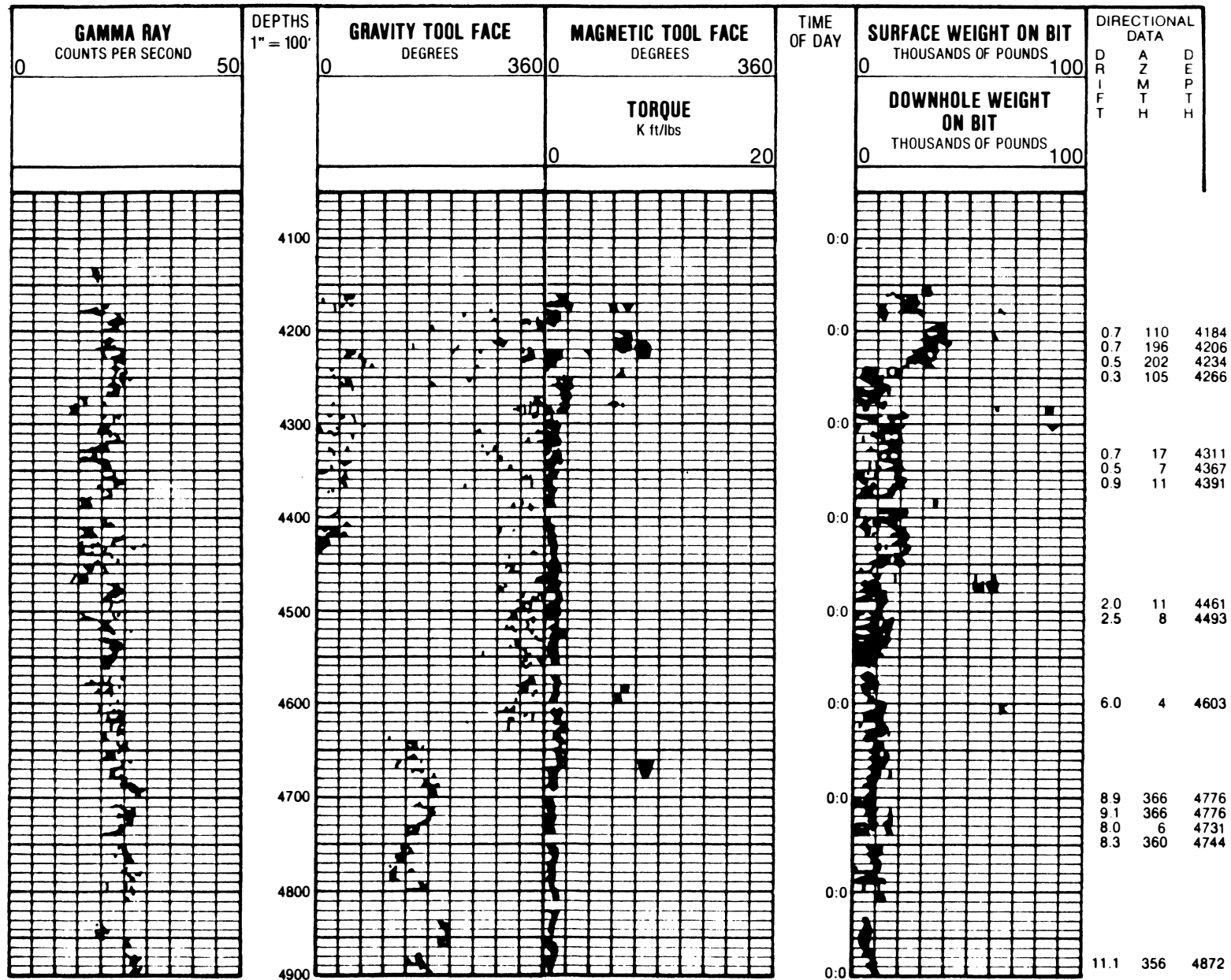


Fig. 8.61B—Typical multisensor MWD output.

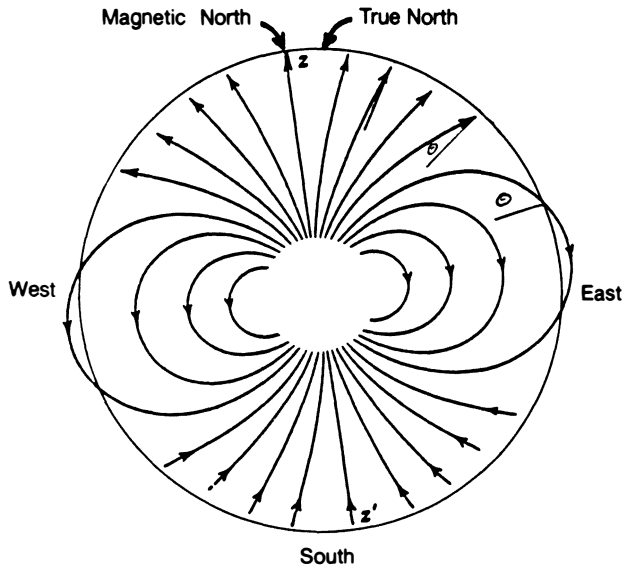


Fig. 8.62—Earth's magnetic field.

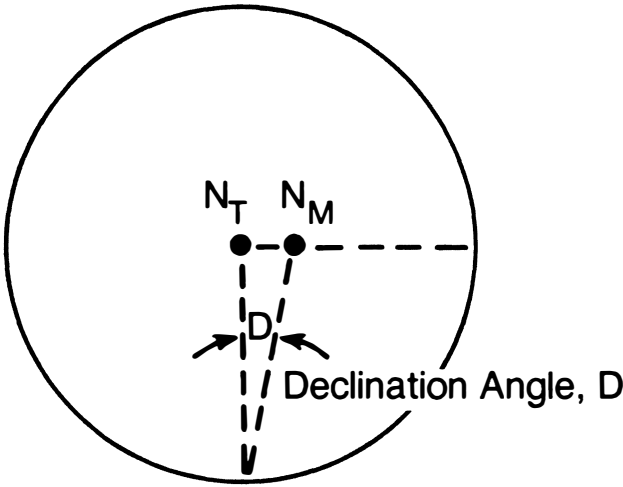


Fig. 8.63—Declination.

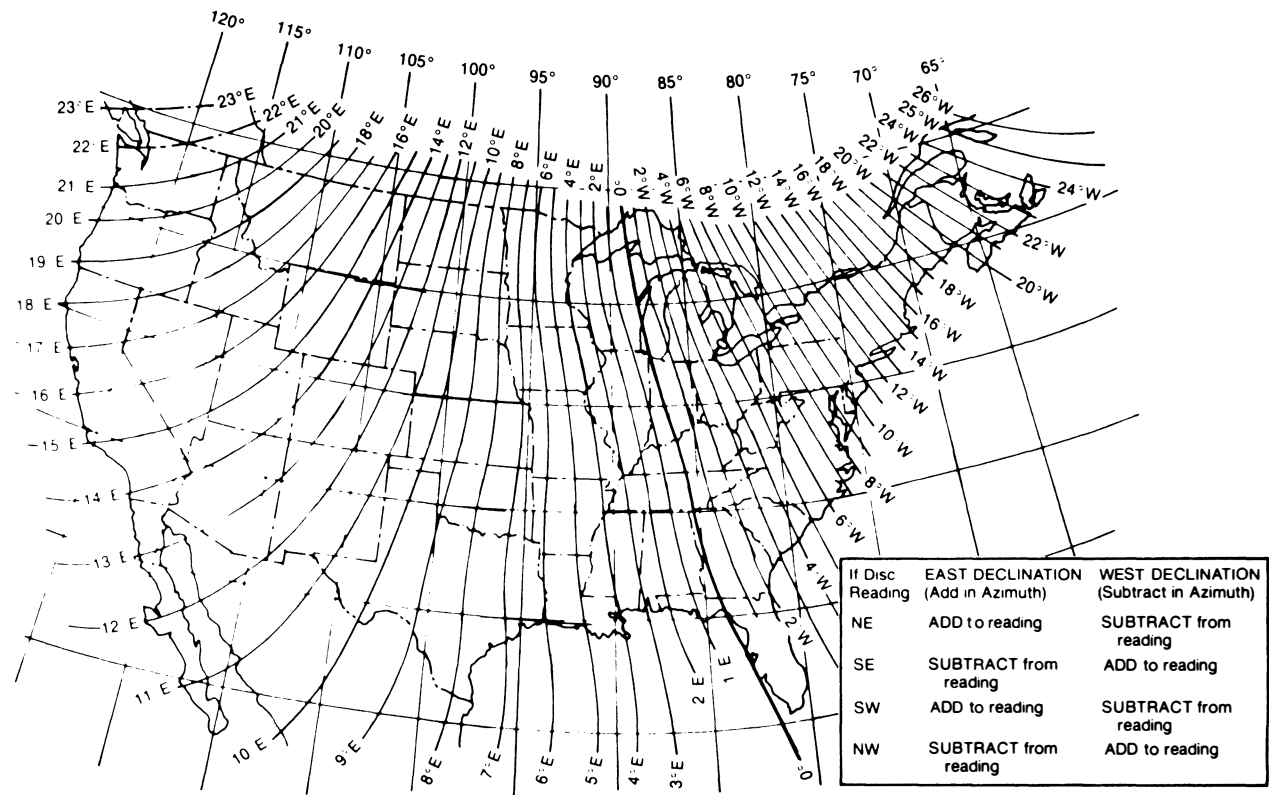


Fig. 8.64—Isogonic chart for the U.S.

**TABLE 8.7—CORRECTION FOR DECLINATION**

Direction Reading	East Declination	West Declination
NE	Add to reading	Subtract from reading
SE	Subtract from reading	Add to reading
SW	Add to reading	Subtract from reading
NW	Subtract from reading	Add to reading

above and below the compass unit. The number of required nonmagnetic collars depends on the location of the wellbore on the earth and the inclination and direction of the wellbore. Fig. 8.66 is a compilation of empirical data that are fairly reliable in selecting the number of nonmagnetic drill collars.

First, a zone is picked where the wellbore is located. Then the expected inclination and direction are used to locate the curve, either A, B, or C.

**Example 8.14.** Select the number of nonmagnetic drill collars needed to drill a well to 55° inclination at a direction of N40E on the north slope of Alaska.

**Solution.** The north slope of Alaska is in Zone III. From the empirical data charts for Zone III at 55° inclination and N40E, the point falls just below Curve B, indicating the need for two nonmagnetic collars with the compass unit 8 to 10 ft below the center.

The effect of the magnetic interference is illustrated further by Fig. 8.67, which shows typical directional errors in the Gulf of Mexico area when 14-, 25-, 31-, and two 31-ft nonmagnetic collars are used for drilling at various inclinations and directions. A well drilled in the Gulf of Mexico with one 31-ft nonmagnetic collar at an inclination of 30° and a direction of S75W has a directional error of approximately 1.3°.

### 8.5.6 Gyroscopic Measurement

A gyroscopic compass is used when magnetic surveying instruments cannot be used because of the magnetic interference of nearby casing or when a borehole with casing already set is being surveyed.

There are various kinds of gyroscopic instruments: single- and multishot gyroscopes, the surface-recording gyroscope, the rate or north-seeking gyroscope, and the Ferranti tool (a highly precise, inertial guidance tool similar to that used on modern commercial aircraft). Of the gyroscopic instruments used for surveying cased boreholes, the multishot is the most common.

Fig. 8.68 depicts a Cardan-suspended horizontal gyroscope. A high-frequency AC current drives a squirrel-cage rotor at a speed of 20,000 to 40,000 rpm; as long as the rotor runs at its reference speed and there are no external forces, the gyroscope stays fixed.

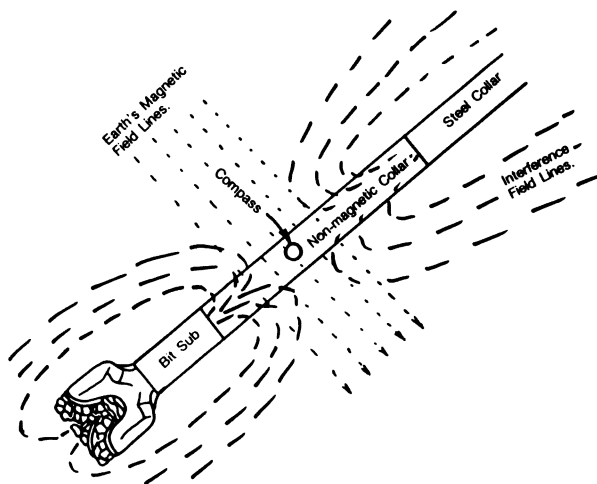
Fig. 8.69 shows a complete gyroscope assembly. The upper part of the tool holds the batteries, camera assembly, and multishot clock. The lower part of the tool contains the inclinometer, the Cardan-suspended gyroscope motor, electronic components for the gyroscope, and the shock absorber.

Even though the gyroscope is not influenced by magnetic interference, its very design introduces unique problems associated with obtaining accurate survey information. If the gyroscope could be supported exactly at its center of gravity, it would be free of influences by external forces. However, such accuracy is practically impossible to achieve. Consequently, a slightly off-center gyroscope will tend to show a force,  $F$ , caused by gravity, in the direction indicated in Fig. 8.68. The gyroscope compensates for the gravitational and frictional forces caused by the bearings by rotating about its vertical axis in a direction commensurate with the right or left side of the downward force on the horizontal gimbal axis. (Fig. 8.68 shows a counterclockwise movement for the force on the right side.) The amount of this rotation determines the accuracy of the gyroscope. The tilt of the horizontal gimbal is corrected by a sensor that detects any departure of the gyroscope from the horizontal axis and sends a signal to a servo motor. This corrects the gyroscope by rotating the vertical axis until the horizontal axis is properly adjusted. The gyroscope is not as rugged as the magnetic instrument and must be handled more carefully. Unlike the magnetic tools, the gyroscope must be run on a wireline. When it is run, the survey stations usually are made going into the hole with a few check shots coming out; this is done mainly to make accounting for drift easier.

Drift is caused by the rotation of the earth. Fig. 8.70 shows the amount of drift per hour, which is dependent on the latitude. At either pole the drift is at a maximum, and at the equator there is no apparent drift. When a gyroscopic survey is run, the effects of drift must always be determined.

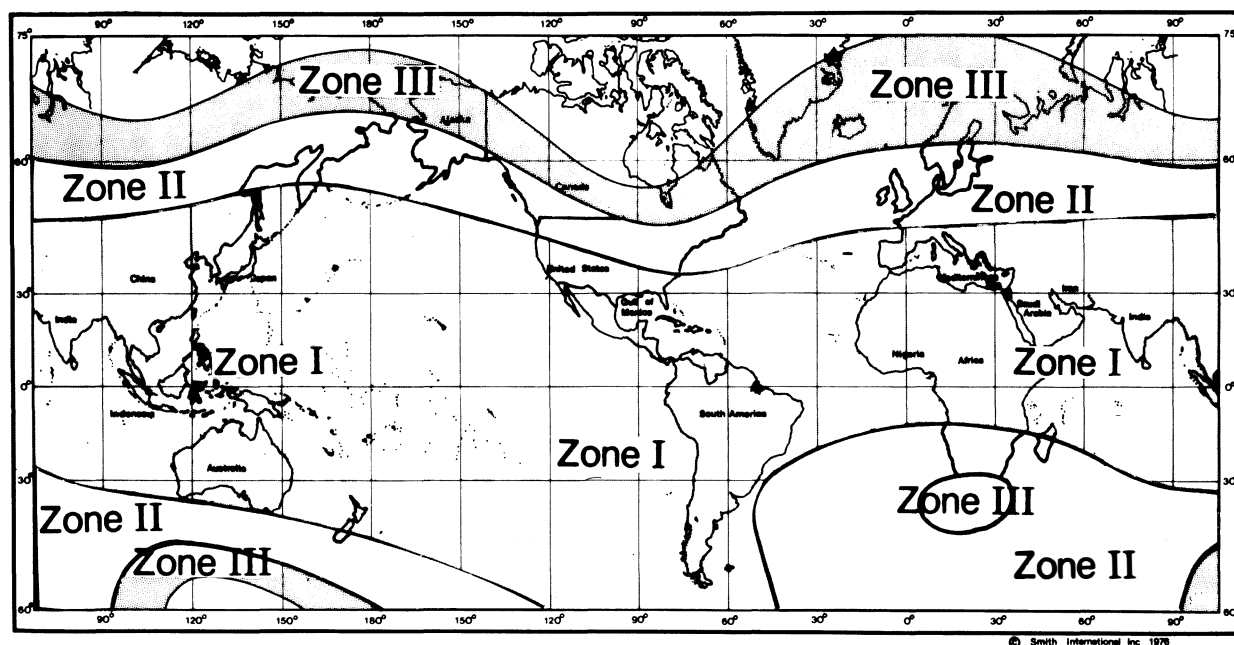
The first step in running a gyroscopic survey is to orient the gyroscope. Fig. 8.71 shows the direction face of a gyroscope. The solid triangle is always pointed at the stake or reference point (see Fig. 8.72). Because the bearing or direction of the reference point is known, it is relatively easy to determine the direction of the “zero” spin axis on the inner scale.

The reference direction is determined by making a sighting from some point over the wellbore, either to a stake fixed some distance from the wellbore or to a constant

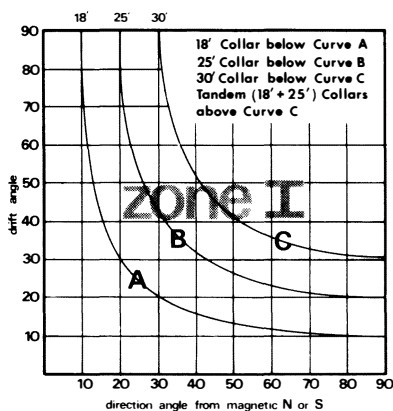
**Fig. 8.65—Source of magnetic interference.**



The Earth's horizontal magnetic intensity varies geographically, and the length of nonmagnetic drill collars used in a bottom hole assembly should fit the requirements of the particular area. This map is used to determine which set of empirical data should be used for a given area.

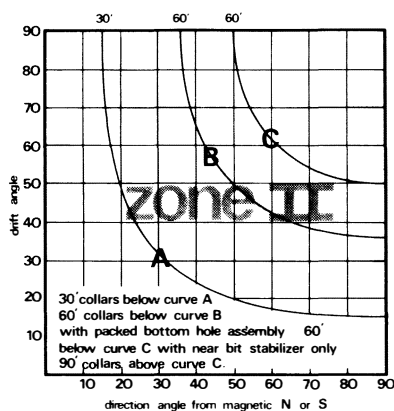


### Empirical Data Charts



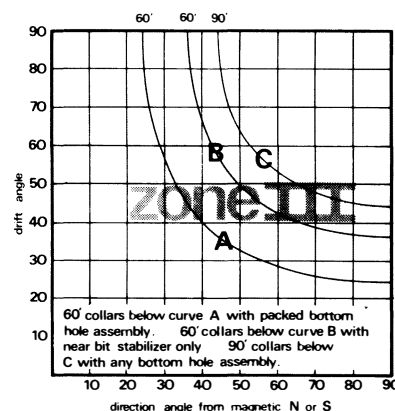
#### Compass Spacing

18' collar: 1' to 2' below center  
25' collar: 2' to 3' below center  
30' collar: 3' to 4' below center  
tandem 18' + 25': center of bottom collar



#### Compass Spacing

30' collar: 3' to 4' below center  
60' collars: at center (curve B)  
60' collars: 8' to 10' below center (curve C)  
90' collars: at center



#### Compass Spacing

60' collars: at center (curve A)  
60' collars: 8' to 10' below center (curve B)  
90' collars: at center

Fig. 8.66—Zone-selection map and charts to determine how many nonmagnetic drill collars are required (courtesy Smith Intl. Inc.).

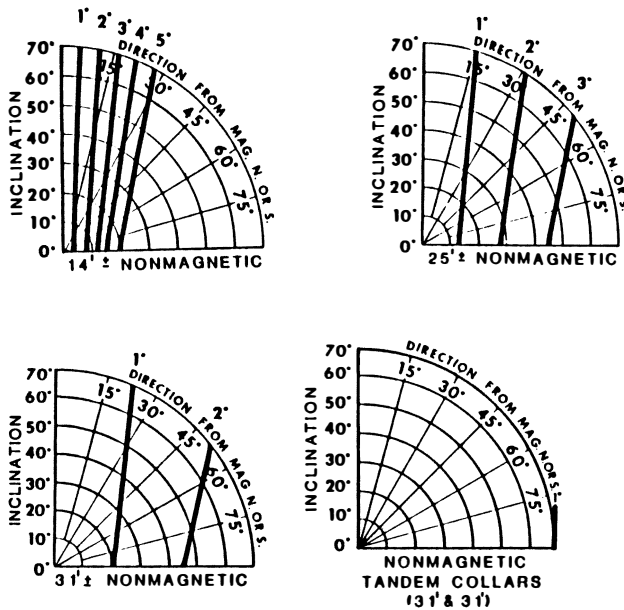


Fig. 8.67—Typical direction errors resulting from magnetic interference—Gulf Coast (courtesy NL Sperry-Sun).

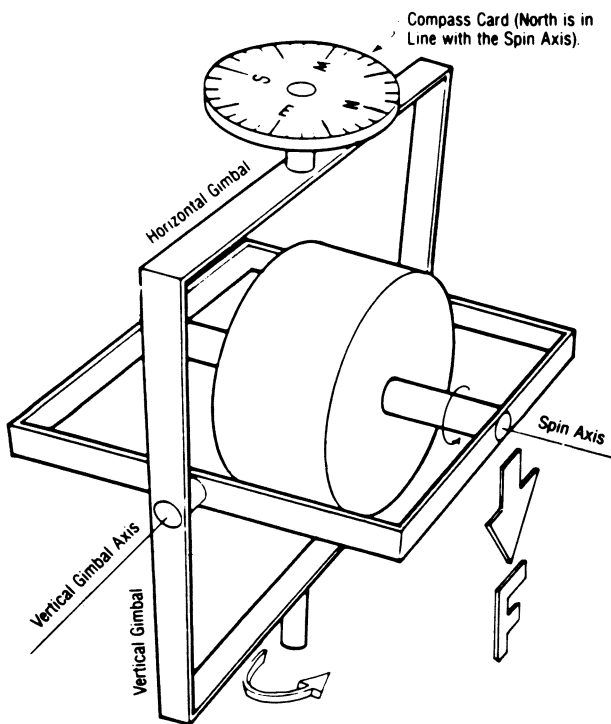


Fig. 8.68—Typical gyroscope.

reference point away from the wellbore, such as a building, another drilling rig, or some other object. Fig. 8.72 shows a typical example of a reference sighting.

When the gyroscope is referenced initially, one of two procedures, depending on the maximum inclination that is expected, is followed. If the inclination is to be less than  $10^\circ$ , the case index (see Fig. 8.71) is lined up with the reference marker—i.e., in the stake direction ( $D_s$ ). Refer to the example presented by Fig. 8.72, in which the stake is N20E or  $20^\circ$ . The gyroscope spin axis—i.e., index setting ( $i_s$ )—is moved until  $20^\circ$  is opposite the case index, thereby aligning the spin axis with north. Below  $10^\circ$  inclination, the 3D instrument correction is negligible. (This will be covered later and is called the intercardinal correction.) Above  $10^\circ$ , the 3D correction must be considered. Again, the case index must be aligned with the reference object, but the index setting is determined by Eq. 8.58.

$$i_s = D_s - \delta_{dr}, \dots \dots \dots (8.58)$$

where  $\delta_{dr}$  is the assumed hole direction.

For example, if the  $D_s$  is S17W or  $197^\circ$  and the  $\delta_{dr}$  is N20E or  $20^\circ$ , the index setting is determined as follows:

$$197^\circ - 20^\circ = 177^\circ.$$

When the case index is aligned with  $177^\circ$ , the gyroscope north will be aligned with the  $\delta_{dr}$  of  $20^\circ$ , and errors resulting from gyroscope tilt will be minimized. Every survey reading should be adjusted for the initial offset of  $20^\circ$ , as well as for drift correction and the intercardinal correction.

After the initial gyroscope orientation, or “gyro orientation” (GO), the tool case is oriented to what is called a “case orientation” (CO). From these initial checks, an initial drift is estimated. The tool is run in the wellbore, making stops for survey pictures. At 10-minute intervals, drift is checked by keeping the tool still for 3 minutes or more. Fig. 8.73 shows a typical drift data sheet for a gyroscope survey. Note that most of the check stops were made going into the wellbore; only two were made coming out.

Once the data are obtained, the drift correction must be made by the construction of a drift correction plot. Fig. 8.74 is a plot for the drift data on Fig. 8.73. The vertical axis, measured in degrees, is the scale for the correction values that will be applied to directional data to correct for drift during the survey. The horizontal scale is the surveying time in minutes.

The range of the vertical axis is determined by taking the correction factor,  $F_C$ , which is determined from Eq. 8.59,

$$F_C = D_s - i_s, \dots \dots \dots (8.59)$$

and by scaling above and below this factor in  $1^\circ$  increments. For the example presented in Fig. 8.74,  $F_C$  is 19.8 (the case was actually indexed at  $177.2^\circ$  rather than the calculated  $177.0^\circ$ ), and the scale ranges from +19.0 to +26.0. The horizontal scale should cover the entire survey from the gyroscope start to end; for this survey, the duration was 101.00 minutes.

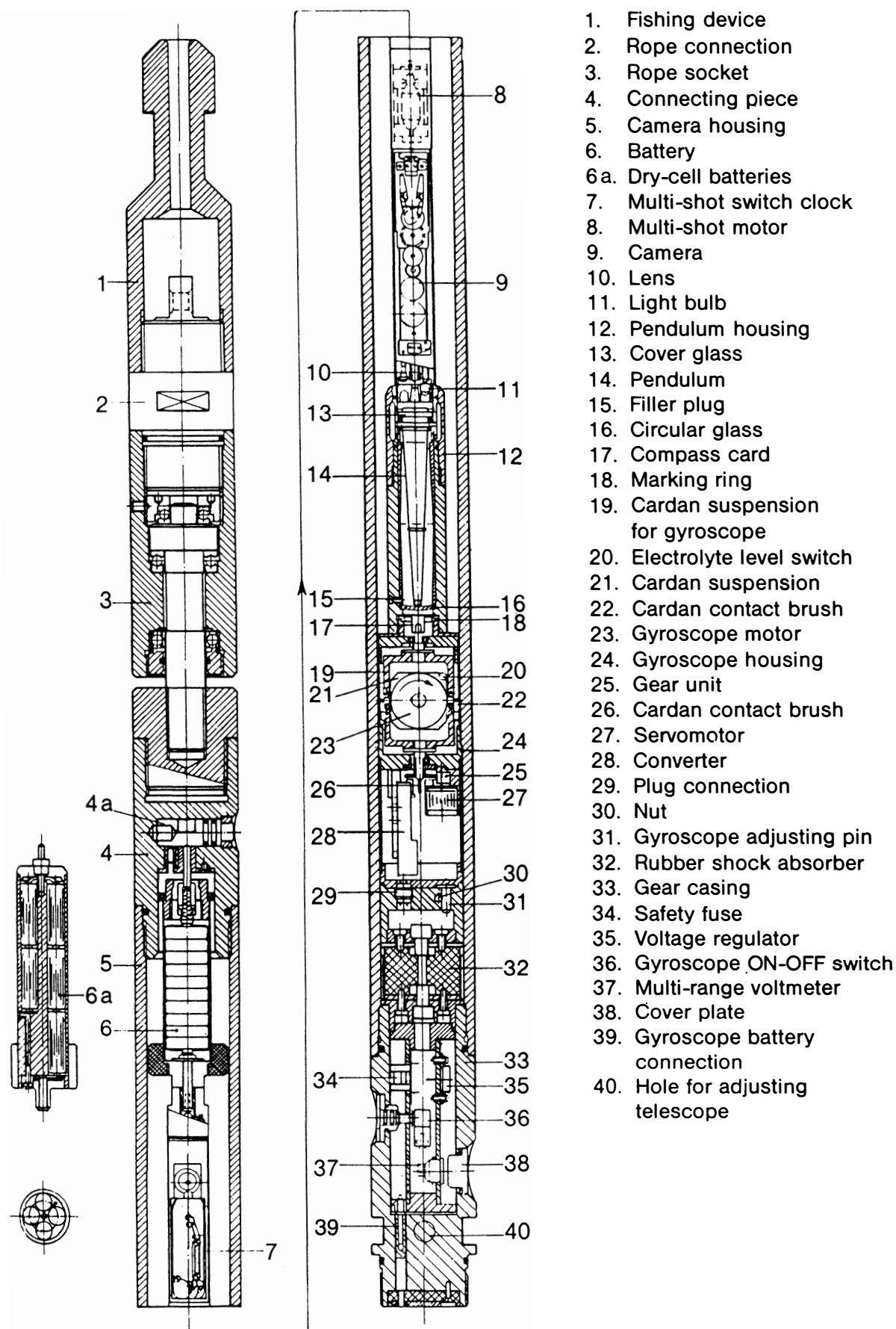


Fig. 8.69—Components of a gyroscope compass instrument (after Eikelberg *et al.*<sup>8</sup>).

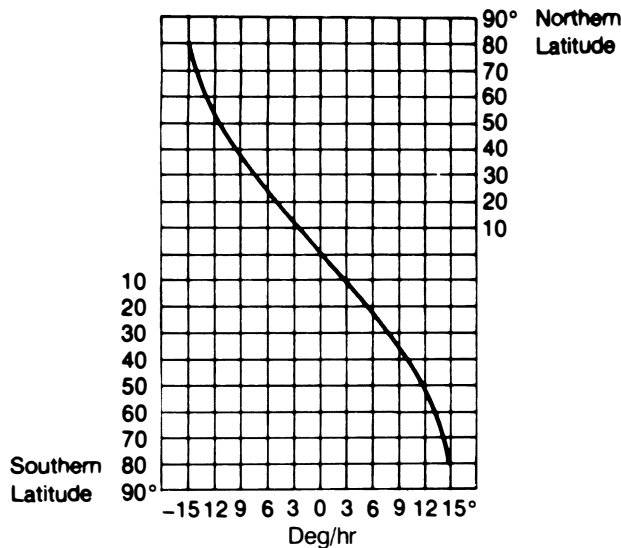


Fig. 8.70—Diagram of apparent drift for every point on Earth, depending on geographical latitude (after Eikelberg *et al.*<sup>8</sup>).

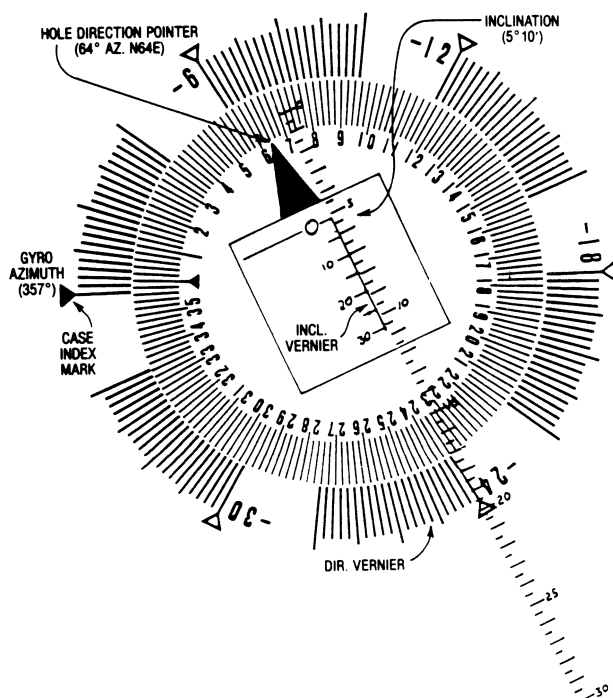


Fig. 8.71—Gyroscope face.

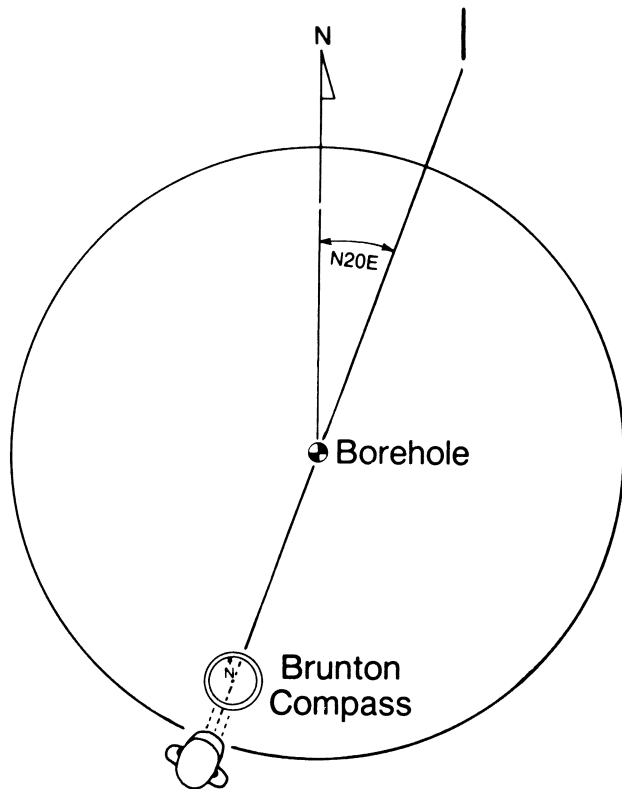


Fig. 8.72—Sighting of reference object.

The sequence of events for the survey begins with turning on the gyroscope at 2 minutes : 20 seconds. At 7 minutes : 20 seconds, the CO is performed. Following that are eight drift-check stops interspersed with the survey stops, which are taken every 100 ft up to 1,815 ft and then coming out of the hole at 1,200 ft, 200 ft, and at the surface. At the end of the survey, a final case orientation is performed before the gyroscope is turned off. (Although it was not done on this survey, rotational shots sometimes are taken at the end of the survey to determine the true wellbore center and to correct any misalignment of the survey tool with the wellbore. The rotational shots are obtained by the lowering of the surveying tool into the wellbore until the stabilizers center the tool in the casing. Six survey records are taken at 60° increments. Once the film is processed, the true center of the survey tool can be determined, and the misalignment errors in inclination and direction can be corrected. Problem 8.47 presents this type of data.)

The first drift check—between 7 minutes : 20 seconds and 9 minutes : 40 seconds—lasts 2 minutes : 20 seconds; this is entered as a block on the time scale. The same procedure is followed for each drift check. Next, a centerline is determined by the marking of the halfway point between each two blocks of drift time. The rate of drift (rate/hour) for each drift check is plotted, starting with the CO point at 7 minutes : 20 seconds, by drawing the correct slope from this point to the point where it intersects the next centerline (15 minutes : 0 seconds). The next slope (+3.6°/hr) is plotted from the new point to the next centerline, and so on.

**DRIFT DATA SHEET - L.R.**

CUSTOMER SMITH OIL CO. RUN NO 1

JOB NO SU 73-0802-1 GYRO NO. 242-LR TYPE 3" L.R. DATE 8-2-73

DATE RUN 8-2-73 READ BY SWG DATE 8-2-73 CHECKED BY E.J.B. DATE 8-4-73

SD TRUE NORTH AZIM 197 IS INDEX NORTH AZIM 177 CF +SD - IS CORRECTION +20 -/+

TIME AZIMUTH

GYRO START 02-00 END 101-00 START 177.0 END 173.1 CORR +3.9 -/0

FILM ORIENT 05-20 99-00 177.2 172.8 CORR +4.4 -/0

CASE ORIENT 07-20 87-20 177.2 172.8 CORR +4.4 -/0

REF PT CHECK TIME 1 INCL DIR BOTTOM TIME 59-20 DEPTH 1815'

DRIFT CHECK NO	DEPTH	TIME	DELTA TIME	GYRO AZIM	INCL	HOLE DIRECT	REAL HOLE DIR.	DELTA HOLE DIR.	RATE / HR. HOLE DIR.
1	0	07-20	140	177.2	0°	—	—	0.1	2.57
		09-40		177.1		—	—		
2	500	20-20		042.0		344.0	344.20	0.2	3.60
		23-40	200	041.8	9°-15'	343.8	344.00		
3	1000	31-20		061.9		344.0	346.24	0.43	8.60
		34-20	180	062.4	31°-20'	344.5	346.67		
4	1400	41-40		067.8		351.0	353.44	0.15	3.00
		44-40	180	067.6	43°-25'	350.8	353.29		
5	1800	52-20		097.7		027.0	20.91	0.57	10.26
		55-40	200	097.0	41°-25'	026.3	20.34		
6	1200	65-00		064.8		346.5	349.19	0.16	2.88
		68-20	200	064.6	37°-20'	346.3	349.03		
7	200	77-40		104.0		020.0	020.00	1.5	15.00
		83-40	360	102.5	0°-15'	018.5	018.5		
8	0	93-40		190.7	0°	316.0	316.0	0	0
		96-20	160	190.7		316.0	316.0		

CASE ORIENT AT 87:20

Fig. 8.73—Typical drift data on surveying data sheet.

The plotted slopes yield a calculated drift curve. The straight line connecting the initial CO and the ending CO is the average drift rate for the survey interval. In this case (Fig. 8.74), it is +4.4° over the 80 minutes between the initial and final CO's.

A straight line is drawn between the initial CO at 7 minutes : 20 seconds and the final CO at 87 minutes : 20 seconds. The difference, *A*, between the two lines is subtracted from the calculated drift curve at each drift correction point. Note that if the average survey line is above the calculated average survey drift rate, the delta increment would be added to the calculated survey points. Connecting each of the new drift-correction points forms the adjusted correction curve, which will be used to correct the observed gyroscopic data for drift.

As mentioned before, whenever the inclination is greater than 10°, a correction must be made to account for

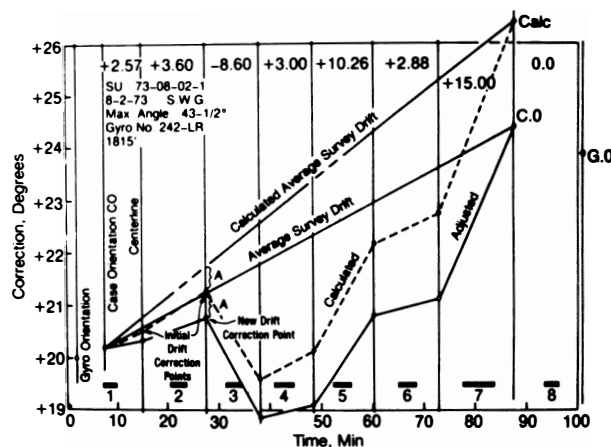


Fig. 8.74—Drift correction plot.



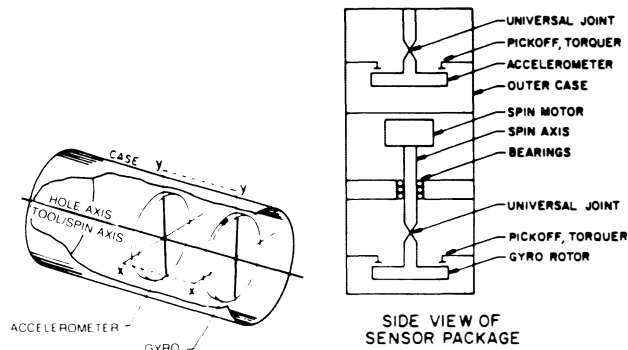


Fig. 8.76—A dual-axis, dynamically tuned rate gyro with dual-axis accelerometer (after Utrecht and deWardt<sup>10</sup>).

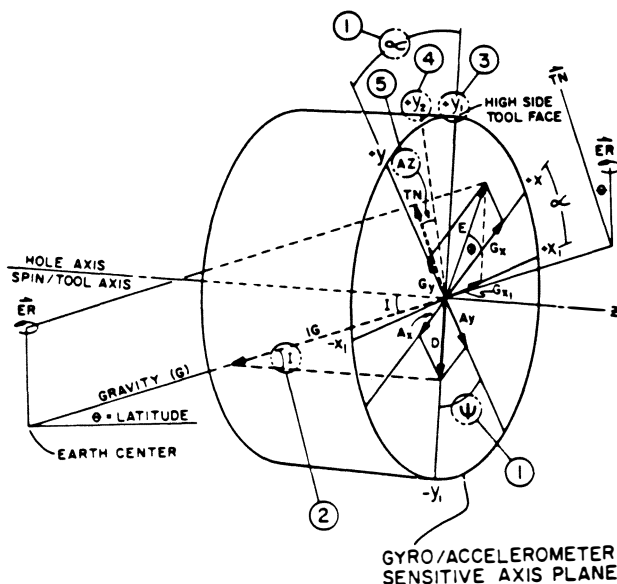


Fig. 8.77A—Vector analysis of combined gyro and accelerometer readings (after Utrecht and deWardt<sup>10</sup>).

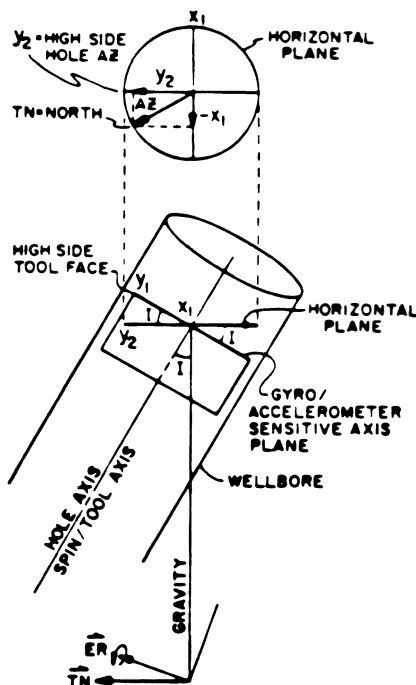


Fig. 8.77B—Mathematically rotating the sensing plane to horizontal creates a compass (after Utrecht and deWardt<sup>10</sup>).

12,000 rpm is reached, the rotor is free to precess at right angles to the tool axis ( $x$ - $y$  planes). The tool always tries to maintain a null position between the rotor and the case with torques and pickoffs. The measured torque necessary to maintain the null position is proportional to the rate of angular motion of the case at right angles to the  $x$ - $y$  spin plane. When the tool is still, the earth's spin causes it to detect the movement of the case, to return the rotor automatically to a null position, and to measure the rate of the earth's rotation.

Figs. 8.77A and 8.77B show the relationship between the earth and the tool axis, which is aligned with the hole axis. Uttecht<sup>10</sup> showed that the orientation of the tool's axis to the gravity vector is given by Eq. 8.61.

$$\Psi = \arctan \frac{A_x}{A_y}, \dots \dots \dots (8.61)$$

where  $\Psi$  is the angle between the  $y$  axis and  $D$ , which is the direction of the low side of the hole.  $A_x$  and  $A_y$  are sensed by the accelerometer. The wellbore inclination can be derived since gravity,  $g$ , is a known vector:

$$\arcsin[(A_x^2 + A_y^2)^{1/2}/g] = \arcsin(D/g). \dots \dots (8.62)$$

Knowing the gravity vector in the  $x$ - $y$  plane, the  $x$ - $y$  plane can be rotated by  $\Psi$  around the  $z$  axis until the  $y$  axis is oriented to the high side of the hole and the  $x$  axis is the horizontal plane.

The gyroscope detects the earth's spin vector,  $ER$ , which is Vector  $E$ :

$$\overline{g_y} + \overline{g_x} = \overline{E}. \dots \dots \dots (8.63)$$

The angle  $\phi$  is defined as the angle between  $E$  and the  $x$ - $y$  plane and by the rotation of  $\Psi$  from  $x$  and  $y$  to  $x_1$  and  $y_1$ ;  $E$  stays constant, and  $\phi + \Psi$  is the angle between  $x_1$  and  $E$ .  $g_{x_1}$  in the horizontal plane can now be determined.

Because the horizontal component of the earth rate,  $T_e$ , is known for a given latitude,  $\theta$ :

$$T_e = ER \cos(\theta). \dots \dots \dots (8.64)$$

The earth-rate component in the horizontal axis is

$$g_{y_2} = (T_e^2 - g_{x_1}^2)^{1/2}, \dots \dots \dots (8.65)$$

and the hole azimuth  $A_z$  is as follows:

$$A_z = \arctan \left( \frac{x_1}{y_2} \right). \dots \dots \dots (8.66)$$

Fig. 8.78 shows the rate gyroscope system, consisting of a power source, printer, CPU, and sonde, which is run on electric wireline. Because drift stops are not required, surveying time is shorter than that required for running a normal gyroscope. As with all gyroscopes, the nearer the poles and the higher the inclination, the less accurate the tool. For a typical rate gyroscope, this starts becoming significant at inclinations exceeding 70° and at latitudes of 70°.

## Gyroscopic Directional Survey System

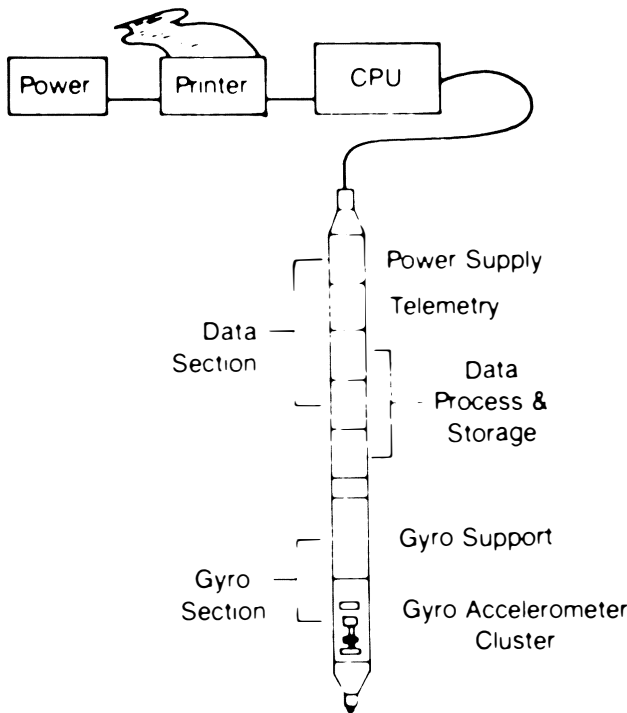


Fig. 8.78—The downhole survey probe and surface equipment (after Utrecht and deWardt<sup>10</sup>).

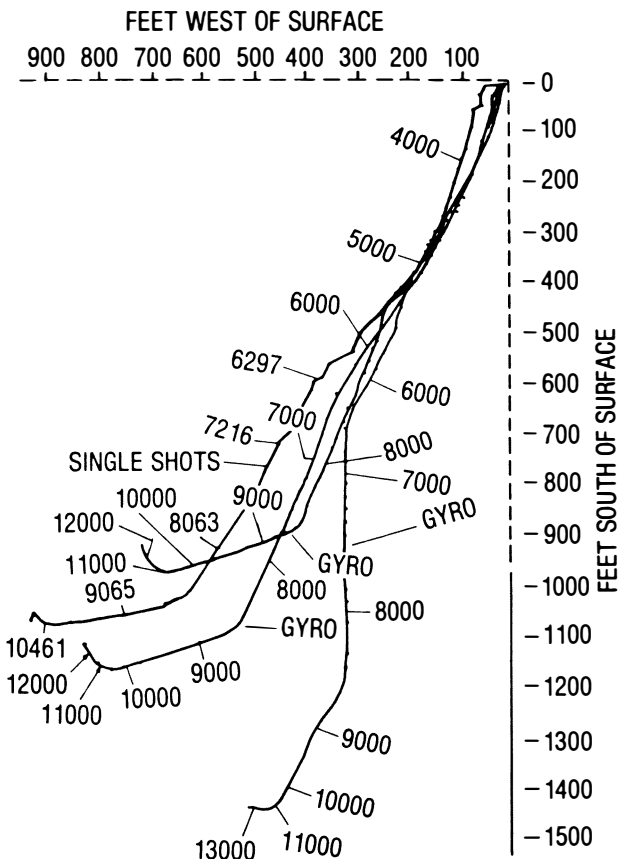


Fig. 8.79—Plan view of wellbore based on four different surveys.

Another type of surface-recording gyroscope uses a gyroscope-stabilized single-axis platform with an orthogonal set of accelerometers to measure direction and inclination. This gyroscope requires short survey station stops of 2 to 4 seconds and conventional 10-minute drift correction checks. A microprocessor performs all the calculations and displays all the results almost instantaneously. The tool is run on electric wireline and is powered at the surface.

### 8.5.7 Surveying Accuracy and the Position of the Borehole

Fig. 8.79 shows the plan view of a borehole that has been surveyed four times: once with magnetic single-shots while the well was being drilled and later with three separate gyroscope surveys. The position of the wellbore becomes particularly relevant if a well blows out and a relief well must be drilled to intercept the wellbore of the blown-out well at a desired point. Knowing the exact position of the wellbore is also extremely important in other applications: (1) in drilling near a cluster of wellbores from a multiwell directional pad or platform where there is a risk of intersecting other wellbores; (2) in intersecting the target exactly for closely spaced infill drilling where sweep efficiencies are critical; and (3) in drilling a sidetrack to ensure that the new wellbore does not re-enter the old wellbore.

Both magnetic and gyroscopic survey instruments have inherent inaccuracies. Magnetic compasses are subject to magnetic interference by the surrounding drillstring and are affected by the position of the survey on the earth. The conventional gyroscope has a drift error because of the spin of the earth and the position of the survey on the earth. Along with the major measuring problems, there may be errors caused by magnetic storms (which can change the north reading), declination variation, hot spots on the nonmagnetic collars, or inaccurate readings. Also, inaccuracy may be caused by compass or inclinometer alignment or by excessive bearing friction that leads to compass and inclinometer drag.

Gyroscope errors can occur from improper orientation at the surface, misalignment of the gimbal assembly, excessive bearing drag, high inclinations (gyroscopes cannot be run at inclinations exceeding 70°), or excessive drifts resulting from lengthy survey times.

All the inaccuracies can be shown to be systematic<sup>10</sup> and can be related to five major categories: compass reference, compass instrument, inclination, misalignment, and depth errors.

Fig. 8.80 is an example of a gyroscopic well survey that shows erratic and excessive drifts. Fig. 8.81 is an example of poor magnetic survey data taken with two different magnetic multishot tools. Which one is correct? Fig. 8.82 is an example of surveys taken off depth.

Fig. 8.83 shows data on a well surveyed first with single-shots, then with an MWD tool, and later with a magnetic multishot at the intermediate casing depth. The multishot surveys indicated that the trajectory would miss the target, while the MWD and single-shot surveys indicated the trajectory was on course. When the BHA and the location of the compass unit of the multishot was checked, the compass was found to be directly opposite a steel clamp-on stabilizer that caused a consistent systematic error in all the directional readings.



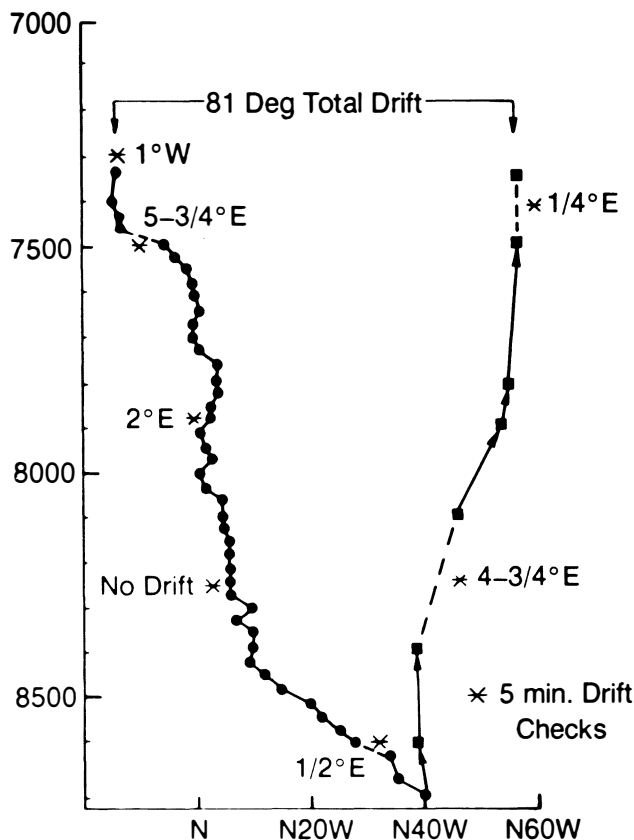


Fig. 8.80—Example of gyro survey with excessive and erratic drift.

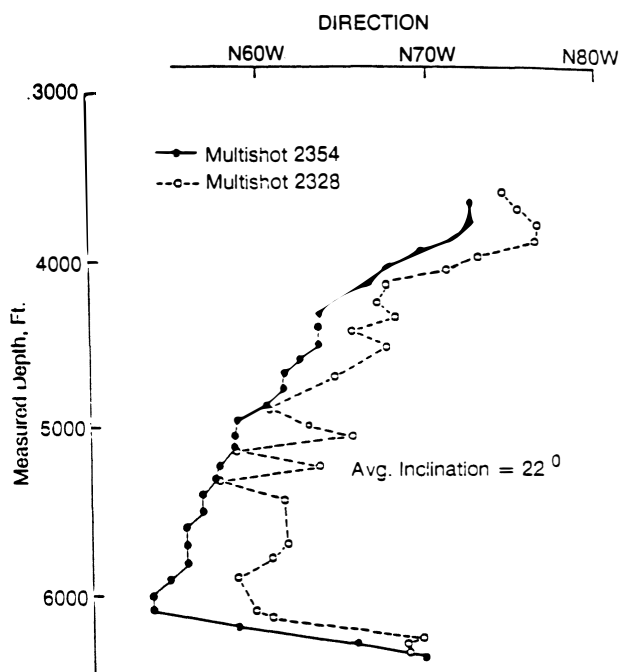


Fig. 8.81—Example of poor-quality survey.

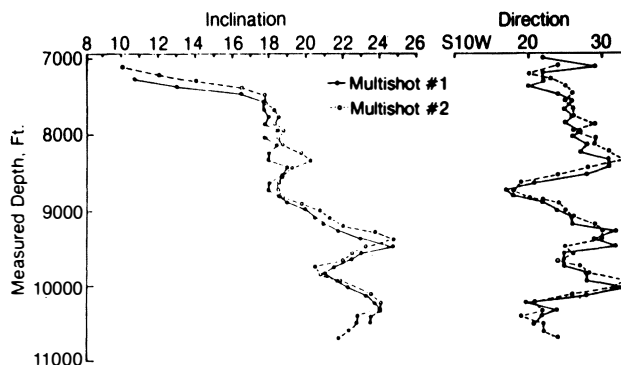


Fig. 8.82—Example of off-depth survey for a Gulf Coast well.

An example of magnetic interference on the compass can be related to an equation derived by Wolfe and deWardt.<sup>11</sup>

$$\Delta C = \sin \alpha \sin \epsilon \left( \frac{\Delta M_E}{M_F} \right), \dots \dots \dots (8.67)$$

where  $\Delta C$  is the actual compass deflection,  $\alpha$  is the inclination,  $\epsilon$  is the azimuth, and  $M_F$  is the magnetic field, which varies between  $40 \mu\text{T}$  at the equator and  $0 \mu\text{T}$  at the north and south poles.  $\Delta M_E$  is the strength of the magnetic error field. Eq. 8.67 implies that the greater the inclination and the more east or west the direction, the higher the change in  $\Delta C$ . Anything that increases the magnetic error field, such as hot spots or improper positioning of the compass in the nonmagnetic collars, increases  $\Delta C$ . Moving south or north from the equator also increases  $\Delta C$ . Maximum deflections occur at greater inclinations east or west in the northern and southern latitudes, such as in the North Sea and Alaska and toward the South Pole.

**Example 8.15.** Calculate the azimuth error for a north slope well in Alaska where the wellbore is at  $60^\circ$  inclination and N70E. Assume a magnetic strength of  $10.2 \mu\text{T}$  for the north component and  $2.0 \mu\text{T}$  because of the collars and drillstring.

**Solution.** The azimuth error is calculated with Eq. 8.67:

$$\Delta C = \sin(60^\circ) \sin(70^\circ) \left( \frac{2}{10.2} \right) = 0.1596.$$

$$\text{Azimuth error} = 0.1596 \text{ rad.}$$

$$57.295^\circ/\text{rad} = 9.14^\circ.$$

The maximum survey error can be estimated with Fig. 8.84, which is based on typical measuring for good and poor gyroscope surveys and good and poor magnetic surveys (east/west). Table 8.9 shows the typical values used to construct Fig. 8.84.

TABLE 8.9—TYPICAL VALUES FOR MEASURING ERRORS

	Relative Depth $\epsilon$ $10^{-3}$	Misalignment $\Delta I_m$ (degrees)	True Inclination $\Delta I_{to}$ (degrees)	Reference Error $\Delta C_1$ (degrees)	Drillstring Magnification $\Delta C_2$ (degrees)	Gyro Compass $\Delta C_3$ (degrees)
Good Gyro	0.5	0.03	0.2	0.1	—	0.5
Poor Gyro	2.0	0.2	0.5	1.0	—	2.5
Good Magnification	1.0	0.1	0.5	1.5	0.25	—
Poor Magnification	2.0	0.3	1.0	1.5	$5.0 \pm 5.0$	—
Weighting	1	1	$\sin I$	$\sin I$	$\sin I \sin A$	$(\cos I)^{-1}$

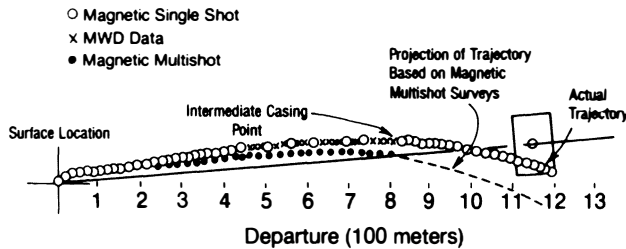


Fig. 8.83—Example of surveying a hole with a magnetic multishot before running intermediate casing where the multishot does not agree with single-shot and MWD surveys.

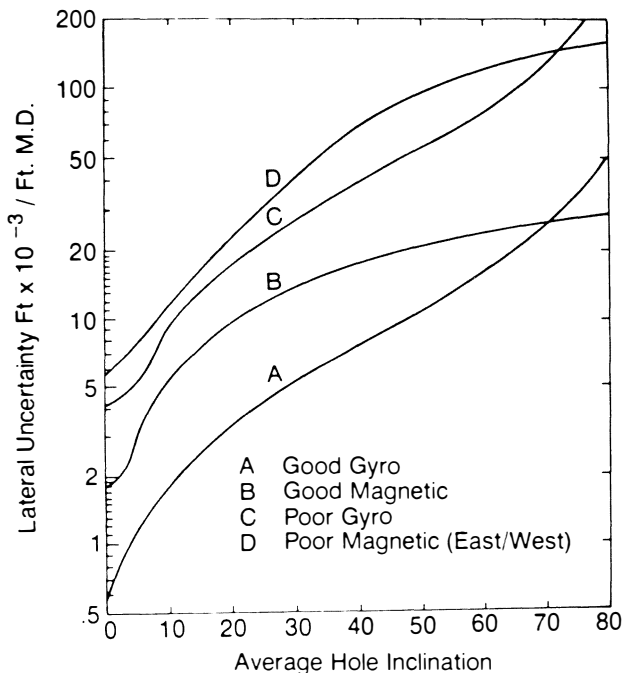


Fig. 8.84—Chart to determine lateral uncertainty for typical good and poor magnetic and gyro surveys (after Wolff and deWardt<sup>11</sup>).

**Example 8.16.** Determine the maximum expected survey error for the well described below. Assume that a good and a poor magnetic survey are available.

Well's inclination:

0 to 5,000 ft	vertical
5,000 to 6,500 ft	0 to 30° (constant build)
6,500 to 10,000 ft	30° average

**Solution.** According to Fig. 8.84, the first interval from 0 to 5,000 ft shows 0.0018 ft/ft MD; 5,000 to 6,500 ft is 0.0075 ft/ft MD, and 0.014 ft/ft MD for 30° inclination. The following is the maximum survey error:

$$\begin{aligned}
 5,000 \text{ ft} \times 0.0018 \text{ ft/ft MD} &= 9 \text{ ft} \\
 1,500 \text{ ft} \times 0.0075 \text{ ft/ft MD} &= 11 \text{ ft} \\
 3,500 \text{ ft} \times 0.0140 \text{ ft/ft MD} &= 49 \text{ ft} \\
 &\underline{\hspace{1.5cm}} \\
 &69 \text{ ft}
 \end{aligned}$$

With this method, the error for the poor survey is 193 ft.

As stated previously, surveying errors appear to be systematic, not random. Data from each survey station form an ellipsoid reflecting the amount of depth, inclination, and directional error. Fig. 8.85 shows the ellipsoids at three different depths for the MWD survey on the basis of the ellipsoids. It was determined that the real wellbore was south of the wellbore derived from the conventionally calculated surveys. Later, it was found that the actual well did come within a few feet of the blowout wellbore at this depth. In this case, the single-shot surveys predicted the most accurate trajectory.

The mathematics needed for the calculation of the three axes of the ellipsoid are presented by Wolfe and deWardt.<sup>11</sup>

To minimize surveying errors, all tools should be test-stand calibrated over the range of inclinations and directions expected. All multishots should be run back to the highest point possible for comparison, and all inclination and directional data should be plotted over the overlapped sections to assure repeatability.

## 8.6 Deflection Tools

Sec. 8.4 explained how to make a controlled trajectory change. Whether a whipstock, mud motor, or jetting bit is used, the principles for determining the total angle change, dogleg severity, new inclination angle, direction, and tool-face setting are all the same. Once a trajectory is reached, there are various ways of implementing it. One can use a positive displacement motor (PDM) with a bent

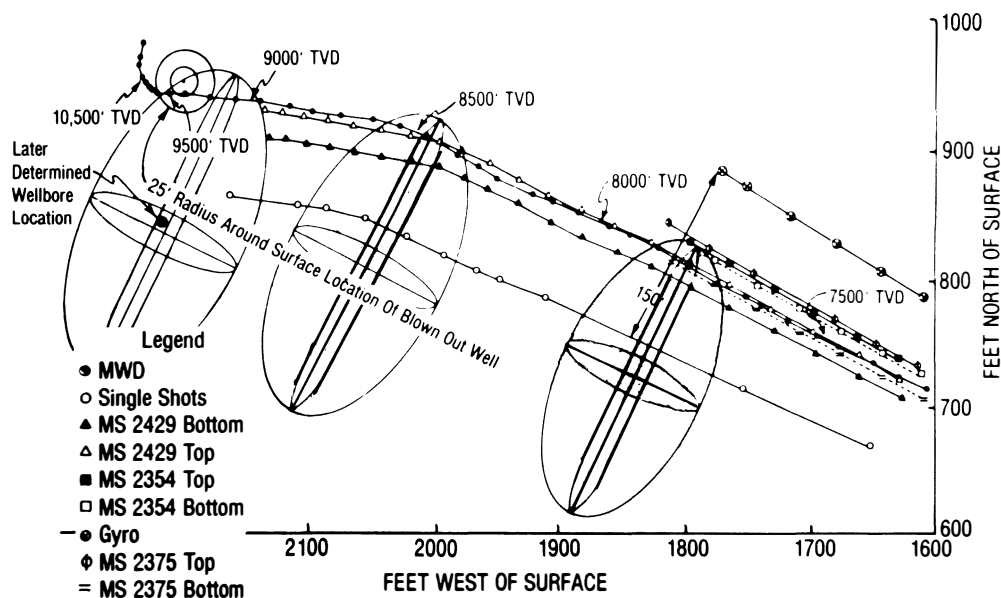


Fig. 8.85—Plan view of various surveys run in a relief well designed to intersect a blowout.

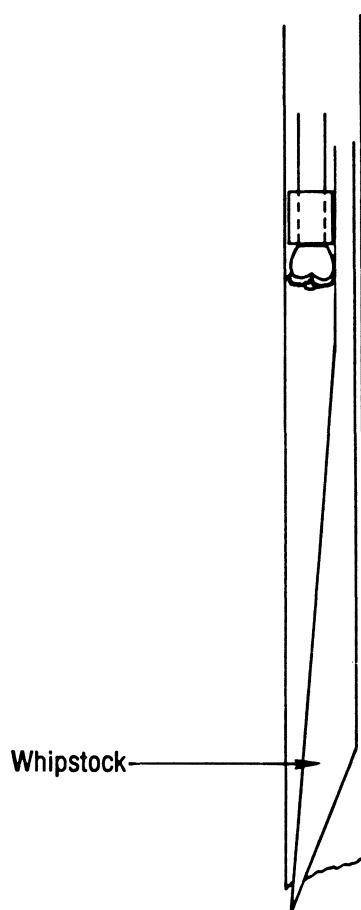


Fig. 8.86—Openhole whipstock.

sub or bent housing and regular tricone bits or diamond or polycrystalline diamond bits. Instead of a PDM, a mud-powered turbine can be used with a bent sub or an eccentric stabilizer. A whipstock or a jetting bit can also be used.

This section describes various tools used in changing trajectories and the principal factors affecting their use.

### 8.6.1 Openhole Whipstocks

The whipstock was the first widely used deflection tool for changing the wellbore trajectory. Fig. 8.86 shows a typical openhole whipstock, and Fig. 8.87 is a diagram of the principle of operation. A whipstock is selected according to the wedge needed to effect the desired deflection. A bit that is small enough to fit in the hole with the whipstock is then chosen; at the start of the running mode, the bit is locked to the top of the whipstock. When the whipstock is positioned at the kick-off depth, whether it is the total depth of the wellbore or the top of a cement plug, it is carefully lowered to bottom, and the center line of the toe is oriented in the desired direction by a conventional nonmagnetic collar with a mule-shoe sub and by a single-shot survey. With the whipstock assembly oriented, enough weight is applied to the toe of the wedge so that it will not move when rotation begins.

Additional weight is applied to shear the pin that holds the drill collars to the wedge; then rotation can begin. Forcing the bit to cut sideways as well as forward, the wedge deflects the bit in an arc set by the curvature of the whipstock. When the bit reaches the end of the wedge, it ordinarily continues in the arc set by the wedge. Drilling continues until the top of the whipstock assembly reaches the stop (Fig. 8.87). Fig. 8.88 (a through d) depicts the operation.

The entire whipstock assembly is pulled, and a pilot bit and hole opener are run to the kick-off point. The wellbore is enlarged to the original hole size, and the assembly is pulled again. The drilling BHA finally is run, and normal drilling is resumed (Fig. 8.88 e and f).

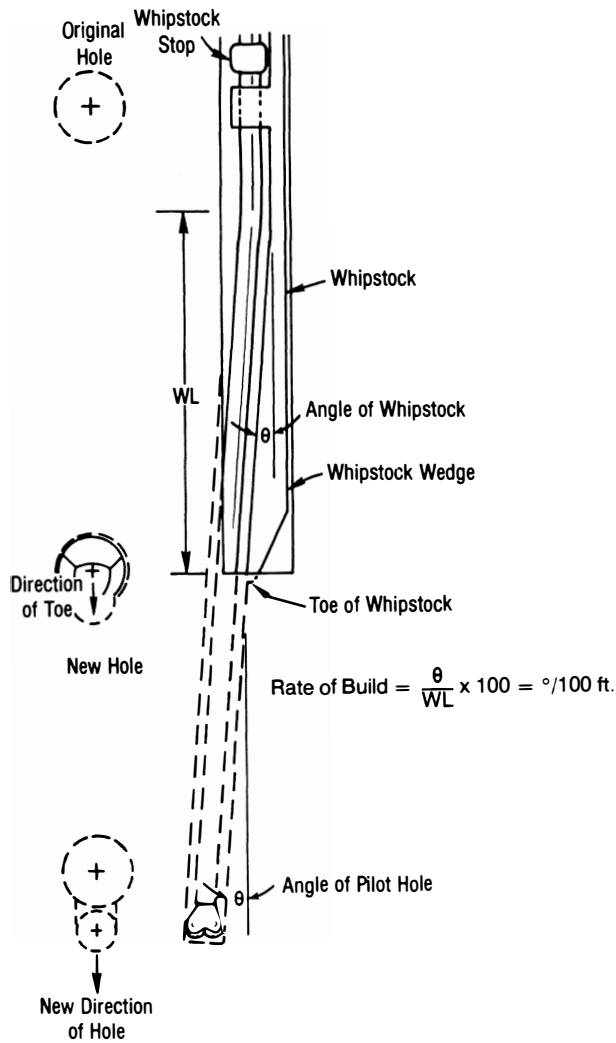


Fig. 8.87—Diagram of retrievable whipstock operation.

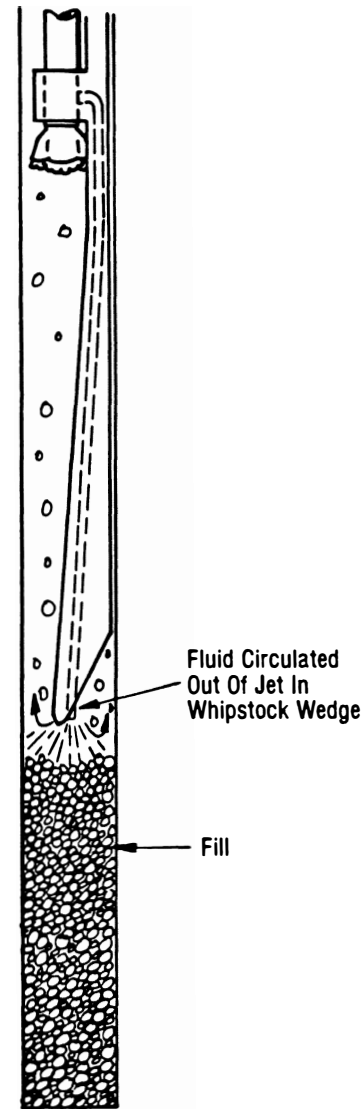


Fig. 8.89—A jetting whipstock.

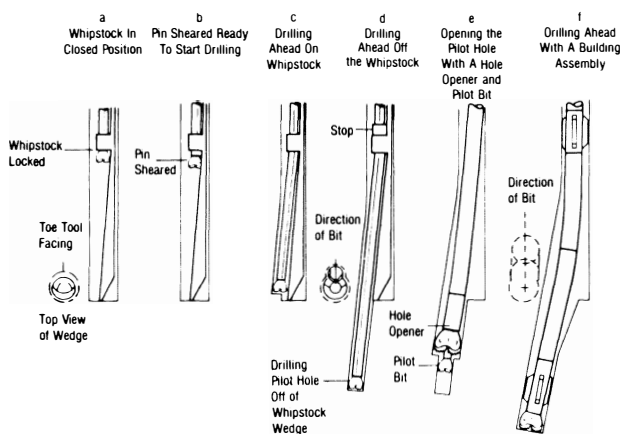
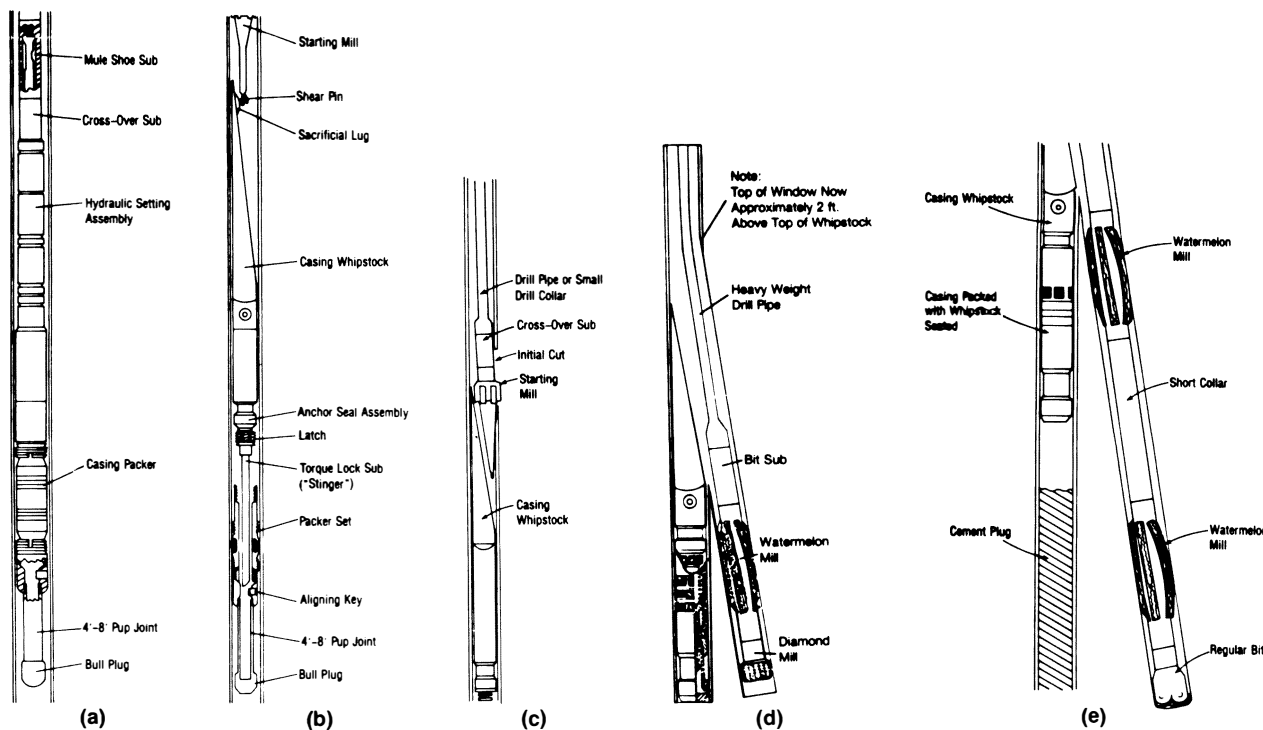


Fig. 8.88—Drilling with a retrievable whipstock.

The foregoing description is of an ideal kick-off with an openhole whipstock. Many factors, however, can cause the whipstock operation to deviate from the norm. If the bottom of the hole is covered with fill and the whipstock is set in the fill, a number of complications can occur. The unstable bottom can cause the toe of the whipstock to rotate when drilling starts. The fill tends to wash away, causing the bit to slide down the side of the wellbore and the entire whipstock assembly to rotate. Even if a kick-off is achieved with fill in the hole, entering the deviated borehole with the drilling assembly is usually impossible because the fill washes away and lowers the bottom of the hole. Fig. 8.89 is a diagram of a jetting whipstock that can be used to jet out the fill so that the whipstock can proceed to the bottom of the hole and, then, can seat properly.

Even when the toe is firmly seated on the bottom of the hole, the driller must be careful not to unseat the toe, to change the orientation, or to rotate the bit off the wedge. The critical stage occurs when the bit leaves the end of the whipstock wedge. If the rock is too soft and the circulation too high, the bit can lose the curvature the whipstock has started and continue drilling nearly straight.



**Fig. 8.90**—(a) Setting the packer and whipstock seat. (b) Locking the whipstock into the packer assembly. (c) Cutting the casing with the starting mill. (d) Cutting a window in the casing with a side packing mill. (e) Drilling ahead with a tricone bit through a window in the casing.

Openhole whipstocks are almost never used because changing the trajectory is very complicated and because too much experience is required to run the tools properly. In certain circumstances, however, they are still useful, such as in very hard rocks and in wellbores where temperatures are too high for mud motors.

### 8.6.2 Casing Whipstocks

Another type of whipstock is the casing whipstock. Unlike the openhole whipstock, the casing whipstock is used routinely to sidetrack out of cased wellbores. Cagle *et al.*<sup>12</sup> described the most common technique for the use of a casing whipstock. A permanent packer is run to the desired kick-off point either on wireline (for a blind kick-off) or on drillpipe carrying a mule-shoe sub for orientation. Once the packer is set, a retrievable starting mill is run on the whipstock. The whipstock assembly is locked into the packer (see Figs. 8.90a and b). Weight is applied, shearing the starting mill off the whipstock (Fig. 8.90c). The starting mill is used to start a cut in the casing and then is pulled out of the hole. A sidetracking mill or diamond bit replaces the starting mill (Fig. 8.90d). The whipstock forces the sidetracking bit through the side of the casing, making a window about 8 to 12 ft long. Once outside the casing, the same bit drills a pilot hole. Then that bit is pulled and replaced with a taper mill and a BHA of string and watermelon mills to make the casing window large enough to accommodate a conventional BHA. After the window is dressed, the assembly is pulled and the taper mill is replaced with a conventional tricone or drag bit (Fig. 8.90e). The conventional bit and watermelon mill assembly are used to drill ahead. When the hole is tripped out, the watermelon mills can be used to ream

the window to ensure that it is large enough to accommodate similar BHA's with conventional stabilizers.

The most common method of sidetracking out of casing, especially when considerable drilling is to follow, is to mill a length of casing with a section mill and then to divert the trajectory with a mud motor and bent sub or bent housing.

When considering the use of a section mill, one should first check for cement behind the portion of casing to be milled. If there is no cement or the cement bonding is poor, milling problems are inevitable. The rotating mill causes the unsupported casing to vibrate, which slows progress, and the mill may torque up and jam. Either the section must be cemented remedially, or another section with better cement bonding must be selected.

Assuming that the casing is well cemented, the section chosen should start immediately below a casing coupling, thereby minimizing the number of couplings that must be milled in a normal 30- to 60-ft milling operation.

Fig. 8.91 shows a section mill with the arms retracted. Fig. 8.92 a through c shows the operation, in which a section mill is run into the hole, the arms are extended, and the casing is milled. At the bottom of the milled section, a cement plug is set to isolate the new open hole from the casing below it. After the appropriate section is milled, a mud motor with a deflecting device is used to leave the old wellbore and start a new one (Fig. 8.92 d and e).

Generally, the more drilling in the new wellbore, the longer the section milled. The disadvantage of the casing/whipstock method is that the casing window is too short. Numerous trips and long hours of rotation can wear or damage the casing, sometimes making it difficult to trip out the BHA through the casing window.

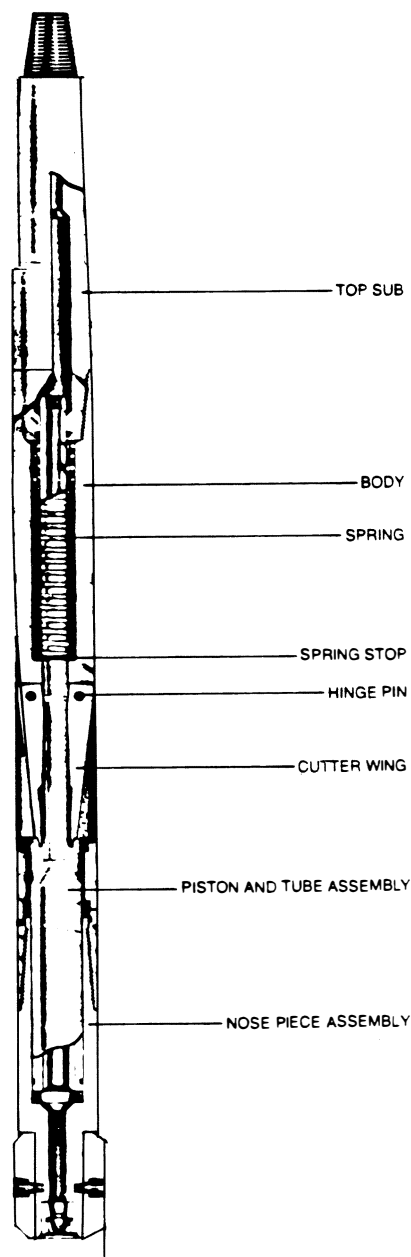


Fig. 8.91—Typical section mill with arms retracted (courtesy of A-Z Intl. Tool Co.).

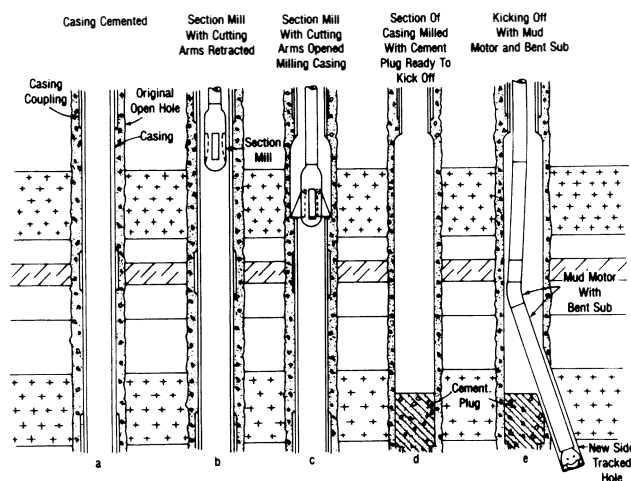


Fig. 8.92—Using a section mill to prepare for a kick-off.

### 8.6.3 Jetting Bits

Another effective means of changing the trajectory of a borehole is jetting. A bit with one large nozzle (see Fig. 8.93) is oriented to the desired tool-face setting. The mule-shoe sub is oriented in the same line as the jetting nozzle.

In jetting, the hydraulic energy of the drilling fluid erodes a pocket out of the bottom of the borehole. The drilling assembly is advanced without rotation into the jetted pocket for a distance of 3 to 6 ft. Rotation is started and conventional drilling proceeds until a depth of 20 to 25 ft is reached; at that point, a survey is taken to evaluate the last jetting interval. If more trajectory change is required, the jetting assembly is oriented again, and the jetting sequence is repeated. This procedure is continued until the desired trajectory change is achieved. Fig. 8.94 shows a typical jetting operation.

Geology is the most important influence on where jetting can be used; next in importance is the amount of hydraulic energy available for jetting. Sandstones and oolitic limestones that are weakly cemented are the best candidates for jetting. Unconsolidated sandstones and some other types of very soft rocks can be jetted with some degree of success. Very soft rocks erode too much, making it difficult to jet in the desired direction; when rotation begins, the stabilizers cut away the curved, jetted section and return to a nearly vertical well path. Sometimes this problem can be overcome by the use of smaller drill collars in the jetting assembly than those normally used in a hole of the same size. Another solution is to reduce the circulation rate to a level at which a regular pocket can be eroded.

Even though shales may be soft, they are not good candidates for jetting. Most medium-strength rock is too well cemented to jet with conventional drilling rig pumps, so it limits the depth to which jetting can be applied. Higher pressures and more hydraulic energy can extend the depth to which jetting is practical.

The principal advantage of jetting is that the same BHA can be used to change the trajectory and to drill ahead. If the geology is conducive, jetting is more economical than running a mud motor. An important secondary advantage of jetting is that slight trajectory alterations can be made after the original trajectory has been established.

Typically, jetting operations take place in wells that have alternating sandstones and shales. A two-cone jetting bit and a single-stabilizer building assembly are used for the operation. The kick-off depth is selected, and the large nozzle is oriented in the general direction desired. To set and to maintain a specific direction at very low inclinations (less than  $1^\circ$ ) are virtually impossible. The first jetting operation is primarily to build the inclination to  $1$  to  $2^\circ$ . A drilling break usually indicates a sandstone; in sandstone at shallow depths, jetting an interval of 3 to 6 ft in 3 to 10 minutes is possible. The harder the rock is or the more shale there is in the rock, the slower the jetting will be. If the jetting procedure is not one that is familiar in that particular drilling area, normal drilling is resumed until another drilling break signifies a possible formation for jetting. After jetting begins a curve, normal drilling is continued until a survey can be run to evaluate the success of the previous jetting. When the inclination exceeds  $1$  to  $2^\circ$ , another jetting interval in which the jetting nozzle can be oriented to achieve the desired

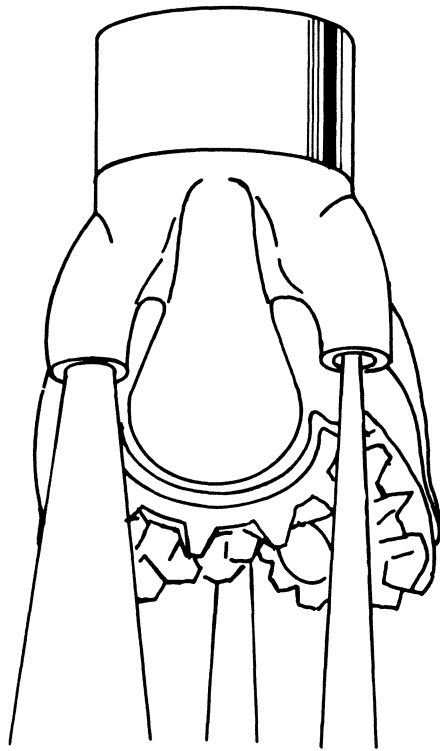


Fig. 8.93—Jetting bit.

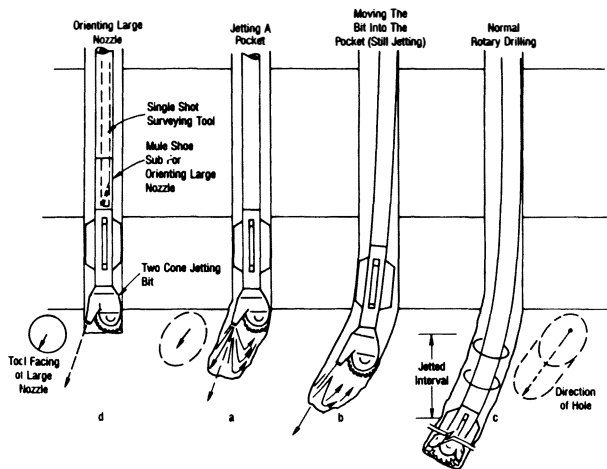


Fig. 8.94—Jetting a trajectory change.

direction and inclination is found. Sometimes this can require as many as four attempts. Hence, a number of jetting intervals should appear over a few hundred feet.

A major drawback to jetting is that the formation must be favorable at a shallow depth or in the desired kick-off interval; otherwise, the technique is no better than the use of a mud motor with a deflecting device. Another problem is that if jetting is continued too long without conventional drilling being resumed, large doglegs can be created. However, if only short intervals are jetted and surveys cover at least 30 ft, the dogleg problem is controllable. If excessive curvature is detected within 30 ft, the borehole can be reamed with the drilling assembly to try to remove the curvature.

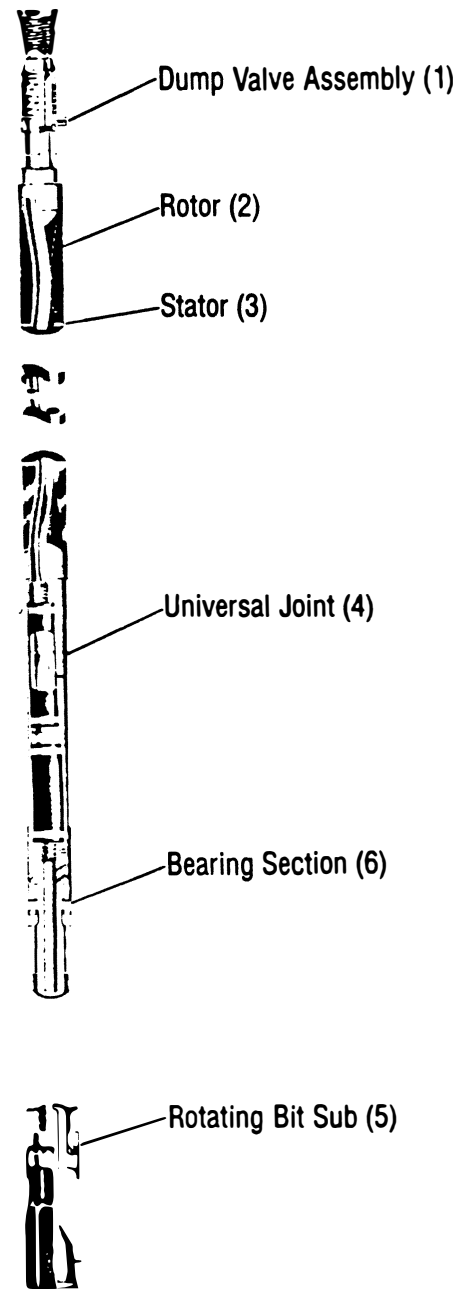


Fig. 8.95—A typical positive-displacement mud motor (PDM) (courtesy Dyna-Drill).

#### 8.6.4 Positive Displacement Mud Motors

The most important advancement in trajectory control is the use of the PDM and the turbine with a bent sub, bent housing, or eccentric stabilizer for making a controlled trajectory change.

Without a bent sub or bent housing, both types of motors can be used for normal directional and straight-hole drilling.

The PDM was developed in 1966, and 2 years later the PDM began to be used in the U.S., primarily as a directional tool. Since then the PDM has been used worldwide as both a directional and a straight-hole drilling tool.

The PDM is based on the Moineau principle. Fig. 8.95 is a cross section of a typical half-lobe profile PDM. The

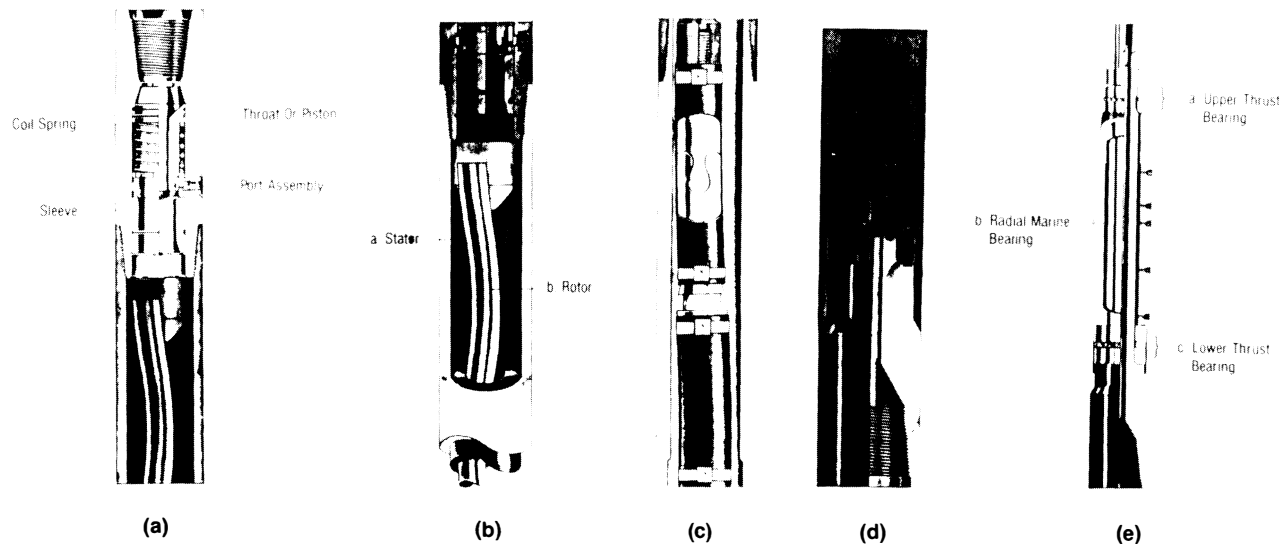


**Fig. 8.96**—(a) Dump-valve assembly. (b) Multistage motor. (c) Universal joint. (d) Rotating-bit sub. (e) Bearing and drive-shaft assembly (courtesy Dyna-Drill).

dump valve (1) is used to bypass the fluid while it flows in and out of the hole (Fig. 8.96a). When circulation begins, fluid forces the piston down, thereby closing the ports and directing the fluid through the stator. Because of the eccentricity of the rotor (2) in the stator (3) (Fig. 8.96b), the circulated fluid imparts a torque to the rotor, causing the rotor to turn and to pass the fluid from chamber to chamber. Rotation from the stator is transmitted to the bit by a universal joint (Fig. 8.96c) (4) to a rotating sub (5) to which the bit is connected (Fig. 8.96d). Thrust and radial bearings (6) (Fig. 8.96e) are used to withstand axial and normal loads on the bit and rotating sub. An upper-thrust bearing guards against hydraulic loads when the bit is off bottom and when there is circulation (Fig. 8.96E).

The operating life of a PDM is limited primarily by wear of the stator, thrust bearings, and drive components—such as the universal joint load coupling. It is important to maintain operating histories of key components, to conduct thorough inspections after each run, and to replace parts regularly before they fail downhole. Operators most often rent PDM's and thus are dependent on the service tool companies for strict quality-assurance procedures.

The stator is a vulnerable portion of the motor because it is subjected to continuous rubbing and deformation by the rotor. The stator rubber must have the resiliency to provide an effective hydraulic seal around the rotor while permitting the rotor to turn freely. It is essential that the stator consist of a correctly formulated elastomer compound that is bonded securely to the motor housing. Stators are occasionally subjected to chemical attack by aromatic hydrocarbons in the diesel phase of oil mud systems. Diesel fuels are typically “winterized” by the addition of aromatic compounds to lower the temperature at which the fuel gels. The aniline point of a diesel fuel—the temperature at which aniline becomes soluble in the diesel—is an inversely related indicator of aromatic content. Fuels with aniline points less than 155°F are potentially detrimental to PDM stators.

Excessive pressure drops across each motor stage accelerate stator wear. This problem is reduced in multilobed motors because the rotational speed and pressure drop per stage is less. However, the higher operating torques of multilobed motors tend to make the universal joint and related drive train components the weak link in the system.

Motor bearings can fail because of fluid erosion of mud-lubricated (nonsealed) systems, excessive loading of either the off-bottom or on-bottom thrust bearings, and normal attrition. When trajectory changes are made, the motor run is usually short enough that bearing life is not exceeded. Bearing life can be the limiting factor during longer trajectory changes or straight-hole drilling. Early PDM designs permitted only low pressure drops across the bearings; thus bit pressure drop was limited to similarly low values (about 250 psi). Higher pressure drops caused erosion of the restrictor used to control mud flow through the bearings. Newer nonsealed designs permit up to 1,000 psi pressure drop while sealed bearings operate at pressure differentials up to 1,500 psi. Unusual operating practices—such as considerable washing and reaming or running at abnormally low WOB—can hasten wear of off-bottom bearings. Abnormally high WOB accelerates on-bottom bearing wear. Normal attrition is the usual wear mode. Advances in bearing materials technology are making PDM bearing wear a less significant factor than in the past.\*

The most common PDM is called a half-lobe motor, which means that the rotor has one lobe or tooth ( $n_r = 1$ ) and the stator has two lobes or teeth ( $n_{st} = 2$ ). A key aspect of PDM design is that the stator always has one more lobe than the rotor, thus forming a series of progressive fluid cavities as the rotor turns:

$$n_{st} = n_r + 1. \quad (8.68)$$

The rotor has a diameter  $d_r$  and an eccentricity  $e_r$ , as shown in Fig. 8.97. Fig. 8.98 shows the pitch and lead of a half-lobe PDM. The rotor pitch,  $P_r$ , is equivalent

\*The following information has been provided by Baker Service Tools Co.



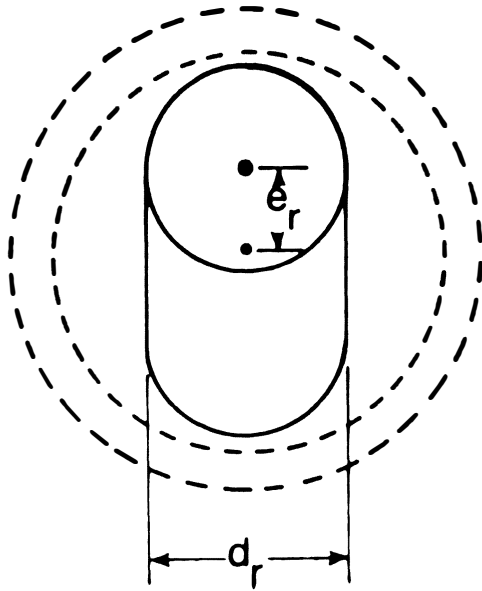


Fig. 8.97—Cross section of a half-lobe PDM showing the diameter and eccentricity of the rotor.

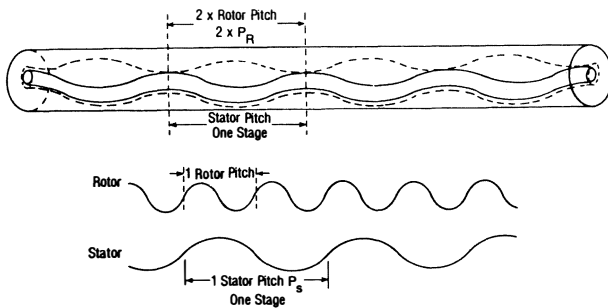


Fig. 8.98—A half-lobe PDM showing the stator and rotor pitches.

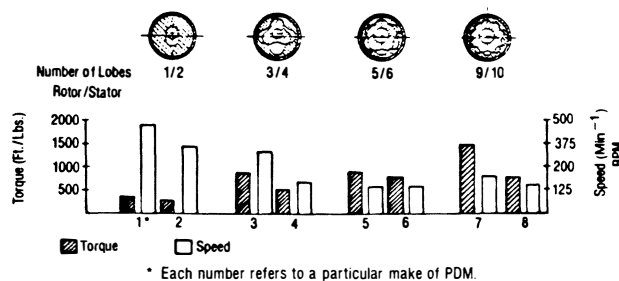


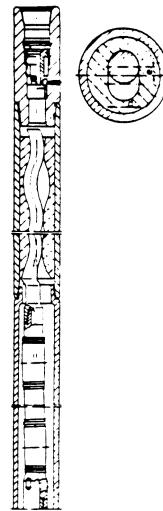
Fig. 8.99—Characteristics of various multilobe PDM profiles (after Jürgens<sup>13</sup>).

to the wavelength of the rotor. The rotor lead,  $L_r$ , is the axial distance that a tooth advances during one full rotor revolution. For any PDM the rotor pitch and stator pitch are equal while the rotor and stator leads are proportional to the number of teeth:

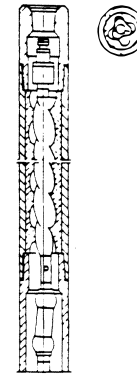
$$P_r = P_{st}, \dots \dots \dots (8.69a)$$

$$L_r = n_r P_r, \dots \dots \dots (8.69b)$$

1/2 Lobe PDM



3/4 Lobe PDM



9/10 Lobe PDM



Fig. 8.100—Multilobe PDM designs (after Eickelberg *et al.*<sup>8</sup>).

and

$$L_s = n_{st} P_{st}, \dots \dots \dots (8.69c)$$

For example, in a half-lobe PDM, the pitch and lead of the rotor are the same while the stator lead is twice the pitch.

In addition to half-lobe PDM's there are multilobe designs with  $\frac{3}{4}$ ,  $\frac{5}{6}$ , and  $\frac{9}{10}$  profiles, as shown in Figs. 8.99 and 8.100. Motor torque increases as the number of lobes increases, with a proportionate decrease in bit speed. The bit speed of some multilobe PDM's is low enough to permit lengthy straight-hole runs with journal-bearing roller-cone bits.

**Example 8.17.** What is the stator pitch ( $P_{st}$ ), rotor lead ( $L_r$ ), and stator lead ( $L_s$ ) of a  $\frac{3}{4}$ -lobe PDM with a 7-in. rotor pitch?

**Solution.** The stator pitch is equal to the rotor pitch.

$$P_{st} = P_r = 7 \text{ in.}$$

The rotor lead is equal to the pitch times the number of rotor teeth.

$$L_r = 7 \text{ in.} \times 3 = 21 \text{ in.}$$

The stator lead is equal to the pitch times the number of stator teeth.

$$L_s = 7 \text{ in.} \times 4 = 28 \text{ in.}$$

The starting point for PDM-design calculations is to determine the specific displacement,  $s$ , per revolution of the rotor. This is equal to the cross-sectional area of the fluid times the distance the fluid advances.

$$s = n_r \times n_{st} \times P_r \times A, \dots \dots \dots (8.70)$$

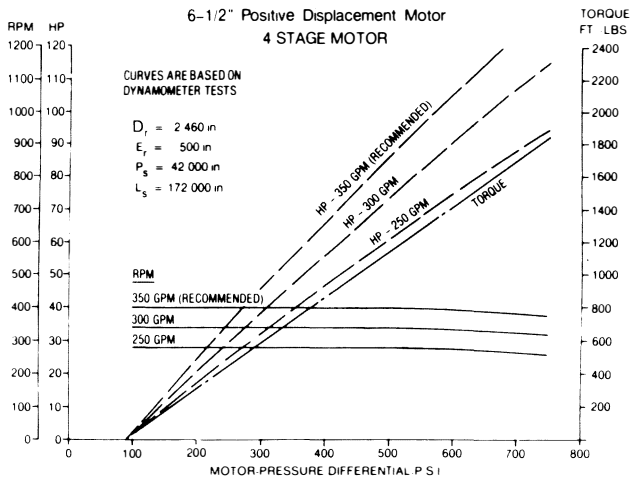


Fig. 8.101A—Data for four-stage 6½-in. positive-displacement motor (courtesy of Dyna-Drill).

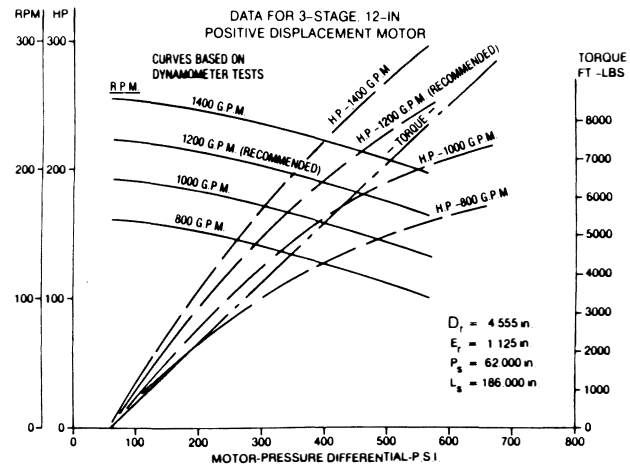


Fig. 8.101B—Data for three-stage 12-in. positive-displacement motor (courtesy of Dyna-Drill).

The fluid cross-sectional area is approximated by

$$A = \frac{\pi d_o^2}{4} \frac{2n_{st} - 1}{(n_{st} + 1)^2}, \quad (8.71a)$$

where  $d_e$  = stator gear OD.

For a half-lobe PDM,

$$A = 2e_r d_r. \quad (8.71b)$$

Bit speed is simply the flow rate divided by the specific displacement.

$$N_b = \frac{231q}{s}, \quad (8.72a)$$

where  $q$  is in gallons per minute and  $s$  is in cubic inches per revolution.

The bit speed of a half-lobe PDM is equal to

$$\frac{57.754q}{e_r d_r P_r}. \quad (8.72b)$$

Motor torque is obtained by relating mechanical horsepower output to hydraulic horsepower input and substituting Eqs. 8.70 and 8.72a to yield Eq. 8.73b:

$$\frac{M \times \text{rpm}}{5252} = \frac{q \times \Delta p}{1714} \times \eta, \quad (8.73a)$$

$$M = \frac{3.064q\Delta p E}{\text{rpm}} = 0.0133n_r n_{st} p_r A \Delta p \eta, \quad (8.73b)$$

where  $M$  is measured in foot-pounds mass and  $\Delta p$  is measured in pounds per square inch. Motor efficiency rarely exceeds 80% ( $\eta = 0.80$ ) for half-lobe PDM's and 70% for multilobe PDM's.

**Example 8.18.** Find the torque of a half-lobe 8-in.-OD PDM with 1.75-in. rotor eccentricity, 2.5-in. rotor diameter, and 24-in. rotor pitch; the total pressure drop is 465 psi. What is the bit speed at a flow rate of 600 gal/min?

**Solution.** Eq. 8.73c is developed by a combination of Eqs. 8.72b and 8.73b.

$$M_{1/2} = \frac{3.064q\Delta p \eta}{57.754q/e_r d_r p_r} = 0.0531 e_r d_r p_r \eta \Delta p; \quad (8.73c)$$

$$M_{1/2} = 0.0531 (1.75)(2.5)(24)(0.80)(465) = 2,074 \text{ ft-lbf.}$$

The bit speed is given by Eq. 8.72b.

$$N_{b1/2} = \frac{57.754q}{e_r d_r p_r} = \frac{57.754 (600)}{(1.75)(2.5)(24)} = 330 \text{ rpm.}$$

Notice from Eq. 8.73c that PDM torque is directly proportional to  $\Delta p$  and is independent of rotary speed. Also, torque decreases as eccentricity decreases; if eccentricity is zero, then motor torque is zero.

The number of motor stages is

$$n_s = \frac{L}{P_{st}} - (n_{st} - 1), \quad (8.74)$$

where  $L$  is the length of motor section only.

Ideally, the bit speed of a PDM should be linear with pump rate, as implied by Eq. 8.72a. The stator is made of an elastomer, and as the pressure drop across the motor increases (i.e., as the torque increases), the elastomer deforms, allowing a small portion of the fluid to bypass, thus reducing the bit speed. This is a nonlinear effect, as shown clearly by Figs. 8.101a and 8.101b.

### 8.6.5 Turbines

Turbines were first used in the Soviet Union in 1934. The use of turbines increased from 65% in 1953 to 86.5% of all drilling in 1959. Currently, turbines are used in the Soviet Union for 50 to 60% of all drilling.

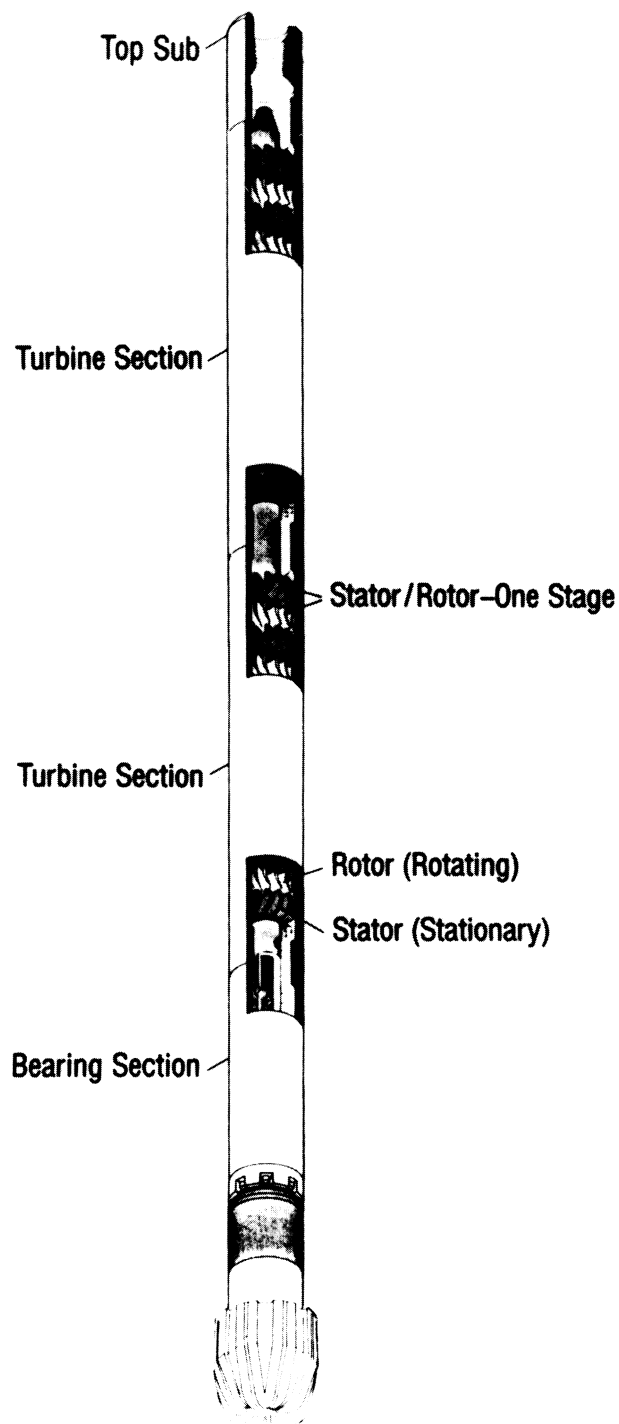


Fig. 8.102—Typical turbine design (courtesy of Baker Tool Co.).

In 1959, the first successful drilling with turbines outside the Soviet Union took place in southern France. Turbines were introduced to the U.S. in 1960, but less than 1% of footage drilled in the U.S. has been with turbines. They are used more extensively in parts of Europe and the North Sea, although not as much as they are in the Soviet Union.

Fig. 8.102 shows a typical turbine design. The fluid enters the top sub and travels past the stators and rotors (one stator and one rotor compose one stage). The lower part of the turbine is the main thrust-bearing section.

Unlike the PDM, the turbine's power output is optimal over only a limited range of operating conditions. Fig. 8.103 shows a common curve of torque, speed, and power for a typical directional-drilling turbine where the pump rate is 500 gal/min. For the given pump rate, which is the input power, the output power varies, reaching an optimum at 820 rpm. Fig. 8.104 shows a similar curve for a straight-hole turbine. The torque and power curves exhibit a much narrower range of operation.

At lower speeds and higher torques, the efficiency of turbine drilling is reduced significantly. Two- and three-cone rock bits require high axial loads and lower speeds to drill and, therefore, are impractical for use with turbines. Diamond bits and the new polycrystalline diamond cutter (PDC) bits are better suited for the turbine. Diamond bits have not been used with turbines as much as roller-cone bits because it is difficult to match certain diamond bit designs with particular types of formations. Even engineers in the Soviet Union, who usually drill with turbines, use principally roller-cone bits. This approach has forced them to build mud motors with slower speeds.

The type of thrust bearings used also affects the performance of a turbine significantly. Rubber bearings were designed so that the axial thrust load balances the downward velocity of the fluid against the drive section of the turbine. If a properly designed bit is selected for a given formation and allowance is made for the appropriate axial WOB to balance the thrust and to optimize the output power, a successful turbine run can be achieved. This assumes that the operator can keep the turbine drilling at the correct torque and speed. Clearly, without some means of monitoring downhole performance (i.e., torque and speed), it is much harder to drill with a turbine than with a PDM. (Because torque is proportional to the differential operating pressure for a PDM, the standpipe pressure can be used to indicate operating torque; and, because the bit speed is proportional to the pump rate, the bit speed can be monitored by keeping track of the pump strokes.) Rubber bearings, which must be balanced to help prolong motor life, are not as durable as balanced roller bearings. The testing of newer bearing materials promises to increase bearing life and to extend the hours for a turbine run.

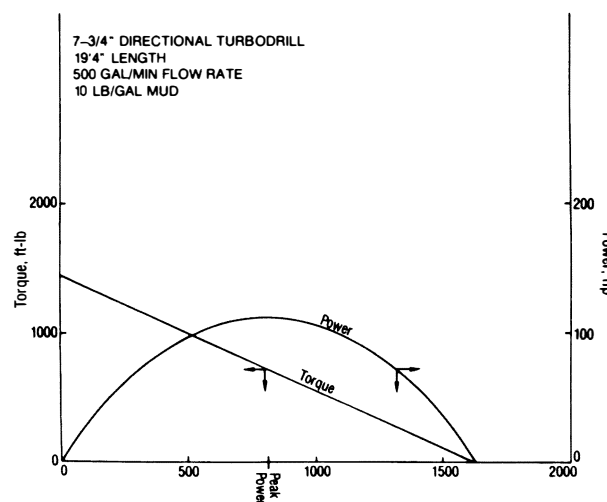


Fig. 8.103—Typical torque/power curves for a turbine.

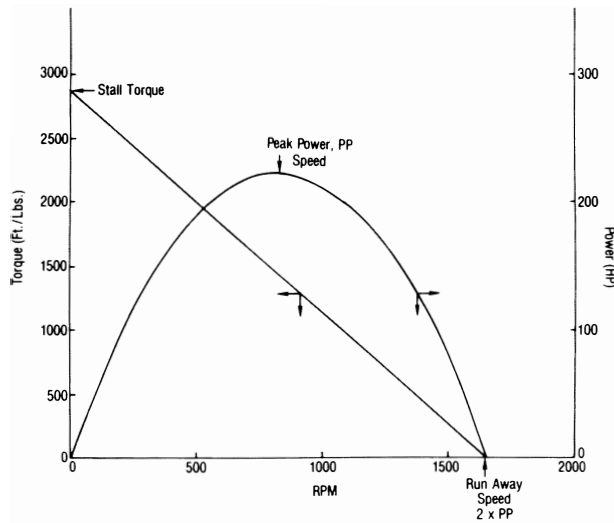


Fig. 8.104—Typical torque/power curves for a turbine at a pump rate of 500 gal/min, 10-lbm/gal mud.

The stall torque of any turbine can be determined with Eq. 8.75<sup>13</sup>:

$$M = 1.38386 \times 10^{-5} \eta_H \eta_M \tan \beta n_s W_m q^2 / h, \dots (8.75)$$

where

- $\eta_H$  = hydraulic efficiency,
- $\eta_M$  = mechanical efficiency,
- $\beta$  = exit blade angle, degrees,
- $n_s$  = number of stages,
- $W_m$  = mud weight, lbm/gal,
- $q$  = circulation rate, gal/min, and
- $h$  = height of vane, in.

Fig. 8.105 shows the side view of a single turbine stage.

The runaway bit speed of a turbine can be calculated with Eq. 8.76:

$$N_b = 5.85 \eta_V \tan \beta q / r^2 h, \dots (8.76)$$

where  $\eta_V$  is the volumetric efficiency and  $r$  is the median blade radius.

From Fig. 8.104 it is apparent that the function that relates turbine torque to turbine speed is of the form

$$M_i = M_{ts} - B \times N_b, \dots (8.77)$$

where

- $M_i$  = instantaneous torque,
- $M_{ts}$  = turbine stall torque, and
- $B$  = constant.

And if torque is equal to a constant times bit speed and if Eqs. 8.75 and 8.76 are combined, where  $K_1$  is the slope and a constant, then

$$M_i = M_{ts} - K_1 N_b, \dots (8.78)$$

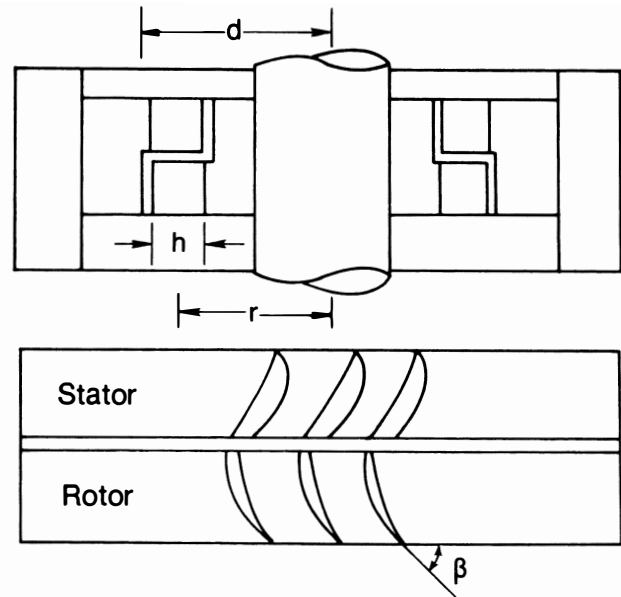


Fig. 8.105—Side view of a single-stage turbine. (after Jürgens<sup>13</sup>).

Expanding Eq. 8.78 yields Eq. 8.79:

$$M_i = M_{ts} - \left( \frac{r^2 h}{231 \eta_V \tan \beta} \right) \times \left( \frac{4.46 \times 10^{-4} \eta_H \eta_M \tan \beta n_s W_m q}{h} \right) N_b, \dots (8.79)$$

where

$$K_2 = \frac{r^2 h}{231 \eta_V \tan \beta},$$

$$K_3 = \frac{4.46 \times 10^{-4} \eta_H \eta_M \tan \beta n_s W_m q}{h},$$

and

$$K_2 K_3 = K_1.$$

It can be seen from Eq. 8.79 that, for a given number of stages, mud weight, and pump rate, the torque is linear with bit speed, as depicted in Figs. 8.103 and 8.104. Eq. 8.75 implies that the addition of stages can increase the torque. This assumes all other variables are held constant. Eq. 8.79 states that as the bit speed increases, the overall turbine torque decreases. However, increasing the flow rate and/or the mud weight will increase the overall torque stall point. The necessity of higher pump rates required to drive the turbine precluded the use of turbines on most land rigs and on some offshore drilling rigs until the

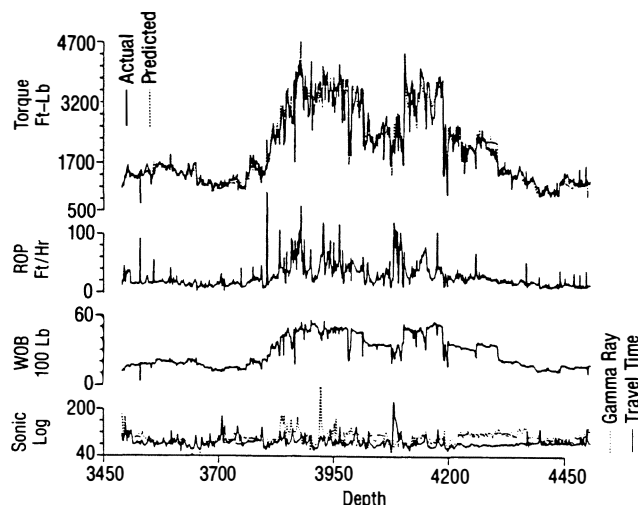


Fig. 8.106—Observed and predicted torque for an overthrust well with a 12¼-in. IADC Series 5-1-7 bit.

mid-1970's; finally, drilling contractors upgraded their pump sizes to accommodate the deeper drilling. Now, in both the U.S. and Europe, more drilling rigs can run turbines than ever before.

Once the torque/speed relationship of a turbine is known, the mechanical power output can be calculated by Eq. 8.71, and the hydraulic power can be determined from Eq. 8.70 if the pressure drop across the motor ( $\Delta p$ ) is known. The ratio of the two is the overall efficiency.

**Example Problem 8.19.** Determine the mechanical efficiency of the turbine presented by Fig. 8.103. The following information is also known:

Number of stages = 100,  
Radius of blade = 3.0 in.,  
 $\eta_v = 0.80$ , and  
 $\eta_H = 0.45$ .

**Solution.** From the torque curve presented in Fig. 8.103, the slope is 1.67 ft-lbf/rpm. Because the slope is  $K_1$  and  $K_1 = K_2 K_3$ , the mechanical efficiency can be calculated by Eq. 8.76.

$$\begin{aligned}\eta_M &= \frac{(K_1)(5.85)\eta_v}{1.38386 \times 10^{-5} n_s W_m q E_H r^2} \\ &= \frac{(1.67)(5.85)(0.80)}{1.38386 \times 10^{-5} (100)(10)(500)(0.45)(3.0)^2} \\ &= 0.279 = 27.9\% \text{ efficiency at 500 gal/min.}\end{aligned}$$

### 8.6.6 Using the PDM for Directional and Straight-Hole Drilling

Drilling with the PDM is much easier than with a turbine because the surface standpipe pressure reflects the PDM

torque. As the motor torque increases, the standpipe pressure increases; as the motor torque decreases, the standpipe pressure also decreases. Therefore, the driller should use the standpipe pressure or a downhole torque indicator as a primary output indicator to advance the bit. The tool face of a wireline orienting tool or an MWD tool is influenced by the bit torque and, therefore, can indicate the bit torque. This will be covered later in this section.

The relationship between the motor torque and the torque used to drill a given formation with a tricone bit is developed by Warren.<sup>14</sup>

$$M = \left[ C_3 + C_4 \sqrt{\frac{q_p}{N_b \cdot d_b}} \right] (d_b W_b) f_{(\text{tooth wear})}, \quad (8.80)$$

where

$C_3$  = bit constant (dimensionless),  
 $C_4$  = bit constant (dimensionless),  
 $q_p$  = penetration rate (ft/hr),  
 $N_b$  = bit speed (rpm),  
 $d_b$  = bit diameter (in.),  
 $W_b$  = weight on bit (1,000 lbf), and  
 $f_{(\text{tooth wear})}$  = function to relate tooth wear to footage drilled.

Warren<sup>14</sup> cites a derived torque relationship for a 12¼-in. bit drilling a section between 3,484 and 4,510 ft. Fig. 8.106 shows the data for such a bit run. From a regression analysis of the data the constants  $C_3$ ,  $C_4$ , and  $f_{(\text{bit wear})}$  are obtained:

$$M = \left( 3.79 + 19.17 \sqrt{\frac{R}{N_b \cdot d_b}} \right) (d_b W_b) \cdot \left( \frac{1}{1 + 0.0021 L_t} \right), \quad \dots \dots \dots (8.81)$$

where  $L_t$  is the total footage drilled with this series 5-1-7 bit. Warren also cites other experimental work that verifies Eq. 8.80 (see Fig. 8.107a and b).

The torque the PDM experiences is (1) the torque required to overcome the off-bottom torque so that the rotor can rotate against the stator and against the friction of the bearings and (2) the torque required to drill a given formation with a specific bit, bit diameter, bit speed, and WOB. Rearranging Eq. 8.68, combining it with Eq. 8.80, and adding a term for off-bottom rotational torque yields

$$\begin{aligned}\Delta p = \frac{M}{K_3} &= \frac{1}{K_3} \left[ \left( C_3 + C_4 \sqrt{\frac{q_p}{N_b \cdot d_b}} \right) \right. \\ &\quad \left. \times (d_b W_b) f_{(\text{tooth wear})} \right] + p_m, \quad \dots \dots \dots (8.82)\end{aligned}$$

where

$$K_3 = \frac{1}{0.636 e_r d_r P_s},$$

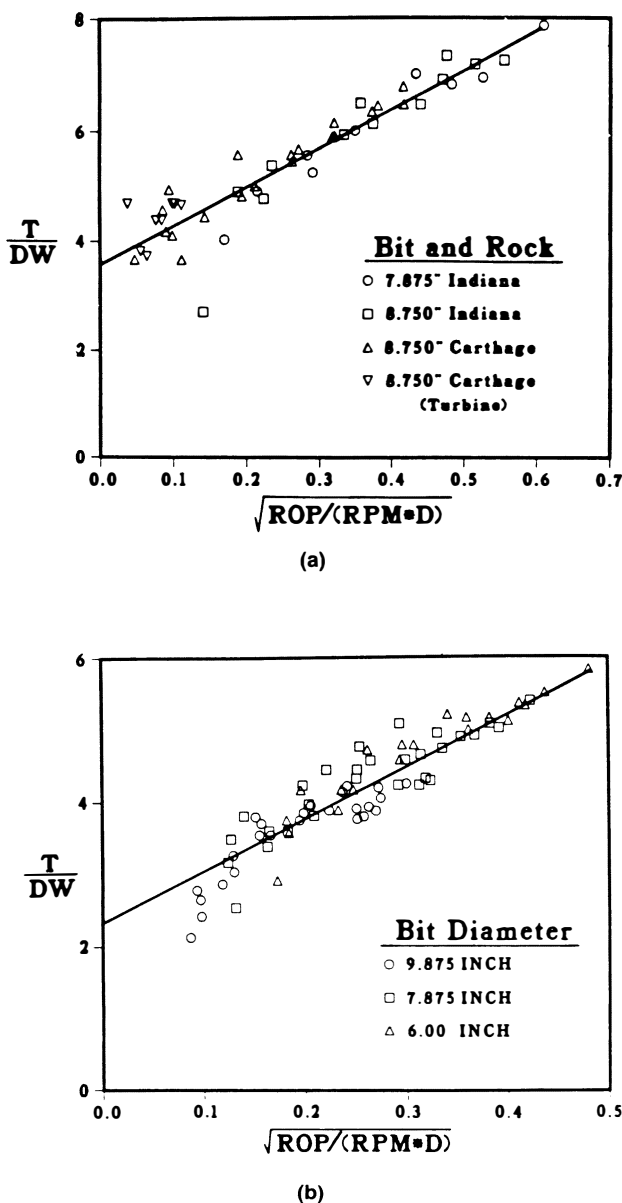


Fig. 8.107—Results of bit tests to verify torque relationship for three-cone rotary bits.

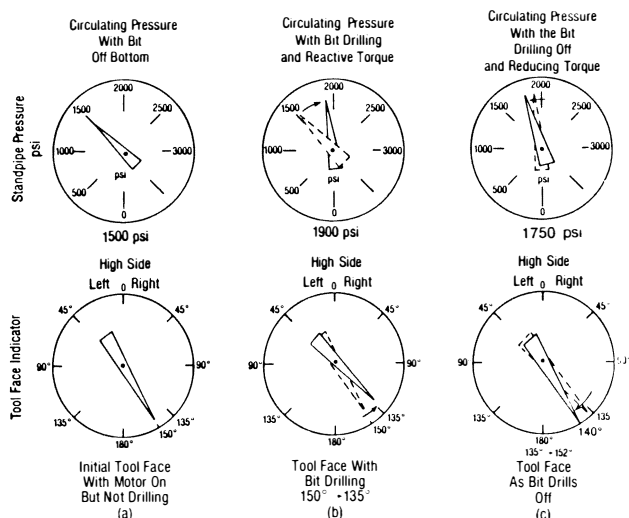


Fig. 8.108—Drilling with a PDM—typical standpipe pressure and tool-face indicator responses.

and  $p_m$  is the off-bottom pressure drop caused by the friction of the stator and rotor and bearings. The standpipe pressure can reflect the pressure variation of the motor torque if all the pressure losses are considered:

$$p_{sp} = p_{dl} + \Delta p_{(PDM)} + p_{bl} + p_{al}, \dots \dots \dots (8.83)$$

where  $p_{sp}$  is the pressure of the standpipe,  $p_{dl}$  is the pressure of the drillstring loss,  $\Delta p_{(PDM)}$  is the pressure difference of a PDM,  $p_{bl}$  is the pressure of a bit loss, and  $p_{al}$  is the pressure of the annulus loss. If all the pressures are constant for a given circulation rate,  $p_{sp}$  will directly reflect  $\Delta p_{(PDM)}$ .

Fig. 8.108 shows what a driller sees while drilling with a PDM when there is no noticeable sideforce on the bit. The  $p_{sp}$  will go up nearly linearly as WOB is added. This is true for roller cones or for polycrystalline diamond bits with jets but not for natural diamond bits. (The reason for this nonlinear increase in pressure for natural diamond bits will be covered later when bit pump-off is discussed.) As the penetration rate increases and rock strength decreases, the torque and the  $p_{sp}$  go up. Conversely, the torque and  $p_{sp}$  decrease in harder formations. The  $p_{sp}$  increase for variations in penetration rate response is less than an equivalent increase in WOB, because  $\Delta p$  is proportional to the square root of penetration rate.

While the PDM driller feeds out line through the brake, WOB is increased; torque also increases and causes the  $p_{sp}$  to increase. If the maximum  $p_{sp}$  is not exceeded and the driller stops adding WOB, the torque and  $p_{sp}$  will decrease as the bit drills off. If WOB is increased, causing maximum  $p_{sp}$ , the bit speed and penetration rate will decrease. The PDM will stall if too much weight is applied. If the motor is left in the stall position too long, seals can break, allowing the circulating fluid to bypass and necessitating the tripping out of the PDM.

In the foregoing discussion, it is assumed that all the torque is developed by the penetration of the formation by the bit and the overcoming of the internal friction in the PDM. In directional drilling with a PDM, a bent sub, bent housing, or a PDM as part of a directional assembly, torque is developed as the bit cuts sideways out of the vertical plane. This additional torque is related to the total torque used by a PDM as

$$M_m = M_b + M_{mf} + M_s, \dots \dots \dots (8.84)$$

where  $M_m$  is motor torque,  $M_b$  is bit torque,  $M_{mf}$  is motor-friction torque, and  $M_s$  is sidecutting torque.

When a directional driller monitors the tool-face angle on a surface display with a PDM with a bent sub, he observes the following occurrences (see Fig. 8.108). Circulation begins with the bit off bottom. As the motor reacts to the clockwise rotation of the rotor against the stator and the bearings, the tool face begins to rotate counterclockwise. As the bit engages the side of the borehole, a right readjustment occurs; and finally, as the bit face engages, a counterclockwise rotation of the tool face takes place. As the bit drills off, the left rotation decreases. If the data are obtained frequently enough, the driller can use this information to advance the bit more accurately than he can with the coarser-reading pressure gauge. If

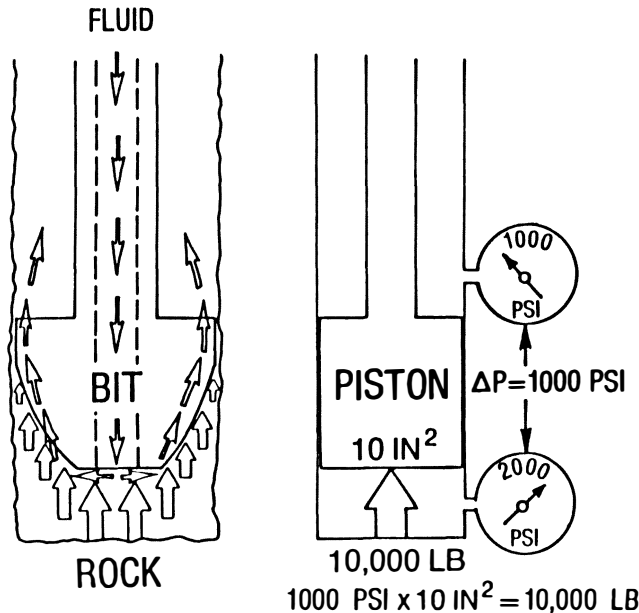


Fig. 8.109—Pressure differential caused by circulation of the drilling fluid.

the data are obtained only infrequently, however, as with most MWD tools, the use of the tool-face readings for drilling is difficult.

The higher the inclination angle, the greater the bit's sidcutting effect; sometimes the tool-face orientation varies more than 90°. The tool face oscillates so severely that a visual running average is required to direct the orientation of the bit. This oscillation usually occurs when the inclination is greater than 50°, the formation is medium soft, and aggressive bits are used.

### 8.6.7 Drilling With a PDM

When a drag-type bit is used (diamond, polycrystalline diamond, or a combination of the two), the pump-off of the bit must be considered in the design of the motor bit system and in the determination of the amount of effective WOB to be applied at the surface to obtain a desired WOB at the bit. Fig. 8.109 illustrates how the circulation of the drilling fluid causes a 1,000-psi pressure difference across the bit. This equates to a pump-off force of 10,000 lbf across a 10-sq-in. piston.

Winters and Warren<sup>15,16</sup> verified the pump-off force in the field and with controlled laboratory tests. Their work showed that the pump-off force can be obtained in the field by observing the hook load and standpipe pressures for what is called a "pump-off test." Eq. 8.85 relates the pump-off force  $F_h$  to the difference between the hook load with the bit off bottom,  $F_{ob}$ , and the hook load with the bit just drilled off,  $F_{do}$ .

$$F_h = F_{do} - F_{ob} \quad (8.85)$$

The difference between the standpipe pressure with the bit off bottom,  $p_{ob}$ , and that with the bit just drilled off,  $p_{do}$ , is the pressure drop across the bit,  $\Delta p_b$ , and is related by Eq. 8.86:

$$\Delta p_b = p_{do} - p_{ob} \quad (8.86)$$

### OFF-BOTTOM PUMPED DRILLING OFF

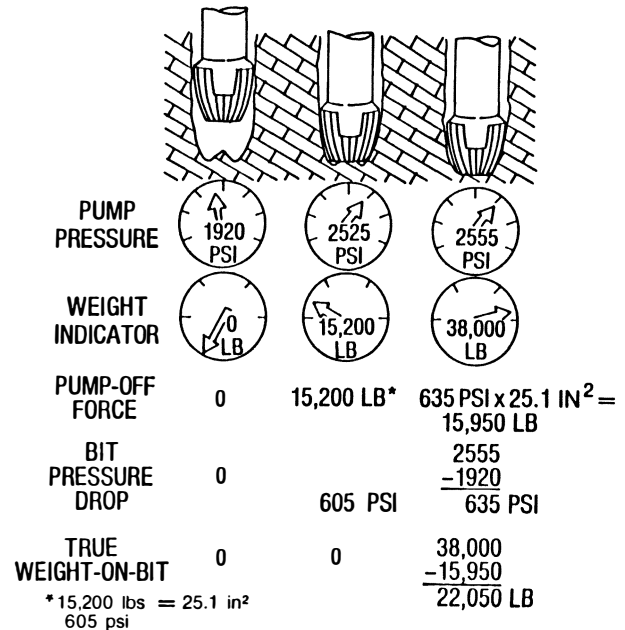


Fig. 8.110—Pumpoff pressure and weight (after Winters and Warren<sup>16</sup>).

Fig. 8.110 shows how the pump-off pressure and weight are obtained and how the effective pump-off area of the bit can be determined.

With the bit off bottom, the pump pressure is 1,920 psi and the  $\Delta$  hook load is 0.0 lbf. The pump-off force is 0.0 lbf and the bit pressure drop is 0.0 psi. There is no WOB. The pump-off force and pressure can be found in one of two ways: the bit can be advanced until it drills or the brake can be locked so that the bit can drill off. The point at which the bit will be just drilled off is the point of pump-off pressure and weight. Fig. 8.111A plots a carefully controlled drill-off test. However, the plot of WOB vs. time does not define the pump-off clearly. When pump pressure vs. WOB is replotted, the true pump-off point is discernable (see Fig. 8.111B). As the drillstring is lowered slowly, the  $\Delta$  hook load and the standpipe pressure are recorded until the pump-off is noted. Fig. 8.112 shows how this is done. At 0.0 lbf  $\Delta$  hook load, the  $\Delta$  standpipe pressure is 0.0 psi. As the bit is lowered, the pressure starts to increase and continues to increase almost linearly until a pressure difference of 595 psi is reached at a  $\Delta$  hook load of 9,000 lbf. Further addition of  $\Delta$  hook load causes the bit to drill ahead, as indicated by the change in slope of the data. The pump-off force of the new bit is 9,000 lbf, and its pump-off area is determined to be 9,000 lbf/595 psi = 15.1 sq in. Fig. 8.112 indicates that as the bit dulled, its pump-off area increased to 25.1 sq in.

As the example in Fig. 8.110 shows, the determined pump-off point is 2,525 psi at a  $\Delta$  hook load of 15,200 lbf. The bit pressure drop is

$$\Delta p_b = 2,525 \text{ psi} - 1,920 \text{ psi} = 605 \text{ psi.}$$

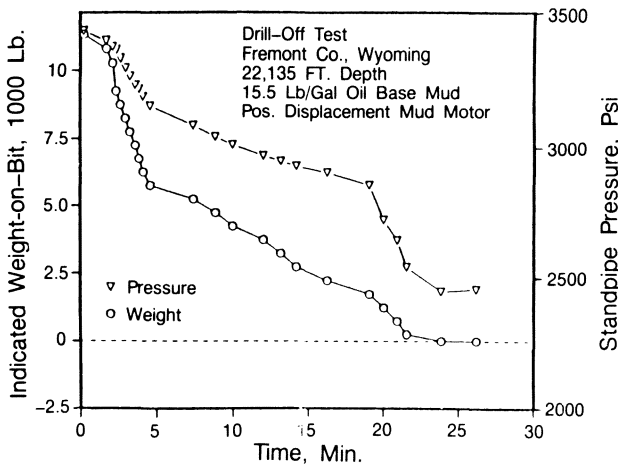


Fig. 8.111A—Drill-off test with an 8½-in. standard crossflow bit.

The true WOB is still 0.0 lbf at this point. The pump-off area,  $A_{po}$ , of the bit is calculated with

$$A_{po} = \frac{F_h}{\Delta p_b} \quad (8.87)$$

For the values presented by Fig. 8.110, the pump-off area is

$$A_{po} = \frac{15,200 \text{ lbf}}{605 \text{ psi}} = 25.1 \text{ sq in.}$$

If the pump-off area and the off-bottom pump pressure are known, the true WOB for any pump rate can be determined.

Fig. 8.110 shows a drilling example in which the surface-indicated WOB is 38,000 lbf and the standpipe pressure is 2,555 psi. The bit pressure drop is

$$\Delta p_b = 2,555 \text{ psi} - 1,920 \text{ psi} = 635 \text{ psi};$$

the pump-off force is

$$F_b = 635 \text{ psi} \times 25.1 \text{ sq in.} = 15,939 \text{ lbf};$$

and the true WOB is

$$W_b = 38,000 - 15,939 \text{ lbf} = 22,061 \text{ lbf.}$$

A typical example of drilling with a sidetracking diamond bit and a PDM with a bent housing is shown by Fig. 8.113. (Note that the downward arrows indicate each time the driller slacked off weight.)

At time  $T_1$  the bit was off bottom with 0.0 lbf WOB. The off-bottom pressure was 1,540 psi. At  $T_2$  the string was lowered slowly, causing the standpipe pressure to increase until  $T_3$ , when the pump-off point was noted. Additional WOB ( $T_4$ ) caused the motor to drill, reaching a  $\Delta p$  of 100 psi for a WOB of 13,400 lbf. As the bit drilled off, the standpipe pressure and WOB decreased until the pump-off point was reached. Then the slope changed ( $T_5$ ). WOB was again applied ( $T_6$ ), causing the standpipe pressure to increase to 2,270 psi and giving a motor  $\Delta p$  of 210 psi ( $T_7$ ). The bit drilled off at a fairly constant rate until the pump-off point was again reached at  $T_8$  when, again, the rate of decline of the standpipe pressure and WOB increased. The driller slacked off weight

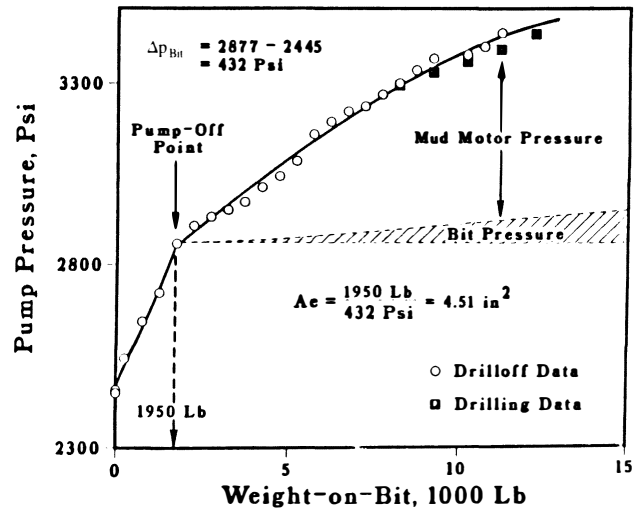


Fig. 8.111B—Point of pump-off (after Winters and Warren<sup>16</sup>).

three times, but there was no apparent torque response because of hole drag. Then at  $T_9$ , the excessive weight reached the bit, and the motor stalled. The standpipe stall pressure was 2,880 psi, and the  $\Delta p$  motor stall pressure was 820 psi.

This typical field example shows the principal operating features of the motor and diamond-bit system. The pump-off force is 13,700 lbf at a standpipe pressure of 2,060 psi. The bit pressure drop is 2,060 psi minus the off-bottom pressure of 1,540 psi, which is 520 psi. The pump-off area is 26 sq in. The actual motor  $\Delta p$  is any pressure above that at the pump-off point, in this case 2,060 psi. The actual WOB can be calculated by multiplication of the bit  $\Delta p$  and the pump-off area.

The motor  $\Delta p$  relates to the amount of torque necessary for a given type of bit to drill a particular type of formation. The torque relationships for drag bits are similar to those for three-cone bits. Fig. 8.114A is a typical plot of diamond bit torque and penetration rate vs. WOB for a given pump rate and rotary speed.

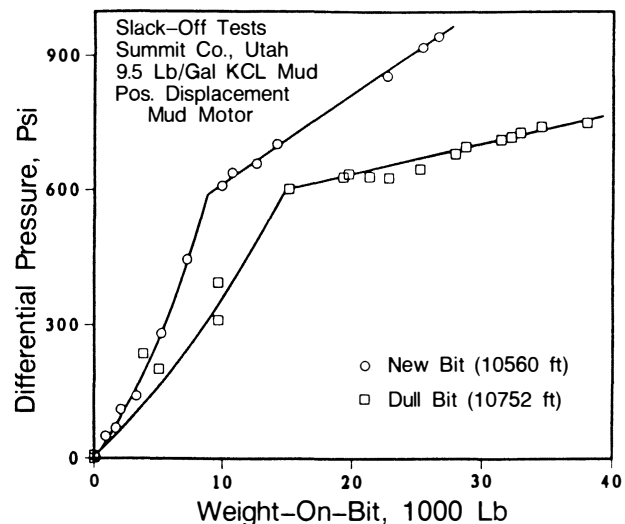


Fig. 8.112—Slack-off test data with 12¼-in. flat profile radial flow bit.



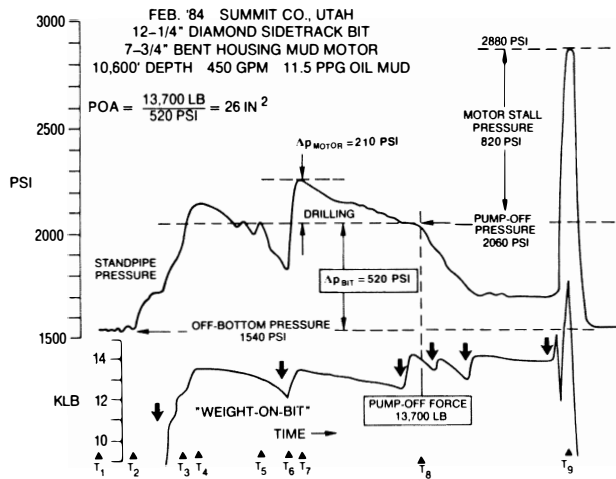


Fig. 8.113—Drilling with a sidetracking diamond bit and bent housing mud motor.

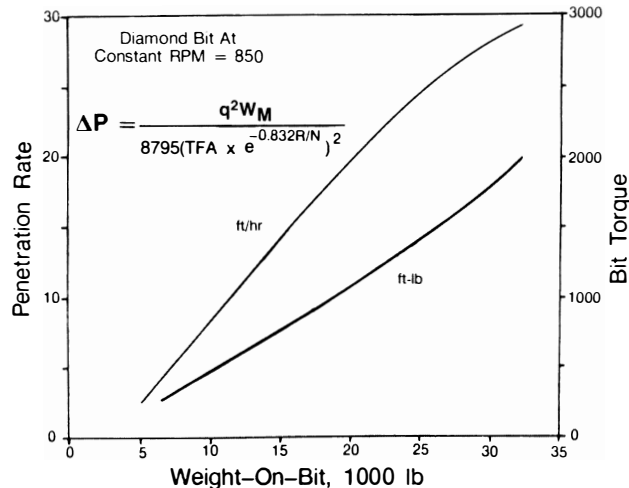


Fig. 8.114A—Diamond-bit penetration rate and torque analysis at 850 rpm.

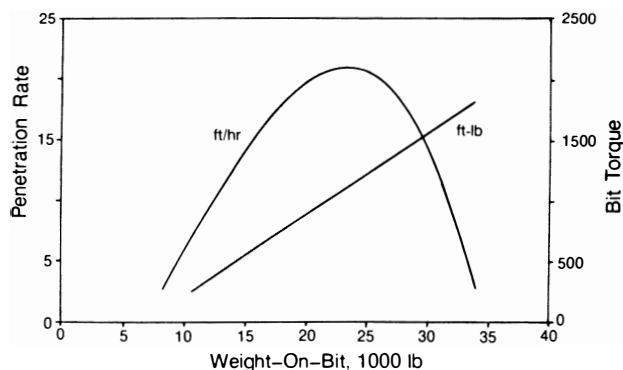


Fig. 8.114B—130-stage turbine with diamond bit.

### 8.6.8 Effect of Standpipe Pressure Change on Drillpipe Elongation

When a PDM is used, the change in the internal drillpipe pressure causes an elongation of the drillstring. This effect can be related by

$$\Delta L = \left[ \frac{-\Delta W_b}{E \times A_s} + \frac{\Delta p_i \times A_i}{E \times A_s} - \frac{2\mu}{E} \frac{\Delta p_i}{(F_d^2 - 1)} \right] L, \quad \dots \dots \dots (8.88)$$

where  $\Delta L$  is the change in drillpipe length,  $\Delta W_b$  is the change in WOB,  $\Delta p_i$  is the change in internal drillpipe pressure,  $A_s$  is the cross-sectional area of steel in drillpipe,  $A_i$  is the internal drillpipe area,  $F_d$  is the ratio of drillpipe,  $E$  is the Young's modulus for steel ( $29 \times 10^6$  psi),  $\mu$  is the Poisson's ratio for steel (0.3), and  $L$  is the length of drillpipe.

For a 5-in. drillpipe, Eq. 8.88 reduces to

$$\Delta L = \left( \frac{-\Delta W_b}{15.82 \times 10^7} + \frac{\Delta p_i}{2.76 \times 10^7} \right) L. \quad \dots \dots \dots (8.89)$$

**Example 8.20.** If the driller slacks off 0.95 ft of 15,000 ft of 5-in. drillpipe, what is the indicated WOB? This slack-off causes an increase of 155 psi, which causes an increase in WOB. How much must be drilled off to maintain the indicated WOB?

**Solution.** With no change in motor pressure ( $\Delta p = 0$ ), the slack-off weight is

$$W_b = \frac{15.82 \times 10^7}{15,000} (0.95) = 10,000 \text{ lbf.}$$

An increase of 10,000 lbf WOB causes a  $\Delta p$  of 155 psi. This increases the WOB, so  $(155 \text{ psi} / 2.76 \times 10^7 \text{ psi}) \times 15,000 \text{ ft} = 0.08 \text{ ft}$  must be drilled off to maintain 10,000 lbf WOB.

### 8.6.9 Planning a Trajectory Change With a PDM

The following are steps for planning and executing a trajectory change when a PDM is used.

1. Design the hydraulics in such a way that the pressure drop across the bit does not exceed the manufacturer's limits and supplies enough pressure and circulation rate to power the motor throughout the trajectory change. Select a PDM with enough power to rotate a bit of the size and type necessary both to drill a given series of formations and to cause the trajectory change.

2. Once the motor, bit, and hydraulics are designed, select the appropriate bent sub (depending on the desired trajectory change).

3. Trip the bit, motor, bent sub, mule-shoe sub, and the remainder of the BHA into the hole.

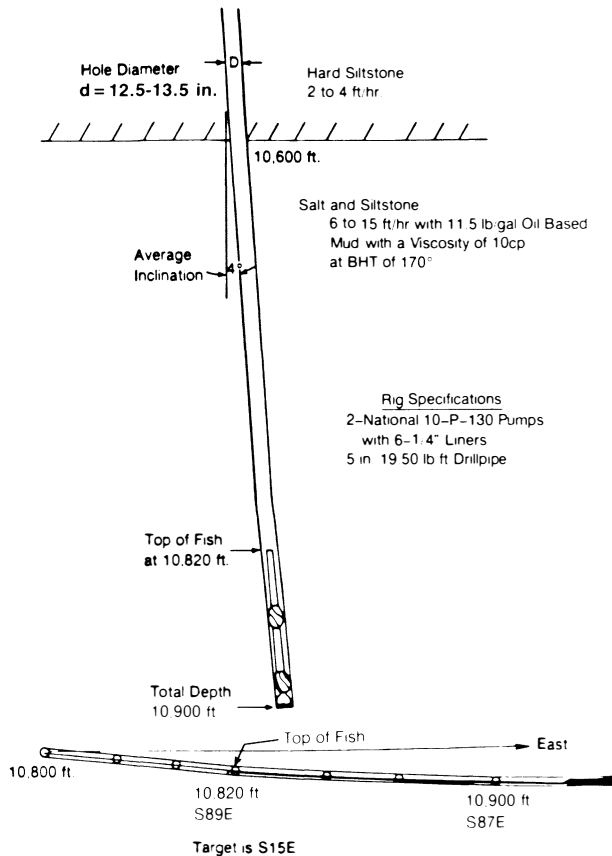


Fig. 8.115—Wellbore situation for Example 8.21.

4. On the basis of the calculations presented in Sec. 8.4 and allowing for the reactive torque of the motor, orient the tool face before starting the motor by orienting the pipe at the surface while moving the drillpipe up and down to reduce the static friction of the drillstring and the bent-sub or bent-housing knee. Or the bit face can be adjusted and the pipe worked to transmit the torque to the bit.

5. Start the motor by circulating the mud and bringing up the circulation rate to the desired level.

6. Advance the bit until a reactive torque is indicated by the standpipe pressure and/or by the tool-face indicator; this implies a bit/formation interaction. (If Step 4 is performed correctly, there should be very little readjustment of the tool face at the surface. If that step is omitted, however, the driller must keep readjusting the tool face until the final trajectory change is obtained. Such changing can cause severe, unplanned doglegs.)

7. Generally, plan to make a direction change when the inclination exceeds  $2^\circ$ . To control the dogleg severity, change the direction over a drilled section and use the motor to hold the direction as constant as possible while building inclination over a course length that covers the controlling section of the next BHA. If a bent housing is used, the general strategy is to change the trajectory over a course length that does not exceed the dogleg criteria and then to replace the PDM bent housing with a PDM bent-sub arrangement.

8. If a trajectory change is required at a higher inclination, use a longer tool run (multiple tool runs may be required) to keep the dogleg severity to a predetermined

limit. In such cases, the bit run must be optimized to last the life of the motor to maximize the interval drilled.

**Example 8.21.** A bit and two stabilizers are stuck in the hole and cannot be retrieved economically. It is decided to sidetrack around the fish and to continue with the drilling. Fig. 8.115 shows the wellbore situation. The siltstone section above the salt is extremely hard to drill with the existing 11.6-lbf/gal mud. Penetration rates vary in this interval from 2 to 4 ft/hr. The salt-and-siltstone section below 10,600 ft is easier to drill, with penetration rates varying from 10 ft/hr for the 100% siltstone to 30 ft/hr for 100% salt. The mud is a low-fluid-loss oil/water emulsion. The average wellbore diameter varies between 12.5 and 13.5 in. Surveys at 10,820 ft and 10,900 ft report the inclination at  $4.0^\circ$  and  $4.5^\circ$ , and the directions S84E and S87E, respectively. The top of the fish is at 10,820 ft. Design an optimum sidetrack to get around the fish without drilling any of the harder siltstone above the salt. To be safe at the top of the fish, the new wellbore should be two diameters laterally displaced from the old wellbore. The drillpipe is 5.0-in., 19.50-lbm/ft Grade E.

**Solution.** First, place a hard cement plug from the top of the fish to at least 200 ft above the salt. This ensures that at the top of the salt where the kick-off needs to start, there is good, consistently hard cement. A regular  $12\frac{1}{4}$ -in. Series 1-1-1 bit or a good rerun bit can be used to drill the cement to the top of the salt. Next, select the proper size and type of motor, the bit, and the bent-sub angle, and design the hydraulics program to run the motor over the expected range of pressures.

There are a number of possible motor types and sizes that could be used for the sidetracking operation (see Tables 8.10 and 8.11).

Because this sidetrack will be done over a minimum section of hole (approximately 220 ft to miss the top of the fish; Fig. 8.115), the shortest motor offers the best chance of changing the angle off the plug. This assumes that a bent sub, not a bent housing, will be used for the deflection. Of the eight possible choices, the  $7\frac{3}{4}$ -in. Type D motor, which is 21 ft long, is the shortest. This motor develops 50.8 to 73.3 hp with a maximum torque of 1,160 ft-lbf. The maximum pressure differential is 360 psi. Pump rates of 325 to 450 gal/min drive the bit at 230 to 332 rpm.

TABLE 8.10—TYPICAL  
MOTOR SIZES  
USED FOR SIDETRACKING

Type	OD (in.)	Stator/Rotor	Length (ft)
A	8	$\frac{5}{8}$	23
B	$9\frac{1}{2}$	$\frac{5}{8}$	24
B	8	$\frac{1}{2}$	26.5
B	$9\frac{1}{2}$	$\frac{1}{2}$	33
C	8	$\frac{1}{2}$	23.8
C	$9\frac{1}{2}$	$\frac{1}{2}$	24.9
D	$7\frac{3}{4}$	$\frac{1}{2}$	21.0
D	$9\frac{3}{8}$	$\frac{1}{2}$	26.5

TABLE 8.11—TYPICAL OPERATING PARAMETERS FOR VARIOUS MOTORS

TYPE A										
Tool Size OD (in.)	Recommended Hole Size (in.)	Pump Rate (gal/min)		Bit Speed Range	Maximum Differential Pressure	Maximum Torque (ft/lbf)	Horsepower Range	Thread Connection Bit Sub, Box Down	Length (ft)	Weight (lbm)
		min.	max.							
4¾	6 to 7⅞	80	155	90-180	580	920	17 to 32	3½ (in.)-Reg.	17.4	750
6¾	7⅞ to 9⅞	185	370	85-185	580	2,065	36 to 73	4½ (in.)-Reg.	19.8	1,760
8	9½ to 12¼	300	600	75-150	465	3,400	49 to 97	6⅝ (in.)-Reg.	23.0	2,430
9½	12¼ to 17½	425	845	80-160	465	4,490	69 to 137	6⅝ (in.)-Reg.	24.6	3,970
11¼	17½ to 26	525	1,050	65-130	465	6,850	85 to 170	7⅝ (in.)-Reg.	26.6	5,950
TYPE B										
3¾	4¼ to 5⅞	80	190	325-800	580	320	20 to 52	2⅞ (in.)-Reg.	20.8	470
4¾	6 to 7⅞	100	240	245-600	580	585	27 to 67	3½ (in.)-Reg.	21.5	840
6¼	7⅞ to 9⅞	170	345	200-510	580	1,015	39 to 98	4½ (in.)-Reg.	24.0	1,760
6¾	8⅜ to 9⅞	200	475	205-485	580	1,500	58 to 138	4½ (in.)-Reg.	26.6	2,160
8	9½ to 12¼	245	635	165-380	465	2,085	66 to 151	6⅝ (in.)-Reg.	26.5	2,800
9½	12¼ to 17½	395	635	230-380	810	3,730	163 to 270	6⅝ (in.)-Reg.	33.0	5,200
11¼	17½ to 26	525	1,055	120-250	465	5,385	123 to 256	7⅝ (in.)-Reg.	30.0	7,300
TYPE C										
3¾	4¼ to 5⅞	60	145	340-855	580	245	16 to 40	2⅞ (in.)-Reg.	16.8	400
4¾	6 to 7⅞	80	185	270-680	580	415	21 to 53	3½ (in.)-Reg.	17.5	680
6¼	7⅞ to 9⅞	170	345	200-510	580	1,015	39 to 98	4½ (in.)-Reg.	25.0	1,760
6¾	8⅜ to 10⅝	160	395	140-480	465	995	27 to 91	4½ (in.)-Reg.	21.9	1,585
8	9½ to 12¼	200	475	160-400	465	1,475	45 to 112	6⅝ (in.)-Reg.	23.8	2,430
9½	12¼ to 17½	240	610	135-340	465	2,280	59 to 148	6⅝ (in.)-Reg.	24.9	3,970
11¼	17½ to 26	290	690	115-290	465	2,990	65 to 165	7⅝ (in.)-Reg.	26.0	5,950
TYPE D										
3⅞	4⅝ to 6	100	150	380-580	625	412	29.8 to 45.5	2⅞ (in.)-Reg.	22.5	530
5	6½ to 7⅞	180	250	350-482	360	480	32.0 to 44.1	3½ (in.)-Reg.	19.9	911
6½	8⅜ to 9⅞	250	350	292-431	360	801	44.5 to 65.7	4½ (in.)-Reg.	19.9	1,582
7¾	9⅞ to 12¼	325	450	230-332	360	1,160	50.8 to 73.3	6⅝ (in.)-Reg.	21	2,350
9¾	12¼ to 17½	500	800	200-420	360	1,775	67.6 to 142.1	7⅝ (in.)-Reg.	26.5	4,350
12	17½ to 26	800	1,200	125-188	360	5,666	134.8 to 202.8	7⅝ (in.)-Reg.	33.2	8,100

Next, determine the horsepower necessary to drive the motor and to provide enough pressure across the bit to satisfy the pressure-drop requirements for the bearings and for drilling with a Series 5-1-7 bit.

Table 8.10 shows that the maximum recommended pump rate of the 7¾-in. PDM is 450 gal/min. A 10-P-130 pump operating at 112 strokes/min will pump 448 gal/min (this assumes 100% volumetric efficiency and 85% mechanical efficiency), which is well within the operating range of the pump.

To determine how many drill collars might be needed, consider how much torque will be necessary to drill the salt at a maximum penetration rate of 15 ft/hr. With Eq. 8.81, the maximum WOB for the maximum PDM torque is

$$1,160 = \left[ 3.79 + 19.7 \sqrt{\frac{15(\text{ft/hr})}{332(\text{rpm})(12.25 \text{ in.})}} \right] \times 12.25 W_b,$$

where  $W_b = 19,000$  lbf.

The drill collars are 7¾ in. OD by 3 in. ID. The weight is 116 lbm/ft in air and  $0.825 \times 116$  lbm/ft in 11.5 lbm/gal mud or 95.7 lbf/ft. Because 19,000 lbf are needed, and

because a 20% safety factor is needed to keep the drillpipe in tension, the number of collars ( $n_C$ ) needed is

$$n_C = \left[ \frac{19,000 \text{ lbf}}{(95.7 \text{ lbf/ft})(30 \text{ ft/collar})} \right] \frac{1}{0.80} = 8.3 \text{ collars.}$$

For convenience, nine collars (three stands) could be used. This leaves 10,330 ft of 5-in., 19.5-lbm/ft XH drillpipe with an ID of 4.276 in. The pressure losses in the drillstring and up the annulus minus the bit and PDM pressure at a pump rate of 448 gal/min are as follows.

Pressure loss* through surface equipment	24 psi
(Case 4: 45 ft of 4-in.-ID standpipe,	
55 ft of 3-in.-ID hose,	
6 ft of 3-in.-ID swivel,	
40 ft of 4-in.-ID kelly)	
Pressure loss through drillpipe	710 psi
Pressure loss through drill collars (3-in. ID)	89 psi
Pressure loss up the drillpipe annulus	161 psi
Pressure loss up the drill collar annulus	56 psi

\*Pressure-loss calculations are based on a power-law model; a yield value of 9 lbf/100 sq ft is assumed.

The total pressure drop for the 10,600-ft string is calculated as

$$\Delta p_t = 24 \text{ psi} + 710 \text{ psi} + 89 \text{ psi} + 161 \text{ psi} + 56 \text{ psi}$$

$$= 1,040 \text{ psi circulating pressure open ended.}$$

To design the optimum PDM motor run correctly, the maximum bit pressure drop should be determined on the basis of the hydraulic thrust and bit-weight balance. The maximum WOB for this application is 20,000 lbf. Fig. 8.116 shows that the on-bottom bearing load at a WOB of 20,000 lbf is 4,600 lbf for a bit  $\Delta p$  of 750 psi and 8,000 lbf for a bit  $\Delta p$  of 500 psi, the maximum recommended bit pressure differential. If a balanced bearing load is desired at a  $\Delta p$  of 500 psi, the maximum WOB should not exceed 12,000 lbf. Because this will be a short motor run, the on-bottom bearing load can be increased as much as 5,000 lbf (to 17,000 lbf WOB). The actual pressure drop of the bit must be corrected for mud weight before the use of Table 8.12.

$$500 \text{ psi} = \frac{\text{pressure loss} \times \text{actual mud weight}}{10 \text{ lbm/gal}},$$

and

$$\text{pressure loss} = 500 \text{ psi} \frac{10 \text{ lbm/gal}}{11.5 \text{ lbm/gal}} = 435 \text{ psi.}$$

The nozzles should be sized for a bit  $\Delta p$  of 435 psi and a mud weight of 11.5 lbm/gal. Table 8.12 shows that 2 $\frac{1}{32}$ - and 1 $\frac{1}{32}$ -in. nozzles are required to give the approximate  $\Delta p$ .

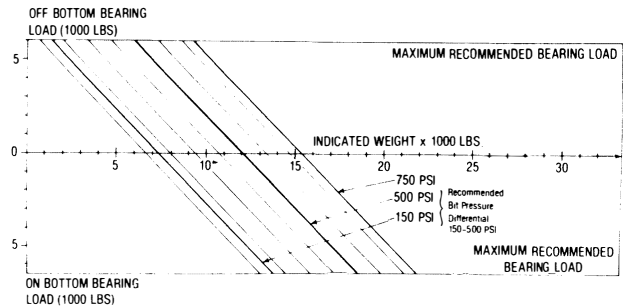


Fig. 8.116—Hydraulic thrust and bit weight balance (courtesy of Dyna-Drill).

The total standpipe pressure, including the PDM  $\Delta p$ , would be as follows (at 450 gal/min):

$$\begin{aligned} \text{Drillstring} &= 1,040 \text{ psi} \\ \Delta p_b &= 500 \text{ psi} \\ \text{Maximum } \Delta p \text{ for motor torque} &= 360 \text{ psi} \\ \text{Total standpipe pressure} &= 1,900 \text{ psi} \end{aligned}$$

The next step is to design a trajectory for the sidetrack that will miss the top of the fish by at least two bit diameters, which means that the side of the new wellbore will be about 24 in. from the side of the old wellbore. The minimum average change to offset the fish by two bit diameters is 0.78°. Because the desired target for the well is S15E, the plan should call for a right turn away from the old wellbore. A simple direction change with no inclination change would be risky; therefore, a drop and right turn should be planned to ensure that the new borehole will not re-enter the old borehole. It must be

TABLE 8.12—PRESSURE LOSS THROUGH THE JET NOZZLES (PSI)

Flow Rate (gal/min.)	JET NOZZLE SIZE AREA*											
	15 15 15 (0.5177 sq in.)	15 15 16 (0.5415 sq in.)	15 16 16 (0.5653 sq in.)	16 16 16 (0.5890 sq in.)	16 16 18 (0.5412 sq in.)	16 18 18 (0.6934 sq in.)	18 18 18 (0.7455 sq in.)	18 18 20 (0.8038 sq in.)	18 20 20 (0.8621 sq in.)	20 20 20 (0.9204 sq in.)	20 20 22 (0.9048 sq in.)	20 22 22 (0.0492 sq in.)
410	578	528	485	446	377	322	279	240	208	183	160	141
420	606	554	508	468	395	338	292	251	219	192	168	148
430	635	581	533	491	414	354	306	264	229	201	176	155
440	665	608	558	514	434	371	321	276	240	210	184	162
450	696	636	584	537	454	388	336	289	251	220	192	169
460	727	665	610	562	474	405	351	302	262	230	201	177
470	759	694	637	586	495	423	366	315	274	240	210	185
480	792	724	664	612	516	441	382	328	286	250	219	193
490	825	754	692	637	538	460	398	342	298	261	228	201
500	859	785	721	664	560	479	414	356	310	272	237	209
510	894	817	750	690	583	498	431	371	322	283	247	218
520	929	849	779	718	606	518	448	385	335	294	257	226
530	965	882	810	746	629	538	465	400	348	305	267	235
540	1,002	916	840	774	653	559	483	416	361	317	277	244
550	1,039	950	872	803	678	580	501	431	375	329	287	253
560	1,078	985	904	832	702	601	520	447	389	341	298	262
570	1,116	1,021	936	862	728	622	538	463	403	353	309	272
580	1,156	1,057	970	893	754	644	557	480	417	366	319	281
590	1,196	1,093	1,003	924	780	667	577	496	431	378	331	291
600	1,237	1,131	1,038	956	806	690	597	513	446	391	342	301
610	1,279	1,169	1,073	988	834	713	617	530	461	405	353	311
620	1,321	1,207	1,108	1,020	861	736	637	548	476	418	365	322
630	1,364	1,247	1,144	1,053	889	760	658	566	492	432	377	332

\* Nozzle Size (32/100 in.). Nozzle Area (sq. in.)

(Courtesy of Dyna Drill)

TABLE 8.13—DEFLECTION ANGLE RESULTING FROM BENT-SUB ANGLE AND HOLE SIZE

Bent-Sub Angle (degrees)	BENT-SUB ASSEMBLY									
	3 7/8 in.		5 in.		6 1/2 in.		7 3/4 in.		9 5/8 in.	
	Hole Size (in.)	Deflection Angle (deg/100 ft)	Hole Size (in.)	Deflection Angle (deg/100 ft)	Hole Size (in.)	Deflection Angle (deg/100 ft)	Hole Size (in.)	Deflection Angle (deg/100 ft)	Hole Size (in.)	Deflection Angle (deg/100 ft)
1	4 1/4	4°00'	6	3°30'	8 3/4	2°30'	9 7/8	2°30'	13 1/2	2°00'
1 1/2		4°30'		4°45'		3°30'		3°45'		3°00'
2		5°30'		5°30'		4°30'		5°00'		4°30'
1	4 3/4	3°00'	6 3/4	3°00'	9 7/8	1°45'	10 5/8	2°00'	15	1°45'
1 1/2		3°30'		4°15'		3°00'		3°30'		2°30'
2		4°00'		5°00'		3°45'		4°15'		3°45'
2 1/2		5°00'		5°45'		5°00'		5°30'		5°00'
1	5 7/8	2°00'	7 7/8	2°30'	10 5/8	1°15'	12 1/4	1°45'	17 1/2	1°15'
1 1/2		2°30'		3°30'		2°00'		2°30'		2°15'
2		3°00'		4°30'		3°00'		3°30'		3°00'
2 1/2		3°30'		5°30'		4°00'		5°00'		4°30'

remembered when sidetracking in harder formations that the bent-sub assembly will not always respond as predicted. Therefore, a safe design would be based on a 2°/100-ft right turn and drop away from the old wellbore.

Based on the 2°/100 ft dogleg severity over 220 ft, the total angle change is

$$\beta = \frac{2(220)}{(100)} = 4.4^\circ.$$

The current inclination,  $\alpha$ , is 4°. Assuming a 2° inclination drop, what should be the tool-face setting to maintain a total angle change of 4.4° and achieve a maximum direction change  $\Delta\epsilon$ ? First, calculate the tool face setting with Eq. 8.48:

$$\gamma = \arccos \left[ \frac{\cos(4) \cos(4.4) - \cos(2)}{\sin(4) \sin(4.4)} \right] = 153^\circ.$$

With a tool-face setting of 153° right of the high side, the maximum direction change can be calculated with Eq. 8.42.

$$\Delta\epsilon = \arctan \left[ \frac{\tan(4.4) \sin(153^\circ)}{\sin(4) + \tan(4.4) \cos(4) \cos(153^\circ)} \right]$$

$$= 87.8^\circ$$

The reactive torque for the bit and the PDM can be calculated from Eq. 8.57 with a maximum motor torque of 1,160 ft-lbf.

$$\theta = \frac{13,920 \text{ in. lbf}}{11.5 \times 10^6 \text{ psi}} \left( \frac{125,160 \text{ in.}}{-32.8 \text{ in.}^4} + \frac{3,240 \text{ in.}}{346 \text{ in.}^4} \right)$$

$$= 4.61.$$

$$\theta = \frac{4.61(36)}{2\pi} = 264^\circ.$$

Note that the PDM is omitted because its short length makes it a negligible term.

The reactive torque from the PDM and the Series 5-1-7 bit is significant and requires that a steering tool be run so that the tool face will always be at the proper setting. Because the reactive torque calculation allows for no friction, it would be wise to plan initially to set the tool face at N48E, to engage the bit with near-maximum WOB (20,000 lbf), and to observe the reactive torque response. The full reactive torque probably will not be observed because of friction, and the tool face will need to be adjusted less than the calculated 264° to obtain the tool-face setting of 153°. A few tries with the steering tool should be ample to set the tool face and to start the sidetrack. The calculated tool-direction change is more than enough to head the wellbore toward the target. Because the drilling is slow, the direction can be watched and corrected to a lesser tool-face setting (90 to 120°), which will result in a smaller  $\Delta\epsilon$ .

The last part of the design is to select a bent sub that will give an angle change of approximately 2.0°/100 ft. From Table 8.13, a 1° bent sub on a 7 3/4-in. PDM in a 12 1/4-in. hole should yield an angle change of nearly 1.75°/100 ft. A 1.5° bent sub would give an angle change of 2.5°/100 ft. Because the formations are harder and the response is less than those included in Table 8.13, the safest plan would be to run the 1.5° bent sub.

### 8.6.10 The Use of a Turbine for Directional and Straight-Hole Drilling

Drilling economically with a turbine is more complicated than with a PDM. The bit must be chosen for a given turbine, and the drilling rig must be able to deliver the required flow rates at pressures that will operate the turbine at maximum efficiency. In addition, the operator must be capable of operating the turbine at speed and torque ranges that will achieve maximum horsepower most of the time.

Because, unlike the PDM, neither the bit speed nor the torque is related to the standpipe pressure, the only way to be certain a turbine is performing properly is to measure downhole bit speed and/or torque. A surface-reading tachometer is needed to control a turbine accurately, unless the operator is very familiar with the formations in the drilling area, can pick the appropriate bit and motor

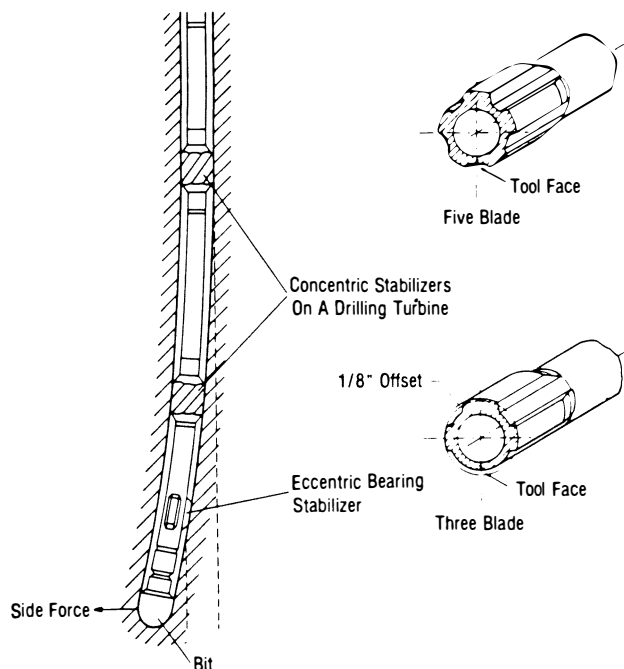


Fig. 8.117—Eccentric stabilizer (after Feenstra and Kamp<sup>17</sup>).

size, and knows the capabilities of the turbine thoroughly. Even with such experience, the operator must watch the turbine constantly to keep it from stalling and to drill with the right WOB to ensure optimum drilling conditions. This is another reason for the slow acceptance of turbines outside the Soviet Union and Europe.

To emphasize the problem, consider Eq. 8.78 rewritten as

$$N_b = \frac{1}{K}(M_{ts} - M_i).$$

The torque relationship for an 8.5-in. polycrystalline diamond bit is similar to any drag bit. Neglecting the torque to overcome friction yields the following relationship:

$$M_i = \left( 8.537 + 203 \times \frac{\sqrt{F_d}}{n} \right) d_b W_b, \dots \dots \dots (8.90)$$

If the pump stroke, bit size, and mud weight are maintained at constant levels, the addition of WOB will increase the turbine torque, which in turn reduces both the bit speed and the penetration rate. The reduction in penetration rate causes the torque to decrease and the bit speed to increase. If the bit speed is not controlled so that it is kept at the peak of the power curve, optimal performance of the turbine and the bit is not obtained. Unlike using the hook-load indicator in drilling with a rotary system and a tricone bit or using the standpipe pressure gauge in drilling with a PDM, drilling with a turbine requires a bit-speed indicator.

Properly engineered, the turbine can be economically competitive in many drilling situations, especially with

the advanced designs of the new polycrystalline diamond bits. For kicking off and making trajectory changes, turbines have not been as widely used as PDM's. In areas of soft formations, turbines have been used with tricone bits to make successful (though not necessarily economical) trajectory changes. For most trajectory changes, however, operating a turbine with a tricone bit is too difficult because of the previously mentioned bit speed and bit side-force problems. Where formations dictate a less aggressive bit, such as a diamond or other type of drag bit, the turbine is more likely to be successful. A properly designed turbine and bit combination with a tachometer can be as successful in making a trajectory change as a PDM.

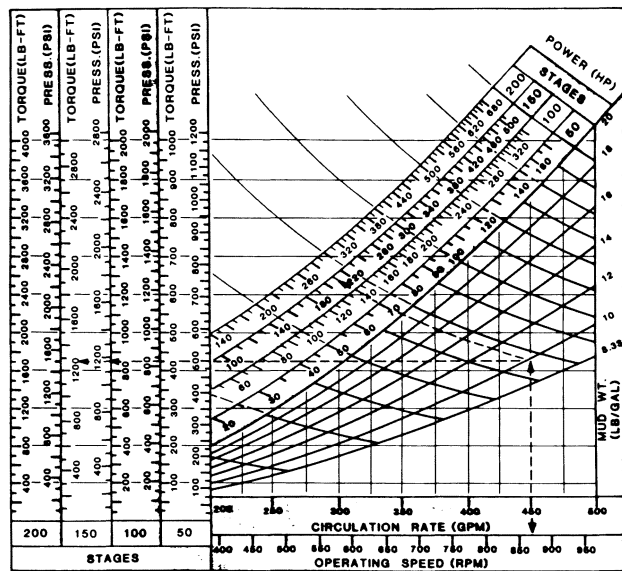
One way of making controlled trajectory changes is to use an eccentric stabilizer on the turbine near the bit (see Fig. 8.117). The undergauge blade is oriented as a bent sub or bent housing and the drillstring does not rotate. After the desired trajectory change is achieved, drillstring rotation is begun with the eccentric stabilizer, a part of the controlling BHA. This system is frequently used with a building BHA. (See Sec. 8.7 for a description of a building assembly.)

The turbine is commonly used as part of the BHA for normal directional drilling. Unlike most rotary directional drilling systems, the reactive torque of the turbine gives a strong left or counterclockwise component to the bit direction. Rotating the drillstring counteracts this reactive torque to varying degrees, dependent on the bit type and BHA, and it reduces some of the left or counterclockwise tendency.

**Example 8.22.** Determine whether it is economical to run a diamond bit with a turbine in a situation where 8½-in. Series 6-2-7 bits average 3 ft/hr at a depth of 17,520 ft. The bits usually drill 120 to 140 ft and are graded 4 to 6 and ⅛-in. in gauge. Use the same rig as in Example 8.21. The oil-mud density is 16.2 lbm/gal, the plastic viscosity is 22 cp, and the yield value is 15 lbf/100 sq ft. A Series 6-2-7 bit costs \$4,400. The diamond bit costs \$19,500 assuming 50% salvage. A 7-in. turbodrill costs \$500 per rotating hour. Round-trip time is 16 hours. Rig cost is \$800/hr. Fig. 8.118A is a nomograph for a 7-in. turbine with 50, 100, 150, and 200 stages. The turbine develops maximum horsepower at about 850 rpm. Fig. 8.114A shows the theoretical torque, penetration rate, and pressure-drop characteristics of the new diamond bit under downhole conditions at a constant rotary speed of 850 rpm. The bit has a pump-off area of 10 sq in. Assume that the penetration rate and torque of the diamond bit when dull is about half that of the new bit. Select the appropriate flow rate and number of stages for the turbine, and size the total flow area ( $A_{tf}$ ) of the diamond bit to provide at least 2.0 to 2.5 hhp/sq in.

**Solution.** Refer to the nomograph in Fig. 8.118A to find that the turbine requires 440 gal/min to develop its maximum power at 850 rpm. The nomograph and Fig. 8.114A provide the information found in Table 8.14.

Roughly calculate the number of drill collars required, assuming that 25,000 lbf will be applied initially and that it will take 50% additional weight to maintain bit torque as the bit dulls and as its pump-off effect increases.



## - EXAMPLE -

GIVEN : Circulation rate : 450 GPM  
Mud weight : 10 LB/GAL

FIND : Operating pressure drop, torque, power, and speed for 150 stage motor.

SOLUTION : Enter graph at circulation rate of 450 GPM. Following dashed line, turn at intersection with mud weight of 10 LB/GAL and read pressure drop of 1180 PSI and torque of 1260 LB-FT. Also at intersection follow horsepower line and read 210 HP. Project down from circulation rate of 450 GPM and read speed of 870 RPM.

Fig. 8.118A—Seven-inch turbine drilling motor operating characteristics (courtesy Baker Service Tools).

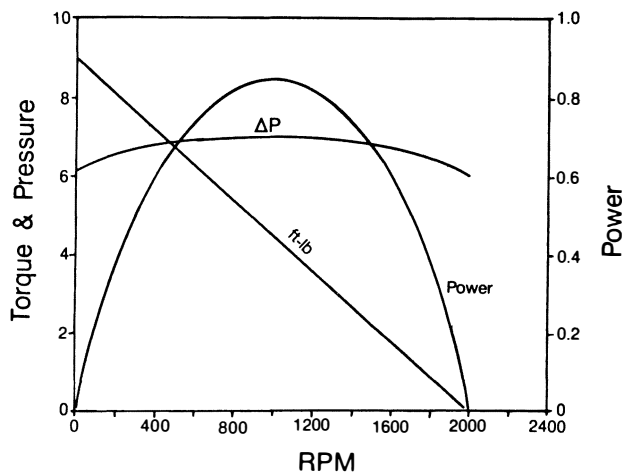


Fig. 8.118B—One-stage turbodrill characteristics.

Calculate the collars required for 37,500 lbf, using a 20% safety factor for collars having a buoyed weight of 81.3 lbf/ft.

$$n_c = \frac{37,500 \text{ lbf}}{(87.3 \text{ lbf/ft})(30 \text{ ft/collar})(0.80)}$$

$$= 17.9 \text{ collars} = 6 \text{ stands.}$$

Using a penetration rate of 18 ft/hr, determine the diamond bit  $A_{if}$  required for 2.0 hhp/sq in.

A minimum of 113 hhp is required, which at 440 gal/min equates to 442 psi  $\Delta p$  at the bit. Use of the equation from Fig. 8.114A yields

$$A_{if} = \left[ \sqrt{\frac{(440)^2 16.2}{8,795(442)}} \right] \div 0.983 = 0.91 \text{ sq in.}$$

The  $A_{if}$  should be no larger than 0.91 sq in.

Can the turbine be operated at 440 gal/min without exceeding the pressure limit of the drilling rig? It depends on the size of the liners that are run in the pump and on the pressure capacity of all other components in the circulating system. For the 10-P-130 pump, a good choice is to install 6-in. liners. The pump is rated to 140 strokes/min, and only 125 strokes/min will be required.

$$440 \text{ gal/min} \div (3.7 \text{ gal/stroke} \times 0.95 \text{ pump efficiency})$$

$$= 125 \text{ strokes/min.}$$

The pump is rated to 3,900 psi maximum with 6-in. liners, so 3,705 psi will be the maximum planned standpipe pressure.

$$3,900 \text{ psi} \times 0.95 \text{ pump safety factor} = 3,705 \text{ psi.}$$

Now calculate the component pressure losses in the circulating system for a power law fluid:

Surface equipment, psi	24
Drillpipe bore, psi	1,638
Drill collar bore, psi	219
Drill bit, psi	442
Drill collar annulus, psi	310
Drillpipe annulus, psi	456
Total, psi	3,089

TABLE 8.14—TURBINE OPERATING RANGE  
SELECTED FROM FIGS. 8.114A and 8.118A

No. Stages	Turbine $\Delta p$ (psi)	Turbine Torque (ft/lbf)	Turbine (hp)	Bit Weight (lbm)	Rate of Penetration (ft/hr)
50	800	680	110	13.5	12.2
100	1340	1360	220	24.5	24.1
150	1890	2040	330	32.5	29.3

**TABLE 8.15—DRILLSTRING PRESSURES LOSSES AT VARIOUS FLOW RATES FOR PROBLEM 8.22**

Components	Pressures (psi)				
	at 100 gal/min	at 200 gal/min	at 300 gal/min	at 400 gal/min	at 500 gal/min
Surface equipment	—	4	11	19	31
Drillpipe bore	77	460	878	1,401	2,021
Drill collar bore	20	60	117	188	272
Drill bit	23	92	207	369	576
Drill collar annulus	24	48	91	144	207
Drillpipe annulus	78	133	248	391	561
Total standpipe	222	797	1,552	2,512	3,668
Available pressure, psi	3,483	2,908	2,153	1,193	37
Available power, hp	203	339	377	278	11

Available pressure for the turbine:  $3,705 - 3,089 = 616$  psi.

The pressure losses in the system are too great for even the 50-stage turbine, which consumes 800 psi at 440 gal/min with 16.2-lbm/gal mud. This does not mean that the problem is solved and that a turbine can be run. The problem cannot be solved until it is analyzed properly as follows.

The correct procedure is to analyze the entire circulating system.

1. Compute the component pressure losses at several flow rates, such as 100, 200, 300, 400, and 500 gal/min. Add the component losses to determine the total standpipe pressure for each flow rate.

2. Plot standpipe pressure vs. flow rate. Mark a horizontal line at the maximum recommended standpipe pressure.

3. Determine the remaining available standpipe pressure at each flow rate (the difference between maximum and calculated standpipe pressure). On a separate graph, plot the available pressure vs. flow rate.

4. Compute the available hydraulic power at each flow rate, and plot on the same graph available power equals available psi times gallons per minute divided by 1,714.

5. Locate the maximum available power on the curve, and note the flow rate at which it occurs. This is the flow rate at which the turbine should be operated. The corresponding available pressure is the pressure drop for which the turbine should be sized. It may not necessarily agree with the flow rate and pressure at which a particular turbine was designed to operate, in which case the turbine is mismatched to the system and a different turbine must be considered.

The foregoing procedure is applied to this problem (see Table 8.15) and is shown graphically in Figs. 8.119A and B.

The optimal flow rate for this system is approximately 300 gal/min, as shown in Fig. 8.119B. That is the flow rate at which the most hydraulic horsepower is delivered to a downhole motor for conversion to mechanical horsepower at the bit. Without changing something in the system, such as switching to larger drillpipe, no other flow rate will affect mechanical horsepower more strongly at the bit. The nomograph (Fig. 8.118A) shows that at 300 gal/min, turbine speed is only 575 rpm and the resultant power is reduced to 115 hp with 150 stages and 153 hp with 200 stages. Fig. 8.119B shows that at 300 gal/min, 377 hhp is available from the system. Assuming roughly a 55% power conversion factor, a turbine that develops

about 207 hp ( $377 \times 0.55 = 207$ ) at 300 gal/min with 16.2-lbm/gal mud is best suited to this system. It becomes clear that even if there were no standpipe-pressure limitation, even the 200-stage turbine in Fig. 8.118A would be less than optimal with its 153 hp. The problem now becomes one of selecting a turbine that is matched to the system.

Fig. 8.118B shows the characteristics for one stage of a 7-in. turbodrill designed to operate in the range of 275 to 325 gal/min. This turbine can deliver more power to the bit in this particular situation than the turbine represented previously in Fig. 8.118A. Fig. 8.118B is based on 300 gal/min with water. Notice that peak power occurs at 1,000 rpm and that  $\Delta p_1 = 7$  psi (for water). Therefore  $\Delta p_1$  equals 14 psi for 16.2-lbm/gal mud ( $16.2 \times 7/8.33 = 14$ ).

Resize the pump liners, if possible, and adjust the  $A_{tf}$  of the diamond bit to give 2.5 hhp/sq. in. at 300 gal/min flow rate. For the 10-P-130 pump, a good choice is 5½-in. liners. The pump is rated to 140 strokes/min, but only 102 will be required.

$$300 \text{ gal/min} \div (3.1 \text{ gal/stroke} \times 0.95 \text{ pump efficiency}) \\ = 102 \text{ strokes/min.}$$

The pump is rated to 4,645 psi with 5½-in. liners; however, although 95% of 4,645 psi is 4,413 psi, both the contractor and operator agree in this case not to exceed 3,950 psi because of the limitations of the standpipe, kelly hose, and swivel.

**TABLE 8.16—SYSTEM PRESSURE DROP AT VARIOUS FLOW RATES WITH A DIAMOND BIT TFA OF 0.42 SQ IN.**

Flow Rate (gal/min)	Bit $\Delta p$ (psi)	Standpipe Pressure (psi)	Available Standpipe Pressure (psi)	Available Hydraulic Horsepower (hp)
100	90	289	3,661	214
200	361	1,066	2,884	337
300	811	2,156	1,794	314
400	1,443	3,586	364	85
500	2,254	5,346	—	—



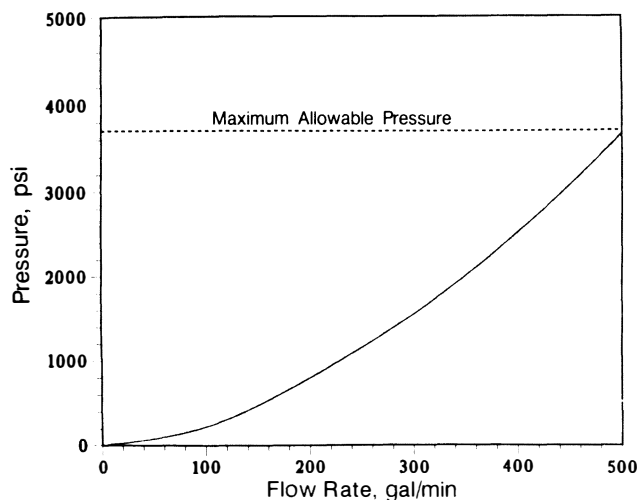


Fig. 8.119A—Standpipe pressure vs. flow rate.

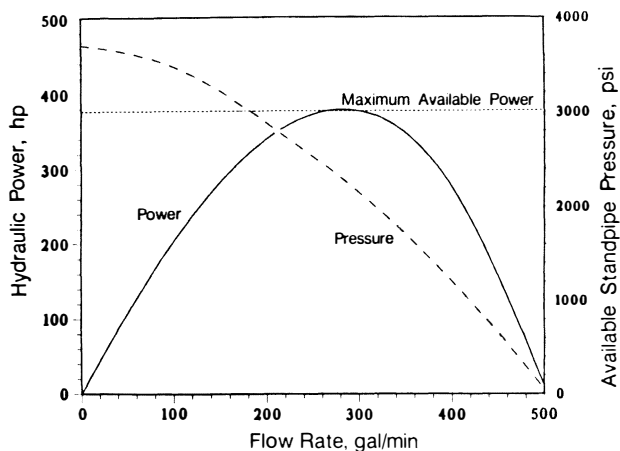


Fig. 8.119B—Available pressure and power vs. flow rate.

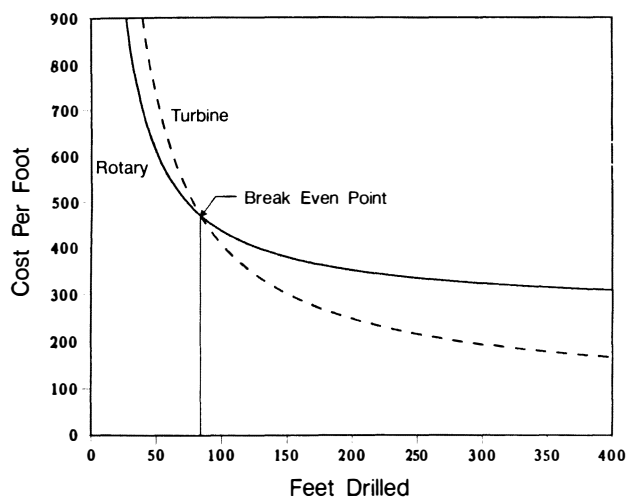


Fig. 8.119C—Analysis of cost per foot—rotary vs. turbine drilling.

The  $A_{tf}$  of the diamond bit must be reduced to provide 2.5 hhp/sq in. at the bit. A pressure drop of 810 psi is required at 300 gal/min to give 2.5 hhp/sq in.:

$$2.5 \text{ hhp/sq in.} \times 56.7 \text{ sq in.} = 142 \text{ hhp,}$$

$$142 \text{ hhp} \times 1,714/300 = 811 \text{ psi.}$$

A minimum  $A_{tf}$  of 0.46 sq in. is required. Now recalculate the system pressures using the 0.46-sq-in.  $A_{tf}$ . See Table 8.16 for system pressure drops at various flow rates. With the  $A_{tf}$  reduced, the optimal flow rate of the system has shifted to about 260 gal/min, but it is decided to operate at 300 gal/min to operate the turbine at its optimal design rate and to provide adequate bit cleaning and annular cuttings transport. Bit cleaning is important because the turbine is designed to divert at least 5% of the mud flow through the bearings; therefore, no more than 285 gal/min will be flowing through the bit, thus giving a bit  $\Delta p$  of 730 psi rather than the 811 psi shown in the previous table. Bit hydraulic horsepower is 2.1 hhp/sq in., which is marginal, and the available turbine pressure will be adjusted by 81 psi because of the diversion of fluid. Available turbine pressure ( $p_{at}$ ) is calculated as

$$p_{at} = 1,794 + 81 = 1,875.$$

Calculate the number of turbine stages:

$$\Delta p_E = 1,875 \text{ psi,}$$

$$\Delta p_1 = 14 \text{ psi/stage,}$$

$$n_s = \Delta p_E / \Delta p_1 = 1,875 / 14 = 134 \text{ stages.}$$

The 7-in. turbine represented in Fig. 8.118B is readily available as a 130-stage tool.

Determine the power output of a 130-stage turbine. Note in Fig. 8.118B that one turbine stage develops a maximum of 0.87 hp at 300 gal/min with water. Therefore,

$$0.87 \times (16.2 \text{ lbm/gal}) / (8.33 \text{ lbm/gal})$$

$$= 1.7 \text{ hp/stage with 16.2-lbm/gal mud.}$$

$$1.7 \text{ hp/stage} \times 130 \text{ stages} = 221 \text{ } H_m \text{ at the bit.}$$

The 130-stage turbine will deliver 221 hp at the bit, compared with 153 hp with the 200-stage turbine referred to in Fig. 1.118A. This does not mean that the 200-stage turbine is not a good tool; however, it is highly mismatched to the system in this example.

It must be determined now whether the 130-stage turbine and natural diamond bit will be economical.

Fig. 8.114B shows the penetration rate and torque curves for a new diamond bit on the 130-stage turbine. This figure indicates that at about 7,000 lbf, the bit is pumped off and at 35,000 lbf the turbine is stalled. Peak penetration rates of 20 to 21 ft/hr are achieved in the 20,000- to 26,000-lbf range. Remember that the rate of penetration of the bit will decrease by about half when the bit is dulled, so assume an average penetration rate of 15 ft/hr over the entire run. Also, remember that bit

torque will decrease by 50% as the bit dulls; therefore, WOB must be increased throughout the run to maintain turbine operation at peak power. Also, diamond bit pump-off force is likely to increase about 50% as the bit dulls, thus requiring still more weight to maintain torque. The result is that initial WOB should be about 23,000 lbf and the final WOB should be about 36,000 lbf, which means that the original calculation calling for six stands of drill collars still applies.

The rotary drilling cost per foot, using the Series 6-2-7 bit, is

$$C_{\text{rot}} = \frac{(\text{trip time} + \text{rotating time})(\text{rig cost}) + \text{bit cost}}{\text{feet drilled}}$$

$$= \frac{(16 \text{ hr} + 40 \text{ hr})(\$800/\text{hr}) + \$4,400}{120}$$

$$= 410 \text{ \$/ft.}$$

and for 140 ft, the cost per foot is \$390.

The cost per foot for the turbine is

$$C_{\text{turbine}} = \frac{(\text{trip time} + \text{rotating time})(\text{rig cost}) + \text{bit cost}}{\text{feet drilled}} + \frac{(\text{rotating time})(\text{turbine cost})}{\text{feet drilled}}$$

Assuming the penetration rate averages 15 ft/hr, the costs per foot for 120 and 140 ft are

$$C_{120} = \frac{(16 + 8)(\$800/\text{hr}) + \$19,500 + (8 \text{ hrs})(\$500/\text{hr})}{120}$$

$$= \$356/\text{ft.}$$

and

$$C_{140} = \$317/\text{ft.}$$

The break-even point for the turbine/diamond-bit combination is at a drilled interval of 84 ft. The cost per foot and interval drilled can be calculated with the equation for turbine cost per foot. Fig. 8.119C shows the break-even point at 5.6 hours for a drilled interval of 84 ft. If the average penetration rate decreases to less than 15 to 12 ft/hr, it will take 7.9 hours and a drilled interval of 95 ft for the turbine/diamond-bit combination to break even.

## 8.7 Principles of the BHA

The BHA is the portion of the drillstring that affects the trajectory of the bit and, consequently, of the wellbore. Its construction could be simple, having only a drill bit, collars, and drillpipe, or it may be complicated, having a drill bit, stabilizers, magnetic collar, telemetry unit, shock sub, collars, reamers, jars, crossover subs, heavyweight drillpipe, and regular drillpipe. Fig. 8.120 depicts two BHA's.

In the earlier days of drilling, the slick assembly (bit with drill collars) was the most common. Later, Lubinski and Woods<sup>18</sup> showed that the pendulum assembly

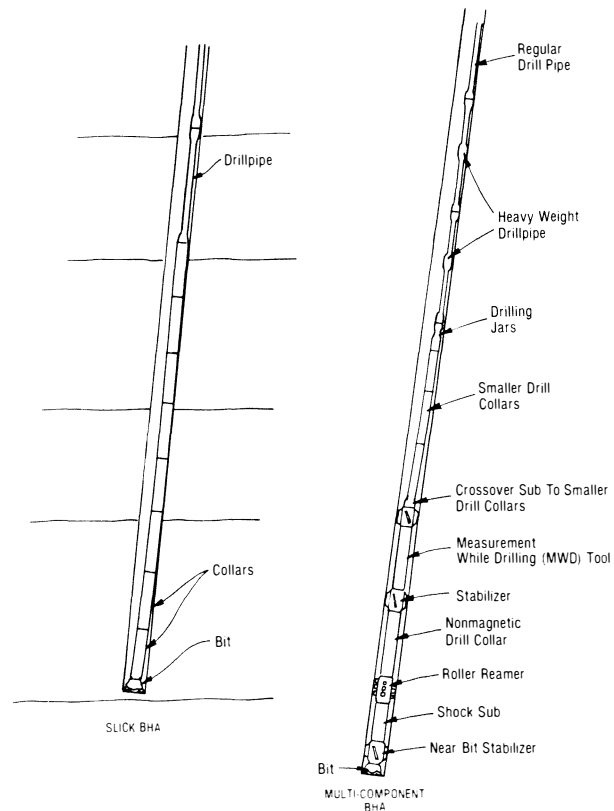


Fig. 8.120—Bottomhole assemblies.

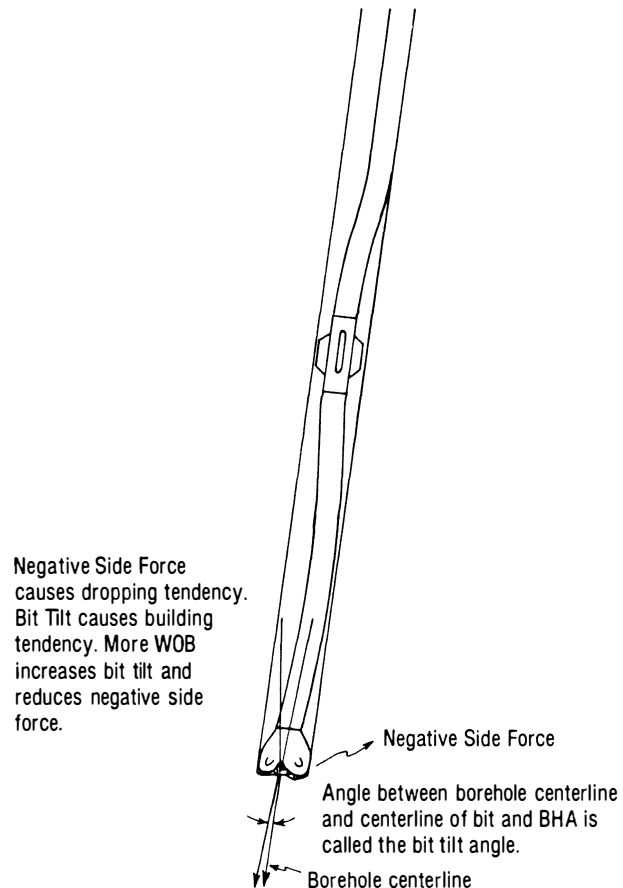


Fig. 8.121—Example of bit tilt for a pendulum BHA.

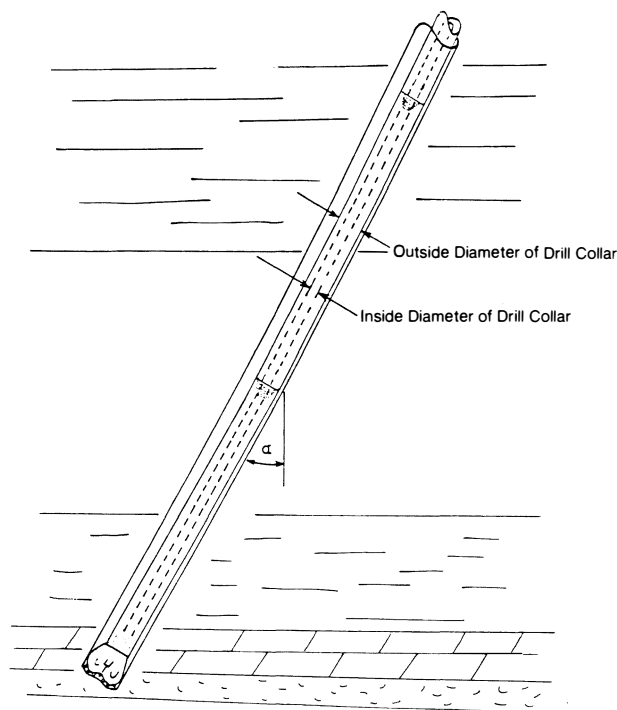


Fig. 8.122—Typical slick BHA drilling ahead at an inclination  $\alpha$ .

could be used for deviation control. Multistabilizer BHA's became popular because of directional drilling and, later, were shown effective in some attempts for deviation control.

All BHA's cause a side force at the bit that makes the bit build or drop or makes it hold an angle and turn to the left or right. Furthermore, the stabilizers and parts of the BHA that contact the wellbore exert side forces on the formation or casing. Sometimes these forces are so great that the contacting equipment wears a hole in the casing, mechanically wears or cuts the formation, and wears the pipe or stabilizer blades touching the wellbore. The forces and displacements for a given WOB and the rotary speed for any BHA can be determined accurately if the physical properties of each BHA component are known, and if the shape, size, and trajectory of the wellbore can be described.

Bit tilt is another factor in BHA mechanics that influences bit direction and inclination, especially in drilling softer formations. The curvature of the BHA centerline is transmitted to the bit, causing some tilt and movement in the direction of the centerline (see Fig. 8.121). The softer the rock, the more the bit tilt controls the trajectory of the bit. On the other hand, the harder the rock, the more the bit side force predominates. A bent housing works on the bit-tilt principle; with a bent sub, however, either a bit tilt or a side-force mechanism or both may exist.

This section will present the principles that govern BHA design and performance. The properties that govern the elastic behavior of a simple BHA will provide the basis for the more complex analysis of the single- and multi-stabilizer BHA's. Most of the BHA (bit and drill collars) analysis will apply to a 2D static system. The effects of drillstring rotation on the inclination and direction bit forces will be covered briefly at the end of this section.

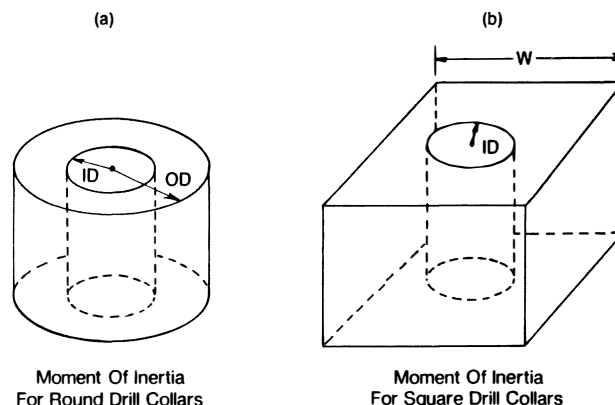


Fig. 8.123—Moment of inertia representation.

### 8.7.1 Statistics of the Tubular Column

Fig. 8.122 is a BHA consisting of drill collars and a bit in an inclined borehole. The types of metals that compose the collars dictate the weight of the collars and their elastic behavior.

From the shape and dimensions of the collars, the axial moment of inertia,  $I$ , and the polar moment of inertia,  $J$ , can be determined. Most drilling components used in a BHA can be represented as a thick-walled cylinder or as a square column with a cylindrical hole in the center (see Fig. 8.123).

The axial moment of inertia for a thick-walled cylinder is expressed as follows.

$$I = \frac{(d_e^4 - d_i^4)\pi}{64} \quad \dots \dots \dots (8.91)$$

The polar moment of inertia for the cylinder,

$$J = \frac{1}{32}\pi(d_e^4 - d_i^4) \text{ or } J = 2I. \quad \dots \dots \dots (8.92)$$

**Example 8.23.** Calculate the axial and polar moments of inertia for a 6-in. round collar with a  $2\frac{3}{8}$ -in. ID ( $I_6$  and  $J_6$ , respectively) and for an 11-in. collar with a 3-in. ID ( $I_{11}$  and  $J_{11}$ , respectively).

**Solution.**

$$I_6 = (6.0^4 - 2.1875^4)\pi/64 = 62.5 \text{ in.}^4$$

$$J_6 = 2(62.5) = 125.0 \text{ in.}^4$$

$$I_{11} = (11.0^4 - 3.0^4)\pi/64 = 715 \text{ in.}^4$$

$$J_{11} = 2(715 \text{ in.}^4) = 1,430 \text{ in.}^4$$

In Example 8.24, the moment of inertia is increased an order of magnitude by increasing the OD from 6 to 11 in. If the ID's in both examples are neglected, the difference would be small (i.e.,  $I_6 = 63.6 \text{ in.}^4$  and

TABLE 8.17—TYPICAL PROPERTIES OF SOME COMMON ALLOYS AND METALS

Metal	Melting Point (°F)	Density (lbm/cu ft)	Modulus of Elasticity (10 <sup>6</sup> psi)	Tensile Strength (10 <sup>3</sup> psi)	Yield Strength (10 <sup>3</sup> psi)	Electrical Resistance Microhms (cm <sup>3</sup> )	Thermal Conductivity (BTU/hr/sq ft/°F/ft)	Brinell Hardness
<b>Iron Base Alloys</b>								
Steel, Low Carbon	2760	491	29.0	60	40	10	30	100 to 300
Cast Iron	2150	449	13.5 to 21	18 to 60	8 to 40	66	—	50
Ni Resist-Type 1	2250	456	—	—	—	140	—	30
Cr-Mo Steels	2500	491	27.4 to 29.9	63 to 84	40 to 56	10	15 to 19	70
12 Cr Steel	2720	484	29.2	89	47	9	13.0	70
Stainless 304	2590	501	27.4	85	35	72	9.4	160
Stainless 316	2550	501	28.1	90	42	74	9.4	165
Stainless 317	2550	501	—	85	40	74	—	165
Worthite Alloy 20	2650	501	—	—	—	75	—	160
25 Cr-12 Ni Steel	2650	501	—	80	57	78	8.0	160
25 Cr-12 Ni Steel	2650	501	28.2	88	33	78	8.0	165
Incoly 800	2525	503	28.5	82	43	93	8.0	184
<b>Nickel Base Alloys</b>								
Monel 400	2460	551	26.0	81	32	48	12.6	44
Monel k-500	2460	529	26.0	160	111	48	10.1	50
Nickel 200	2640	556	30.0	67	22	7	32.5	20
Inconel 600	2600	526	31.0	85	36	103	8.6	40
Hastelloy B	2460	577	31.0	131	56	135	6.5	23
Hastelloy C	2380	558	29.8	121	58	133	7.3	23
<b>Super Alloys</b>								
Nimonic 80	2590	515	27.0	155	87	124	7.0	185
Inconel X-750	2600	515	31.0	178	122	122	6.92	176
Refractaloy 26	2450	513	30.6	154	91	92	—	250
Haynes Alloy 31	2500	538	28.0	172	87	98	8.6	340
<b>Other Metals</b>								
Aluminum	1220	170	10.6	28	25	3	131	20
Titanium	3135	281	16.0	85	63	61	11.5	150
Tungsten	6200	1205	51.5	200	—	60 ± 18	95	230

$I_{11} = 718.7 \text{ in.}^4$ ). If the ID in the 6-in. example is increased to 3 in., the moment is decreased only to 59.6 sq in. or 4.6%.

Young's modulus,  $E$ , relates the amount of strain of a material to a given amount of stress. This assumes that the material strains linearly when stressed and is in the Hooke's-law region. Most of the time the drillstring and BHA are in the elastic region. Sometimes, however, the pipe can be pulled beyond its elastic limit, resulting in plastic deformation and possible failure. Table 8.17 presents the values of some common alloys and metals. Note that the modulus of aluminum is nearly one-third that of mild steel and that the modulus of tungsten is nearly double. The modulus slightly decreases with an increase in temperature.

The product of the moment of inertia and the modulus of elasticity is called the stiffness of a material,  $EI$ . Fig. 8.124 is a plot of the stiffness of various drillstring and BHA components as a function of OD and ID.

**Example 8.24.** Determine the stiffness of a tungsten collar having an OD of  $6\frac{1}{4}$  in. and an ID of  $2\frac{3}{16}$  in.

**Solution.**

$$\begin{aligned}
 EI &= (51.5 \times 10^6 \text{ lbf/sq in.}) \\
 &\times \frac{(\pi)[(6.25 \text{ in.})^4 - (2.1875 \text{ in.})^4]}{64} \\
 &= 3.80 \times 10^9 \text{ sq in.-lbf.}
 \end{aligned}$$

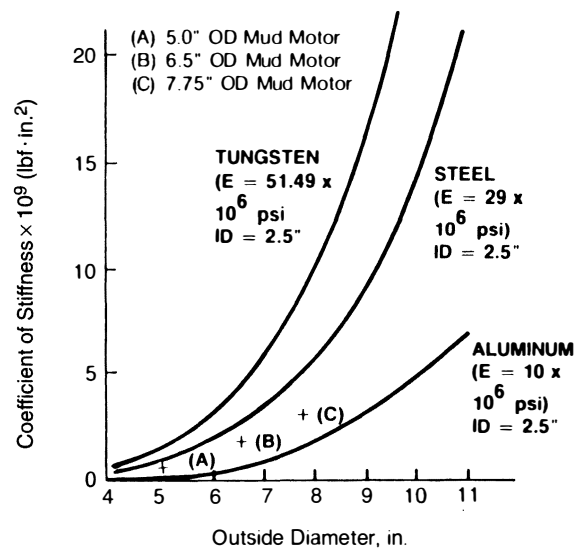


Fig. 8.124—Drill-collar stiffness (after Millheim<sup>19</sup>).

The air weight of any BHA component can be determined if the density, cross-sectional area, and length are known (see Table 8.11). For most round drill collars, this can be determined if the ID, OD, and length are known. However, even the round drill collars can weigh less than the calculated air weight if, for example, they have machined grooves or if the OD at both ends has been decreased so that the collar can be picked up with elevators. Determining air weights of other BHA components—such as stabilizers, reamers, motors, shock subs, telemetry collars, jars, thick-walled drillpipe, and other downhole tools—is more complex because the cross-sectional geometries vary with length. Another reason the calculated air weight can differ from the actual air weight is that the wear on the outside of the component may not be uniform, so the cross-sectional shape of the component may be more elliptical than circular.

When any BHA component is placed in a fluid-filled hole, the air weight is reduced by the buoyancy of the component. The buoyancy correction factor,  $B_c$ , can be determined from Eq. 8.93:

$$B_c = \frac{(\rho - W_m)}{\rho}, \dots \dots \dots (8.93)$$

where  $\rho$  is the density of the metal of the BHA component and  $W_m$  is the weight of the mud in consistent units.

**Example 8.25.** Determine the weight of 45 steel collars whose OD is 10 in., ID is  $3\frac{1}{16}$  in., and  $\rho_s$  is 490 lbm/cu ft. Each collar is 31 ft long, and the mud weight is 16 lbm/gal.

**Solution.**

$$\text{Weight of String in Air} = W_s$$

$$= (490 \text{ lbm/cu ft}) \left( \frac{\pi}{4} \right) \left( \frac{1 \text{ sq ft}}{144 \text{ sq in.}} \right)$$

$$\times (10^2 - 3.06^2) \text{ sq in. (45) (31 ft)}$$

$$= 337,909 \text{ lbm.}$$

$$\text{Weight of String in Mud} = W_s B_c$$

$$= (337,909 \text{ lbm}) \left[ 490 \text{ lbm/cu ft} - \frac{16 \text{ lbm/gal}}{8.33 \text{ lbm/gal}} \right. \\ \left. \times (62.4 \text{ lbm/cu ft}) \right] \div (490 \text{ lbm/cu ft}) = 255,255 \text{ lbm.}$$

### 8.7.2 Slick BHA

Fig. 8.125 depicts a slick BHA (a) and a typical pendulum assembly (b). Each BHA has a negative component of side force,  $F_B$ , caused by gravity. At the bit, this component can be determined from

$$F_B = -0.5W_c L_T B_c \sin \alpha, \dots \dots \dots (8.94)$$

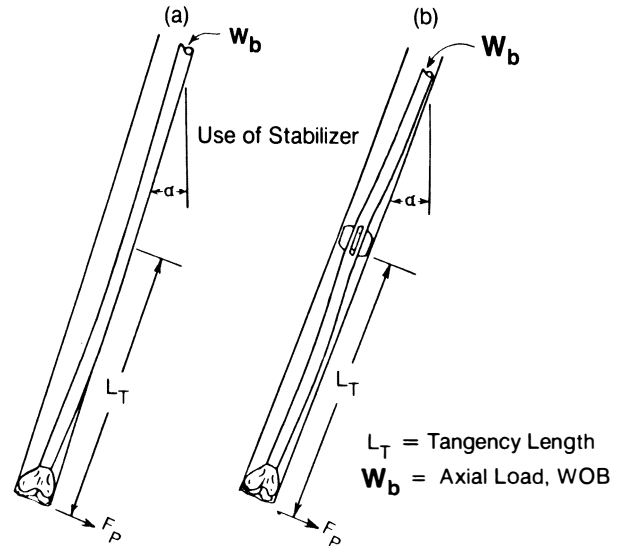


**Fig. 8.125—Tangencies for slick and pendulum BHA's.**

where  $W_c$  is the weight of the collar in lbm/linear ft in air,  $L_T$  is the length of the BHA between the bit and the first point of tangency (Fig. 8.125a and b) in feet, and  $\alpha$  is the inclination angle.

**Example 8.26.** Determine the negative side force, in a 9-lbm/gal mud, for a slick BHA whose air weight is 98.6 lbm/ft. The wellbore is at an inclination of  $4^\circ$  and length to the point of the tangency ( $L_T$ ) is 25 ft.

**Solution.**

$$F_B = -(98.6 \text{ lbf/ft})(25 \text{ ft}) \left\{ [489 \text{ lbf/cu ft} \right. \\ \left. - \frac{9 \text{ lbf/gal}}{8.33 \text{ lbf/gal}} (62.4 \text{ lbf/cu ft}) / 489 \text{ lbf/cu ft} \right\} \\ \times \frac{\sin(4^\circ)}{2} = -74.1 \text{ lbf.}$$

If axial weight is applied to the bit, a positive force component, called the bending force, must be considered. Fig. 8.126 shows the zero axial load (a) and a BHA with the pipe bending as an axial load is applied (b). To determine the positive component of any BHA, one must assess the bending moments occurring over the active portion of the BHA. (Active portion refers to all parts of the BHA below the main tangency point.)

Eq. 8.95, presented by Jiazhi<sup>20</sup> and based on Timoshenko's<sup>21</sup> method of "Three Moment Equations," shows both the negative and the positive components, which are functions of WOB or applied axial load.

$$F_B = -0.5W_c B_c L_T \sin \alpha \\ + (P_B - 0.5W_c B_c L_T \cos \alpha) / L_T, \dots \dots \dots (8.95)$$

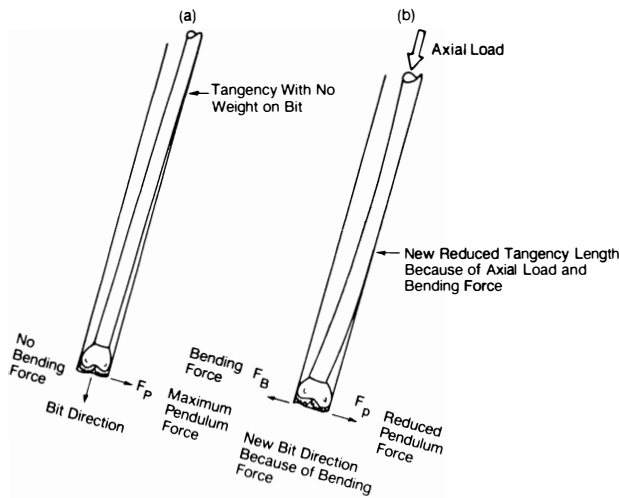


Fig. 8.126—Slick BHA without axial load and with axial load.

(Note that the sign convention used by Jiazhi is changed to be consistent with the present practice in BHA analysis of using a positive sign to mean a building side force and a negative sign to indicate a dropping side force.)

In Eq. 8.95  $F_B$  is the bit side force (lbf),  $p_B$  is the axial or compressive load on the bit (lbf), and  $\ell$  is the clearance radius of the drill collars (in.). Because  $L_T$  is unknown in both the negative and positive sides of the equations, it must be determined before  $F_B$  can be calculated.

The clearance of the drill collar is related by

$$\ell = 0.5(d_b - d_{dc}), \dots \dots \dots (8.96)$$

where  $d_b$  is the diameter of the bit and  $d_{dc}$  is the diameter of the drill collars.

For Jiazhi's solution, one must initially guess the tangency length,  $L_T$ . If the guess agrees with the length calculated by Eq. 8.97, Eq. 8.95 can be used to calculate the side force for a slick BHA with a constant inclination and drill collars of the same diameter:

$$L_T^4 = \frac{24EI\ell}{W_c B_c \sin \alpha X}, \dots \dots \dots (8.97)$$

where  $X$  is a transcendental function related by Eq. 8.98.

$$X = \frac{3(\tan u - u)}{u^3}, \dots \dots \dots (8.98)$$

where  $u$  is in radians and is given by

$$u = \frac{L_T}{2} \left( \frac{p_c}{EI} \right)^{0.5} \dots \dots \dots (8.99)$$

The compressive load on the collars,  $p_c$ , can be determined by

$$p_c = p_B - 0.5W_c B_c L_T \cos \alpha. \dots \dots \dots (8.100)$$

**Example 8.27.** Determine the resultant side forces for a slick BHA for 0-, 10,000-, 30,000-, 50,000-, 70,000-, and 80,000-lbf WOB. At what WOB will the BHA start building for a formation force of 0 and 525 lbf? Plot the negative and positive side-force components and the resultant side force, considering the 0- and 525-lbf formation forces. The drill bit diameter is 8.75 in.; the steel collars have 7.0-in. OD's and  $2\frac{3}{16}$ -in. ID's. Mud weight is 9.2 lbm/gal. Inclination is  $3.2^\circ$ .

**Solution.** An initial estimate of 40 ft is made for the case of 30,000-lbf WOB. The weight of the drill collars in 9.2-lbm/gal mud is

$$W_c = \frac{\pi}{4(144)} \frac{\text{sq ft}}{\text{sq in.}} (7.0^2 - 2.188^2) \text{ sq in.}$$

$$\times (489 \text{ lbm/cu ft}) B_c,$$

$$W_c = 118 \text{ lbm/ft } B_c,$$

$$B_c = \left[ 489 \text{ lbm/cu ft} - \frac{9.2 \text{ lbm/gal}}{8.33 \text{ lbm/gal}} \right. \\ \left. \times (62.4 \text{ lbm/cu ft}) \right] / (489 \text{ lbm/cu ft}) - 0.859,$$

$$W_c B_c = 118(0.859) = 101.4 \text{ lbm/ft},$$

$$\ell = 0.5(8.75 - 7.0) \text{ in.} \left( \frac{\text{in.}}{12 \text{ ft}} \right) = 0.0729 \text{ ft},$$

$$P_c = 30,000 \text{ lbf} - 0.5(101.4 \text{ lbf/ft})$$

$$\times (40 \text{ ft})(\cos 3.2) = 27,977 \text{ lbf},$$

$$u = \frac{40}{2} \left[ \frac{27,977 \text{ lbf}}{(4.18 \times 10^9 \text{ lbf/sq ft})(5.63 \times 10^{-3} \text{ ft}^4)} \right]^{0.5} \\ = 0.69,$$

$$X = \frac{3[\tan(0.69) - 0.69]}{(0.69)^3} = 1.24,$$

and

$$L_T =$$

$$\left[ \frac{24(4.18 \times 10^9 \text{ lbf/sq ft})(5.63 \times 10^{-3} \text{ ft}^4)(0.0729 \text{ ft})}{(101.4 \text{ lbf/ft})(1.24)(\sin 3.2)} \right]^{0.25} \\ = 49.2 \text{ ft.}$$

Because the calculated  $L_T$  does not agree with the initial estimate of  $L$ , a second estimate of the average of the initial estimate and the calculated value should be used.

$$L_T = \frac{49.2 + 40}{2} = 44.6 \text{ ft.}$$

**TABLE 8.18—RESULTING SIDE FORCES  
AND TANGENCY LENGTH FOR VARIOUS WOB**

Weight on Bit (lbf)	0 Formation Force $F_B$ (lbf)	525 lbf Formation Force $F_B$ (lbf)	$L_T$ (ft)
0	-147	378	51.9
10,000	-133	392	50.8
30,000	-94	431	48.0
50,000	-51	474	45.3
70,000	-6	519	42.9
80,000	18	543	41.7

Successive iterations yield the value of  $L_T=48.0$  ft.

The side force at the bit is found as follows:

$$\begin{aligned}
 F_B &= -0.5(101.4 \text{ lbf/cu ft})(48 \text{ ft})(\sin 3.2) \\
 &\quad + [30,000 \text{ lbf} - 0.5(101.4 \text{ lbf/cu ft})(48 \text{ ft})(\cos 3.2)] \\
 &\quad \times (0.0729 \text{ ft})/48 \text{ ft}, \\
 &= -93.8 \text{ lbf}.
 \end{aligned}$$

The negative sign indicates a net dropping tendency with 0 lbf of formation forces and 431.2 lbf of build tendency with a 525-lbf formation force.

Similar calculations yield the results found in Table 8.18 for the other WOB's.

Fig. 8.127 is a plot of the results of Example 8.28 for 0-lbf formation force and 525-lbf formation force. The bending or positive side force and negative side force components also are plotted vs. WOB. It appears that, for this particular BHA with 0-lbf formation force, nearly 80,000-lbf WOB would be required to start a slight build, and for 525-lbf formation force there would be a moderate building tendency, even at the very low bit weights.

The tendency of the bit in the foregoing example to build, to hold, or to drop angle is based on a positive, zero, or negative side force. Essentially, this would be the case for hard formations (i.e., drilling rates of 1 to 10 ft/hr). When the formation is soft to medium-hard, the side-force tendency is not the only component that will influence the inclination and direction of the bit. Because of the curvature of the BHA near the bit, the bit is canted or tilted in some resultant direction and inclination, somewhat like the bent housing and bent sub. The magnitude of the tilt is directly influenced by the strength of the formation. Just as a deflection tool will not obtain the maximum curvature for which it was designed in harder formations, so it is with a BHA and a given bit tilt. In very soft formations (drilling rates exceeding 100 ft/hr), the side force again can be the predominant mechanism and will, in many cases, mitigate the effects of BHA bit tilt. This is especially true when the larger, stiffer collars are run.

When the formations are soft to medium-hard (drilling rates from 10 to 100 ft/hr), effects of the bit tilt can be significant. To determine the bit tilt, one must know the curvature of both the wellbore and the BHA near the bit. Analytical BHA solutions, such as Jiazhi's, are difficult and cumbersome to use with the varying wellbore incli-

nations and directions and to describe the curvature of the BHA. To calculate bit tilt, one of the finite-element BHA algorithms or similar solutions are better suited.<sup>20,21</sup> To be truly accurate, the dynamic effects of the BHA must be considered. However, a strong understanding of the basic BHA mechanics with Jiazhi's technique will give an insight to the ideal 2D behavior of most common BHA's.

In the special case of the slick BHA, no stabilizers are used. In the previous example calculation, 7-in. collars are used in an 8.75-in. wellbore, which generates side forces ranging from a low of -147 lbf at 0 lbf WOB to a high of 18 lbf at 80,000 lbf WOB. If the formation forces are 525 lbf, the slick BHA is going to build angle, no matter what weight is used on the bit, until an equilibrium inclination angle is reached at which the formation force is offset by the negative side force.

**Example 8.28.** For the previous example, estimate the inclination at which the slick BHA will cease building angle (assume no WOB).

**Solution.** Assuming the calculated tangency length will not change substantially,

$$525 = 0.5(101.4 \text{ lbf/ft})(48 \text{ ft})\sin \alpha$$

and

$$\alpha = 12.46^\circ \text{ inclination.}$$

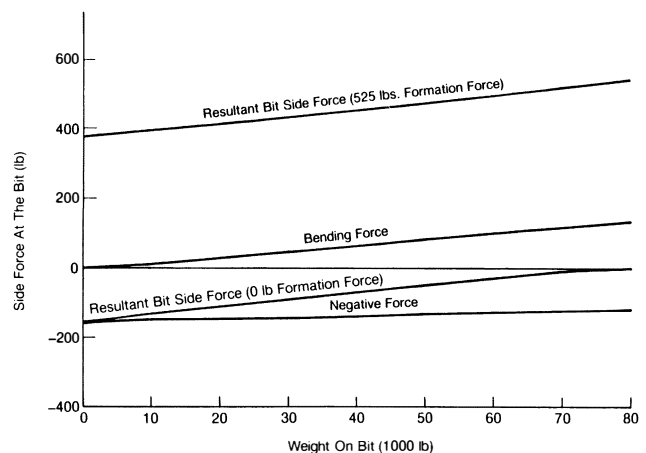


**Fig. 8.127—Results of BHA calculation for slick BHA.**

If it is desired to maintain a low inclination angle with a strong formation force of 525 lbf in the 8.75-in.-OD hole, the 7-in.-OD collars are as large as they can be for safe use. An alternative is to drill a larger wellbore so that collars with larger diameters can be used.

**Example 8.29.** Estimate the collar OD, assuming a 2 $\frac{1}{8}$ -in.-ID collar and a 9 $\frac{7}{8}$ -in.-diameter wellbore, 9.2-lbm/gal mud, and a maximum tolerable inclination of 3.2° to offset the 525-lbf formation force.

**Solution.**

$$525 \text{ lbf} = \frac{\pi}{4(144)} \left( \frac{\text{sq ft}}{\text{sq in.}} \right) (d_e^2 - 2.8125^2) \text{ sq in.}$$

$$\times (48 \text{ ft})(489 \text{ lbm/cu ft})(0.859)(\sin 3.2^\circ),$$

$$d_e = 9.67 \text{ in.} \approx 9.5 \text{ in.-OD collars.}$$

The 9.5-in. collars would be too large for a 9 $\frac{7}{8}$ -in. wellbore but could be used in a 12 $\frac{1}{4}$ -in. wellbore. If the hole size cannot be enlarged, the only other possibility is to increase the tangency length of the BHA. With the use of a stabilizer to move the tangency point farther up the wellbore, more negative force can be obtained. A pendulum assembly is one that has a stabilizer to control the tangency length.

### 8.7.3 Single-Stabilizer BHA

The same type of analysis performed for a slick BHA can be applied to a single-stabilizer BHA (see Fig. 8.128). Again, one must estimate a tangency length that agrees with the calculated length  $L_T^2$  in Eq. 8.101.

$$L_T^4 = \frac{24EI_2(\ell_2 - \ell_1)}{q_2x_2} - \frac{4m_1L_T^2W_2}{q_2x_2}, \dots \dots (8.101)$$

The unknown bending moment,  $m$ , is calculated from the relationship

$$2m_1 \left( V_1 + \frac{L_2I_1}{L_1I_2} V_2 \right) = -\frac{q_1L_1^2}{4}x_1 - \frac{q_2L_2^3I_1}{4L_1I_2}x_2$$

$$+ \frac{6EI_1\ell_1}{L_1^2} + \frac{6EI_1(\ell_1 - \ell_2)}{L_1L_2}, \dots \dots \dots (8.102)$$

where  $q_1 = W_{c1}B_c \sin \phi$ ,  $q_2 = W_{c2}B_c \sin \phi$ ,  $W_{c1}$  is the weight of the drill collars from the bit to the stabilizers, and  $W_{c2}$  is the weight of the collars from the stabilizers to the point of tangency.

The coefficients  $W_i$  and  $V_i$  can be calculated from Eqs. 8.103 and 8.104.

$$W_i = \frac{3}{u_i} \left[ \frac{1}{\sin(2u_i)} - \frac{1}{2u_2} \right] \dots \dots \dots (8.103)$$

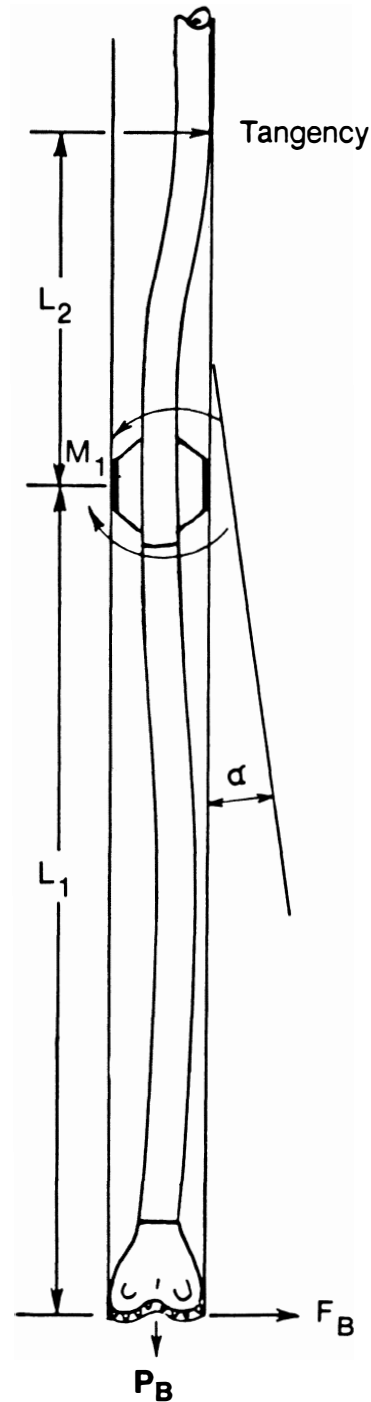


Fig. 8.128—Typical single-stabilizer BHA.



and

$$V_i = \frac{3}{2u_i} \left[ \frac{1}{2u_i} - \frac{1}{\tan(2u_i)} \right], \dots\dots\dots (8.104)$$

where  $i=1$  or  $2$ . Coefficients  $X_i$  and  $u_i$  are determined from Eqs. 8.98 and 8.99, considering the collars from the bit to the stabilizer and from the stabilizer to the point of tangency.

$$X_i = \frac{3[\tan(u_i) - u_i]}{u_i^3},$$

where

$$u_i = \frac{L_i}{2} \left( \frac{P_{ci}}{EI_i} \right)^{0.5}.$$

Eq. 8.96 is used to calculate the clearances for each section of collar where  $d_s$  is the diameter of the stabilizer and  $d_2$  is the diameter of the collars that achieve tangency.

$$\ell_1 = 0.5(d_b - d_s)$$

and

$$\ell_2 = 0.5(d_b - d_2).$$

The compressive load for the first section is calculated with Eq. 8.103, and

$$P_{c1} = P_B - \left[ \left( \frac{L_1}{2} W_{c1} B_c \right) \cos \phi \right],$$

while the compressive load of the second section is given by Eq. 8.105.

$$P_{c2} = P_B - \{[(W_{c1} B_c L_1) + (0.5 W_{c2} B_c L_2)] \cos \phi\}.$$

..... (8.105)

If the estimated value of  $L_2$  equals  $L_T$ , Eq. 8.106 can be used to calculate the side force at the bit.

$$F_B = -0.5 B_c W_{c1} L_1 \sin \phi + \frac{P_{c1} \ell_1}{L_1} - \frac{m}{L_1}. \dots (8.106)$$

If the estimated value of  $L_2$  does not agree with the value of  $L_T$ , the new assigned value should be an average of  $L_2$  and  $L_T$  and the same calculation procedure should be repeated until  $L_2 = L_T$ .

**Example 8.30.** Consider the case of a single-stabilizer building BHA on which the distance between the bit and the first stabilizer is 5.0 ft and the wellbore diameter is 12¼ in. All the drill collars have an OD of 8.0 in. and an ID of 2⅓ in. The diameter of the stabilizer blade is 12.21875 in.; the inclination angle is 10°, and the mud weight is 10.5 lbm/gal.

Calculate the bit side forces ( $F_B$ ) for WOB's of 10,000, 20,000, 30,000, 40,000, and 50,000 lbf.

**Solution.** For 30,000-lbf WOB, the initial estimate for  $L_2$  is 40 ft. The stepwise calculation is shown below. Note that for  $W_{c1} B_c$ , the weight of the collars in mud,

$$W_{c1} = W_{c2} = 149.6 \text{ lbf and } B_c = 0.839,$$

$$W_{c1} B_c = (149.6 \text{ lbf})(0.839) = 125.5 \text{ lbf/ft},$$

$$E = 4.176 \times 10^9 \text{ lbf/sq ft},$$

$$I = 9.55 \times 10^{-3} \text{ ft}^4,$$

$$\ell_1 = 0.5 \left( \frac{\text{ft}}{12 \text{ in.}} \right) (12.25 - 12.21875) \text{ in.} = 0.00130 \text{ ft},$$

$$\ell_2 = 0.5 \left( \frac{\text{ft}}{12 \text{ in.}} \right) (12.25 - 8.0) \text{ in.} = 0.17708 \text{ ft},$$

$$P_{c1} = 30,000 - 0.5(125.5 \text{ lbf/ft})(5 \text{ ft})(\cos 10^\circ)$$

$$= 29,691 \text{ lbf},$$

$$P_{c2} = 30,000 - [(125.5 \text{ lbf/ft})(5 \text{ ft})$$

$$+ 0.5(125.5 \text{ lbf/ft})(40 \text{ ft})](\cos 10^\circ) = 26,900 \text{ lbf}.$$

$$u_1 = \left( \frac{5 \text{ ft}}{2} \right)$$

$$\times \left[ \frac{29,691 \text{ lbf}}{(4.176 \times 10^9 \text{ lbf/sq ft})(9.55 \times 10^{-3} \text{ ft}^4)} \right]^{0.5}$$

$$= 6.82 \times 10^{-2},$$

$$u_2 = \left( \frac{40 \text{ ft}}{2} \right)$$

$$\times \left[ \frac{26,900 \text{ lbf}}{(4.176 \times 10^9 \text{ lbf/sq ft})(9.55 \times 10^{-3} \text{ ft}^4)} \right]^{0.5}$$

$$= 5.20 \times 10^{-1},$$

$$x_1 = 3 \frac{\tan(0.0682) - 0.0682}{(0.0682)^3} = 1.00185,$$

$$x_2 = 3 \frac{\tan(0.520) - 0.520}{(0.520)^3} = 1.12117,$$

$$W_2 = \frac{3}{(0.520)} \frac{1}{\sin(2 \times 0.520)} - \frac{1}{2(0.520)} = 1.142,$$

$$V_1 = \frac{3}{2(0.0682)} \frac{1}{2(0.0682)} - \frac{1}{\tan(2 \times 0.0682)}$$

$$= 1.00124,$$

$$V_2 = \frac{3}{2(0.520)} \frac{1}{2(0.520)} - \frac{1}{\tan(2 \times 0.520)} = 1.08025,$$

and

$$q_1 = 125.5 \text{ lbf/ft} (\sin 10^\circ) = 21.8 \text{ lbf/ft.}$$

Therefore,

$$\begin{aligned} 2m \left[ 1.00124 + \frac{(40)(1.08025)}{5} \right] \\ = - \frac{(21.8 \text{ lbf/ft})(5 \text{ ft})^2}{4} (1.00185) \\ - \frac{(21.8 \text{ lbf/sq ft})(40 \text{ ft})^3}{4(5 \text{ ft})} (1.12117) \\ + \frac{6(3.987 \times 10^7 \text{ lbf/sq ft})(0.00130 \text{ ft})}{(5 \text{ ft})^2} \\ + \frac{6(3.987 \times 10^7 \text{ lbf/sq ft})(0.00130 - 0.17708)}{(5 \text{ ft})(40 \text{ ft})}. \end{aligned}$$

Therefore,

$$m = -14,318 \text{ ft-lbf.}$$

$$\begin{aligned} L_T^4 = \frac{24(3.987 \times 10^7 \text{ lbf/sq ft})(0.17708 - 0.00130) \text{ ft}}{(21.8 \text{ lbf/ft})(1.12117)} \\ - \frac{4(-14,318 \text{ ft-lbf})(L_T^2)(1.142)}{(21.8 \text{ lbf/ft})(1.12117)}. \end{aligned}$$

Therefore,

$$L_T = 57.8 \text{ ft.}$$

Because  $L_T$  does not equal  $L_2$ , 48 ft should be used for  $L_2$  in the next try.

Successive tries will show that  $L_T = L_2 = 65.5$  ft and that

$$\begin{aligned} F_B = - \{ [0.5(125.5 \text{ lbf/sq ft})(5 \text{ ft})(\sin 10^\circ)] \\ + \frac{(29,691 \text{ lbf})(0.00130 \text{ ft})}{(5 \text{ ft})} - \frac{(-15,552)}{5 \text{ ft}} \} \\ = 3,058 \text{ lbf.} \end{aligned}$$

Table 8.19 summarizes the solutions according to bit weight.

This solution indicates that the additional WOB of 20,000 lbf increases the bit side force from 3,058 to 3,086 lbf and reduces the tangency length from 65.5 to 64.2 ft.

Fig. 8.129 shows bit side force as a function of distance of the stabilizer from the bit for WOB's of 10,000 to 60,000 lbf for the BHA cited in Example 8.31. Fig. 8.130 is a similar plot for 6½-in. collars. (A finite-element BHA code<sup>20</sup> was used to generate these plots. The tech-

**TABLE 8.19—SUMMARY OF BIT SIDE FORCES FOR VARIOUS WOB'S**

Weight on bit (lbf)	Bit Side Force $F_B$ (lbf)	Tangency Length $L_T$ (ft)	Bending Moment $M$ (ft-lbf)
10,000	3,030	66.9	15,410
20,000	3,044	66.2	15,466
30,000	3,058	65.5	15,522
40,000	3,072	64.9	15,579
50,000	3,086	64.2	15,638

nique used in Example 8.31, however, can be used to calculate the same data up to the point where tangency between the bit and the stabilizer occurs.)

The stabilizer near the bit causes a building or positive side force. As the stabilizer is moved away from the bit, between 30 and 35 ft, a 0-lbf bit side force is achieved. This assembly is called a neutral BHA. If the stabilizer is positioned beyond 30 ft, the bit side force becomes negative and decreases to a maximum negative value. The single-stabilizer negative assembly is called a pendulum or dropping assembly. The maximum pendulum or negative bit side force is reached at the point where the drill collars achieve tangency between the bit and the stabilizer. The BHA solution by Jiazhi cannot predict this tangency. Other BHA algorithms that can calculate the maximum pendulum force when tangency occurs indicate that the maximum negative side force occurs between 75 and 85 ft for bit loads of 10,000 to 60,000 lbf. For the smaller-diameter wellbores and drill collars, the maximum negative side force occurs between 55 and 80 ft for bit loads of 10,000 to 60,000 lbf.

#### 8.7.4 Two-Stabilizer BHA's

The two-stabilizer BHA's can also be solved with Jiazhi's<sup>20</sup> technique. Fig. 8.131 depicts a typical two-stabilizer building BHA;  $L_1$  and  $L_2$  are known lengths between the bit and the first stabilizer and between the first and second stabilizers. The distance,  $L_3$ , between the second stabilizer and the point of tangency is unknown, and, as in the case of the slick and single-stabilizer solutions,  $L_3$  must be estimated initially.

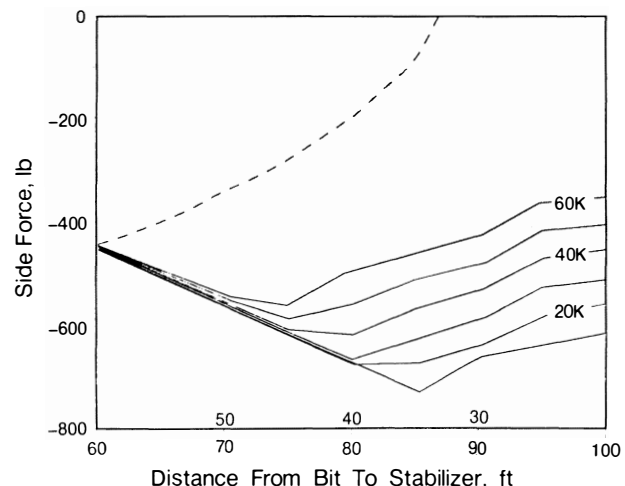


**Fig. 8.129—Side force vs. pendulum collar length; 12¼-in. hole, 8-in. collars, 10½-lbm/gal mud; 10° inclination.**

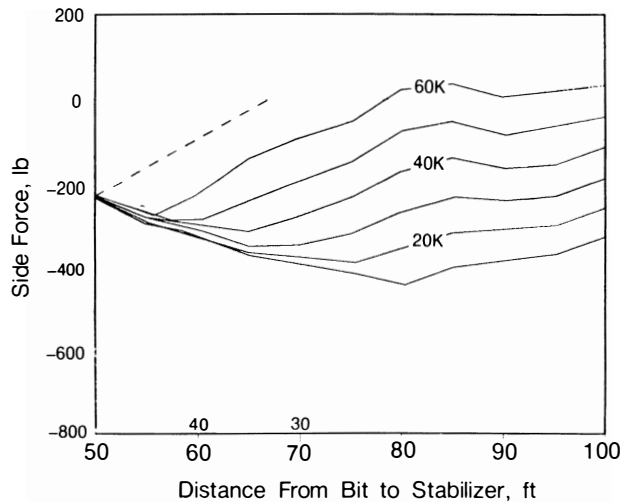


**Fig. 8.130**—Side force vs. pendulum collar length; 12¼-in. hole, 6½-in. collars, 10½-lbm/gal mud, 10° inclination.

Three different collar diameters and material types can be used in the solution. Once a correct tangency length is obtained, the two moments,  $M_1$  and  $M_2$ , can be determined, and the bit side force can be calculated.

As in Eq. 8.96, the clearance between the stabilizers and the wellbore and the last collar and the wellbore are given by

$$\ell_1 = 0.5(d_b - DS_1)/12,$$

$$\ell_2 = 0.5(d_b - DS_2)/12,$$

and

$$\ell_3 = 0.5(d_b - DC_3)/12.$$

Eq. 8.107 can be used to calculate the bit side force.

$$F_B = -0.5W_c B_c L_1 \sin \phi + P_{c1} \ell_1 / L_1 - m_1 / L_1. \quad \dots \dots \dots (8.107)$$

Everything is known in Eq. 8.108 except  $m_2$ . To determine  $m_2$ , a value of  $L_3$  must be estimated. If the estimated  $L_3$  agrees with  $L_T$  in Eq. 8.108, the equivalent value of  $m_2$  can be used in Eq. 8.108, and  $m_1$  can be used in the bit-side-force calculations.

$$L_T^4 = \frac{24EI_3(\ell_3 - \ell_2)}{q_3 X_3} - \frac{4m_2 L_3^2 W_3}{q_3 X_3}, \quad \dots \dots \dots (8.108)$$

and

$$q_i = W_c B_c \sin \phi,$$

where  $i=1, 2$ , or  $3$ .

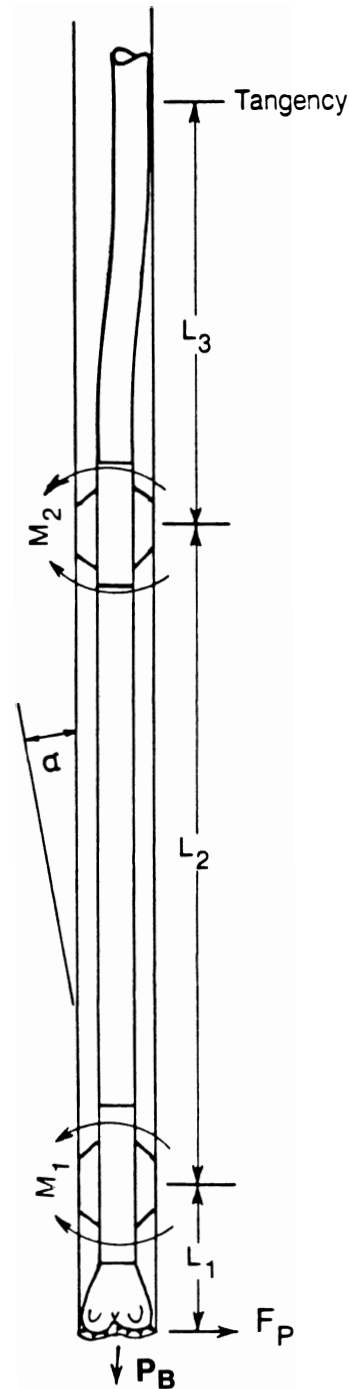


**Fig. 8.131**—Typical two-stabilizer BHA.

The relationships for the first and second moments are given by Eqs. 8.109 and 8.110.

$$2m_1 \left( V_1 + \frac{L_2 I_1}{L_1 I_2} V_2 \right) + m_2 \frac{L_2 I_1}{L_1 I_2} W_2$$

$$= -\frac{q_1 L_1^2}{4} X_1 - \frac{q_2 L_2^3 I_1}{4 L_1 I_2} X_2 + \frac{6EI_1 \ell_1}{L_1^2}$$

$$+ \frac{6EI_1 (\ell_1 - \ell_2)}{L_1^2} \dots \dots \dots (8.109)$$

$$m_1 W_2 + 2m_2 \left( V_2 + \frac{L_3 I_2}{L_2 I_3} V_3 \right)$$

$$= -\frac{q_2 L_2^2}{4} X_2 - \frac{q_3 L_3^3 I_2}{4 L_2 I_3}$$

$$- \frac{6EI_2 (\ell_1 - \ell_2)}{L_2^2} - \frac{6EI_2 (\ell_3 - \ell_2)}{L_2 L_3} \dots \dots \dots (8.110)$$

$X_i$ ,  $W_i$ , and  $V_i$  can be calculated from Eqs. 8.98, 8.103, and 8.104, where  $i=1, 2$ , or  $3$ .

$$X_i = \frac{3[\tan(u_i) - (u_i)]}{u_i^3},$$

$$W_i = \frac{3}{u_i} \left[ \frac{1}{\sin(2u_i)} - \frac{1}{2u_i} \right],$$

and

$$V_i = \frac{3}{2u_i} \left[ \frac{1}{2u_i} - \frac{1}{\tan(2u_i)} \right],$$

where

$$u_i = \frac{L_i}{2} [(p_{ci}/EI_i)^{0.5}];$$

and

$$p_1 = p_B - [(0.5W_{c1}B_cL_1)\cos\phi], \dots \dots \dots (8.111)$$

$$p_2 = p_B - \{[(W_{c1}B_{c1}L_1) + 0.5W_{c2}L_2]\cos\phi\},$$

$$\dots \dots \dots (8.112)$$

and

$$p_3 = p_B - \{[(W_{c1}B_{c1}L_1) + (W_{c2}B_{c2}L_2) + (0.5W_{c3}L_3)]\cos\phi\}. \dots \dots \dots (8.113)$$

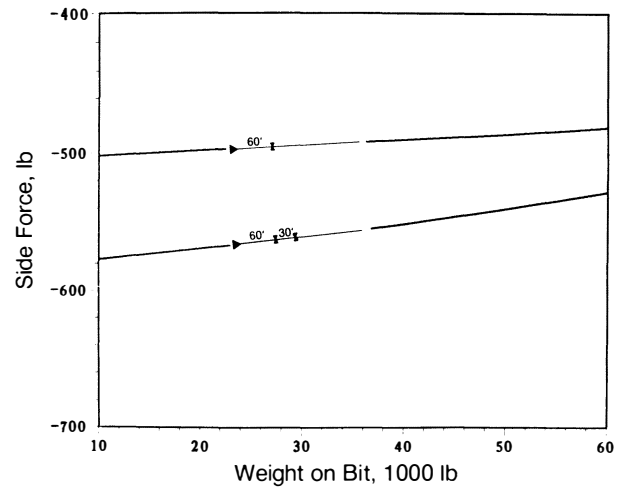


Fig. 8.132—Effect of adding a stabilizer; 12¼-in. hole, 8-in. collars, 9-lbm/gal mud, 10° inclination.

Fig. 8.132 shows the solution for a single-stabilizer, 60-ft pendulum assembly at 10° inclination vs. the two-stabilizer pendulum assembly. The second stabilizer increases the negative side force by reducing the effect of the positive bending force.

The slick, the single-stabilizer, and the two-stabilizer BHA's can be analyzed with the foregoing algorithms. Also, the scheme proposed by Jiazhi<sup>20</sup> can be expanded to handle multistabilizer BHA's, including those with three, four, and five stabilizers.

For the slick BHA there is no solution, except at the tangency length  $L_T$ , when  $u_i < 1.57$  and  $p_{c1} > 0$ . This means that the solution technique is valid only as long as the lower part of the BHA is in compression. The same applies for the single stabilizer. When  $u_i > 1.57$  and  $p_{c1} < 0$ , there is no solution; and when  $u_2 > 1.57$  and  $p_2 < 0$ , there is no solution except at the final tangency length,  $L_T$ , where  $u_2 < 1.57$  and  $p_2 > 0$ . The two-stabilizer BHA has no solution when  $u_1 > 1.57$ ,  $p_{c1} < 0$ ,  $u_2 > 1.57$  and  $p_{c2} < 0$ . When  $u_3 > 1.57$  and  $p_3 < 0$ , there is no solution except at the final tangency length, where  $u_3 < 1.57$  and  $p_3 > 0$ .

This BHA analysis technique does not allow for hole curvature and cannot handle cases in which tangency occurs between the bit and the first stabilizer or between the two stabilizers. Furthermore, the wellbore must be a constant gauge. Adding too much WOB can result in no solution because the collars usually reach tangency between the bit and the first stabilizer or between the two stabilizers. This technique is only 2D and static and does not give a directional side-force component. If the neutral point is below the tangency length, no solution is obtained. In this analytical technique, blade lengths are ignored, and it is assumed that point-contact stabilizers are used.

Even with all those restrictions, the technique can provide basic insights into the mechanics of a number of BHA configurations and can help explain why BHA's behave in a certain manner for different hole sizes, inclinations, collar diameters, and applied WOB. Certain programmable hand calculators can be used to solve the slick, single-stabilizer, and multistabilizer problems.

### 8.7.5 Multistabilizer BHA Analysis

A solution technique for the slick, one-, and two-stabilizer BHA's has been presented. Other techniques, developed by Walker<sup>22</sup> and by Millheim and Apostol,<sup>23</sup> solve the three-dimensional (3D) BHA case. Both techniques yield inclination and direction side-force components. They also handle wellbore curvature, variable gauge holds, and combination BHA components. Unlike the analytical solution, these more generalized solutions can handle situations in which tangency occurs between the bit and stabilizer or between the stabilizers, as well as the cases in which increases in WOB force the creation of additional points of tangency.

Fig. 8.133A shows the two-stabilizer pendulum cases in which tangency occurs between the bit and the stabilizer because of the pendulum length and inclination angle. Fig. 8.133B shows a two-stabilizer, 90-ft building BHA in which the tangency occurs between the two stabilizers; Fig. 8.133C shows the effect of increasing the WOB.

Hole curvature also can influence the response of a BHA significantly. Fig. 8.134 shows how a curvature affects bit side force for a build rate of 1°/100 ft to 12° inclination. A case of constant inclination of 12° is shown also. All BHA's try to reach equilibrium for a given set of conditions—i.e., geology, penetration rate, WOB, speed, BHA configuration, inclination, and hole condition. As long as the conditions remain essentially constant, the average curvature is constant (see Fig. 8.135).

Whenever a BHA is run in a section of hole that has not been created by a BHA of that configuration, the curvature of the hole can cause various consequences: the new BHA may not be able to reach the bottom of the wellbore; the bit may stop rotation; or the BHA responds in a manner counter to that for which it was designed. Curvature can also accelerate a BHA response, especially with building BHA's.

If a formation is soft, the hole curvature caused by a mud motor with a bent sub or a bent housing usually causes the BHA to drill ahead with increased torque and to ream out the hole. The harder the formation, the greater the effects of hole curvature. When a trajectory has been changed with a mud motor in harder formations, the BHA that is used later usually reverses the original curvatures of the wellbore; this is called "bounce back."

Hole curvature can significantly affect more than just the bit side forces. A good example is a pendulum assembly that is run in a hole to reduce angle. Even when the pendulum side force is adequate to reduce angle, the curvature effects can cause the BHA to build angle beyond the point of equilibrium. The curvature of the wellbore can contribute to a bit-tilt effect that is stronger than the side-force effect.

$$G = (F_B C_1 + C_2) 100, \dots \dots \dots (8.114)$$

where  $C_1 = \text{deg/lbf-ft}$ ,  $C_2 = \text{deg/ft}$ , and  $G$  is the resultant bit curvature in degrees/100 ft.

**Example 8.31.** Determine the resultant bit angle for a bit side force of -162 lbf, where the side-force side-cutting response is 0.0001°/lbf-ft and the bit tilt effect caused by the BHA bit tilt and hole curvature is 0.025°/ft.

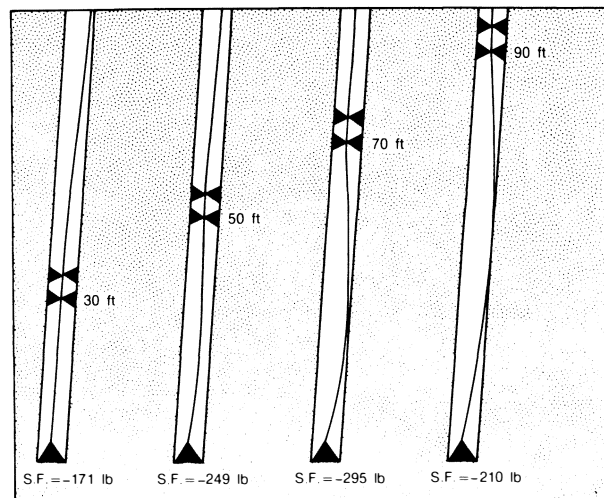


**Fig. 8.133A—**Tangency between bit and stabilizer resulting from pendulum length and inclination; 9 7/8-in. hole, 6 3/4-in. collars, 8° inclination, 30,000-lbf WOB.

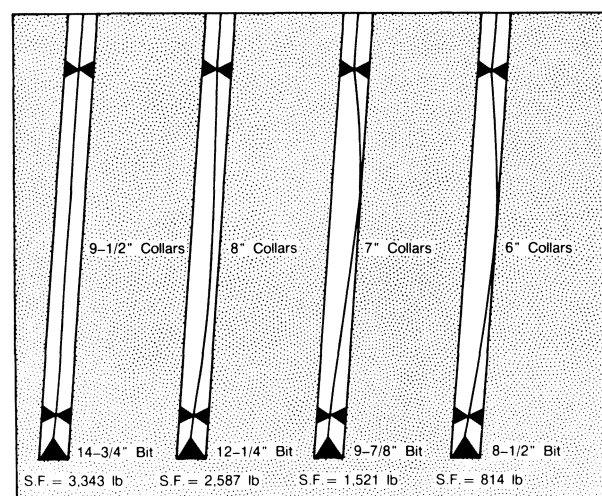


**Fig. 8.133B—**Tangency between bit and stabilizer; 90-ft building assembly, 10° inclination, 30,000-lbf WOB.

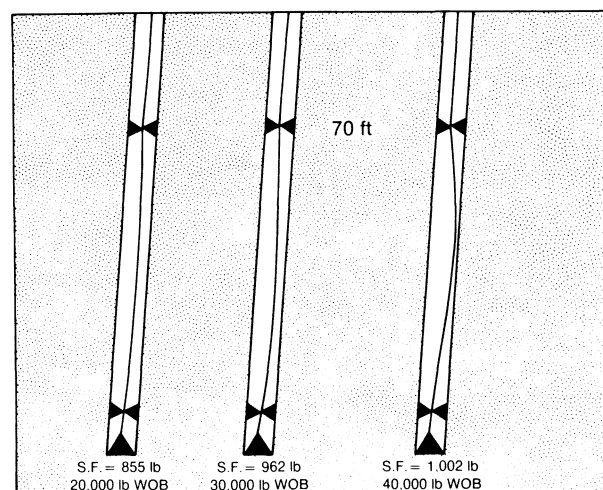


**Fig. 8.133C—**Tangency resulting from increasing WOB; 8 1/2-in. hole, 6-in. collars, 10° inclination, 70-ft tangency length.

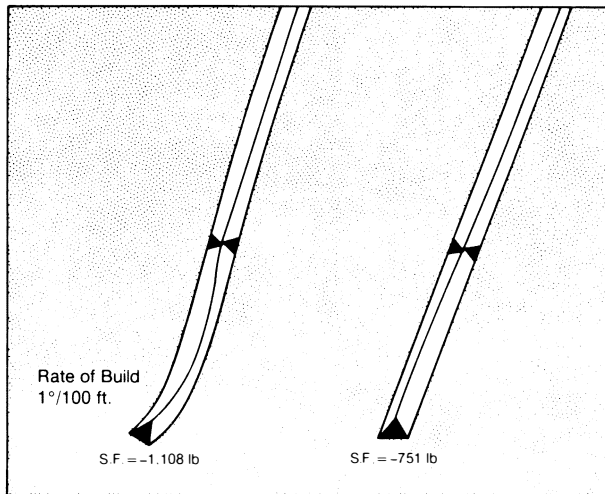


Fig. 8.134—Curvature and its effect on bit side force; 12¼-in. hole, 9-in. collars, 30,000-lbf WOB, 14° constant inclination.

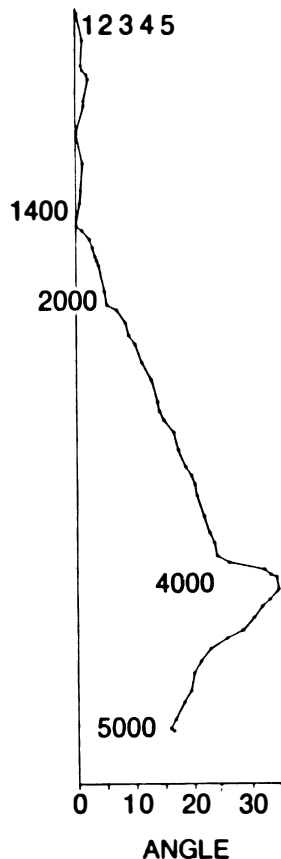


Fig. 8.135—Data showing constant inclination.

*Solution.*

$$G = [(-162 \text{ lbf})(0.0001^\circ/\text{lbf ft}) + 0.025^\circ/\text{ft}]100$$

$$= 0.88^\circ/100 \text{ ft.}$$

### 8.7.6 BHA's for Building Inclination Angle

Fig. 8.136 presents various commonly used BHA's for building inclination angle. Fig. 8.137 shows the side-force response of the building BHA's for 8-in. drill collars in a 12¼-in. wellbore as a function of inclination angle from 5 to 60° for a WOB of 30,000 lbf. These cases were solved with a finite-element algorithm presented by Millheim.<sup>19</sup>

The most building side force is generated by the 90-ft building BHA, except at lower inclinations, where the single-stabilizer building assembly can generate more side force. Rates of build ranging from 2 to 5°/100 ft can be achieved with these building assemblies. Addition of WOB, depending on collar size, increases the rate of build. This is caused not so much by the bit side force as by the increase in bit tilt. The smaller the collar size relative to the diameter of the hole, the greater the influence of bit tilt.

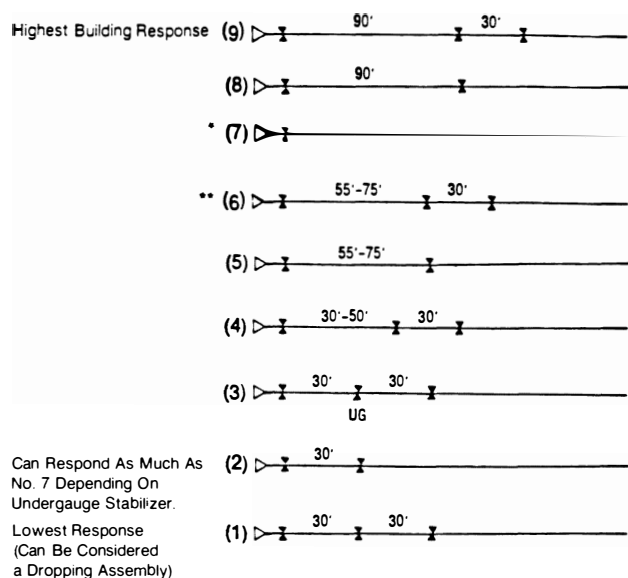
In the earlier days of directional drilling in the Gulf of Mexico, smaller drill collars were used for most BHA's (6 to 6½-in. drill collars in 9⅞- to 12½-in. wellbores). Such building assemblies were very sensitive to WOB, sometimes responding to changes of less than 5,000 lbf.

In harder rocks, the 90-ft BHA is not as responsive as in softer rocks and is less affected by bit tilt. Rates of build of 1 to 2°/100 ft are fairly common.

The single-stabilizer building assembly can achieve a response approaching that of the 90-ft BHA, especially when the smaller drill collars are used. With larger collars—8 to 11 in.—the response is usually less than that for the 90-ft BHA. The single-stabilizer building BHA is more responsive than the intermediate—55- to 75-ft—building assemblies that generate rates of build from 1 to 3°/100 ft. Response also depends on the geology, inclination, wellbore diameter, and collar diameter. As the inclination increases, the general response of all building assemblies increases (see Fig. 8.137).

The rate of build with the three-stabilizer, 30- to 50-ft building assemblies varies from slight to moderate; in some situations those assemblies could even be considered holding assemblies. The two-stabilizer, 30- to 50-ft BHA's with 8-in. collars function as dropping BHA's for the complete range of inclinations. These assemblies are almost unaffected by bit tilt. They are generally used to regain inclination in the hold section. Similarly, the BHA with an undergauge stabilizer in the middle (No. 3 in Fig. 8.136) is used as a slight- to medium-building assembly, depending on how much under gauge the mid-stabilizer is and how responsive to weight the BHA is.

In modern directional drilling, especially in soft formations, the practice is to use the fewest drill collars and stabilizers possible to accomplish a given objective. Thick-walled or heavy drillpipe replaces regular drill collars, eliminating the need for stabilizers that hold the drill collars off the wellbore wall.



\* At lower inclinations this BHA is the most responsive.

\*\* Fig. 8.137 shows that the level of building tendency changes with inclination where BHA's 6 and 7 generate more side force at higher angles.

Fig. 8.136—BHA's for building inclination angle.

A typical building BHA has a bit or near-bit stabilizer placed 3 to 5 ft from the bit face to the leading edge of the stabilizer blade. Beyond the last stabilizer are three to six drill collars and enough heavy drillpipe to satisfy the WOB requirements.

### 8.7.7 BHA's for Holding Inclination Angle

Holding BHA's do not maintain inclination angle; rather, they minimize angle build or drop. All the BHA's in Figs. 8.138 and 8.139 have either a slight building or a slight dropping tendency. The four-stabilizer holding BHA (No. 7) shows the least change with side force as the inclination increases (see Fig. 8.139). Using more than five stabilizers for deviation control has no added effect on the neutrality of the BHA. At lower inclinations, however, the five-stabilizer BHA is most effective. At higher

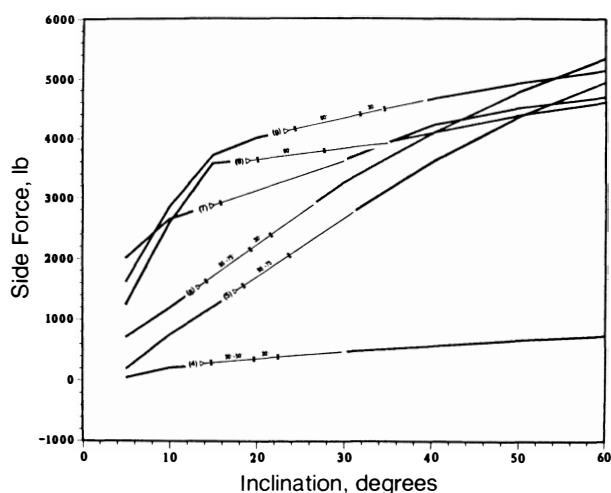


Fig. 8.137—Side-force response as a function of inclination angle, for building BHA's referred to in Fig. 8.136.

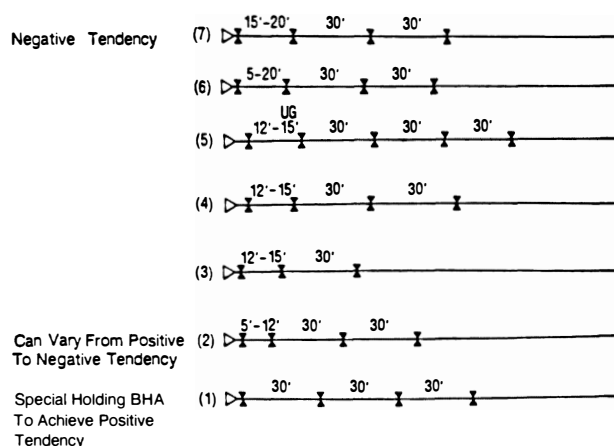


Fig. 8.138—BHA's for holding inclination angle.

inclinations, the fifth stabilizer can add too much torque for the rotary system, so the three- or four-stabilizer BHA's usually are used. With 8-in. collars, they have a negative or dropping tendency. Fig. 8.139 shows the bit-side-force tendencies as a function of inclination for the BHA's depicted in Fig. 8.138. The holding BHA undergauge second stabilizer is used when a slight positive side force or building tendency is required: for example, where the geology or hole conditions are such that the normal BHA's drop too quickly. Also, an undergauge second stabilizer causes a slight bit tilt.

A holding BHA is actually a BHA designed to build or to drop inclination slightly, opposing the formation characteristics in such a way as to prevent a rapid change in inclination angle. Minimal bit tilt, as well as stiffness of the BHA near the bit, also helps maintain inclination angle. Also characteristic of the holding BHA is the small variation in bit side force as a function of WOB change. (See Fig. 8.140.)

Assembly No. 1 in Fig. 8.138 can have either a building or a dropping tendency, which is dependent on a variety of conditions. If the near-bit stabilizer becomes undergauge or the formation around the bit and the stabilizer is eroding, this BHA can respond similarly to

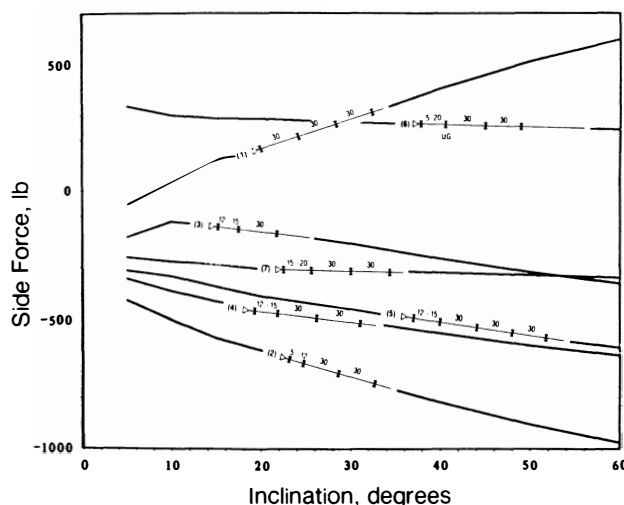


Fig. 8.139—Bit side force tendency as a function of inclination angle, for holding BHA's referred to in Fig. 8.138.

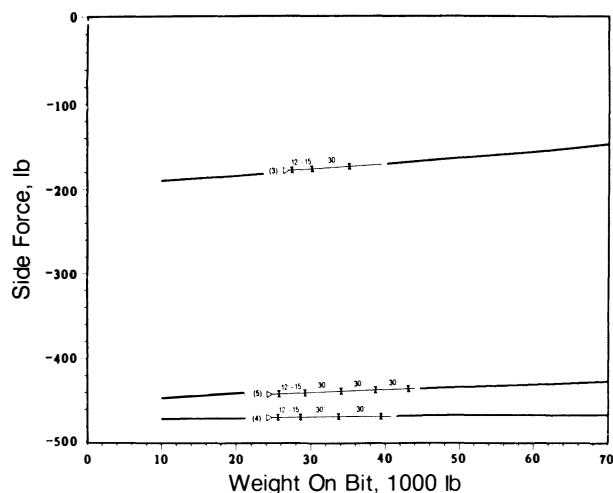
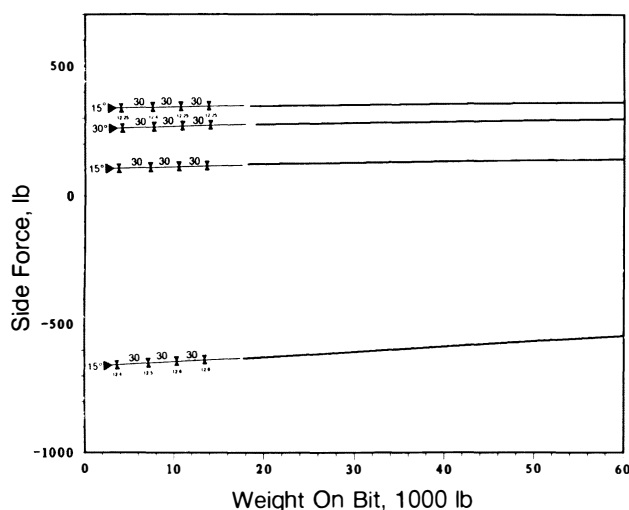


Fig. 8.140—Bit side force as a function of WOB, for holding BHA's.





**TABLE 8.21—COMPARISON OF LOW RPM RESULTS BETWEEN A STATIC BHA ALGORITHM WITH AN EQUIVALENT TORQUE AND A FULL DYNAMIC SOLUTION**

Rotary Speed	Solution	Side Force, Direction (lbf)	Side Force, Inclination (lbf)
50	Dynamic	-809	1,934
50	quasi Dynamic (Static)	-819	1,934
100	Dynamic	-880	1,825
100	quasi Dynamic (Static)	-895	1,847
125	Dynamic	-955	1,497
125	quasi Dynamic (Static)	-919	1,815

\*Solution no longer approximates full 3D dynamic solution.

### 8.7.9 Rotation of the Drillstring

The BHA analysis discussed earlier assumes that the drillstring is static and 2D. This is adequate for estimating the inclination tendency of the BHA and the bit. To find the direction or the “bit-walk” component of the bit trajectory, however, the rotation of the drillstring and the 3D forces and displacements of the BHA must be considered, as must the effects of bit-face torque and the rotating friction of the stabilizer(s). Dynamic analysis by Millheim and Apostol<sup>23</sup> showed also that the 3D static analysis, which includes inclination and direction forces, can be in error if the drillstring is rotated faster than 100 to 125 rpm. If the rotation is at or below 100 rpm, a quasi-dynamic solution that includes torque and neglects inertial effects can be used to approximate a 3D dynamic solution. Table 8.21 gives results of a static quasidynamic solution and a full dynamic solution for a slick BHA at 50, 100, and 125 rpm. Note the close agreement of the 50- and 100-rpm cases and the difference between the two 125-rpm solutions.

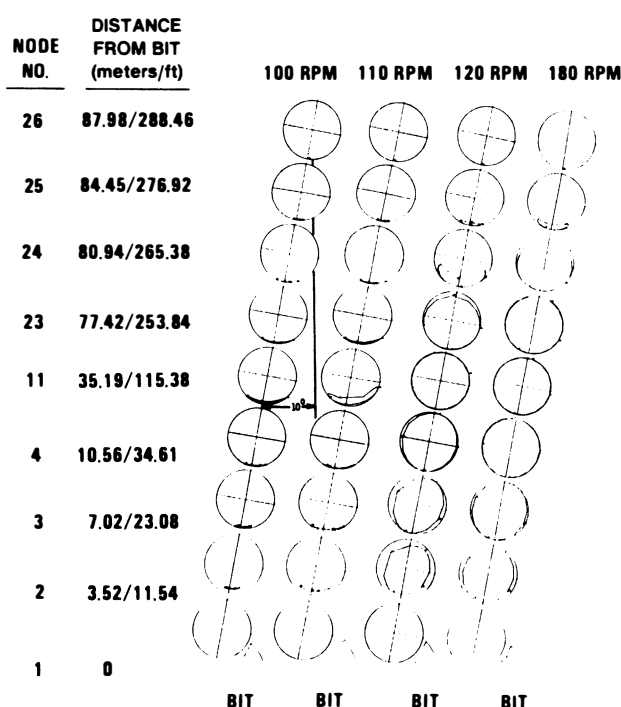


**Fig. 8.143—Effect of rotation on orbital path; 97/8-in. hole, 7-in. collars (after Millheim and Apostol<sup>23</sup>).**

The rotation of the drillstring with an axial load on the bit causes a number of occurrences: (1) the bit generates a bit-face torque and a side-cutting friction or torque; (2) the stabilizers generate a torque or side-cutting friction; and (3) the inertial energy of the drill collars causes a certain orbital path that changes as the speed increases or decreases (see Fig. 8.143). The inertial energy and the varying orbit followed by each component of the BHA can cause the inclination side force to change with changes in speed.

Consider a slick BHA with a tricone bit, drill collars, and drillstring. The total torque that the rotary motor must supply to rotate this system is

$$M_{rd} = M_{bf} + M_{bsc} + M_{dc} + M_{ds}, \dots \dots \dots (8.115)$$

where  $M_{rd}$  is the torque of a rotary drive,  $M_{bf}$  is the torque of a bit face,  $M_{bsc}$  is the torque of a bit side cutting,  $M_{dc}$  is the torque of a drill collar, and  $M_{ds}$  is the torque of a drillstring. The torques that affect the bit trajectory most are the bit torque and the bit side cutting torque. The torque needed to rotate the drill collars and drillstring is negligible. The speed and inclination, however, contribute to the resultant direction and inclination vector, as well as the final tilt of the bit.

The bit-face-torque relationship presented in Sec. 8.6 for tricone bits by Warren<sup>14</sup> can also be used for dynamic BHA analysis. For polycrystalline diamond compact and diamond bits, another torque function similar to Eq. 8.90 represents the bit-face torque.

Bit-face torque, like the PDM- and turbine-torque response discussed in Sec. 8.6, causes a reactive left, or counterclockwise, bit tendency. Bit side cutting can have either a left or a right tendency, dependent on whether the inclination side forces are building (left) or dropping (right). This also holds true for stabilizer side cutting. For example, a slick BHA with a dropping tendency and with a bit-face torque less than the resultant bit-side torque will turn right. If this same assembly starts building, it could turn left (see Figs. 8.144A and B).

If a single stabilizer is added as a building assembly, the bit has a left tendency, even though the stabilizer itself can have a strong right tendency (see Fig. 8.145). The resultant direction tendency can be predicted, in this case, only with the aid of a BHA algorithm that can resolve the magnitudes of the various side forces and torques. A single-stabilizer dropping assembly has a strong right tendency because both the bit and the stabilizer have side-force negative components yielding right-direction force tendencies (see Fig. 8.146).

Determining the side forces for a multistabilizer building BHA is not as easy as for slick and single-stabilizer BHA's. Fig. 8.147 shows the inclination and direction side forces at the bit for a 60-ft building BHA as a function of stabilizer side friction and bit side friction for constant WOB and speed. Notice that, as the stabilizer friction increases, the building assembly goes from a left-direction tendency to a right-direction tendency, dependent on the bit side friction. Bit-face torque is not included. If it had been, it would have negated some of the right tendency, dependent on the rock type, bit type, WOB, speed, and bit diameter. The greater the bit-side cutting torque, the greater the tendency of the bit to resist the effects of the increased stabilizer friction. This is logical because the

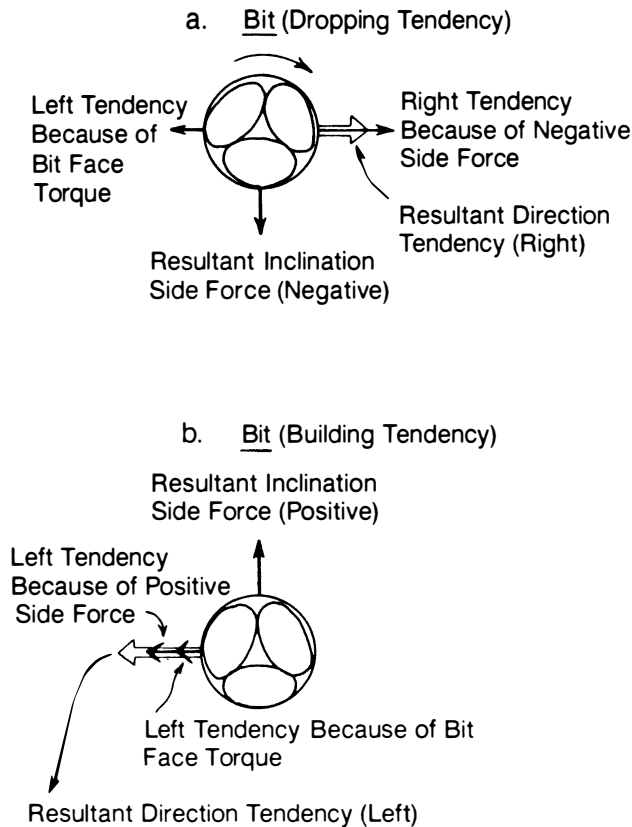


**Fig. 8.144**—Rotation of slick BHA causing direction (bit turn) tendency.

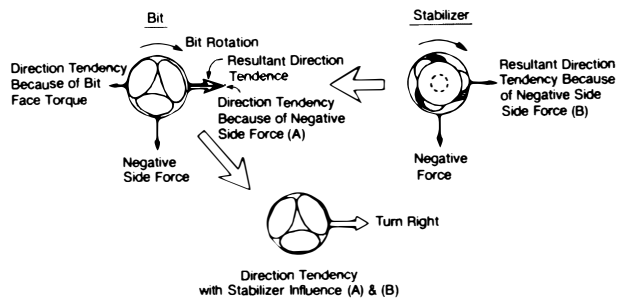


**Fig. 8.145**—Rotation of single-stabilizer pendulum BHA causing direction (bit turn) tendency.

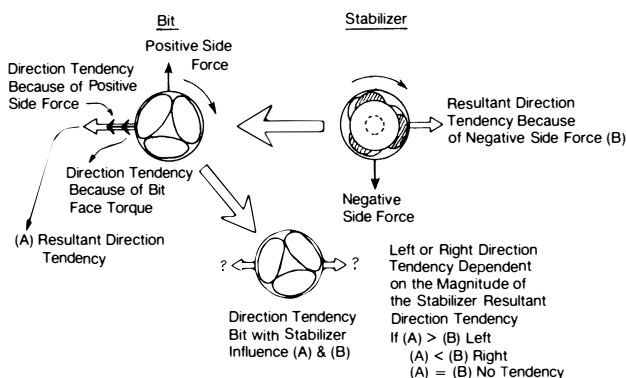


**Fig. 8.146**—Rotation of single-stabilizer building BHA causing direction (bit turn) tendency.

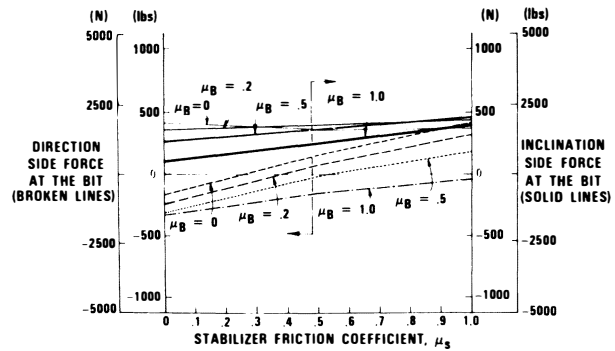


**Fig. 8.147**—Inclination and direction side force at the bit as a function of stabilizer and bit side friction for constant WOB and rpm. Building assembly. (After Millheim and Apostol<sup>23</sup>.)

bit side force is positive, making the direction component left. As the stabilizer influence increases, however, the overall rotational forces favor a right-direction tendency, except for a bit friction,  $\mu_B = 1.0$ . This is why adding two near-bit stabilizers (increasing  $\mu_s$ ) can cause more of a right-direction tendency for building BHA's.

Multistabilizer holding BHA's are influenced more by the bit side friction and force than by the stabilizer friction. Fig. 8.148 shows the bit forces for a holding BHA. Because the resultant inclination force is negative, the bit direction force is positive or right. As the bit side friction increases, the direction tendency also increases (opposite that of the building BHA). Bit torque can reduce or even alter the overall tendency, dependent on its magnitude.

**Example 8.32.** Determine the direction tendency for a building BHA that has the following configuration, side forces, and bit-face torque. There is no formation tendency.

- Bit side force: +1,200 lbf
- Bit face torque: 1,000 ft-lbf (equal to 200 lbf of bit side force)
- First stabilizer: -2,000 lbf (5 ft from bit face)
- Second stabilizer: -1,500 lbf (15 ft from bit face)
- Third stabilizer: -1,000 lbf (100 ft from bit face)

**Solution.** The +1,250 lbf of bit side force has a left tendency, as does the bit-face torque. However, all the stabilizers have strong negative or right-turn tendencies. The closer the stabilizer is to the bit, the more influence it has on the turning tendency. Because there are two near-bit stabilizers with nearly 2,100 lbf more of negative side force, the probability that this assembly will turn right is very high.

Following the rules and analytical procedures presented in this section will show how direction and inclination tendencies of the bit can be estimated for the basic building, dropping, and holding BHA's. Accurate predictions of a BHA's inclination and direction tendencies require

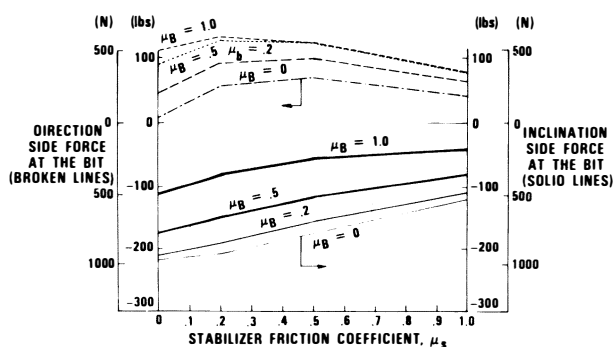


Fig. 8.148—Inclination and direction side force at the bit as a function of stabilizer and bit side friction for constant WOB and rpm. Holding assembly. (After Millheim and Apostol<sup>23</sup>.)

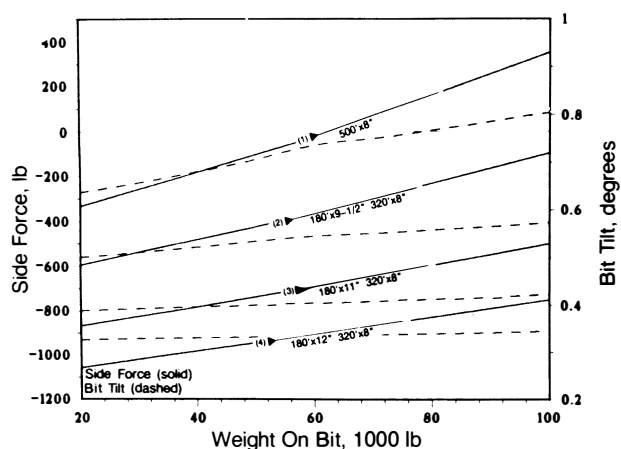


Fig. 8.149—Side force and bit tilt for a slick BHA; 17 1/2-in. hole, 10-lbm/gal mud, 5° inclination.

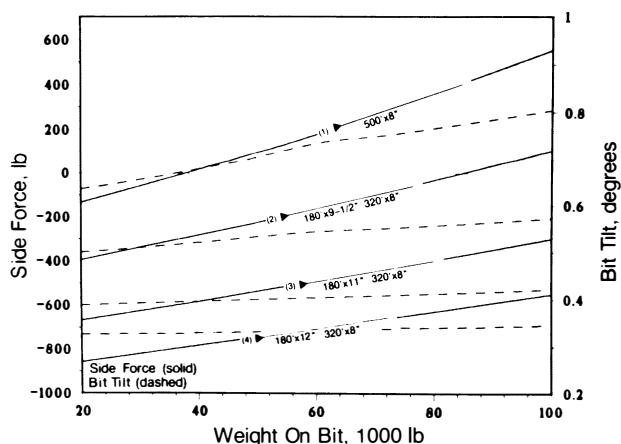


Fig. 8.150—Side force and bit tilt for a geological force of 200 lbf; 17 1/2-in. hole, 10-lbm/gal mud, 5° inclination.

the use of an algorithm that can account for all the variables influencing the BHA forces and displacements, such as bit-force torque, hole curvature, BHA configuration, bit type, penetration rate, hole shape, and other factors. Even the mud properties and hydraulics can affect the final trajectory tendencies of a BHA.

The total interplay of the bit, BHA, geology, and other factors make directional drilling a subsystem of the overall drilling system. An understanding of each component of the drilling system presented in the previous chapters and of the basics presented in this chapter will bring about an understanding of the overall system that controls the bit's trajectory and how it is used in directional-drilling engineering.

## 8.8 Deviation Control

Directional drilling was used first for deviation control, which is concerned specifically with limiting the inclination or horizontal departure of the wellbore within some predescribed limits. At first, such problems as premature sucker-rod failure and damage caused when sucker rods rubbed the tubing were thought to result from the greater wellbore inclinations. Later experience proved that the cause was not the magnitude of inclination but the severity of the doglegs.

The principal use of deviation control is to limit the inclination angle for such reasons as keeping the wellbore from crossing lease lines or remaining within specific drainage boundaries. The practice of hitting a target is considered directional drilling and not deviation control, even though the inclinations and departures might be small.

This section will present the typical deviation-control practices for contending with the following drilling situations: (1) controlling the large-diameter hole (from 12 1/4 to 26 in.), (2) drilling complex geologies, and (3) general deviation control.

### 8.8.1 Deviation Control for Drilling Large-Diameter Wellbores

In most exploration and development wells that are deeper than 10,000 ft, portions of the surface and intermediate hole are from 12 1/4 to 26 in. in diameter. Deeper wells and wells that require multiple casing strings usually require even larger intermediate and surface holes. When the trajectory for such wells is planned, the aim is to hold the dogleg severity to less than 1°/100 ft to prevent casing wear and failure. Other factors that determine inclination are lease boundaries and reservoir drainage constraints.

Deviation control problems associated with large holes usually result from the larger size of the bit and the conditions necessary to make the bit drill. For an optimal WOB, a 17 1/2-in. bit might require from 2,000 to 5,000 lbf/in. If the BHA is not designed properly for the optimal WOB, it is possible that the bit will build inclination angle.

Fig. 8.149 presents the side forces and bit tilts for four slick BHA's used for drilling a 17 1/2-in. hole. Collars with OD's of 8, 9 1/2, 11, and 12 in. are used. The WOB varies from 20,000 to 100,000 lbf. Both bit side force and bit tilt increase with increased WOB. Fig. 8.150 presents the same data with geological forces of +200 lbf. If the geological forces are substantial, the 11- and 12-in. collar diameters provide significantly more bit side force and less bit tilt than the 8- and 9 1/2-in. collars. However, even

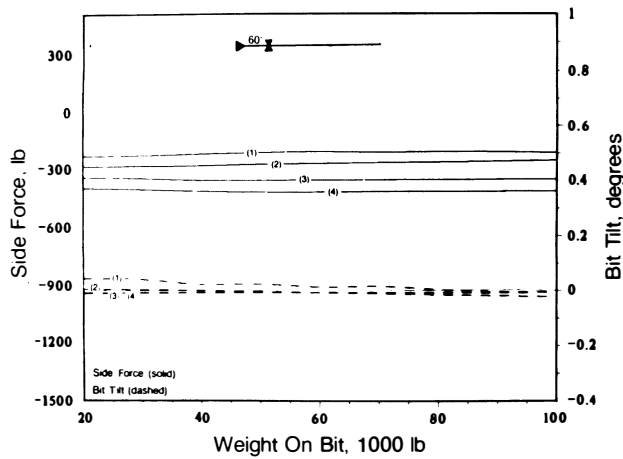


Fig. 8.151A—Single-stabilizer BHA; 17½-in. hole, 10-lbm/gal mud, 5° inclination.

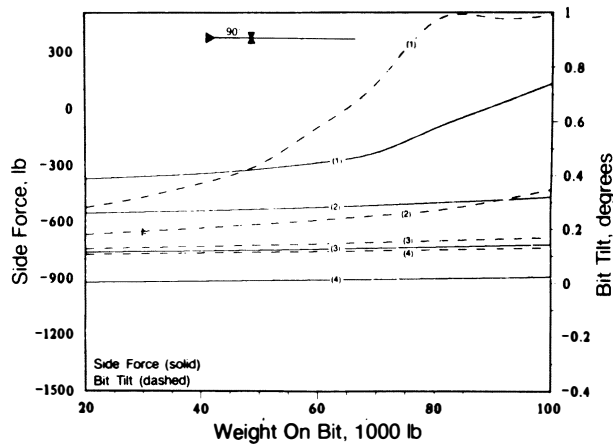


Fig. 8.151B—Single-stabilizer BHA; 17½-in. hole, 10-lbm/gal mud, 5° inclination.

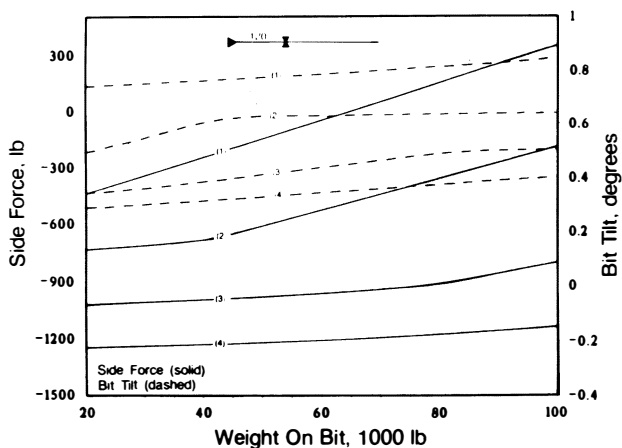


Fig. 8.151C—Single-stabilizer BHA; 17½-in. hole, 10-lbm/gal mud, 5° inclination.

the 12-in. collars will build angle if the geological force is strong enough. The inclination will continue to increase until some equilibrium angle is reached.

A common alternative to the slick BHA is the pendulum. In the larger-diameter wellbore where the big collars are used, tangency lengths can be as great as 120 ft when the inclination is low. Figs. 8.151A through 8.151C show the side forces and bit tilts for the same collars and conditions presented by Figs. 8.149 and 8.150, except that a stabilizer is placed at 60, 90, and 120 ft. Figs. 8.152A through 8.152C show the same cases, except that a two-stabilizer pendulum is used. The second stabilizer is 30 ft from the first stabilizer.

Deviation control with a slick or a pendulum BHA in a large-diameter hole relies on the negative side force to offset the bit tilt and geological effects that tend to build angle. The pendulum and slick BHA's work best when the geological forces are small, the formations are fairly homogeneous, and the formation strength is low. When the geological forces are significant, when the lithology is varied, and when the formation strengths are medium to hard, the multistabilizer BHA usually effects better results.

Fig. 8.153 presents the typical packed BHA's used for deviation-control drilling in large holes. Figs. 8.154A through 8.154C show the side forces and bit tilts for the same BHA's with 8-, 9½-, 11-, and 12-in.-OD drill collars.

If the geological forces are strong, all the packed BHA's will build inclination at some constant rate until the geological force ceases. Once a building curvature is started with a packed BHA, however, there is a tendency for the build to continue until a major change occurs to break the curvature. This can be a change in the BHA configuration, in the geology, or in operating practices.

The use of multistabilizer BHA's has positive and negative aspects for deviation-control drilling. Stabilizers—especially large-diameter stabilizers—add torque and, in some instances, reduce the amount of weight that can be applied at the bit. Chemical and hydraulic actions can weaken certain formations, and stabilizers can accelerate the erosion of a wellbore by mechanically cutting, wearing, and striking the wellbore wall. Trip times are increased because of the handling of the stabilizers; with larger-diameter holes, this is especially true because of the greater makeup torques of the larger tool joints. Tables 8.22 and 8.23 present some of the makeup torques for various drill collars. If the makeup torques are not achieved, tool joints can be overtorqued during drilling; this can crack the boxes and can make breaking the tool joint at the surface difficult. In unstable wellbores, there is a risk of excessive drag in tripping out of the hole with multistabilizer BHA's. Moreover, fishing is more difficult.

The virtues of multistabilizer BHA's are many. Bit performance is usually better because of the small bit tilts and better dynamics. If the bit becomes worn in drilling an abrasive formation, the near-bit stabilizer will ream the hole to the original bit diameter. When these stabilizer blades become worn and undergauge, the rotary torque increases and the penetration rate decreases, signaling that something is wrong and that the bit should be pulled. The chances are reduced, therefore, of drilling undergauge holes and pinching new bits in tripping back into the hole.

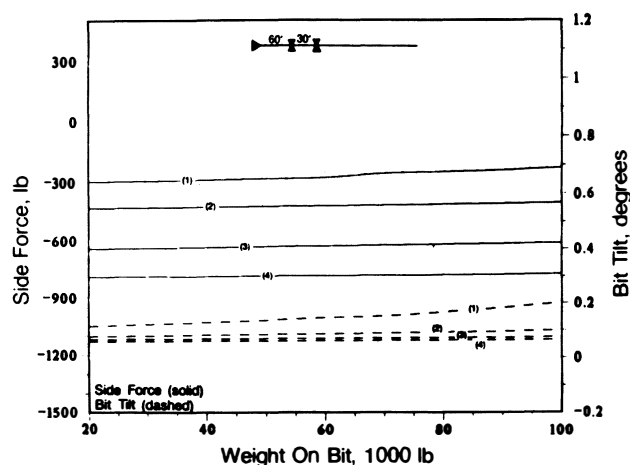


Fig. 8.152A—Two-stabilizer BHA; 17½-in. hole, 10-lbm/gal mud, 5° inclination.

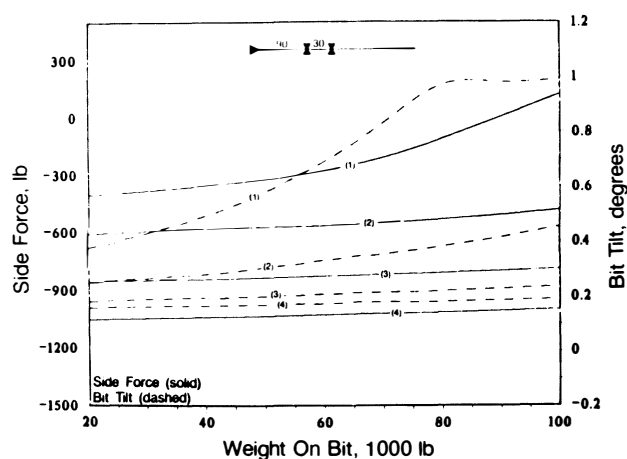


Fig. 8.152B—Two-stabilizer BHA; 17½-in. hole, 10-lbm/gal mud, 5° inclination.

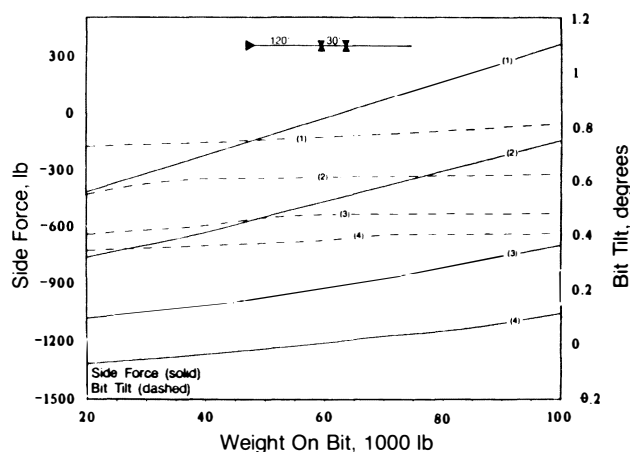


Fig. 8.152C—Two-stabilizer BHA; 17½-in. hole, 10-lbm/gal mud, 5° inclination.

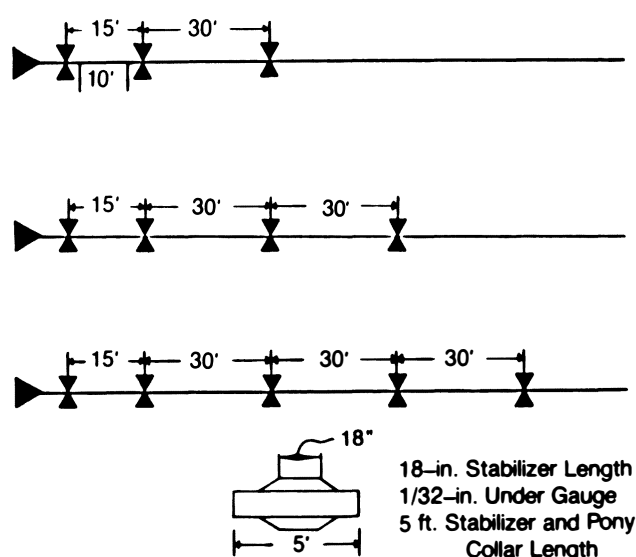


Fig. 8.153—Packed BHA's used for deviation control.

Multistabilizer BHA's permit the use of extreme WOB without incurring appreciable changes in the bit side force or bit tilt. This does not mean that the packed BHA will not build angle; it will at a constant curvature. Variation in lithology does not affect the packed BHA nearly as much as it does a slick or pendulum BHA. Also, the potential for a severe dogleg is much less with a packed BHA. Usually it is easier to place casing into a section of hole newly drilled with a packed BHA than a pendulum or slick BHA.

The selection of a BHA to drill larger wellbores depends on such factors as geological forces and stratigraphy, depth of hole, inclination and dogleg severity constraints, desired penetration rates, trip times, risk of fishing, and drilling-rig capabilities. Of all those factors, geological effects have the greatest bearing on deviation control and on whether wellbores are to be large or small.

### 8.8.2 Geological Forces and Deviation Control

Geological forces that cause deviation control problems are associated with medium-soft to medium-hard formations with significant interbedding and dip angles ranging from 5 to 90°. Such conditions are usually present where there is folding and faulting.

Fig. 8.155 depicts a typical anticlinal structure where most of the wellbores trend toward the crest of the structure. For dip angles less than about 45°, the tendency of the bit is to build angles perpendicular to the strike. The opposite tendency to drill downdip occurs when the beds dip more than about 60°. When the beds are 80 to 90°, the bit tends to follow the dip of the formation, but at a reduced penetration rate. At formation dip angles between 45 and 75°, the bit tends to follow the strike of the formation.

The magnitude of the dips, the formation hardness, and the amount of interbedding dictate the overall formation strength. Another complication is that dips and strike (dip direction) vary with depth. The variation in dip is a function of the position of the well on the structure and the attack angle of the bit with the dipping formations. Fig. 8.156A is an example of a typical series of geological

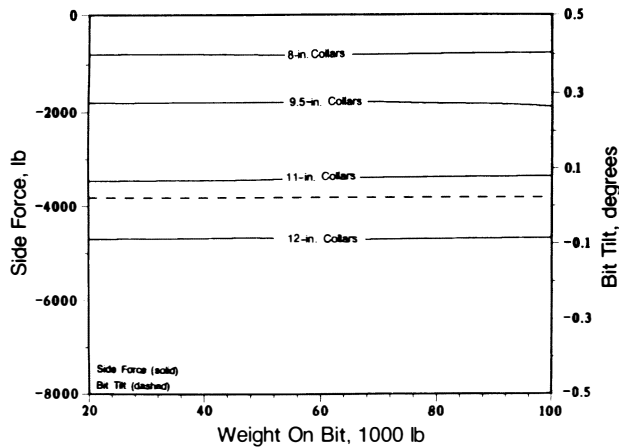


Fig. 8.154A—Three-stabilizer BHA; 17½-in. hole, 10-lbm/gal mud, 5° inclination.

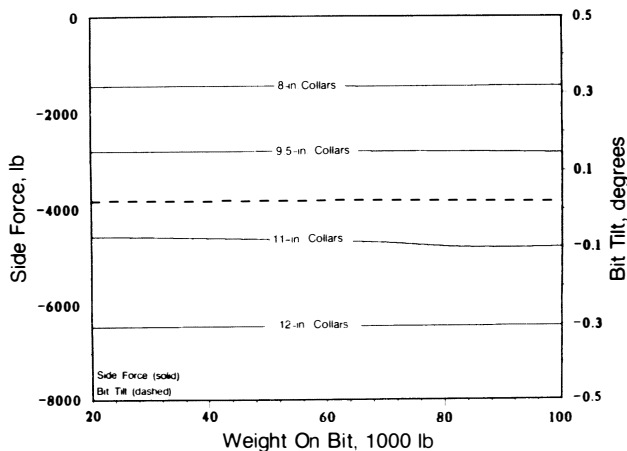


Fig. 8.154B—Four-stabilizer BHA; 17½-in. hole, 10-lbm/gal mud, 5° inclination.

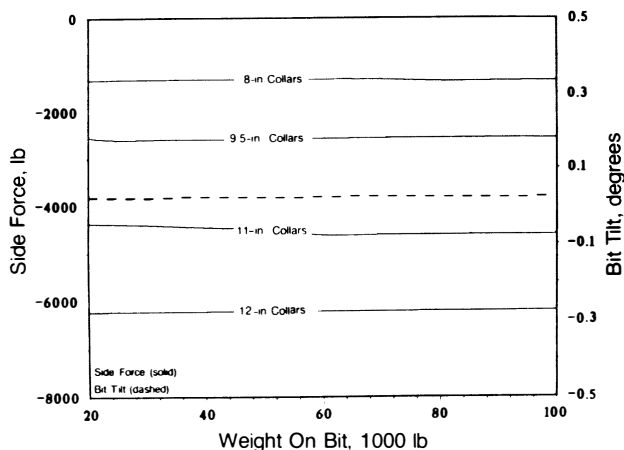


Fig. 8.154C—Five-stabilizer BHA; 17½-in. hole, 10-lbm/gal mud, 5° inclination.

events that caused various dips and dip directions (Fig. 8.156B). The initial 4,000 ft is medium-soft Tertiary sediments deposited over an erosional surface, having only a slight regional dip of 2 to 5° with a westerly dip direction. Below the unconformity is an anticlinal structure that has been thrust faulted, causing dips as high as 50° on the eastern side. The Cretaceous sediments are highly interbedded, while the Jurassic and Triassic sediments are fairly uniform shales. Below the shales, the formations dip severely and are also very hard.

During the drilling of the main structure, there is very little bit-building tendency through the fairly flat Tertiary formations. Below the unconformity, the dips are greater and vary in direction and angle. If a slick, pendulum, or packed BHA is used to drill through the interface of the unconformity where the dip direction changes, the borehole, more than likely, will change direction and trend perpendicular to the strike and up dip. If the inclination of the wellbore is between 1 and 5°, there is a strong probability that the wellbore direction will not change during drilling through the interface. Above 5°, the change in direction may not be too drastic. Once in the interbedded dipping beds, the slick and pendulum BHA's will continue to build angle until equilibrium is achieved. This equilibrium depends on a balance between the resultant bit side force and the formation force, as discussed in Sec. 8.7.4. A packed BHA will reach an equilibrium curvature and continue on this curvature until some major change occurs.

Drilling into shales that are fairly uniform and of medium strength, the slick, pendulum, and packed BHA's will all tend to drop angle even though the dips of the shale formations are similar to those of the overlying sediments. The underlying sandstones and limestones are much harder, and they dip more than the overlying sediments. Any change in direction or inclination will be slow and slight, regardless of the BHA used. For example, if an inclination occurs when the harder formations are being penetrated, it will probably remain unchanged whether a pendulum, slick, or packed BHA is used. Starting a drop of inclination angle usually requires a mud motor.

### 8.8.3 Theoretical Investigations Pertaining to Deviation Control

Lubinski and Woods<sup>24</sup> defined the anisotropy index,  $h$ , as a way to account for the geological forces that cause a bit to deviate when the rock properties change abruptly. Their theory, however, could not explain down dip deviation in steeply dipping formations. Other investigators tried to postulate the deviation of a bit in a variety of ways. The miniature whipstock theory proposed by Rollins<sup>25</sup> and further researched by Murphey and Cheatham<sup>26</sup> explained that brittle material subjected to compressional forces will fail normal to the bedding planes. In dipping formations, this failure leads to miniature whipstocks that cause the bit to deviate (see Fig. 8.157). The miniature-whipstock theory does not explain down dip deviation in steeply dipping beds.

Fig. 8.158 illustrates a theory presented by Knapp,<sup>27</sup> who suggests that drilling in a soft formation and intersecting a dipping, hard formation will deviate down dip. This theory is not consistent with field results. In contrast to Knapp's theory, Sultanov and Shandalov's<sup>28</sup> theory states that a bit drilling in a soft formation and

TABLE 8.22—MAKE-UP TORQUE FOR DRILL COLLARS (ft-lbf)

CONNECTION			BORE OF DRILL COLLAR SIZE (in.)										+ WEAK MEMBER
SIZE (in.)	TYPE	OD (in.)	1	1-1/4	1-1/2	1-3/4	2	2-1/4	2-1/2	2-13/16	3		
API	NC 23	3	2,500	2,500	2,500							BOX	
		3-1/8	3,300	3,300	2,600							PIN	
		3-1/4	4,000	3,400	2,600							PIN	
2-7/8	PAC (See Note 4)	3		3,800	3,800	2,900						PIN	
		3-1/8		4,900	4,200	2,900						PIN	
		3-1/4		5,200	4,200	2,900						PIN	
2-3/8	API IF or NC 26 or SLIM HOLE	3-1/2		4,600	4,600	3,700						PIN	
		3-3/4		5,500	4,700	3,700						PIN	
2-7/8	EXTRA HOLE or DBL STREAMLINE or MOD. OPEN	3-3/4		4,100	4,100	4,100						BOX	
		3-7/8		5,300	5,300	5,300						BOX	
		4-1/8		8,000	8,000	7,400						PIN	
2-7/8	API IF or NC 31 or SLIM HOLE	3-7/8		4,600	4,600	4,600						BOX	
		4-1/8		7,300	7,300	7,300						BOX	
		4-1/4		8,800	8,800	8,100						PIN	
3-1/2		10,000	9,300	8,100							PIN		
API	NC 35	4-1/2				8,900	8,900	8,900	7,400			PIN	
		4-3/4				12,100	10,600	9,200	7,400			PIN	
		5				12,100	10,600	9,200	7,400			PIN	
3-1/2	EXTRA HOLE or SLIM HOLE or MOD. OPEN	4-1/4				5,100	5,100	5,100	5,100			BOX	
		4-1/2				8,400	8,400	8,400	8,200			PIN	
		4-3/4				11,900	11,700	10,000	8,200			PIN	
3-1/2	API IF or NC 38 or SLIM HOLE	5				13,200	11,700	10,000	8,200			PIN	
		5-1/4				13,200	11,700	10,000	8,200			PIN	
		5-1/2				13,200	11,700	10,000	8,200			PIN	
3-1/2	API IF or NC 38 or SLIM HOLE	4-3/4				9,900	9,900	9,900	8,300			PIN	
		5				13,800	13,800	12,600	10,900	8,300		PIN	
		5-1/4				18,000	14,600	12,800	10,900	8,300		PIN	
3-1/2	H-90 (See Note 3)	4-3/4				8,700	8,700	8,700	8,700	8,700		BOX	
		5				12,700	12,700	12,700	12,700	10,400		PIN	
		5-1/4				16,900	16,700	15,000	13,100	10,400		PIN	
4	FULL HOLE or NC 40 or MOD. OPEN or DBL STREAMLINE	5				18,500	16,700	15,000	13,100	10,400		PIN	
		5-1/4				10,800	10,800	10,800	10,800	10,800		BOX	
		5-1/2				15,100	15,100	15,100	14,800	12,100		PIN	
4	H-90 (See Note 3)	5-1/2				19,700	18,600	16,900	14,800	12,100		PIN	
		5-3/4				20,400	18,600	16,900	14,800	12,100		PIN	
		6				20,400	18,600	16,900	14,800	12,100		PIN	
4-1/2	API REGULAR	5-1/4				12,500	12,500	12,500	12,500			BOX	
		5-1/2				17,300	17,300	17,300	16,500			PIN	
		5-3/4				22,300	21,500	19,400	16,500			PIN	
4-1/2	API REGULAR	6				23,500	21,500	19,400	16,500			PIN	
		6-1/4				23,500	21,500	19,400	16,500			PIN	
		6-1/2				23,500	21,500	19,400	16,500			PIN	
API	NC 44	5-3/4	FOR LARGER OD's NOT SHOWN, ADD 10% AS STATED IN NOTE 2.			20,600	20,600	20,600	18,000			PIN	
		6-1/4				25,000	23,300	21,200	18,000			PIN	
		6-1/2				25,000	23,300	21,200	18,000			PIN	
4-1/2	API FULL HOLE	5-1/2				12,900	12,900	12,900	12,900	12,900		BOX	
		5-3/4				17,900	17,900	17,900	17,900	17,700		PIN	
		6				23,300	23,300	22,800	19,800	17,700		PIN	
4-1/2	EXTRA HOLE or NC 46 or API IF or SEMI IF or DBL STREAMLINE or MOD. OPEN	6-1/4				27,000	25,000	22,800	19,800	17,700		PIN	
		6-1/2				27,000	25,000	22,800	19,800	17,700		PIN	
		6-3/4											
4-1/2	H-90 (See Note 3)	5-3/4				17,600	17,600	17,600	17,600			BOX	
		6				23,200	23,200	22,200	20,200			PIN	
		6-1/4				28,000	25,500	22,200	20,200			PIN	
5	H-90 (See Note 3)	6-1/2				28,000	25,500	22,200	20,200			PIN	
		6-3/4				28,000	25,500	22,200	20,200			PIN	
		7				34,000	34,000	34,000	34,000			PIN	
5-1/2	H-90 (See Note 3)	6-3/4				41,500	40,000	36,500	34,000			PIN	
		7				42,500	40,000	36,800	34,000			PIN	
		7-1/4				42,500	40,000	36,500	34,000			PIN	
5-1/2	API REGULAR	6-3/4				31,500	31,500	31,500	31,500			BOX	
		7				39,000	39,000	36,000	33,500			PIN	
		7-1/4				42,000	39,500	36,000	33,500			PIN	
5-1/2	API REGULAR	7-1/2				42,000	39,500	36,000	33,500			PIN	
		7-1/2				42,000	39,500	36,000	33,500			PIN	
		7-1/2				42,000	39,500	36,000	33,500			PIN	

(1) Basis of calculations for recommended make-up torque assumed the use of a thread compound containing 40-60% by weight of finely powdered metallic zinc or 60% by weight of finely powdered metallic lead applied thoroughly to all threads and shoulders and using the modified jack screw formula as shown in the IADC Tool Pusher's Manual Sec B 1, p. 7 and API RP 7G, second edition April 1971 Appendix A Sec A 9 and a unit stress of 62,500 PSI in the box or pin whichever is weaker.

(3) H-90 connection make up torque based on 56,250 PSI stress and other factors as stated in note (1).

(2) Normal torque range — tabulated minimum value to 10% greater. Largest diameter shown for each connection is the maximum recommended for that connection. If connections are used on drill collars larger than the maximum shown, increase the torque values shown by 10% for a minimum value. In addition to the increased minimum torque value it is also recommended that a fishing neck be machined to the maximum diameter shown.

(4) 2 7/8 PAC make up torque based on 87,500 PSI stress and other factors as stated in note (1).

Courtesy of Drilco.

TABLE 8.23—MAKE-UP TORQUE FOR DRILL COLLARS (ft-lbf)

CONNECTION			BORE OF DRILL COLLAR SIZE (in.)					+ WEAK MEMBER		
SIZE (in.)	TYPE	OD (in.)	2-1/4	2-1/2	2-13/16	3	3-1/4	3-1/2	3-3/4	
4-1/2	API IF or NC 50 or EXTRA HOLE or MOD. OPEN or DBL. STREAMLINE or SEMI-IF	6-1/4	22,800	22,800	22,800	22,800	22,800			BOX
API		6-1/2	29,500	29,500	29,500	29,500	26,500			PIN
5		6-3/4	36,000	35,500	32,000	30,000	26,500			PIN
5		7	38,000	35,500	32,000	30,000	26,500			PIN
5-1/2		7-1/4	38,000	35,500	32,000	30,000	26,500			PIN
5										
5-1/2	API FULL HOLE	7		32,500	32,500	32,500	32,500			BOX
		7-1/4		40,500	40,500	40,500	40,500			BOX
		7-1/2		49,000	47,000	45,000	41,500			PIN
		7-3/4		51,000	47,000	45,000	41,500			PIN
API	NC 56	7-1/4		40,000	40,000	40,000	40,000			BOX
		7-1/2		48,500	48,000	45,000	42,000			PIN
		7-3/4		51,000	48,000	45,000	42,000			PIN
		8		51,000	48,000	45,000	42,000			PIN
6-5/8	API REGULAR	7-1/2		46,000	46,000	46,000	46,000			BOX
		7-3/4		55,000	53,000	50,000	47,000			PIN
		8		57,000	53,000	50,000	47,000			PIN
		8-1/4		57,000	53,000	50,000	47,000			PIN
6-5/8	H-90 (See Note 3)	7-1/2		46,000	46,000	46,000	46,000			BOX
		7-3/4		55,000	55,000	51,000	49,500			PIN
		8		59,500	56,000	53,000	49,500			PIN
		8-1/4		59,500	56,000	53,000	49,500			PIN
API	NC 61	8		54,000	54,000	54,000	54,000			BOX
		8-1/4		64,000	64,000	64,000	61,000			PIN
		8-1/2		72,000	68,000	65,000	61,000			PIN
		8-3/4		72,000	68,000	65,000	61,000			PIN
		9		72,000	68,000	65,000	61,000			PIN
5-1/2	API IF	8		56,000	56,000	56,000	56,000	56,000		BOX
		8-1/4		66,000	66,000	63,000	59,000			PIN
		8-1/2		74,000	70,000	67,000	63,000	59,000		PIN
		8-3/4		74,000	70,000	67,000	63,000	59,000		PIN
		9		74,000	70,000	67,000	63,000	59,000		PIN
		9-1/4		74,000	70,000	67,000	63,000	59,000		PIN
6-5/8	API FULL HOLE	8-1/2			67,000	67,000	67,000	67,000	66,500	PIN
		8-3/4			78,000	78,000	72,000	72,000	66,500	PIN
		9			83,000	80,000	76,000	72,000	66,500	PIN
		9-1/4			83,000	80,000	76,000	72,000	66,500	PIN
		9-1/2			83,000	80,000	76,000	72,000	66,500	PIN
API	NC 70	9			75,000	75,000	75,000	75,000	75,000	BOX
		9-1/4			88,000	88,000	88,000	88,000	88,000	BOX
		9-1/2			101,000	101,000	100,000	95,000	90,000	PIN
		9-3/4			107,000	105,000	100,000	95,000	90,000	PIN
		10			107,000	105,000	100,000	95,000	90,000	PIN
		10-1/4			107,000	105,000	100,000	95,000	90,000	PIN
API	NC 77	10			107,000	107,000	107,000	107,000	107,000	BOX
		10-1/4			122,000	122,000	122,000	122,000	122,000	BOX
		10-1/2			138,000	138,000	133,000	128,000	128,000	PIN
		10-3/4			143,000	138,000	133,000	128,000	128,000	PIN
		11			143,000	138,000	133,000	128,000	128,000	PIN

CONNECTIONS			WITH FULL FACE					+ WEAK MEMBER
7	H-90 (See Note 3)	8			53,000	53,000	53,000	53,000
		8-1/4			63,000	63,000	63,000	60,500
		8-1/2			71,500	68,500	65,000	60,500
7-5/8	API REGULAR	8-1/2				60,000	60,000	60,000
		8-3/4				71,000	71,000	71,000
		9				83,000	83,000	79,000
		9-1/4				88,000	83,000	79,000
		9-1/2				88,000	83,000	79,000
7-5/8	H-90 (See Note 3)	9				72,000	72,000	72,000
		9-1/4				85,500	85,500	85,500
		9-1/2				98,000	98,000	95,500
8-5/8	API REGULAR	10				108,000	108,000	108,000
		10-1/4				123,000	123,000	123,000
		10-1/2				139,000	134,000	129,000
8-5/8	H-90 (See Note 3)	10-1/4				112,500	112,500	112,500
		10-1/2				128,500	128,500	128,500

CONNECTIONS			WITH LOW TORQUE FACE					+ WEAK MEMBER
7	H-90 (See Note 3)	8-3/4			67,500	67,500	66,500	62,000
		9			74,000	71,000	66,500	62,000
7-5/8	API REGULAR	9-1/4				72,000	72,000	72,000
		9-1/2				85,000	85,000	82,000
		9-3/4				91,000	87,000	82,000
		10				91,000	87,000	82,000
7-5/8	H-90 (See Note 3)	9-3/4				91,000	91,000	91,000
		10				105,000	105,000	98,000
		10-1/4				112,500	108,000	103,500
		10-1/2				112,500	108,000	103,500
8-5/8	API REGULAR	10-3/4				112,000	112,000	112,000
		11				129,000	129,000	129,000
8-5/8	H-90 (See Note 3)	10-3/4				92,500	92,500	92,500
		11				110,000	110,000	110,000
		11-1/4				128,000	128,000	128,000

\* Largest diameter shown is the maximum recommended for these full face connections. If larger diameters are used, machine connections with low torque faces and use the torque values shown under low torque face tables. If low torque faces are not used see note (2) for increased torque values.

+ Notation in this column indicates cross section area (3/4" from base on pin or 3/8" from shoulder on box) is smaller on the member indicated



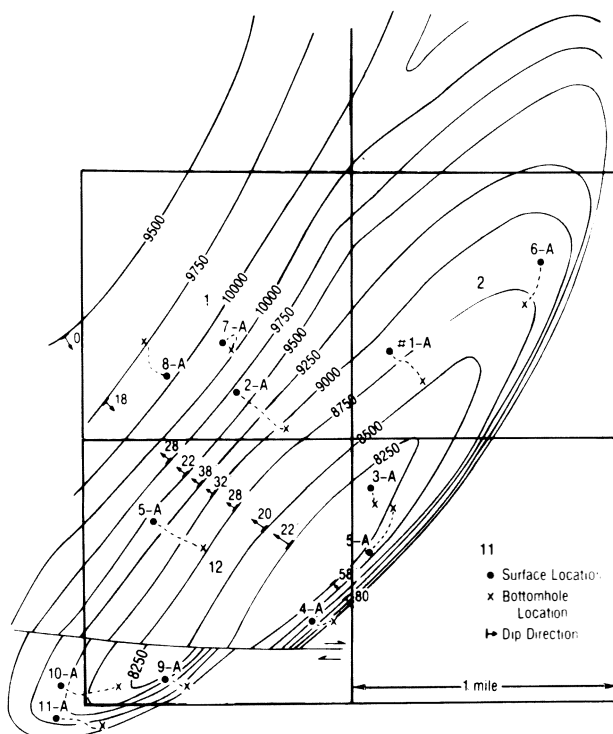


Fig. 8.155—Typical anticlinal structure that can cause deviation control problems.

intersecting a hard formation will deviate updip. Again, the tendency to deviate downdip in steeply dipping beds is not explained. Another theory, presented by Smith and Cheatham,<sup>29</sup> considers the plastic fracture of a formation under a single wedge. The conclusions of their work imply downdip deviation in all cases. This, too, is inconsistent with field observations.

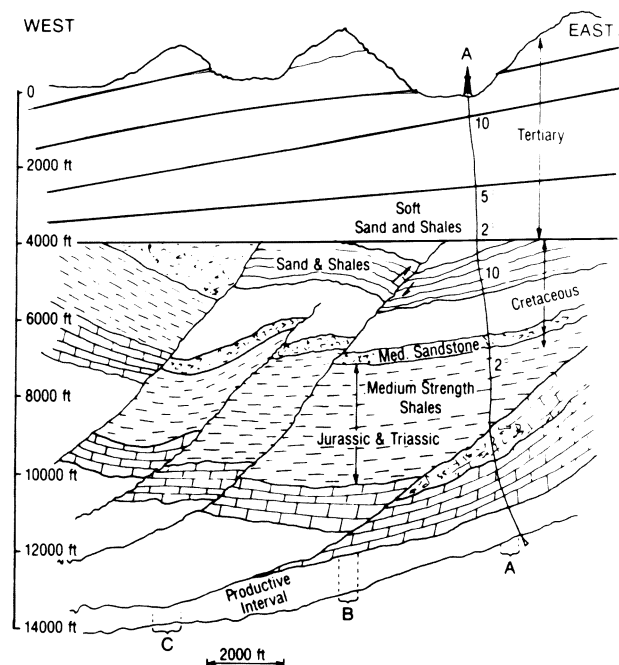


Fig. 8.156A—Typical cross section of complex geology that causes deviation control problems.

A theory that does explain both updip and downdip deviation was initially proposed by McLamore<sup>30</sup> and later expanded by Bradley.<sup>31</sup> It is called the “preferred chip formation” theory. Fig. 8.159 summarizes McLamore’s idea of the interaction of a bit’s tooth with a brittle formation. At time  $T_1$ , a vertical force is imparted to a single wedge with a wedge angle of  $\Omega$  into a formation with a dip,  $\phi$ . At time  $T_2$ , a tensile crack is formed, and a pulverized or plastic zone is immediately below the tooth. At time  $T_3$  a chip breaks loose on the updip side, and at time  $T_4$  a crater is left with more volume removed from the updip side than from the downdip side.

The force to create a chip on either side of the tooth was derived by McLamore.

$$F_i = \frac{2\tau(\rho_i)D_w \sin \Omega \cos \phi}{\cos^2 \left( \frac{\pi/2 + \Omega + \phi}{2} \right)}, \dots \dots \dots (8.116)$$

where  $i$  is 1 for the updip side of the wedge and 2 for the downdip side,  $D_w$  is the depth of the wedge penetration,  $\Omega$  is the included wedge half angle,  $\phi$  is the bedding dip angle relative to the bottom of the hole,  $\rho_1$  equals  $\phi$  plus  $\Omega$ ,  $\alpha_{dh}$  is the bedding dip angle relative to the bottom of the hole,  $\rho_2$  equals  $\phi$  minus  $\Omega$ ,  $\tau(\rho_i)$  is the shear strength of the anisotropic rock along the plane of failure, and  $\phi$  is the angle of internal friction of the anisotropic rock.

The deviation force can be calculated by Eq. 8.117, assuming that the chip will form on the side of the wedge having the lesser amount of fracture force.

$$F_{DEV} = \frac{\tau(\rho_i)D_w \cos \Omega \cos \phi}{\cos^2 \left( \frac{\pi/2 + \Omega + \phi}{2} \right)}, \dots \dots \dots (8.117)$$

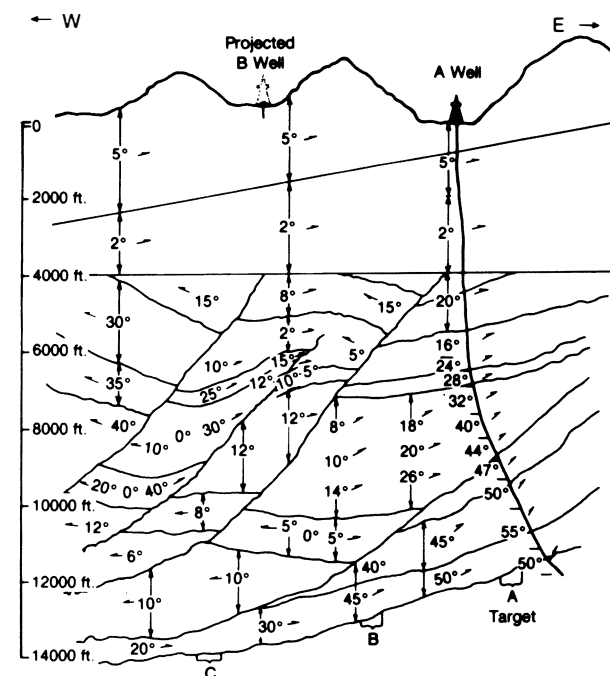


Fig. 8.156B—Projected dips based on Well A and geophysical information.

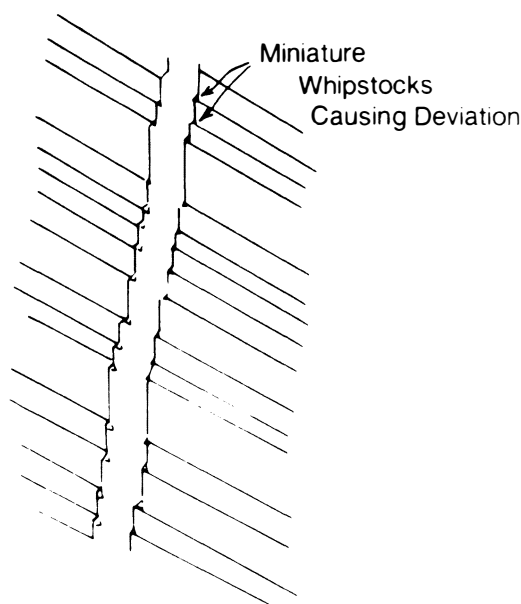


Fig. 8.157—Miniature-whipstock theory (after Rollins<sup>25</sup>).

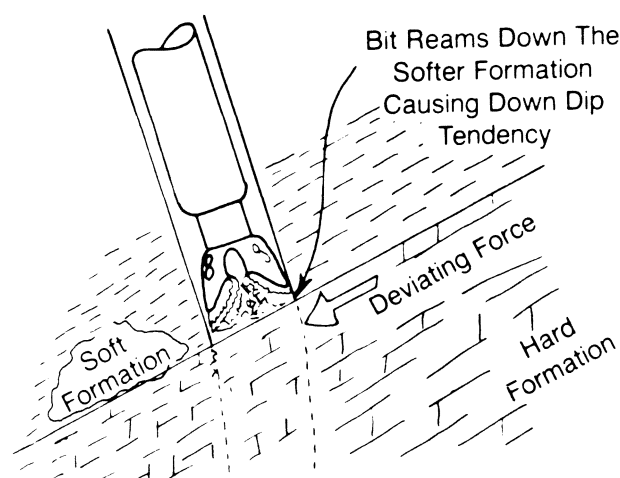


Fig. 8.158—Soft-to-hard downdip theory (after Knapp<sup>27</sup>).

Both parts of Fig. 8.160 were calculated by McLamore with Eq. 8.115. Fig. 8.160a shows that for wedge angles ( $2\Omega$ ) of 35 to 45° and for bed dips of 30°, the tendency is for a positive deviation force (updip); for bed dips of more than 30°, there is a negative deviation force (downdip). Fig. 8.160b shows that, for the large wedge angles, the tendency shifts more to the downdip with the transition dip angle being between 30 and 40°.

McLamore's theory implies that the tooth-wedge angle affects the deviation force. The narrower the wedge, the greater the tendency to drill updip.

#### 8.8.4 General Deviation Control

Sec. 8.8.1 presented deviation control for large-diameter wellbores using BHA's with 8- to 12-in.-diameter drill collars. Drilling intermediate-sized holes—7 $\frac{7}{8}$  to 12 $\frac{1}{2}$ -in.—requires 6- to 10-in. collars. Larger collars can be used if the fishability is not a concern. Usually, 1 $\frac{1}{2}$  in. is subtracted from the wellbore diameter to determine

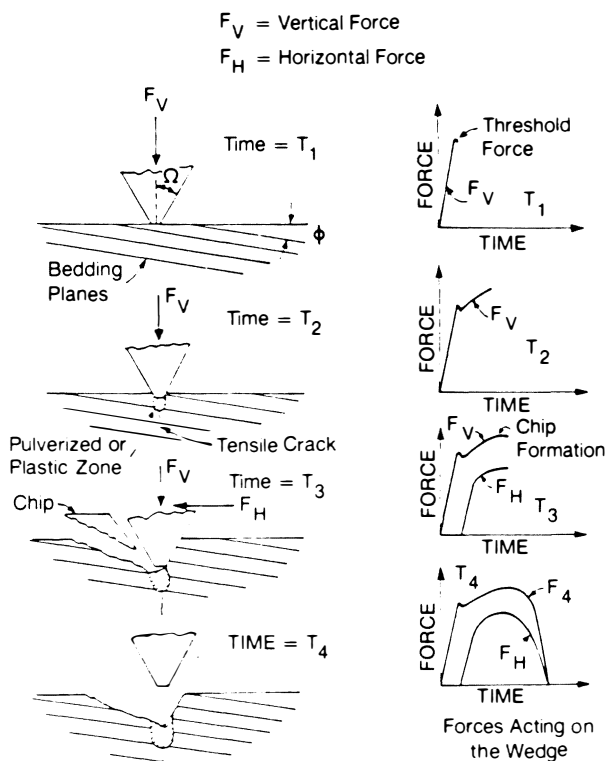


Fig. 8.159—Preferred chip formation model (after McLamore<sup>30</sup>).

the largest collar that can be used if a standard overshoot might be required for a fishing job.

In many drilling situations, the smaller drill collars are not stiff enough to offset moderate to severe formation forces. Even with low WOB's to "fan the formation," it is difficult to keep from building an inclination angle when the formation forces are greater than the maximum 0-lbf WOB case where the negative side force is at its maximum level. Because of the lesser collar stiffness, shorter pendulum BHA's should be used. A 9 $\frac{7}{8}$ -in. hole with 8-in. collars would have a maximum pendulum length of about 80 ft, while a 7 $\frac{7}{8}$ -in. wellbore with 6 $\frac{7}{8}$ -in. collars would have a maximum pendulum length of about 45 ft.

In most situations, using low WOB's to control deviation is not economical, except when a turbine or positive-displacement motor is used. The correct strategy is to determine how much the formation forces will cause the wellbore to deviate over the depth of a well while optimum WOB's and rotary speeds are used. Fig. 8.155 shows surface locations positioned in such a way that the natural tendency of the bit will be to drill updip toward the bottomhole location, which is now a pseudotarget. The positioning of the surface target requires a knowledge of the dips and strikes of all the formations from surface to total depth. Many times a surface location is chosen in expectation of encountering a certain dip direction, but the well is found to be going in a different direction. This usually happens because the near-surface structure is different from that of the deeper formations. Such misjudgments generally occur when the geology of a new structure is undefined, when there is a great deal of faulting (as in the case of piercement domes), and when the drilling is on the flanks of complex structures, such as those depicted in Fig. 8.156.

The best way to determine the horizontal departure of a wellbore from the bottomhole target to the surface location is to determine the optimum WOB's and hole-size requirements and to design the BHA's that will resist the formation forces best. This horizontal distance can be used to determine how far to set the surface location back. This distance can range from a few hundred to more than a thousand feet, depending on the total depth.

Knowing the geological forces and how well a given BHA will respond to them, one can adjust the surface location to take advantage of those factors and optimally drill a well. A packed BHA, for example, will provide a smoother trajectory than a pendulum or a slick BHA. Square drill collars can increase the stiffness of a BHA for a given hole size and can reduce the bending force effects, allowing for more applied WOB than would be possible for round drill collars. As discussed previously, it is not the magnitude of the inclination that causes casing failures, worn pipe, key seats, and production problems with sucker rods and tubing; it is dogleg severity. Accordingly, the same practices used in drilling directional wells to minimize dogleg severity should be used in deviation control.

**Example 8.33.** Your company wants to drill a second well to Bottomhole Location B, as shown in Fig. 8.156A. You need to determine where to position the surface location on the basis of information from Well A and the geological cross section (Fig. 8.156A). You are also required to design the BHA's to hit the bottomhole target. The production string that is required is 7-in., 29-lbm/ft casing. The offset information on Well A is found in Table 8.24. (Note: A valley location costs \$100,000; a mountain location costs \$750,000.)

**Solution.** The calculated trajectory of Well A is presented in Table 8.25.

The total departure of the well is 2,534 ft, which misses the target by 600+ ft. From the surface to the measured depth of 4,558 ft, the rate of angle build is low—i.e.,

less than  $0.1^\circ/100$  ft. At 4,558 ft, the rate of angle build increases to  $0.6^\circ/100$  ft and continues at rates between  $0.4$  and  $0.7^\circ/100$  ft to a measured depth of 9,805 ft, where the rate decreases to  $0.2$  to  $0.3^\circ/100$  ft. From 11,050 to 11,800 ft, the rate of angle build varies between  $0.5$  and  $0.6^\circ/100$  ft. The plot of the trajectory data shows that most of the departure occurs in the Jurassic and Triassic shales and limestone.

Fig. 8.156B shows the interpreted dips based on the Well A dipmeter and geophysical data. Given the 2,540 ft of departure, the surface location of Well B should be 5,000 ft south of Well A. The formation dips that are projected for Well B are much less severe than those for Well A; therefore, if the same BHA's are used, the BHA's would not deviate the trajectory the 2,500 ft north of the surface location. In fact, the wellbore should be nearly vertical down to 6,000 ft. From 6,000 to 10,000 ft, it is possible that the wellbore would deviate much less than that of Well A. Below 10,000 ft, it is possible that the trajectory of Well B would kick to the west away from the target if the wellbore is not east of the  $0^\circ$  dips. Therefore, the trajectory control plan should provide for at least 1,400 ft of north departure when true vertical depth (TVD) of 10,000 ft is reached. This is 400 ft less than Well A. To do this, it might be necessary to design a building BHA that will provide just enough angle build to obtain the necessary departure.

There are three possible approaches for hitting the designated target. The first approach, using a continuous-build trajectory, assumes there will be negligible departure down to the top of the Cretaceous (approximately 4,000 ft). With the continuous build of  $0.5/100$  ft starting at 5,239 ft, the desired departure of 2,540 ft would be reached at the top of the target (12,450 ft TVD) with a final inclination of  $39.0^\circ$  and a measured depth of 13,039 ft. The second approach, using a build-and-hold trajectory, could also be used to hit the target. For example, starting at 4,039 ft and maintaining the same build rate as the continuous-build ( $0.5^\circ/100$  ft), the inclination would be increased to  $22.5^\circ$ , where it would be held constant to total depth. At the top of the target at 12,450 ft, the

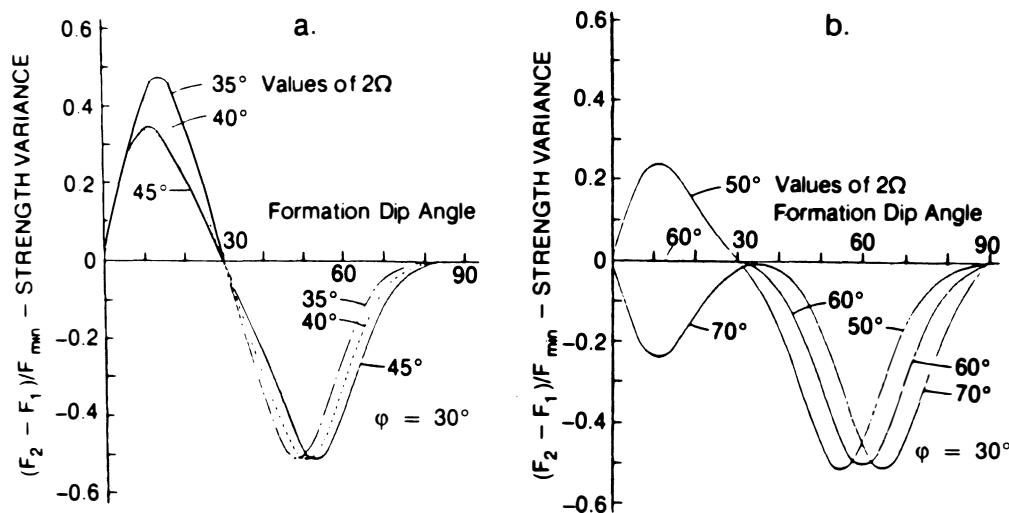


Fig. 8.160—Chip direction preference as a function of wedge angle and formation dip angle (after McLamore<sup>30</sup>).

**TABLE 8.24—OFFSET INFORMATION ON WELL A FOR EXAMPLE 8.33****Hole Sizes and Casing Sizes**

Hole Size (in.)	Casing Size (in.)	Depth
17½ in.	13⅝ in.	Surface to 4,020 ft
12¼ in.	9⅝ in.	4,020 to 9,290 ft
8½ in.	7 in.	9,290 to 11,180 ft

**Drilling Results**

Depth (ft)	Geology	Average Penetration Rate Over Interval (ft/hr)	Inclination	Formation Dip Average Over Interval
0 to 600	Tertiary	30	1°	5°
600 to 1,800	Tertiary	20	1½°	5°
1,800 to 2,801	Tertiary	14	1¾°	2°
2,801 to 3,405	Tertiary	12	2°	2°
3,405 to 4,020	Top of Cretaceous	10	2°	2°
4,020 to 4,558	Cretaceous	35	5°	20°
4,558 to 5,240	Cretaceous	33	8°	20°
5,240 to 5,800	Cretaceous	37	5°	16°
5,800 to 6,350	Cretaceous	8	8.5°	24°
6,350 to 7,010	Cretaceous	24	12.5°	28°
7,010 to 7,500	Jurassic and Triassic	20	16.0°	32°
7,500 to 8,100	Jurassic and Triassic	17	19.5°	40°
8,100 to 8,640	Jurassic and Triassic	15	23.0°	44°
8,640 to 9,290	Jurassic and Triassic	12	27.0°	47°
9,290 to 9,805	Jurassic and Triassic	9	28.0°	50°
9,805 to 10,500	Jurassic and Triassic	8.5	30.0°	55°
10,500 to 11,050		7.0	33.0°	55°
11,050 to 11,470		15.0	35.0°	50°
11,470 to 11,800		12.0	37.0°	50°

**Bottomhole Assemblies**

Interval	Quantity	Equipment
0 to 4,020 ft		17½-in. bit
	9	9.5- × 3.0-in. Drill Collars
	21	8.0- × 2⅜-in. Drill Collars
	12	6.5- × 2⅜-in. Drill Collars 5.0-in. Grade E Drillpipe
4,020 to 9,290 ft		12¼-in. bit
	30	8.0- × 2⅜-in. Drill Collars
	12	6.5- × 2⅜-in. Drill Collars 5.0-in. Grade E Drillpipe
		8.5-in bit
9,290 to 11,800 ft	36	6.5- × 2⅜-in. Drill Collars 5.0-in. Grade E Drillpipe

**Drilling Parameters**

Measured Depth (ft)	Weight on Bit (1000 lb)	Rotary Speed	Pump Pressure (psig)	Pump Rate (gal/min)	Mud Weight (lb/gal)	Viscosity (cp)
600	25	80	3,434	850	9.2	12
1,800	55	80	3,458	850	9.2	12
2,800	70	75	3,433	850	9.2	12
3,405	70	70	3,532	850	9.2	12
4,020	70	70	3,456	850	9.2	12
4,558	55	70	3,431	600	9.2	12
5,240	55	70	3,390	600	9.4	15
5,800	55	70	3,443	600	9.4	15
6,350	55	70	3,491	600	9.4	15
7,040	55	70	3,393	600	9.4	15
7,500	60	65	3,438	600	9.4	15
8,100	60	65	3,489	600	9.6	15
8,640	60	65	3,420	600	9.6	18
9,290	60	65	3,550	600	9.6	18
9,805	35	75	3,401	600	9.6	18
10,500	40	70	3,427	350	9.5	15
11,500	40	70	3,451	350	9.5	15
11,470	40	70	3,471	350	9.5	15
11,800	35	70	3,481	350	9.5	15

departure is 2,540 ft, and the measured depth is 12,896 ft. A third possibility is to drill a build-and-hold trajectory, assuming the kickoff is toward the base of the Jurassic and Triassic section at 8,419 ft. The dips predicted at that depth would cause very little departure. At that point, using a build rate of 2°/100 ft, building to an inclination of 40.5° at a TVD of 10,280 ft, and holding the inclination at 40.5° will achieve the required horizontal departure at 12,450 ft. The measured depth at a TVD of 12,450 ft is 13,298 ft.

Let us examine the three approaches and determine which one would be optimal.

**Case 1—The Continuous Build.** The continuous build would start at 5,239 ft and continue to total depth. If the BHA can be designed to maintain a constant build of 0.5°/100 ft to maximize the WOB, an overall optimization could be achieved. A two-stabilizer building BHA with a spacing between 45 and 55 ft should achieve the desired results. If the second stabilizer is an adjustable slip-on type, the constant rate of build probably could be maintained. The final inclination of 39.0° at total depth is acceptable. The total amount of extra casing necessary for this plan is 589 ft.

**Case 2—Build-and-Hold Starting at 4,039 ft.** The build would start at 4,039 ft at 0.5°/100 ft and would continue to a final inclination of 22.5° at 8,424 ft TVD and 8,539 ft measured depth. At 12,450 ft TVD the measured depth is 12,896 ft, which requires 446 ft of extra casing. However, the final inclination is 16.5° less than that for the continuous-build case. The BHA's used for the continuous-build approach would be suitable for this plan. Maximum WOB could be maintained over the build section. To hold angle, a three-stabilizer BHA could be used, with a spacing of 12 to 15 ft between the lead and second stabilizers and with a 30-ft spacing between the second and third stabilizers.

The problem with this program lies in the hold section. It is doubtful that a constant 22.5° inclination can be maintained against the formation forces below the Jurassic and Triassic section. Because the dips go to the south, the bit probably would have a strong tendency to turn and drop. This would require going back to some type of building assembly and possibly making a motor run to correct the direction.

**Case 3—Build and Hold Starting at 8,419 ft.** It might be possible to start at 8,419 ft and to maintain a rate of build at 2°/100 ft in the 12¼-in. hold if a strongly building BHA is used. A two-stabilizer BHA with 60- to 70-ft spacing might work, as would a single-stabilizer building BHA. Before the bottom of the Jurassic-Triassic interval is reached and the harder limestone is penetrated, the required inclination of 40.5° should have been achieved (10,280 ft TVD). This angle should be held constant to a total measured depth of 13,298 ft. In this case, 848 ft of extra casing would be required, mostly in the 8½-in. hole (with 8-in. casing). This program also calls for a long hold section, but mostly in the hard limestone. It would be much easier to maintain the 40.5° with the holding BHA used in Case 2. The main drawbacks to this approach are that the higher inclinations would cause more drag (which might lead to more time-consuming trips and

TABLE 8.25—CALCULATED TRAJECTORY OF WELL A

Measured Depth (ft)	Depth (TVD) (ft)	North-South	East-West (ft)	Vertical Section (ft)	Departure (ft)	Inclination (degree)	Dog-Leg °/100 ft
600	599.98	0.00	5.24	5.24	5.2	1.00	0.2
1,800	1,799.69	0.00	31.41	31.41	31.4	1.50	0.0
2,801	2,800.29	0.00	59.80	59.80	59.8	1.75	0.0
3,405	3,403.97	0.00	79.56	79.56	79.6	2.00	0.0
4,020	4,018.59	0.00	101.03	101.03	101.0	2.00	0.0
4,558	4,555.59	0.00	133.97	133.87	133.9	5.00	0.6
5,340	5,332.56	0.00	222.39	222.39	222.4	8.00	0.4
5,800	5,789.60	0.00	274.47	274.47	274.5	5.00	0.7
6,350	6,335.79	0.00	339.11	339.11	339.1	8.50	0.6
7,010	6,984.73	0.00	459.39	459.39	459.4	12.50	0.6
7,500	7,459.66	0.00	580.00	580.00	580.0	16.00	0.7
8,100	8,031.09	0.00	762.92	762.92	762.9	19.50	0.6
8,640	8,534.37	0.00	958.64	958.64	958.6	23.00	0.6
9,290	9,123.47	0.00	1,233.34	1,233.34	1,233.3	27.00	0.6
9,805	9,580.28	0.00	1,471.14	1,471.14	1,471.1	28.00	0.2
10,500	10,188.14	0.00	1,808.08	1,808.08	1,808.1	30.00	0.3
11,050	10,657.09	0.00	2,095.45	2,095.45	2,095.5	33.00	0.5
11,470	11,005.29	0.00	2,330.31	2,330.31	2,330.3	35.00	0.5
11,800	11,272.26	0.00	2,524.28	2,524.28	2,524.3	37.00	0.6

damage from key seats and stuck pipe) and that footage would need to be drilled in the harder limestone formations.

**Conclusion.** The analyses of these cases indicate that the continuous-build program is the most attractive approach. Simple two-stabilizer building assemblies can be used with optimal WOB. Because the BHA could always be building angle, the effects of the formation forces could be controlled easily by the adjustment of the second stabilizer either closer to or farther from the lead stabilizer.

Drilling through the abrasive sandstone at the base of the Cretaceous would require 3-point roller reamers instead of stabilizers. These reamers would be necessary in the hard limestones also. To drill through the shale, regular spiral or straight-bladed stabilizers could be used.

The risk in the continuous-build program is that the build might close in the harder limestones and motors would be needed to complete the hole. There is also a danger that the mud program would not stabilize the shales and the hole would enlarge, causing hole instability, key-seating, and other problems that could keep the building assembly from responding in the desired manner. However, good planning and careful selection of the bit, mud system, etc., should minimize those risks.

The foregoing approaches are only a few of the possibilities that can be deduced from the principles presented in Chap. 8. There is no absolute way of drilling a directional or deviation-control well. However, there are better, optimal ways to drill any well. By applying sound drilling engineering analyses, as presented in this textbook, and by treating drilling as a system and using good deductive logic, the drilling engineer can greatly enhance the success of drilling operations.

### Exercises\*

8.1. Derive Eq. 8.19 for  $r_1 > X_3$ .

8.2. Plan a build-and-hold directional well whose surface location on a 640-acre section is 780 ft from the north

line (FNL) and 1,000 ft from the east line (FEL), and whose bottomhole location is 1,250 ft from the south line (FSL) and 2,000 ft FEL. TVD to the target is 10,500 ft. Rate of build should be 1.5°/100 ft. Kick-off depth is 2,450 ft. Your plan should include the following: (1) maximum inclination angle reached, (2) measured depth to the end of the build and to the target, (3) horizontal departure to the end of the build and at TVD's of 5,450, 6,000, and 8,600 ft, and (4) measured depth at TVD's of 5,450, 6,000, and 8,600 ft. *Answer.* (1) Maximum inclination is 25.3°; (2) measured depth at end of build is 4,137 ft, and measured depth at TVD is 11,235 ft; (3) horizontal departures are 3,662; 1020; 1,273; and 2,502 ft, respectively; (4) measured depths are 5,649; 6,258, and 9,134 ft, respectively.

8.3. Derive Eq. 8.20 for  $r_1 < X_3$  and the relationships necessary to calculate (1) measured depth at any TVD and (2) horizontal departure at any TVD or measured depth.

8.4. Plan a build-and-hold trajectory where the kick-off depth is at 2,000 ft, and the target bull's-eye is 5,500 ft from the surface location at a TVD of 8,100 ft. Use a rate of build of 2°/100 ft. Your plan should include the following: (1) maximum inclination angle reached, (2) measured depth to the end of the build and to the target, (3) horizontal departure to the end of the build and at TVD's of 3,100, 5,100, and 7,100 ft, and (4) measured depths at TVD's of 3,100, 5,100, and 7,100 ft.

8.5. Derive the build, hold, and drop relationships (Eq. 8.21) for  $r_1 + r_2 > X_4$  and  $r_1 < X_3$ . Also derive the equations necessary to calculate the measured depth and horizontal departure at any TVD.

8.6. Plan a directional program using a build, hold, and drop trajectory path for which the kick-off depth is 3,100 ft and the maximum required departure is 2,100 ft. Rate of build should be 2°/100 ft, and the rate of drop should be 2°/100 ft. (1) If the TVD is 10,200 ft where the hole returns to vertical, what is the maximum inclination reached? (2) How much casing will you have to purchase for a well with a TVD bottomhole target of 10,200 ft? (3) How long is the hold section? (4) If the drilling plan calls for an intermediate string to be run to a TVD of 8,210 ft, how much casing is needed, and what is the horizontal departure at the casing shoe?

TABLE 8.26—COSTS FOR FIELD DEVELOPMENT

	Case 1	Case 2	Case 3
Cost of Subsea Completion Per Well	\$75 Million	\$7 Million	\$60 Million
Cost of Offshore Platform	\$500 Million	\$15 Million	\$280 Million
Cost of a Drillship, Jackup or Semi-submersible	\$80,000/Day (Semi-submersible or drillship)	\$35,000/Day (Jackup)	\$120,000/Day (Semi-submersible)
Cost of Drilling Rig and Full Support On Fixed Platform	\$40,000/Day	\$30,000/Day	\$80,000/Day
Special Considerations	None	Can drill only 4 months of year because of environmental considerations	None

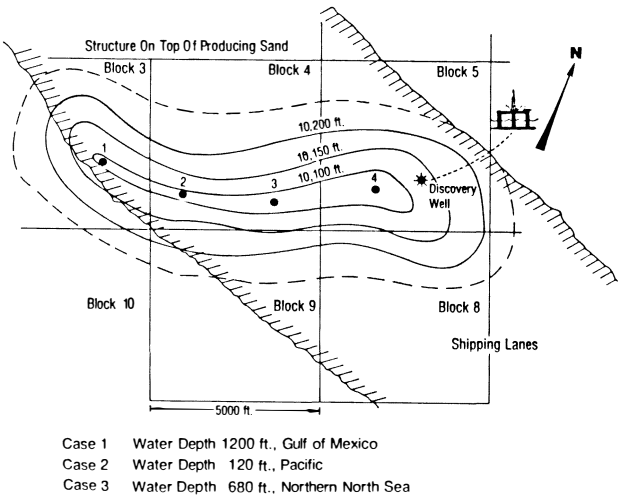


Fig. 8.161—Plot of offshore discovery.

- 8.7. Derive the build, hold, and drop relationships (Eq. 8.22)  $r_1 + r_2 < X_4$  and  $r_1 < X_3$ . Also derive the equations necessary to calculate the measured depth and horizontal departure.
- 8.8. Plan a directional well using a build, hold, and drop trajectory for which the horizontal departure to the target is 9,010 ft and the TVD to the top of the target is 14,100 ft. The rate of build and drop is  $2^\circ/100$  ft. (1) What should be the kick-off depth if the maximum possible angle for hole drop is  $52^\circ$ ? (2) If the intermediate casing is to be run at the end of the build, how much casing is needed, and what are the horizontal departure and the TVD at the casing shoe? (3) Where should the drop begin (TVD and measured depth)? (4) What is the horizontal departure at the beginning and at the end of the drop? (5) How much casing is required from surface to a TVD of 14,100 ft?
- 8.9. Write all the equations for a build, hold, drop, and hold (modified “S”) using Eqs. 8.21 and 8.22. Derive all the relationships to calculate horizontal departures, measured depths, and inclination angle.
- 8.10. Plan a modified “S” trajectory where the target must intersected at a constant inclination of  $20^\circ$ . Kick-off depth is 1,500 ft. Rate of build and drop is  $2^\circ/100$  ft. The desired horizontal departure is 3,100 ft from the surface location at a TVD of 9,075 ft. (1) What is the maximum inclination reached? (2) How much casing is

- needed to go from surface to the end of the build-and-hold section? (3) How much casing is needed from surface to a TVD of 9,075 ft? (4) If the producing interval is logged between 9,355 and 9,420 ft (MD), what are the TVD and the horizontal departure at the top and bottom of the pay?
- 8.11. Repeat Problem 8.10 with a rate of build and drop of  $1^\circ/100$  ft.
- 8.12. An offshore discovery has been made under an active shipping lane (see Fig. 8.161). Further seismic work has defined the anticlinal structure as being almost completely under the shipping lane. (You cannot locate any drilling structure within the shipping lane.) Reservoir analysis dictates drilling the structure with the four bottomhole locations indicated on the plot. Your company owns Blocks 3, 4, and 5. You have permission to drill anywhere outside the shipping lane from Blocks 3, 5, 8, and 10. It is your assignment to determine the best economics to develop this field. (Note: This problem will be referred to in later problems.)

The first part of the study is to determine the economics of different approaches to drilling Wells 1, 2, 3, and 4—i.e., whether to use a semisubmersible and drill some or all of the wells for subsea completions or to set a platform. Table 8.26 gives the various conditions for Cases 1, 2, and 3.

Fig. 8.162 summarizes the results from the discovery well. Determine whether you would set a platform to drill all the wells, set a platform to drill some of the wells and drill the others with a movable drilling vessel and complete them subsea, or drill all the wells with a movable drilling vessel and complete them subsea. You must do the following:

- A. Determine the surface location for each well.
- B. Calculate the trajectory for each well.
- C. Calculate the casing costs on the basis of setting 20-in. surface casing to 3,500 ft (TVD), intermediate  $13\frac{3}{8}$ -in. casing to cover the build section and  $9\frac{5}{8}$ -in. casing to cover the overpressured interval (8,500 ft TVD), and 7-in. casing to total depth. Below is the cost of the casing.

Size (in.)	Cost (\$/ft)
20	105.24
$13\frac{3}{8}$	74.58
$9\frac{5}{8}$	44.73
7	28.82

D. Using the information in Table 8.27, determine the time needed to drill each well for each case. (Maximum inclination is 70° for Case 1, 80° for Case 2, and 60° for Case 3.)

8.13. Replan Problem 8.4 using a target direction of N25E and 18° left of N25E as the amount of lead necessary to offset the expected bit walk. The direction of N7E should be held constant until an inclination of 10° is reached. At what constant rate of right-hand walk will the lead of 18° hit within a 50-ft radius of the target bull's-eye? How much extra casing will be needed because of the bit walk? *Answer.* For Problem 8.4, at 8,085.27 ft, measured depth is 10,423.16 ft; for Problem 8.13, at 8,085.27 ft, measured depth is 10,491 ft.

8.14. Given the trajectory data from an offset well, determine the amount of lead necessary to drill a well to intersect two targets with the following target requirements. How much casing must you buy?

Target 1: Direction of bull's-eye: S75E  
Horizontal departure: 3,570 ft  
TVD to top of target: 10,400 ft  
Radius of target: 150 ft

Target 2: Direction of bull's-eye: S70E  
Horizontal departure: 4,250 ft  
TVD to top of second target: 10,900 ft  
Radius of target: 100 ft

Hint: Plot the offset data in Table 8.28 to determine the total amount of bit walk. Divide the total bit walk by two to estimate the amount of lead to account for the right-hand walk.

8.15. Derive the angle-averaging Eqs. 8.24 through 8.26.

8.16. Using Table 8.29, determine the extra amount of casing you must buy because of bit walk for the trajectories you determined for Problem 12. Use a target radius of 150 ft. How much lead must you have to hit each target?

8.17. Derive the tangential method Eqs. 8.27 through 8.29.

8.18. Determine the trajectory of the well using the tangential method. Did the wellbore intersect the target? Include TVD, north/south and east/west coordinates, the total coordinates, total departure, and the departure angle. The target is a circle with a radius of 600 ft. The top of the target is 7,800 ft TVD at a direction of N13E. See Table 8.30 for survey data.

8.19. Using the angle-averaging method, determine the trajectory of the well on the basis of the surveying data presented in Problem 8.18. How much difference is there in TVD and horizontal departure between the angle-averaging method and the tangential method at total depth? *Answer.* The difference in TVD is +19.03 ft; the difference in horizontal departure is -39 ft.

8.20. Set up a step-by-step procedure using the minimum-curvature method to calculate the TVD, the north/south and east/west coordinates, the total coordinates, the total departures, and the departure angle.

8.21. Determine the trajectory of the well, using the survey data presented in Problem 8.18 and the format derived in Problem 8.20 for the minimum-curvature method. How do the results compare with those of the tangential and angle-averaging methods?

TABLE 8.27—DATA FOR PROBLEM 8.12D

Case 1 Time to Drill =  $[0.016(D_M) - 91](\text{Maximum Inclination Factor})$   
Case 2 Time to Drill =  $[0.013(D_M) - 95](\text{Maximum Inclination Factor})$   
Case 3 Time to Drill =  $[0.015(D_M) - 42](\text{Maximum Inclination Factor})$

Inclination	Maximum Inclination Factor		
	Case 1	Case 2	Case 3
0°-10°	0.9	0.9	0.9
10°-24°	1.0	1.0	1.0
24°-48°	1.3	1.2	1.5
48°-60°	1.5	1.7	2.0
60°-80°	2.0	2.5	—

Sea Floor	
0 ft.	Unconsolidated Tertiary Sands and Shales +300 ft/hr to 60 ft/hr
3550 ft.	Shales and Siltstones +100 ft/hr to 30 ft/hr
6220 ft.	Overpressured Shales and Thin Sandstones 60 to 10 ft/hr
8450 ft.	Normally Pressured Sandstones, Limestones and Shales 30 ft/hr to 10 ft/hr
10,130 ft.	Massive Sandstone With Gas In Top 60 ft. Oil in Next 120 ft. -0.1 Water Contact at 10,310 ft. - +100 ft/hr
Top of Pay	
Days to Drill Discovery Well	Case 1 84 days Case 2 37 days Case 3 110 days

The Maximum Inclination for the Discovery Well in Each Case is 22°

Fig. 8.162—Discovery well information.

8.22. Derive the balanced tangential method from the minimum-curvature method (hint: assume  $L_t = 1.0$ ). Calculate the survey data from Problem 8.18 and determine the trajectory of the well. Is the balanced tangential method comparable with the other methods?

8.23. Using the survey data from two wells drilled from an offshore platform, determine how far apart the wellbores are at their closest point. The survey data are found in Tables 8.31 and 8.32. The surface location of Well 2 is 6 ft due east of Well 1.

motor from 2,140 ft (3° inclination and N5W) to 2,260 ft. The bent sub causes an angle change of 3.5°/100 ft. Tool-face setting is 20° right of high side. *Answer.* N6.7E.

8.25. Determine the new inclination angle for Problem 8.24.

8.26. Determine the tool-face setting to sidetrack out of a wellbore at 8,520 ft for a motor run of 220 ft. The

TABLE 8.28—OFFSET DATA FOR PROBLEM 8.14

Measured Depth (ft)	Inclination (degrees)	Direction	TVD (ft)	Vertical Section	East-West Coordinate	North-South Coordinate	Dogleg Severity (°/100 ft)
646	3	S60W	646	15.6	-14.6	-8.5	0.0
955	1	S61W	955	25.6	-24.0	-13.8	0.65
1,206	1	S71W	1,206	29.4	-28.0	-15.5	0.06
1,468	0.5	S60W	1,468	32.5	-31.2	-17.0	0.20
1,963	0.25	S16E	1,963	35.6	-32.4	-20.0	0.10
2,429	0.25	N45E	2,429	34.8	-30.4	-20.5	0.09
2,861	0.25	N22W	2,861	33.1	-30.0	-18.6	0.06
2,959	2	S20W	2,958	34.3	-31.9	-18.7	2.23
3,057	2.25	S20W	3,056	37.8	-33.2	-22.1	0.23
3,155	4.75	S15W	3,154	43.4	-35.0	-27.8	2.57
3,253	6.75	S20W	3,252	52.6	-37.9	-37.2	2.10
3,322	7.25	S17W	3,320	60.5	-40.6	-45.1	0.89
3,420	8.5	S25W	3,417	73.4	-45.4	-57.7	1.69
3,518	10.5	S25W	3,514	89.2	-52.3	-72.3	2.04
3,616	12.5	S23W	3,610	108.2	-60.2	-90.2	2.08
3,714	14	S22W	3,705	129.8	-68.8	-110.9	1.54
3,812	15.5	S19W	3,800	153.7	-77.5	-134.3	1.72
3,910	17.5	S20W	3,894	180.1	-86.8	-160.5	2.06
4,008	20	S19W	3,987	210.0	-97.2	-190.2	2.57
4,157	20	S21W	4,127	258.6	-114.8	-238.1	0.46
4,281	20	S21W	4,243	299.2	-130.0	-277.7	0.0
4,404	19.75	S22W	4,359	339.4	-145.3	-316.6	0.34
4,528	19.25	S23W	4,476	379.3	-161.1	-354.9	0.48
4,649	19.5	S24W	4,590	418.2	-177.1	-391.7	0.33
4,771	19.75	S25W	4,705	458.1	-194.1	-429.0	0.33
4,891	20.75	S27W	4,818	498.8	-212.3	-466.3	1.01
5,018	20.5	S28W	4,937	542.8	-233.0	-506.0	0.33
5,193	20.75	S30W	5,100	603.7	-262.9	-559.9	0.42
5,368	22.25	S31W	5,263	667.4	-295.4	-615.1	0.88
5,461	22	S32W	5,349	702.2	-313.7	-645.0	0.48
5,492	21.5	S31W	5,378	713.6	-319.7	-654.8	1.98
5,592	20.5	S33W	5,471	749.3	-338.7	-685.2	1.23
5,653	21.5	S33W	5,528	771.1	-350.6	-703.5	1.63
5,718	21.25	S33W	5,589	794.7	-363.5	-723.4	0.34
5,781	20	S34W	5,648	816.8	-375.8	-741.9	2.06
5,874	18	S37W	5,736	847.1	-393.4	-766.5	2.39
5,998	17	S35W	5,854	884.3	-415.3	-796.7	0.94
6,181	17.25	S34W	6,029	938.1	-445.8	-841.1	0.20
6,397	17.5	S38W	6,235	1,002.6	-483.7	-893.3	0.56
6,614	18.75	S36W	6,441	1,070.1	-524.4	-947.2	0.64
6,737	18.25	S39W	6,558	1,109.1	-548.1	-978.2	0.87
6,835	17.5	S38W	6,651	1,139.2	-566.8	-1,001.7	0.82
6,933	15.75	S37W	6,745	1,167.3	-583.9	-1,024.0	1.81
7,031	14.5	S37W	6,840	1,192.8	-599.3	-1,044.4	1.27
7,129	13.5	S36W	6,935	1,216.5	-613.4	-1,063.4	1.05
7,227	12	S35W	7,030	1,238.1	-626.0	-1,081.1	1.54
7,325	10.5	S37W	7,126	1,257.3	-637.2	-1,096.5	1.58
7,423	8.75	S36W	7,223	1,273.6	-646.9	-1,109.7	1.79
7,521	7	S37W	7,320	1,287.1	-654.9	-1,120.5	1.79
7,619	6.25	S37W	7,418	1,298.4	-661.7	-1,129.5	0.76
7,717	4.75	S38W	7,515	1,307.8	-667.4	-1,137.0	1.53
7,815	4	S42W	7,613	1,315.2	-672.3	-1,142.7	0.82
7,913	3.25	S43W	7,711	1,321.4	-676.4	-1,147.3	0.77
7,966	2.5	S47W	7,763	1,324.0	-678.3	-1,149.1	1.46
8,965	4	S80W	8,761	1,375.0	-729.0	-1,174.4	0.23
10,605	3	S65W	10,398	1,425.4	-828.3	-1,161.3	0.14



TABLE 8.29—BIT WALK DATA FOR PROBLEM 8.16

Depth (ft) (TVD)	Inclination (degrees)	Case 1 (°/100 ft)	Case 2 (°/100 ft)	Case 3 (°/100 ft)
0- 3,550	0-80	0.1° left	0°	0.1° right
3,550- 6,220	0-10	0.1° right	0.1° right	0.2° right
	10-30	0.2° right	0.2° right	0.4° right
	30-50	0.3° right	0.2° right	0.3° right
	50-80	0.0	0.0	0.0
6,220- 8,450	0-10	0.1° left	0.1° left	0.1° right
	10-30	0.2° left	0.1° left	0.2° right
	30-50	0.0	0.1° left	0.2° right
	50-80	0.0	0.0	0.0
8,450-10,130	0-10	0.1° right	0.2° right	0.2° right
	10-30	0.2° right	0.5° right	1.0° right
	30-50	0.3° right	1.0° right	0.7° right
	50-80	0.1° left	1.4° right	0.0

inclination is 30° and the direction is N60W. It is necessary to be 3° below the original wellbore. How much direction change can be obtained if the dogleg severity is to be kept below 4°/100 ft?

8.27. For a course length of 300 ft and a dogleg severity of 3.0°/100 ft, determine the tool-face setting for a jetting run whose purpose is to obtain maximum allowable drop while changing the original direction from S10E to S30E. The inclination angle before course change is 15°.

8.28. Derive Eq. 8.50 from Eq. 8.41 by making  $\beta=1$ .

8.29. Derive Eq. 8.51 from Eq. 8.45 by making  $\beta=1.0$ .

8.30. Derive Eq. 8.52 from Eq. 8.41 by making  $\beta=1$ .

8.31. Derive Eq. 8.53 from Eqs. 8.41, 8.45, and 8.48.

8.32. Derive Eq. 8.54 from Eq. 8.53.

8.33. An initial lead of 25° left of N33E has not turned right fast enough to hit the target. A motor must be run to correct the trajectory to N42E. At a measured depth of 4,835 ft, the inclination is 42° and the direction is N15E. How many feet must the motor drill to make the correction without losing inclination and maintaining the dogleg severity below 3.0°/100 ft? What should be the tool-face setting? (Assume no correction for reverse torque.)

and at a direction of S79W. You want to drop the inclination back to 7°. The new desired direction is N66W. What is the dogleg severity if this change is made over 250 ft of course length? What should be the tool-face setting to make this change? How much course length would be necessary if the maximum permissible dogleg severity were 3.5°/100 ft? (Assume no correction for reverse torque.) *Answer.* 266 ft of course length.

8.35. Repeat Problems 8.24, 8.25, and 8.26 using the Ouija Board nomograph.

8.36. Repeat Problems 8.33 and 8.34 using the Ragland diagram.

8.37. Derive Eq. 8.55 from Eq. 8.53. Hint:  $\cos \beta = 1 - 2[\sin(\beta/2)]^2$  and  $\cos \Delta\epsilon = 1 - 2[\sin(\Delta\epsilon/2)]^2$ .

8.38. Calculate the total angle change of 11,050 ft of 5.0-in. Grade E 19.5-lbm/ft drillpipe and 1,200 ft of 8-in. drill collars (2 $\frac{1}{16}$ -in. ID) for a bit-generated torque of 650 ft-lbf. Assume the 8-in. motor has the same properties as the 8-in. collars. Use a shear modulus for steel. *Answer.* 181.97°.

8.39. How much reverse torque could be expected for Problem 8.33 if an 8-in. mud motor were used for the trajectory correction? (The expected maximum torque at

the bit is 1,350 ft-lbf.) In what direction should the face be oriented to offset the reverse torque? The drillstring consists of 5-in., 19.5-lbm/ft Grade E drillpipe, 1,000 ft of 5-in. (3-in.-ID), 49.3-lbm/ft heavyweight drillpipe, and twelve 8-in. (2 $\frac{1}{16}$ -in.-ID) drill collars.

8.40. Generate figures similar to Figs. 8.37 and 8.38 for overall angle changes ( $\beta$ ) of 2, 3, and 5° and for inclinations of 0 to 65°.

8.41. Determine the inclination, direction, and tool-face setting (if applicable) for the single-shot compass card pictures in Fig. 8.163. *Answer.* (1) Inclination=20°, direction=S45E, tool face=S34W; (4) Inclination=11°, direction=N22E, tool face=N55E.

8.42. Determine the inclination and direction from the single-shot compass card pictures in Fig. 8.164.

8.43. Determine the inclination and direction from the survey information found in Table 8.33 and from the multishot pictures in Fig. 8.165. The timer is set for 30 seconds between pictures.

8.44. Correct the single-shot survey data (Problem 8.41) for declination at the following locations: (1) McAllen, TX; (2) Marietta, OH; (3) Cut Bank, MT; (4) Long Beach, CA; (5) Evanston, WY. *Answer.* (1) S37E, (2) S28E, (3) none, (4) N30E, and (5) S47E.

8.45. Correct the multishot survey data (Problem 8.42) for declination at the following locations: Houma, LA; Tyler, TX; Rifle, CO; Casper, WY; Parkersburg, WV.

8.46. Determine how many nonmagnetic drill collars are necessary for drilling the directional wells described in Table 8.34. *Answer.* Zone I, one 30-ft drill collar; compass unit 3 to 4 ft below center.

8.47. Multishot gyroscope data were taken on a shallow directional well near Houston, TX. Table 8.35 supplies general information about the well and the start and end times for the gyroscope. Determine the inclinations and directions, and calculate the trajectory of the wellbore. Table 8.36 lists the tool-drift-check data, while Table 8.37 lists the multishot gyroscope data. *Answer.* measured depth=1,800 ft; TVD=1,590.9 ft; latitude=(N)645.4 ft; departure=191.7 ft (E).

8.48. Calculate the inclination and direction and the direction of the low sides of the hole from the readings taken with a rate gyroscope at a north latitude of 30°. The earth spin rate is 15.042°/hr, and north is positive. Earth's gravity is 1.0, and up is positive. Tool roll, or alpha, is measured clockwise positive from the top of the hole. Table 8.38 gives the measured data from the rate gyroscope.

8.49. It is noted that there is a compass error of 5.8° from a magnetic single-shot instrument in a well with an inclination of 66° and a direction of 165°. The measured magnetic strength at the location is 5.8  $\mu$ T and the dip angle is 60°. What are the resultant magnetic strengths of the collars and drillstring at the location of the compass unit? *Answer.* 11.3  $\mu$ T.

8.50. The measured compass error at an inclination of 32° and a direction of N75W is 10.5°; at 44° and N78W, the error is 13.7° (dip angle is 60°). Was the BHA changed between these surveys?

8.51. Determine the maximum survey error for the following directional well assuming a good magnetic survey.

0 to 2,000 ft	vertical
2,000 to 3,000 ft	10° constant build
3,000 to 5,000 ft	35° constant build
5,000 to 8,000 ft	40° average

**TABLE 8.30—SURVEY DATA FOR  
PROBLEM 8.18**

Depth (md)	Inclination (degrees)	Direction	Depth (md)	Inclination (degrees)	Direction
100	1.20	N11.9W	5,300	46.47	N9.1E
200	1.12	N1.8E	5,400	46.62	N9.5E
300	0.56	N28E	5,500	46.95	N9.2E
400	0.52	N26.1E	5,600	47.49	N9.9E
500	0.65	N21.5E	5,700	47.93	N10.2E
600	0.67	N28.9E	5,800	48.55	N9.6E
700	0.58	N23E	5,900	49.18	N10E
800	0.60	N29.1E	6,000	49.69	N10.1E
900	0.50	N21.7E	6,100	49.79	N9.4E
1,000	0.67	N21.7E	6,200	48.95	N10.3E
1,100	0.74	N22.3E	6,300	50.12	N10.7E
1,200	0.58	N5.4E	6,400	49.95	N10.8E
1,300	0.60	N14.5W	6,500	50.35	N10.7E
1,400	0.51	N5.6W	6,600	50.93	N10.5E
1,500	0.45	N23.7W	6,700	50.19	N11.1E
1,600	0.62	N22.4W	6,800	51.87	N11.7E
1,700	1.04	N2.7W	6,900	53.01	N11.4E
1,800	2.39	N0.3E	7,000	53.72	N12.1E
1,900	4.10	N1.6E	7,100	53.47	N12.6E
2,000	5.85	N2.2W	7,200	53.72	N11.8E
2,100	7.44	N1W	7,300	52.62	N12.7E
2,200	9.60	N1.7E	7,400	53.75	N12E
2,300	11.9	N1E	7,500	52.41	N12.5E
2,400	13.86	N2.9E	7,600	52.90	N12.4E
2,500	16.47	N5.8E	7,700	52.44	N12.9E
2,600	19.8	N5E	7,800	51.59	N12.3E
2,700	22.56	N4.2E	7,900	51.74	N12.2E
2,800	24.88	N4E	8,000	50.56	N12.7E
2,900	26.19	N5.6E	8,100	50.65	N12.3E
3,000	29.28	N4.3E	8,200	49.93	N12.6E
3,100	32.52	N2.8E	8,300	50.06	N12.2E
3,200	35.7	N1.3E	8,400	50.42	N14E
3,300	38.64	N1.1E	8,500	50.75	N15.5E
3,400	41.16	N4E	8,600	51.15	N15.3E
3,500	42.75	N4.9E	8,700	51.79	N15.1E
3,600	42.45	N2.4E	8,800	51.72	N15E
3,700	42.43	N2.7E	8,900	52.13	N15E
3,800	42.47	N2.5E	9,000	52.60	N14.4E
3,900	43.10	N2.7E	9,100	52.90	N14.5E
4,000	43.66	N2.9E	9,200	53.02	N13.9E
4,100	44.23	N3.3E	9,300	53.18	N13.4E
4,200	44.73	N3.4E	9,400	53.67	N12.9E
4,300	45.03	N3.4E	9,500	54.09	N12.4E
4,400	45.55	N3.1E	9,600	54.14	N13.1E
4,500	45.92	N2.5E	9,700	53.05	N12.4E
4,600	46.16	N2E	9,800	52.18	N12.1E
4,700	46.55	N1.4E	9,900	51.44	N12.8E
4,800	46.9	N0.6E	10,000	50.84	N12.5E
4,900	47.23	N0.5E	10,100	50.79	N13.1E
5,000	47.41	N0.7E	10,200	50.93	N13.2E
5,100	46.05	N5.8E	10,300	50.94	N13.8E
5,200	46.08	N9.3E	10,400	51.10	N13.5E

TABLE 8.31—SURVEY DATA FOR WELL A—PROBLEM 8.23

Measured Depth (ft)	Inclination (degrees)	Direction	TVD (ft)	Vertical Section	East-West Coordinate	North-South Coordinate	Dogleg Severity (°/100 ft)
360	0.25	S25W	360	-0.3	-0.3	-0.7	0.0
416	0.25	S36W	416	-0.1	-0.6	-0.7	0.75
596	0.25	N3W	596	0.6	-0.8	0.0	0.06
903	1.5	N6E	903	3.9	-0.7	4.7	0.41
1,245	1.25	N52E	1,245	6.5	3.3	11.9	0.32
1,698	0.75	N34W	1,698	11.4	4.5	19.7	0.31
1,966	2.5	N32W	1,966	18.9	0.4	26.1	0.65
2,064	4.25	N30W	2,064	24.5	-2.6	31.0	1.79
2,162	5.25	N44W	2,161	32.6	-7.5	37.5	1.55
2,260	7	N54W	2,259	43.0	-15.4	44.3	2.08
2,358	8.25	N47W	2,356	55.9	-25.4	52.6	1.59
2,456	9.25	N42W	2,453	70.8	-35.9	63.2	1.28
2,554	10.5	N45W	2,549	87.6	-47.4	75.4	1.37
2,652	12	N47W	2,645	106.7	-61.2	88.7	1.58
2,750	14.75	N48W	2,741	129.3	-77.9	104.0	2.82
2,848	17	N47W	2,835	156.0	-97.7	122.1	2.31
2,946	19	N49W	2,928	186.1	-120.2	142.4	2.13
3,044	21	N52W	3,020	219.4	-146.0	163.7	2.29
3,142	22.5	N53W	3,111	255.1	-174.8	185.8	1.57
3,236	24	N52W	3,198	291.7	-204.3	208.4	1.65
3,330	23.75	N52W	3,283	330.0	-234.9	232.3	0.79
3,424	26.5	N50W	3,368	370.2	-266.4	257.9	2.08
3,517	26.75	N48W	3,451	411.7	-297.9	285.2	1.00
3,640	27	N46W	3,561	467.1	-338.6	323.2	0.76
3,734	26.75	N43W	3,645	509.6	-368.3	353.5	1.46
3,829	27.5	N41W	3,729	552.9	-397.3	385.6	1.24
3,927	26.5	N42W	3,817	597.4	-426.8	419.0	1.12
4,025	26.5	N44W	3,904	641.1	-456.6	450.9	0.91
4,123	26.5	N44W	3,992	684.8	-487.0	482.4	0.0
4,221	26.5	N46W	4,080	728.5	-517.9	513.3	0.91
4,319	25.75	N47W	4,168	771.6	-549.2	543.0	0.88
4,449	26.5	N47W	4,284	828.7	-591.1	582.1	0.57
4,663	26.25	N45W	4,476	923.6	-659.5	648.1	0.43
4,914	26.27	N42W	4,701	1,034.6	-735.9	728.7	0.53
5,012	27.25	N44W	4,789	1,078.7	-766.0	760.9	1.36
5,110	25.5	N49W	4,876	1,122.2	-797.6	790.9	2.88
5,208	25.5	N54W	4,965	1,163.9	-830.6	817.2	2.19
5,302	27.5	N57W	5,049	1,204.8	-865.2	840.9	2.56
5,549	27.75	N58W	5,268	1,315.5	-961.8	902.5	0.21
5,736	27.5	N56W	5,434	1,399.6	-1,034.5	949.7	0.51
5,985	27.5	N54W	5,654	1,511.9	-1,128.7	1,015.6	0.37
6,201	27.75	N53W	5,846	1,610.3	-1,209.2	1,075.2	0.24
6,455	26.5	N52W	6,072	1,724.5	-1,301.1	1,145.7	0.52
6,639	26.5	N50W	6,236	1,805.7	-1,364.9	1,197.4	0.48
6,734	26	N51W	6,322	1,847.4	-1,397.3	1,224.1	0.70
6,853	24.75	N51W	6,429	1,897.8	-1,436.9	1,256.2	1.05
6,944	24.25	N52W	6,512	1,935.1	-1,466.4	1,279.7	0.71
7,038	23	N50W	6,598	1,972.4	-1,495.7	1,303.4	1.58
7,130	21	N52W	6,683	2,006.5	-1,522.5	1,325.1	2.32
7,254	16.75	N51W	6,801	2,046.2	-1,553.9	1,350.1	3.44
7,379	13.25	N49W	6,922	2,078.3	-1,578.7	1,370.8	2.83
7,505	10	N49W	7,045	2,103.5	-1,597.8	1,387.5	2.58
7,630	7	N49W	7,169	2,121.9	-1,611.8	1,399.6	2.40
7,752	5.75	N48W	7,290	2,135.3	-1,621.9	1,408.6	1.03
7,967	4	N43W	7,504	2,153.6	-1,635.0	1,421.4	0.84
8,121	3	N39W	7,658	2,163.0	-1,641.1	1,428.5	0.67
8,439	3	N16W	7,975	2,179.0	-1,648.8	1,443.3	0.38
8,502	4.25	N19W	8,038	2,182.6	-1,650.0	1,447.1	2.00
8,596	5.5	N21W	8,132	2,190.0	-1,652.7	1,454.6	1.34
8,810	5.75	N15W	8,345	2,209.1	-1,659.2	1,474.5	0.30
8,967	4.75	N15W	8,501	2,221.8	-1,662.9	1,488.4	0.63
9,283	3.75	N13W	8,816	2,242.3	-1,668.6	1,511.1	0.32
10,835	3.75	N13W	10,365	2,330.4	-1,691.4	1,610.0	0.0

TABLE 8.32—SURVEY DATA FOR WELL B—PROBLEM 8.23

Measured Depth (ft)	Inclination (degrees)	Direction	TVD (ft)	Vertical Section	East-West Coordinate	North-South Coordinate	Dogleg Severity (°/100 ft)
454	0.25	N15W	454	0.9	-0.3	1.0	0.0
515	1.75	N32W	515	1.9	-0.7	1.9	2.47
606	2.75	N2W	606	5.1	-1.7	5.3	1.66
728	2.5	N34W	728	10.2	-3.5	10.7	1.20
910	2.75	N25W	910	18.3	-7.6	17.9	0.26
1,093	2.5	N30W	1,092	26.3	-11.4	25.4	0.18
1,310	1.5	N22W	1,309	33.6	-14.7	32.2	0.48
1,685	0.75	N30W	1,684	40.6	-18.0	38.8	0.20
1,787	0.5	N80W	1,786	41.7	-18.9	39.4	0.56
1,853	1.25	N55W	1,852	42.6	-19.8	39.8	1.25
1,951	2.5	N62W	1,950	45.7	-22.6	41.5	1.29
2,049	4.25	N69W	2,048	51.0	-27.8	43.9	1.83
2,147	6.25	N64W	2,146	59.3	-36.0	47.4	2.09
2,245	8.5	N58W	2,243	71.2	-47.0	53.5	2.42
2,343	10.5	N62W	2,339	86.7	-61.0	61.6	2.15
2,441	11.5	N57W	2,436	104.6	-77.1	71.1	1.41
2,539	13.25	N55W	2,531	125.1	-94.6	82.9	1.84
2,637	15.5	N55W	2,626	148.9	-114.5	96.8	2.29
2,735	17.5	N58W	2,720	176.0	-137.7	112.2	2.22
2,833	19.75	N59W	2,813	206.1	-164.4	128.5	2.32
2,931	21	N58W	2,905	239.0	-193.5	146.4	1.32
3,029	23.5	N59W	2,996	274.8	-225.1	165.8	2.58
3,089	24.75	N61W	3,050	298.2	-246.4	178.0	2.49
3,187	26.25	N61W	3,139	338.3	-283.3	198.5	1.53
3,286	26.5	N61W	3,228	380.2	-321.7	219.8	0.23
3,410	27.25	N60W	3,338	433.6	-370.5	247.4	0.70
3,533	28.25	N60W	3,447	488.4	-420.1	276.0	0.81
3,660	28.25	N55W	3,559	546.6	-470.8	308.3	1.86
3,782	29	N53W	3,666	604.0	-518.1	342.7	1.00
3,904	30	N52W	3,772	663.2	-565.7	379.3	0.91
4,028	30	N52W	3,880	724.4	-614.6	417.4	0.0
4,215	29.5	N50W	4,042	816.3	-686.7	475.8	0.59
4,401	29.5	N50W	4,204	907.2	-756.9	534.7	0.0
4,557	29.75	N50W	4,339	983.8	-815.9	584.3	0.14
4,746	29.5	N50W	4,504	1,076.5	-887.5	644.3	0.12
4,866	30	N50W	4,608	1,135.6	-933.1	682.6	0.41
4,960	29	N50W	4,690	1,181.6	-968.6	712.3	1.06
5,058	28.5	N46W	4,776	1,228.5	-1,003.6	743.9	2.03
5,156	28	N42W	4,862	1,274.9	-1,035.8	777.3	2.00
5,254	27.75	N39W	4,949	1,320.7	-1,065.6	812.1	1.45
5,352	27.25	N36W	5,035	1,365.7	-1,093.1	848.0	1.50
5,450	28.25	N33W	5,122	1,410.8	-1,119.0	885.6	1.75
5,548	27.75	N33W	5,209	1,456.1	-1,144.0	924.2	0.50
5,686	27.25	N33W	5,331	1,518.9	-1,178.8	977.6	0.35
5,904	27.75	N31W	5,525	1,617.7	-1,232.1	1,063.0	0.48
5,996	26.75	N31W	5,606	1,658.9	-1,253.8	1,099.1	1.08
6,141	26.5	N31W	5,736	1,722.5	-1,287.3	1,154.8	0.15
6,360	25.75	N28W	5,933	1,816.2	-1,334.7	1,238.7	0.69
6,577	25.25	N26W	6,128	1,906.0	-1,377.2	1,322.0	0.46
6,764	24.25	N24W	6,298	1,980.5	-1,410.2	1,392.9	0.70
6,862	23	N25W	6,388	2,017.7	-1,426.5	1,428.7	1.34
6,960	20.25	N23W	6,479	2,051.9	-1,441.2	1,461.6	2.90
7,058	18.75	N24W	6,571	2,082.7	-1,454.3	1,491.6	1.57
7,156	16.25	N24W	6,665	2,110.6	-1,466.2	1,518.6	2.55
7,254	15.25	N24W	6,759	2,135.7	-1,477.1	1,542.9	1.01
7,352	13.5	N21W	6,854	2,158.5	-1,486.4	1,565.4	1.94
7,450	11.75	N22W	6,950	2,178.5	-1,494.2	1,585.3	1.80
7,548	10.75	N19W	7,046	2,196.1	-1,500.9	1,603.2	1.18
7,646	9.25	N16W	7,142	2,211.5	-1,506.0	1,619.4	1.62
7,744	7.75	N15W	7,239	2,224.3	-1,509.9	1,633.4	1.54
7,842	6.5	N14W	7,337	2,235.0	-1,513.0	1,645.1	1.28
7,940	5.25	N13W	7,434	2,243.7	-1,515.3	1,654.9	1.28
8,322	3	N10W	7,815	2,267.2	-1,520.8	1,681.8	0.59
8,515	2.5	N5W	8,008	2,274.7	-1,522.0	1,691.0	0.28
9,288	1	N19E	8,781	2,289.9	-1,519.1	1,714.4	0.21
9,328	1	N19E	8,821	2,290.2	-1,518.9	1,715.1	0.0
10,325	2.5	N64E	9,817	2,293.1	-1,498.7	1,737.9	0.19
10,385	2.5	N64E	9,877	2,292.4	-1,496.3	1,739.0	0.0
11,105	2.5	N64E	10,596	2,283.2	-1,468.1	1,752.8	0.0

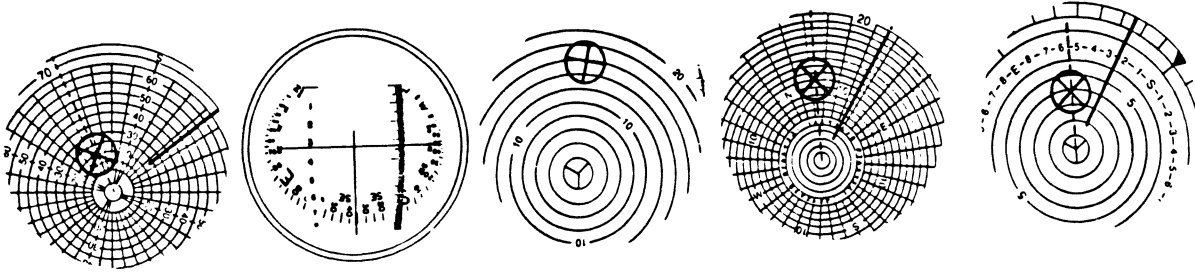


Fig. 8.163—Single-shot compass card pictures for Problem 8.41.

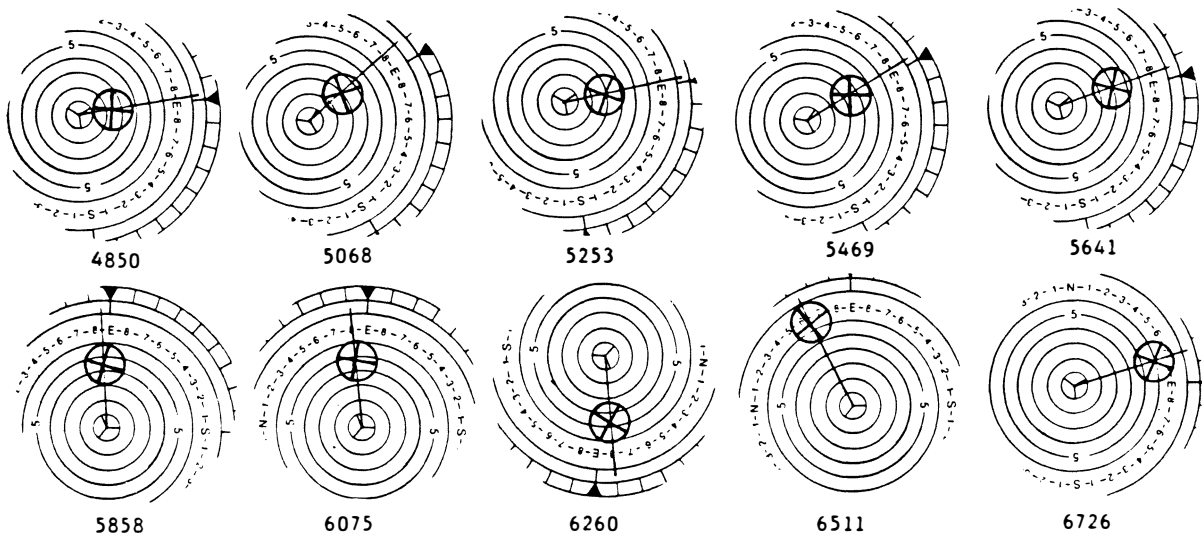


Fig. 8.164—Single-shot compass card pictures for Problem 8.42.

TABLE 8.33—SURVEY DATA  
FOR PROBLEM 8.43

Survey Time	Depth (ft)	Comments
12:45:00	0	Clock off
12:45:20	0	Clock on
12:45:25	0	Tool Dropped
12:45:55		
12:46:25		
12:53:25	8,914	On Bottom
12:53:55	8,914	Wait
12:54:25	8,884	Pull Stand 1/3 Out
12:54:55	8,854	Pull Stand 2/3 Out
12:55:25		Pull Stand Out
12:55:55	8,824	Wait
12:56:25	8,794	Pull Stand 1/3 Out
12:56:55	8,764	Pull Stand 2/3 Out
12:57:25		Pull Stand Out
12:57:55	8,734	Wait
12:58:25	8,704	Pull Stand 1/3 Out
12:58:55	8,674	Pull Stand 2/3 Out
12:59:25		Pull Stand Out
12:59:55	8,644	Wait
12:60:25	8,614	Pull Stand 1/3 Out
12:60:55	8,584	Pull Stand 2/3 Out
12:61:25		Pull Stand Out
12:61:55	8,554	Wait
12:62:25	8,554	Wait
12:62:55	8,524	Pull Stand 1/3 Out
12:53:25	8,914	On Bottom

TABLE 8.34—DIRECTIONAL WELL DATA  
FOR PROBLEM 8.46

Direction of Well	Maximum Inclination	Location
N60E	32°	Corpus Christi, TX
338°	62°	Long Beach, CA
25°	48°	North Sea
S25W	35°	North Slope, AK
N65W	70°	Boss Strait, Australia

8.52. Determine the probable survey error for the survey data of Problem 8.47. *Answer.* For a good gyroscope, 7.7 ft; for a poor gyroscope, 38.6 ft.

8.53. What is the probable survey error for Wells A and B (Problem 8.23), assuming Wells A and B were surveyed with a magnetic multishot?

8.54. You are drilling a directional well in a hot geothermal area where the heat makes turbines and positive displacement motors impractical to run. The kick-off depth is 1,650 ft and the hole size is 12 1/4 in. Design a kick-off program using an open-hole whipstock where the initial inclination is 2.5° and the direction is S45E. The acceptable dogleg severity is 4°/100 ft. In what direction should the toe of the whipstock be pointed to start the bit toward N75W? Can the orientation be achieved in one run? What is the final inclination? Write up a whipstock program for the drilling foreman.

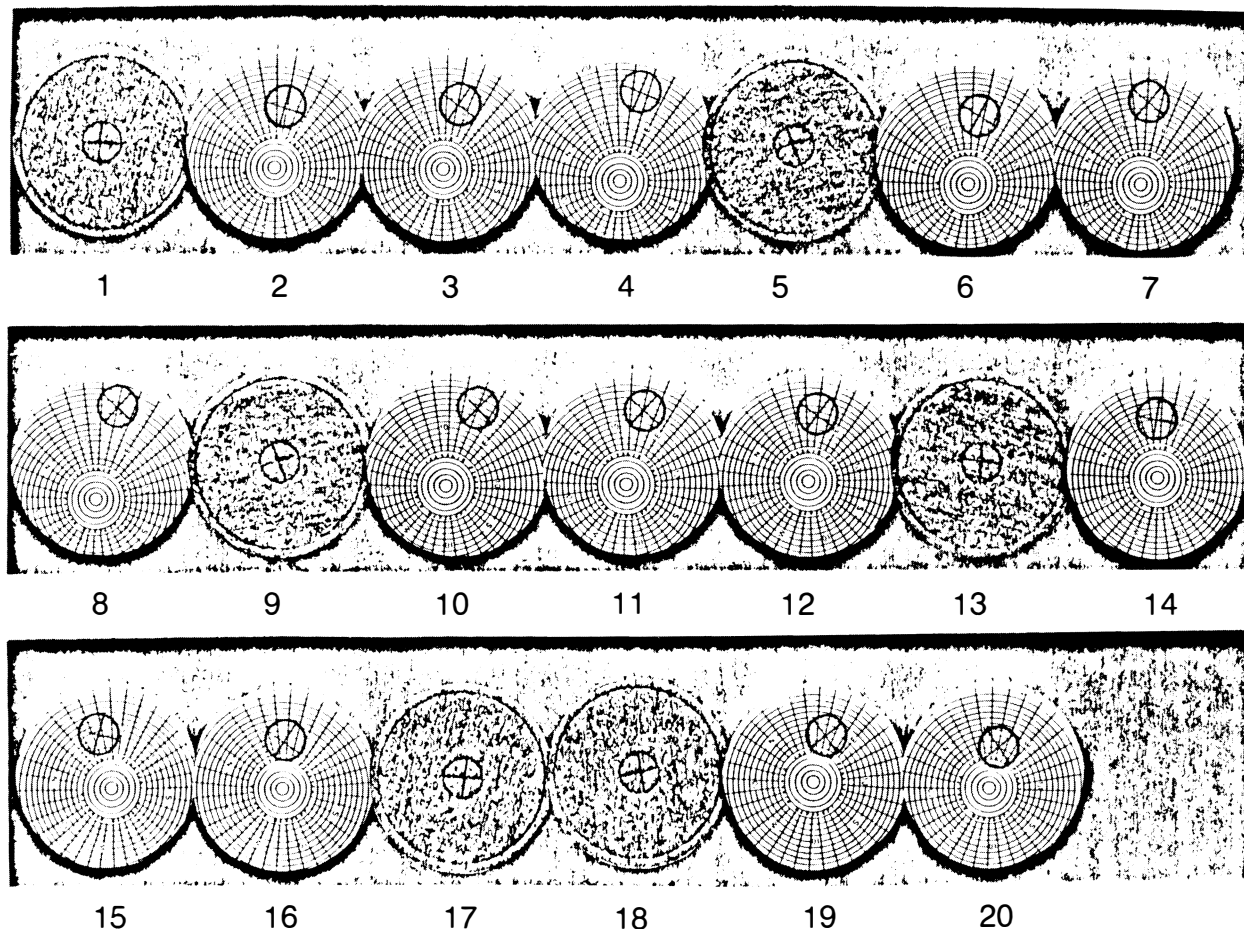


Fig. 8.165—Multishot picture for Problem 8.43.

TABLE 8.35—GENERAL DATA FOR THE WELL IN PROBLEM 8.47

True north azimuth is 197° (SD)				
The index north azimuth is 277° (IS)				
Gyro was started at 13-00				
Gyro ended at 129-00				
Gyro Start: 13-00	End: 129-00	Start: 277.00	End: 297.7	Corr: 20.7
Film Orient: 10-20	128-20	277.40	297.6	20.2
Case Orient: 0-0	127-00	277.80	297.5	19.7

8.55. You have been assigned to sidetrack out of Well B (Problem 8.23) at a measured depth of 5,000 ft and to head in a direction of S60W. The casing size is 10¾ in. The weight is 51 lbm/ft. The cement-bond log shows poor bonding from 4,800 to 3,200 ft. Above 3,200 ft, the bond log looks good. The formation from 3,600 to 6,100 ft is gumbo shale. Choose the best method for sidetracking the wellbore, and give the step-by-step procedure for the sidetracking operation.

8.56. Design a jetting program for kicking off in a 12¼-in. hole. The target direction is S72E; the horizontal departure is 8,500 ft; the TVD is 10,450 ft. Jetting information indicates that 250 hhp is necessary to jet a pocket for a 12¼-in. hole. The rig has a 4.5-in. FH, 16.60 lbm/ft drillpipe, and 7.75-in.-OD (2¼-in.-ID) drill collars. Both pumps are National 9-P-100 with 6- and 5½-in. liners and a 9¼-in. stroke length. Mud weight should be 9.8 lbm/gal. These are sands that can be jetted at 1,050 to 1,160 ft; 1,425 to 1,500 ft; 1,630 to 1,850 ft; and 2,010 to 2,090 ft. Plan the trajectory, hydraulics program, type of bit, jetting program, and BHA's.

TABLE 8.36—TOOL DRIFT CHECK FOR PROBLEM 8.47

Drift Check Number	Depth	Time	Gyro Azimuth	Inclination	Hole Direction
1	Case Surface	0-00	277.8		
		5-40	278.7	1°15'	171
2	25	17-40	60.5		
		21-20	60.8	25'	127
3	225	30-40	220.9		
		34-00	221.1	21'	102
4	475	44-20	60.0		
		49-40	60.9	8°05'	89
5	850	60-40	98.1		
		64-4	98.9	25°50'	102
6	1200	73-00	68.6		
		77-40	69.8	36°35'	100
7	1600	87-20	92.6		
		92-00	93.4	38°40'	118
8	1700	99-00	107.3		
		103-40	108.0	37°55'	131
9	500	113-40	91.2		
		117-40	91.8	9°30'	102
10	Case Surface	123-40	297.4		
		127-00	297.5	45'	58

**TABLE 8.37—MULTISHOT GYRO DATA  
FOR PROBLEM 8.47**

Corrected Time	Measured Depth	Observed Inclination		Observed Hole Azimuth	Gyro Azimuth
		Degrees	Minutes		
Centers					
3-20	(1)		10	97	350.0
4-20	(2)		05	88	56.9
5-00	(3)		05	99	119.9
6-00	(4)		05	106	178.7
6-40	(5)		10	98	238.0
7-40	(6)		10	97	292.5
Data					
17-40	25		25	127	60.5
22-00	50		25	132	24.8
23-40	75		25	140	344.1
25-20	100		20	136	332.5
26-40	125		20	135	326.0
27-40	150		25	127	312.2
29-00	175		15	128	271.5
30-00	200		20	124	247.8
30-40	225		20	102	220.9
35-00	250		25	101	187.4
36-00	275		05	92	147.3
37-20	300		07	76	114.8
38-20	325		05	158	108.0
39-20	350		30	138	100.8
40-40	375	1	40	108	96.5
42-00	400	3	20	106	78.7
43-00	425	5		96	63.4
43-40	450	6	30	92	58.0
44-20	475	8	05	89	60.0
51-20	500	9	20	90	74.5
52-40	550	12	25	94	93.1
53-40	600	14	25	93	89.8
55-20	650	17	30	92	84.7
56-40	700	20	15	94	92.5
58-00	750	22	35	94	91.2
59-40	800	24	20	99	97.0
60-40	850	25	50	102	98.1
65-40	900	27	30	100	87.6
67-00	950	29		96	98.5
68-00	1000	30	55	95	78.0
69-20	1050	32	30	98	89.0
70-20	1100	32	30	103	104.2
72-20	1150	34	25	102	92.6
73-00	1200	36	35	100	68.6
79-00	1250	38	15	98	65.9
80-40	1300	39	50	97	79.3
81-40	1350	42	05	98	77.9
83-20	1400	43		102	80.0
84-20	1450	43	10	106	75.1
85-40	1500	40	55	111	103.1
86-40	1550	36		117	97.2
87-20	1600	38	40	118	92.6
93-00	1650	38	15	124	93.3
94-20	1700	37	55	130	108.0
95-40	1750	39	10	132	99.3
97-40	1800	40	40	130	99.8
99-00	1700	37	55	131	107.3
106-00	1400	43		105	57.9
108-40	1100	32	25	110	79.9
111-40	800	34	20	109	118.4
113-40	500	9	30	102	91.2
120-00	200		20	142	69.6

8.57. If a 17½-in. bit requires 5,325 ft-lbf torque to drill at 25 ft/hr, what is the required pressure drop across a three-stage half-lobe with 62-in. rotor pitch, 1.125-in. eccentricity, and 4.555-in. diameter? *Answer.* 395 psi.

8.58. You are drilling at 3,250 ft with a 12-in. positive-displacement motor. The drillstring and the BHA consist of the following:

- (1) 2,890 ft of 5½-in., 24.7-lbm/ft drillpipe,
- (2) 360 ft of 9.5×3.125-in. drill collars, and
- (3) 17½ Series 1-1-1 bit with two 1½-in. jets and one 1½-in. jet.

You have two pumps that are capable of pumping up to 1,250 gal/min. On bottom with 25,000-lbf WOB, the standpipe pressure is 2,240 psi and the pump rate is 948 gal/min. At 15,000-lbf WOB, the standpipe pressure is 2,040 psi, and the pump rate is 1,040 gal/min. With the bit off bottom and pumping 1,150 gal/min, the standpipe pressure is 1,840 psi.

What are the bit speeds at 25,000 lbf, at 15,000 lbf, and off bottom for mud weights of 9.5 and 13.5 lbm/gal? The plastic viscosity is 15 cp and the yield point is 10 lbm/100 sq ft.

8.59. What is the maximum torque of a multilobe motor with three teeth on the rotor and a stator diameter of 6.25 in.? The stator pitch is 11 in., and the pressure drop across the motor is 235 psi. *Answer.* 2,484 ft-lbf.

8.60. Compare the theoretical motor torque and bit speed of ¼- and ⅝-lobe PDM's.

8.61. Design a positive-displacement motor to meet the following specifications.

Length of motor: 16 to 18 ft.

Hole size: 12¼ to 17½ in.

Power range: 50 to 100 hp.

Maximum differential pressure: 500 psi.

Consider the following:

A. Is it a half-lobe or a multilobe motor? If multilobe, what kind?

B. What are the exact length, diameter, and pitch of the rotor?

C. What is the bit speed as a function of flow rate?

D. What is the maximum motor torque?

8.62. You have just completed drilling the Whale No. 1 to 15,840 ft. This is the first well in a total of 10 to be drilled from a man-made island in the Beaufort Sea. You are the drilling engineer in charge of optimizing the drilling program. While you are planning the second well, a vendor tries to persuade you to drill the second well—from surface to total depth—using a positive-displacement mud motor. Determine whether this would be economical by analyzing the data from this well and using the concepts previously developed. Analyze only the actual drilling data; ignore the intervals cored. The following information is available: round-trip time ( $t_R$ ) is 1.1 times depth, and rig cost is \$47,000/day.

Three PDM types are given along with the corresponding ratings. This information is provided as a possible solution, but it may be wise to analyze other types of PDM's and their corresponding performances. The choice of bits is not limited to those previously used. Table 8.39 lists the available data, and Table 8.40 provides information on the wellbore location.

8.63. What are the torque, power, pressure drop, and bit speed of a 7-in., 200-stage turbine operating at 300, 350, and 450 gal/min for a mud weight of 9.0 and 16 lbm/gal?

TABLE 8.38—SAMPLE DATA FOR PROBLEM 8.48

Station	Ay	Ax	Gy	Gx	Az	Inclination	Alpha
1	0.01543	0.01543	13.14122	0.11446	45	1.25	315
2	0.02072	0.01739	13.12538	-1.06336	45.26	1.55	319.99
3	0.02019	0.02406	13.12611	1.31285	45	1.80	310
4	0.02871	0.02678	13.22877	-0.28081	45.11	2.25	316.99
5	0.02745	0.03390	13.16444	1.53068	45.35	2.50	309
6	0.03675	0.03084	13.23515	-1.02337	45.5	2.75	320
7	0.03701	0.03701	13.29530	0.11037	45.7	3.00	315
8	0.04343	0.03644	13.28324	-0.97261	45.45	3.25	320
9	0.03924	0.04677	13.26710	1.40603	45.3	3.50	310
10	0.04783	0.04460	13.35932	-0.25742	45.55	3.75	317
11	0.04499	0.05556	13.29692	1.58048	45.8	4.10	309
12	0.05810	0.04875	13.37359	-1.00045	45.95	4.35	320
13	0.05671	0.05671	13.43029	0.15586	46.10	4.60	315
14	0.06610	0.05546	13.42072	-1.02263	46.25	4.95	320
15	0.05882	0.07009	13.42063	1.29363	46.5	5.25	310
16	0.07010	0.06537	13.49879	-0.34312	46.55	5.5	317
17	0.06305	0.07786	13.43055	1.59520	46.4	5.75	309
18	0.07874	0.06607	13.49760	-1.01953	46.55	5.90	320
19	0.07575	0.07575	13.55629	0.22624	46.35	6.15	315
20	0.08473	0.07109	13.53810	-0.97534	46.50	6.35	320

8.64. Design a turbine to drill with 8½-in. bits. The maximum power output is 1,500 rpm, and the pump rate is 400 gal/min (mud weight is 10.0 lbm/gal). You are designing for an overall mechanical efficiency of 0.68% and a hydraulic efficiency of 78%. This turbine should be able to drill with a new type of 8½-in. PDC bit that operates at torques of approximately 300 ft-lbf.

8.65. What are the overall power, torque, and bit speed of a combination 6½-in. PDM (Fig. 8.101A) and a 7-in. turbine (Fig. 8.118A) that has two connected shafts? The pump rate is 330 gal/min; the mud weight is 10.0 lbm/gal.

8.66. Your goal is to drill an 800-ft-thick shale section at a starting depth of 13,600 ft with an 8½-in. natural diamond bit on a 7-in., 180-stage turbodrill in 12-lbm/gal oil mud (PV 25, YV 35). The rig has a 10-P-130 pump, and you are using 5¼-in. liners, 5-in., 19.50-lbm/ft drill-pipe, and a string of 6½×2-in. drill collars. The maximum allowable standpipe pressure is 3,825 psi. Laboratory tests at the research department indicate that the 0.45-sq-ft TFA bit will require about 25,000 lbf of true WOB to attain the torque that corresponds to peak turbine power. It is estimated that the bit will have an effective nozzle area of 0.37 sq in. and that the pump-off area will increase from about 12 to 16 sq in. over the 800-ft interval. The expected penetration rate is only 6 ft/hr and requires 133 hours of drilling time. Your supervisor thinks that a 133-hour diamond/turbine run will be too costly. He asks you to determine whether either of two options will reduce the drilling time to a more cost-effective time of 100 hours or less. Both options are aimed at reducing the parasitic power losses in the circulatory system, thus making available more hhp for the turbine.

Option 1. Dilute the 1,500-bbl mud system to what is believed to be a safe density of 10 lbm/gal (estimated PV 21, YV 32).

Option 2. Rent a string of 7-in. drill collars with a 3-in. bore.

Your preliminary investigation shows that it will cost no less than \$52,400 to dilute and to treat the mud. The

mud volume will increase excessively (to approximately 2,750 bbl), but the 1,450-psi reduction in bottomhole mud column pressure can effect a 20% improvement in penetration rate. Renting the collars will cost \$14,700, including delivery, inspection, and rig time required for picking up and laying down. Other expenses for either option include rig and fuel costs at \$500/hr, turbodrill cost at \$500/hr, and a net bit cost of \$18,000. The estimated round-trip time is 16 hours.

The turbine manufacturer has provided the information about the 180-stage tool found in Table 8.41. What do you recommend?

8.67. A drill-off test is performed with an 8½-in. natural diamond bit at a depth of 18,858 ft. The TFA of the bit is 0.40 sq in. The drilling mud is oil based, has a density of 13.5 lbm/gal, and is being pumped at a rate of 285 gal/min. The rotary table is turning at 100 rpm. At an indicated WOB of 14,000 lbf, the drawworks is locked and a drill-off test is run to measure the bit's pump-off force (see Table 8.42).

A. Did the bit drill off to the pump-off point or was the test stopped prematurely?

B. How much pump-off force is there at the pump-off point?

C. How much bit-pressure drop is there at the pump-off point?

D. What is the pump-off area of the bit?

E. What is the apparent nozzle area of the bit?

F. How much pump-off force is there at 14,000-lbf indicated WOB?

G. What is the true WOB at 14,000-lbf indicated WOB?

H. Estimate the bit-pressure drop at 14,000-lbf indicated WOB if the flow rate is increased to 300 gal/min.

I. Estimate the pump-off force at 14,000-lbf indicated WOB and 300 gal/min.

J. How much weight should be applied to get approximately 10,000-lbf true WOB at 300 gal/min?

8.68. A slack-off test is performed with an 8½-in. natural diamond bit at a depth of 10,680 ft. The TFA of the bit is 0.45 sq in. The drilling mud is water based, has a density of 9.0 lbm/gal, and is being pumped at a rate of 380 gal/min. The rotary table is turning at 75 rpm,



TABLE 8.39—AVAILABLE DATA FOR PROBLEM 8.62

## PDM Type 1

Tool size O.D. (in.)	Recommended Hole Size (in.)	Pump Rate (gal/min)		Bit Speed Range (rpm)	Maximum Differential Pressure (psi)	Maximum Torque (ft/lb)	Horsepower Range	Maximum Efficiency (percent)
		min.	max.					
6¾	7⅞- 9⅞	185	370	90-180	580	2,540	44- 87	70
8	9½-12¼	315	610	75-150	465	4,030	58-115	70
9½	12¼-17½	395	335	90-145	640	6,160	106-170	72
11¼	17½-26	525	1,055	70-140	520	8,850	118-236	73
9½	12¼-17½	1,500	2,400	90-145	44	8,350	79-127	72
11¼	17½-26	2,000	4,000	70-140	36	12,000	88-176	73

## PDM Type 2

Tool size O.D. (in.)	Recommended Hole Size (in.)	Pump Rate (gal/min)		Bit Speed Range (rpm)	Maximum Differential Pressure (psi)	Maximum Torque (ft/lb)	Horsepower Range	Maximum Efficiency (percent)	Length (ft)	Weight (lb)
		min.	max.							
4¾	6 - 7⅞	100	240	245-600	580	585	27- 67	83	20.0	840
6¾	8¾- 9⅞	200	475	205-485	580	1,500	59-108	86	26.6	2,160
8	9½-12¼	245	635	145-380	465	2,090	59-152	88	26.9	2,800
9½	12¼-17½	395	740	195-365	695	3,890	145-271	90	32.8	5,200
11¼	17½-26	525	1055	120-250	465	5,380	123-256	90	32.2	7,300

## PDM Type 3

Tool size O.D. (in.)	Recommended Hole Size (in.)	Pump Rate (gal/min)		Bit Speed Range (rpm)	Maximum Differential Pressure (psi)	Maximum Torque (ft/lb)	Horsepower Range	Maximum Efficiency (percent)	Length (ft)	Weight (lb)
		min.	max.							
6¼	7⅞- 9⅞	170	345	200-510	580	1,015	39- 98	85	23.6	1,770
6¾	8¾- 9⅞	160	395	140-480	465	995	27- 91	85	21.7	1,770
8	9½-12¼	200	475	160-400	465	1,475	46-113	87	23.6	2,430
9½	12¼-17½	240	610	130-340	465	2,280	56-148	90	24.6	3,970
9½	12¼-17½	395	900	140-325	290	2,210	59-137	90	24.6	3,970
11¼	17½-26	290	685	115-290	465	2,990	65-165	89	26.6	5,960

## Data for Whale Number A-1:

Bit Program											
Bit No.	Size (in.)	Type	Bit Cost (\$)	Depth out (ft)	Footage (ft)	Drilling Time (Hours)	WOB (lb)	Bit Speed (rpm)	Flow Rate (gal/min)	Pump Pressure (psi)	Types of Nozzles
1	26.00	1-1-1	9,100	1,600	1,200	29	30,000	120	840	1,900	18-18-18
2	17.50	1-1-1	6,300	1,800	200	3	15,000	80	800	2,300	20-20-20 Drl Cement
3	17.50	1-1-6	6,300	2,280	480	5	15,000	350	700	1,800	20-20-20 PDM
4	17.50	1-1-4	6,300	4,300	2,020	19	45,000	200	1,000	3,400	18-18-18
5	17.50	1-1-4	6,300	6,300	2,000	21	40,000	125	950	3,450	16-18-18
6	12.25	1-1-1	5,700	6,500	200	8	15,000	80	480	2,700	12-12-12 Drl Cement
7	12.25	1-1-4	5,700	7,700	1,200	12	40,000	130	530	3,400	12-12-12
8	12.25	1-1-4	5,700	8,650	950	13	45,000	125	550	3,350	12-12-13
9	12.25	4-3-7	8,000	11,200	2,550	66	45,000	80	550	3,300	13-13-13
10	12.25	5-1-7	8,000	12,250	1,050	48	45,000	80	550	3,470	13-14-14
11	8.5	MC201	9,000	12,300	50	5	25,000	75	275	2,000	TFA = .5 Coring
12	8.5	MC201	9,000	12,350	50	5	25,000	75	275	2,000	TFA = .5 Coring/RR
13	8.5	MC201	9,000	12,400	50	5	25,000	75	275	2,000	TFA = .5 Coring/RR
14	12.25	2-1-5	4,000	12,400	0	15	25,000	80	550	3,470	14-14-14 Reaming
15	12.25	5-1-7	8,000	13,550	1,150	61	45,000	80	560	3,450	14-14-14
16	12.25	5-1-7	8,000	14,330	750	59	45,000	80	560	3,450	14-15-15
17	12.25	5-1-7	8,000	15,000	700	49	45,000	75	570	3,450	15-15-16
18	8.50	1-3-5	4,400	15,150	150	18	35,000	90		3,400	10-11-11 Drl Cement
19	8.50	MC201	9,000	15,200	50	5	35,000	75		2,200	TFA = .5 Coring/RR
20	8.50	MC201	9,000	15,250	50	6	25,000	75		2,200	TFA = .5 Coring/RR
21	8.50	MC201	9,000	15,300	50	10	25,000	75		2,200	TFA = .5 Coring/RR
22	8.50	MC201	9,000	15,350	50	10	25,000	75		2,200	TFA = .5 Coring/RR
23	8.50	MC201	9,000	15,400	50	10	25,000	75		2,200	TFA = .5 Coring/RR
24	8.50	MC201	9,000	15,450	50	10	25,000	75		2,200	TFA = .5 Coring/RR
25	8.50	MC201	9,000	15,500	50	10	25,000	75		2,200	TFA = .5 Coring/RR
26	8.50	MC201	9,000	15,500	50	20	25,000	75	275	2,200	TFA = .5 Coring/RR
27	8.50	5-1-7	4,400	15,840	340	56	35,000	90	310	3,400	10-11-11 11,800 TVD

TABLE 8.39—AVAILABLE DATA FOR PROBLEM 8.62 (cont.)

Bottomhole Assemblies		
17½-in. Intermediate I		
Building Interval 1 (1,800 to 2,280 ft)	Building Interval 2 (2,280 to 4,300 ft)	Building Interval 3 (4,300 to 6,100 ft)
17½ Bit	17½-in. Bit	17½-in. Bit
12 Dynadrill Delta 500 PDM	NW RWB Stab.	NB RWP Stab.
1½° Bent Sub	Shock Sub	Shock Sub
1 Jnt. 8-in. NMDC	1 Jnt. 8-in. NMDC	1 Jnt. 8-in. NMDC
MWD	MWD	MWD
1 Jnt. 8-in. NMDC	1 Jnt. 8-in. NMDC	1 Jnt. 8-in. NMDC
2 Jnt 8-in. DC	3 Jnt. 8-in. DC	3 Jnt. 8-in. DC
3 Jnt 6.5-in. DC	3 Jnt. 6.5-in. DC	3 Jnt. 6.5-in. DC
35 Jnt. 5"-in. HWDP	35 Jnt. 5-in. HWDP	35 Jnt. 5-in. HWDP
Air Wt = 81,400 lb	1 Clamp-on NM Stab. 30 ft above first	1 Clamp-on NM Stab. 30 ft above first
	1 Clamp-on NM Stab. 65 ft above first	1 Clamp-on NM Stab. 40 ft above first
	Air Wt = 93,500 lbm	Air Wt. = 93,500 lbm
12¼-in. Intermediate II		
Holding Interval 1 (6,100-19,950 ft)	8½-in. Production	
12¼-in. Bit	Slight Dropping	
NB RWP Stab.	8½ Bit	
Shock Sub	8½ NB Stab.	
1 Jnt. 8-in. NMDC	1 Jnt. 6½-in. short DC	
MWD	1 Jnt. 8½-in. Stab.	
1 Jnt. 8-in. NMDC	1 Jnt. 6½-in. DC	
Full Gauge Stab.	1 Jnt. 8½-in. Stab.	
3 Jnt. 8-in. DC	5 Jnt. 6½-in. DC	
36 Jnt. 5-in. HWDP	24 Jnt. 5-in. HWDP	
3 Jnt. 6¾-in. DC	Jars	
1 Clamp-on NM Stab	12 Jnts 5-in. HWDP	
15 ft from first	Air Wt. = 73,000 lb	
1 Clamp-on NM Stab.		
45 ft from first		
Air Wt. = 93,500 lb		

## Casing Overview

Depth (ft)	Hole Size (in.)	Casing Program	Geologic Interval
0- 200	26.00	30-in. Conductor	
0- 1,600	17.50	20-in. Surface	Below Permafrost
0- 6,300	12.25	13⅜ Intermediate	Below T-5 Coals
0-15,000	8.50	9⅝ Intermediate	100 ft into Sag River
14,500-15,840		7-in. Prod. Liner	11,800 TVD

## Geology Overview

Formation Marker	TVD Subsea (ft)	Estimated Measured Depth from Kelly Bushing (ft)
Kelly Bushing	- 50	0
Bottom of Permafrost	1,600	1,650
Tertiary-Cretaceous Delta	1,600	1,650
T5 Coals	5,100	6,218
Cretaceous Pro Delta	6,400	8,395
Pebble Shale	8,925	11,991
Kuparck	8,050	12,303
Kingate	8,400	12,780
Sag River/Shublik	11,050	14,942
Ivishate	11,200	15,132
Lisburne	11,600	15,629

## Mud Overview

Interval (ft)	Mud Wt (lb/gal)	PV (lb/100 sq ft)	YV (lb/100 sq ft)
0- 1,800	10	14	20
1,800- 2,280	9.9	14	20
2,280- 4,300	9.7	14	20
4,300- 6,300	9.5	14	20
6,300- 8,650	9.5	10	15
8,650-11,200	9.3	10	15
11,200-12,400	9.6	12	18
12,400-15,000	11.5	16	18
15,000-15,500	10.	12	18
15,500-15,800	9.5	12	18

TABLE 8.40—WELLBORE LOCATION FOR PROBLEM 8.62

Measured Depth (ft)	Inclination (degrees)	Direction	True Vertical Depth (ft)	Vertical Section	East-West	North-South	Dogleg Severity (°/100 ft)
100	0.00	N0.00E	100	0.0	0.0	0.0	0.00
1,000	0.00	N0.00E	1,000	0.0	0.0	0.0	0.00
1,000	0.00	N1.00E	1,800	0.0	0.0	0.0	0.00
1,000	3.00	N1.00E	1,899	2.5	0.0	2.6	0.00
2,000	6.00	N1.00E	1,999	10.1	0.2	10.5	3.00
2,100	9.00	N1.00E	2,098	22.6	0.4	23.5	3.00
2,200	12.00	N1.00E	2,197	40.1	0.7	41.7	3.00
2,250	13.50	N1.00E	2,245	50.7	8.9	52.8	2.99
2,350	15.50	N1.40E	2,342	74.8	1.4	77.8	2.00
2,450	17.50	N1.80E	2,430	102.1	2.2	106.2	2.00
2,550	19.50	N2.20E	2,533	132.8	3.3	137.9	2.00
2,650	21.50	N2.60E	2,627	166.6	4.8	172.9	2.00
2,750	23.50	N3.00E	2,709	203.7	6.7	211.1	2.00
2,850	25.50	N3.40E	2,800	244.0	9.0	252.5	2.00
2,950	27.50	N3.80E	2,899	287.4	11.8	297.0	2.00
3,050	29.50	N4.20E	2,987	333.8	15.1	344.6	2.01
3,150	31.00	N4.50E	3,074	383.0	16.9	394.9	1.51
3,250	33.00	N4.80E	3,159	434.4	23.2	447.3	1.51
3,350	34.00	N5.10E	3,242	487.9	27.9	501.9	1.51
3,450	35.50	N5.40E	3,324	543.7	33.2	558.7	1.51
3,550	37.00	N5.70E	3,405	601.7	38.9	617.5	1.51
3,650	38.50	N6.00E	3,484	661.7	45.1	678.4	1.51
3,750	40.00	N6.30E	3,562	723.8	51.9	741.3	1.51
3,850	41.50	N6.60E	3,637	788.0	59.2	806.2	1.51
3,950	43.00	N6.90E	3,711	854.1	67.1	873.0	1.51
4,050	44.50	N7.20E	3,784	922.2	75.6	941.6	1.51
4,150	46.00	N7.50E	3,854	992.2	84.7	1,012.0	1.51
4,250	46.50	N7.70E	3,923	1,063.2	94.3	1,083.6	0.51
4,350	47.00	N7.90E	3,992	1,135.3	104.1	1,155.8	0.51
4,450	47.50	N8.10E	4,060	1,207.8	114.4	1,228.5	0.51
4,550	48.00	N8.30E	4,127	1,280.9	124.9	1,301.8	0.51
4,650	48.50	N8.50E	4,193	1,354.7	135.8	1,375.6	0.51
4,750	49.00	N8.70E	4,259	1,429.1	147.1	1,449.9	0.51
4,850	49.50	N8.90E	4,325	1,504.0	158.7	1,524.8	0.51
4,950	50.00	N9.10E	4,389	1,579.6	170.6	1,600.2	0.51
5,050	50.50	N9.30E	4,453	1,655.7	182.9	1,676.1	0.51
5,150	51.00	N9.50E	4,516	1,732.5	195.5	1,752.5	0.51
5,250	51.50	N9.70E	4,579	1,809.8	208.5	1,829.4	0.51
5,350	52.00	N9.90E	4,641	1,887.7	221.9	1,906.7	0.51
5,450	52.50	N10.10E	4,702	1,966.1	235.6	1,984.6	0.51
5,550	53.00	N10.30E	4,763	2,045.2	249.7	2,063.0	0.51
5,650	53.50	N10.50E	4,822	2,124.7	264.2	2,141.8	0.52
5,750	54.00	N10.70E	4,882	2,204.9	279.0	2,221.0	0.52
5,850	54.50	N10.90E	4,940	2,285.5	294.2	2,300.7	0.52
5,950	55.00	N11.10E	4,998	2,366.7	309.8	2,380.9	0.52
6,050	55.50	N11.30E	5,055	2,448.5	325.8	2,461.5	0.52
6,100	55.75	N11.40E	5,083	2,489.5	333.9	2,502.0	0.50
6,200	55.55	N11.60E	5,139	2,571.7	350.4	2,582.9	0.25
6,300	55.35	N11.80E	5,196	2,653.7	367.1	2,663.5	0.25
6,400	55.15	N12.00E	5,253	2,735.5	384.0	2,743.9	0.25
6,500	54.95	N12.20E	5,310	2,817.2	401.2	2,824.1	0.25
6,600	54.75	N12.40E	5,368	2,898.6	418.6	2,904.0	0.25
6,700	54.55	N12.60E	5,426	2,979.9	436.3	2,983.6	0.25
6,800	54.35	N12.80E	5,484	3,061.1	454.1	3,063.0	0.25
6,900	54.15	N13.00E	5,542	3,142.0	472.3	3,142.1	0.25
7,000	53.95	N13.20E	5,601	3,222.0	490.6	3,220.9	0.25
7,100	53.75	N13.40E	5,660	3,303.3	509.2	3,299.5	0.25
7,200	53.55	N13.60E	5,719	3,383.7	528.0	3,377.0	0.25
7,300	53.35	N13.80E	5,779	3,463.9	547.0	3,455.9	0.25
7,400	53.15	N14.00E	5,839	3,543.9	566.3	3,533.6	0.25
7,500	52.95	N14.20E	5,899	3,623.7	585.7	3,611.1	0.25
7,600	52.75	N14.40E	5,959	3,703.3	605.4	3,688.4	0.25
7,700	52.55	N14.60E	6,020	3,782.7	625.3	3,765.3	0.25
7,800	52.35	N14.80E	6,081	3,861.9	645.4	3,842.0	0.25
7,900	52.15	N15.00E	6,142	3,941.0	665.8	3,918.4	0.25
8,000	51.95	N15.20E	6,204	4,019.8	686.3	3,994.6	0.25
8,100	51.75	N15.40E	6,265	4,098.4	707.1	4,070.4	0.25
8,200	51.55	N15.60E	6,327	4,176.7	728.0	4,146.0	0.25
8,300	51.35	N15.80E	6,390	4,254.9	749.2	4,221.3	0.25
8,400	51.15	N16.00E	6,452	4,332.9	770.6	4,296.3	0.25
8,500	50.95	N16.20E	6,515	4,410.7	792.1	4,371.0	0.25
8,600	50.75	N16.40E	6,578	4,488.2	813.9	4,445.4	0.25
8,700	50.55	N16.60E	6,642	4,565.5	835.8	4,519.6	0.25

TABLE 8.40—WELLBORE LOCATION FOR PROBLEM 8.62 (cont.)

8,800	50.35	N16.80E	6,705	4,642.6	858.0	4,593.4	0.25
8,900	50.15	N17.00E	6,769	4,719.5	880.4	4,667.0	0.25
9,000	49.95	N17.20E	6,833	4,796.2	902.9	4,740.2	0.25
9,100	49.75	N17.40E	6,898	4,872.6	925.6	4,813.2	0.25
9,200	49.55	N17.60E	6,963	4,948.8	948.5	4,885.9	0.25
9,300	49.35	N17.80E	7,028	5,024.8	971.6	4,958.3	0.25
9,400	49.15	N18.00E	7,093	5,100.5	994.9	5,030.4	0.25
9,500	48.95	N18.20E	7,159	5,176.0	1,018.4	5,102.2	0.25
9,600	48.75	N18.40E	7,224	5,251.3	1,042.0	5,173.7	0.25
9,700	48.55	N18.60E	7,290	5,326.4	1,065.9	5,244.0	0.22
9,800	48.35	N18.80E	7,357	5,401.2	1,089.9	5,315.7	0.22
9,900	48.15	N19.00E	7,423	5,475.7	1,114.0	5,386.3	0.22
10,000	47.95	N19.20E	7,490	5,550.1	1,138.4	5,456.6	0.22
10,100	47.75	N19.40E	7,557	5,624.1	1,162.9	5,526.6	0.22
10,200	47.55	N19.60E	7,625	5,698.0	1,187.5	5,596.2	0.22
10,300	47.35	N19.80E	7,692	5,771.6	1,212.4	5,665.6	0.22
10,400	47.15	N20.00E	7,760	5,844.9	1,237.4	5,734.6	0.22
10,500	46.95	N20.20E	7,828	5,918.0	1,262.5	5,803.4	0.22
10,600	46.75	N20.40E	7,897	5,990.8	1,287.8	5,871.8	0.22
10,700	46.55	N20.60E	7,965	6,063.4	1,313.3	5,939.9	0.22
10,800	46.35	N20.80E	8,034	6,135.8	1,338.9	6,007.7	0.22
10,900	46.15	N21.00E	8,103	6,207.8	1,364.7	6,075.2	0.22
11,000	45.95	N21.20E	8,173	6,279.7	1,390.6	6,142.3	0.22
11,100	45.75	N21.40E	8,242	6,351.2	1,416.7	6,209.2	0.22
11,200	45.55	N21.60E	8,312	6,422.5	1,442.9	6,275.7	0.22
11,300	45.35	N21.80E	8,382	6,493.5	1,469.2	6,341.9	0.22
11,400	45.15	N22.00E	8,453	6,464.3	1,495.7	6,407.8	0.22
11,500	44.95	N22.20E	8,524	6,634.8	1,522.3	6,473.4	0.22
11,600	44.75	N22.40E	8,594	6,705.0	1,549.1	6,438.6	0.22
11,700	44.55	N22.60E	8,666	6,775.0	1,576.0	6,603.6	0.22
11,800	44.35	N22.80E	8,737	6,844.7	1,603.0	6,668.2	0.22
11,900	44.15	N23.00E	8,809	6,914.1	1,630.2	6,732.4	0.22
12,000	43.95	N23.20E	8,880	6,983.3	1,657.4	6,796.4	0.22
12,100	43.75	N23.40E	8,953	7,052.1	1,684.8	6,860.0	0.22
12,200	43.55	N23.60E	9,025	7,120.7	1,712.4	6,923.3	0.22
12,300	43.35	N23.80E	9,097	7,189.1	1,740.0	6,986.3	0.22
12,400	43.15	N24.00E	9,170	7,257.1	1,767.0	7,048.9	0.22
12,500	42.95	N24.20E	9,243	7,324.8	1,795.6	7,111.2	0.22
12,600	42.75	N24.40E	9,317	7,392.3	1,823.6	7,173.2	0.22
12,700	42.55	N24.60E	9,390	7,459.5	1,851.7	7,234.9	0.22
12,800	42.35	N24.80E	9,464	7,526.4	1,879.9	7,296.2	0.22
12,900	42.15	N25.00E	9,538	7,593.0	1,908.2	7,357.2	0.22
13,000	41.95	N25.20E	9,612	7,659.3	1,936.6	7,417.8	0.22
13,100	41.75	N25.40E	9,687	7,725.4	1,965.2	7,478.1	0.22
13,200	41.55	N25.60E	9,762	7,791.1	1,993.8	7,538.1	0.22
13,300	41.35	N25.80E	9,836	7,856.6	2,022.5	7,597.8	0.22
13,400	41.15	N26.00E	9,912	7,921.7	2,051.3	7,657.1	0.22
13,500	40.95	N26.20E	9,987	7,986.6	2,080.2	7,716.0	0.22
13,600	40.75	N26.40E	10,063	8,051.1	2,109.2	7,774.7	0.22
13,700	40.55	N26.60E	10,139	8,115.4	2,138.2	7,833.0	0.22
13,800	40.35	N26.80E	10,215	8,179.4	2,167.4	7,890.9	0.22
13,900	40.15	N27.00E	10,291	8,243.0	2,196.6	7,948.6	0.22
14,000	39.95	N27.20E	10,368	8,306.4	2,225.9	8,005.8	0.22
14,100	39.75	N27.40E	10,444	8,369.5	2,255.3	8,067.8	0.22
14,200	39.55	N27.60E	10,521	8,432.2	2,284.8	8,119.4	0.22
14,300	39.35	N27.80E	10,599	8,494.7	2,314.3	8,175.6	0.22
14,400	39.15	N28.00E	10,676	8,556.8	2,343.9	8,231.5	0.22
14,500	39.95	N28.20E	10,754	8,618.7	2,373.6	8,287.1	0.22
14,600	38.75	N28.40E	10,831	8,680.2	2,403.3	8,342.3	0.22
14,700	38.55	N28.60E	10,910	8,741.4	2,433.1	8,397.2	0.22
14,800	38.35	N28.80E	10,988	8,802.3	2,463.0	8,451.6	0.22
14,900	38.15	N29.00E	11,066	8,862.9	2,492.9	8,506.0	0.22
15,000	37.95	N29.20E	11,145	8,923.2	2,522.9	8,559.8	0.22
15,100	37.75	N29.40E	11,224	8,983.2	2,552.9	8,613.3	0.22
15,132	37.68	N29.46E	11,249	9,002.3	2,562.5	8,630.4	0.00
15,232	37.18	N29.46E	11,329	9,061.7	2,592.4	8,683.3	0.49
15,332	36.68	N29.46E	11,409	9,120.4	2,622.0	8,735.6	0.49
15,432	36.18	N29.46E	11,489	9,178.4	2,651.2	8,787.3	0.49
15,532	35.68	N29.46E	11,570	9,235.7	2,680.0	8,838.4	0.49
15,632	35.18	N29.46E	11,652	9,292.3	2,708.5	8,888.9	0.49
15,732	34.68	N29.46E	11,734	9,348.3	2,736.7	8,938.7	0.49
15,832	34.18	N29.46E	11,816	9,403.5	2,764.5	8,987.9	0.49
15,840	34.14	N29.46E	11,823	9,407.9	2,766.7	8,991.8	0.00

while drilling ahead at 10 ft/hr with 22,000-lbf indicated WOB. The drillstring is raised about 1.0 ft off bottom, and then a slack-off test is run to measure the pump-off force.

WOB Indicator (lbf)	Standpipe Pressure (psi)
0.0	1,265
300	1,250
500	1,250
0.0	1,265
300	1,375
1,000	1,475
1,300	1,575
1,800	1,725
2,000	1,825
3,000	1,925
4,300	1,975
7,300	2,025
10,300	2,065
24,000	2,125

- Locate the pump-off point.
- How much bit-pressure drop is there at the pump-off point?
- How much pump-off force is produced by the bit-pressure drop?
- What is the pump-off area of the bit?
- What is the apparent nozzle area of the bit?
- How much pump-off force is there at 22,000-lbf indicated WOB?
- What is the true WOB at 22,000-lbf indicated WOB?
- An offset bit record shows that, in the same interval under comparable conditions, a radial-flow diamond bit with a pump-off area of 12 sq in. averaged 7 ft/hr, compared with 10 ft/hr with the current bit. Both bits have the same diameter and number of diamonds and typically are 50% salvageable after the entire interval is drilled. It appears that the bit that drills the faster is the better bit. Is this a valid conclusion? *Answer.* (B) 685 psi; (D) 4.0 sq in; (G) 18,650 lbf.

8.69. A slack-off test is performed with an 8½-in. matrix body polycrystalline diamond compact bit run on a 6¾-in. positive-displacement mud motor at a depth of 11,168 ft. The mud is oil based with a density of 7.8 lbm/gal and is being pumped at a rate of 380 gal/min. The indicated WOB is 24,000 lbf, and the standpipe pressure is 1,750 psi. The TFA of the bit was 1.0 sq in. when new and has drilled 493 ft. The mud motor is rated to produce maximum power at 580-psi differential pressure.

WOB Indicator (lbf)	Standpipe Pressure (psi)
0.0	1,175
1,000	1,190
2,500	1,190
4,000	1,175
5,000	1,175
6,500	1,200
8,000	1,325
9,000	1,410
11,000	1,450

**TABLE 8.41—DATA ON 180-STAGE TOOL FOR PROBLEM 8.66**

Flow Rate (gal/min)	Mud Weight			
	10 lbm/gal		12 lbm/gal	
	Pressure Drop (psi)	Axial Thrust (lbf)	Pressure Drop (psi)	Axial Thrust (lbf)
250	1,033	18,407	1,240	22,089
270	1,205	21,470	1,446	25,764
290	1,390	24,769	1,668	29,723
310	1,588	28,303	1,906	33,964
330	1,800	32,073	2,160	38,488
350	2,025	36,078	2,429	43,294

**TABLE 8.42—DATA FOR PROBLEM 8.67**

Elapsed Time (min)	WOB Indicator (lbf)	Standpipe Pressure (psi)
0	14,000	2,490
3	13,000	2,490
10	12,000	2,485
15	11,500	2,485
19	11,000	2,485
22	10,500	2,480
30	10,000	2,480
38	9,000	2,475
52	9,000	2,475
(off bottom)	9,000	1,650
13,000		1,510
15,500		1,550
18,000		1,610
20,000		1,650
22,000		1,690
24,000		1,740

A. We know that the on-bottom standpipe pressure is greater than the off-bottom because the mud motor  $\Delta p$  increased in proportion to bit torque. We do not expect much pressure drop (and, therefore, little pump-off force) from a bit rated at 1.0 sq in. TFA. Thus, it appears that the mud motor is being operated very close to its optimal condition of peak power—i.e., On-bottom SPP–Off-bottom SPP =  $1,740 - 1,175 = 565$  psi;  $(565/580) \times 100 = 97\%$  of peak power. Is this a valid conclusion?

B. From the pump-off plot, determine whether the bit has a significant pressure drop and pump-off force.

C. Does the result from Part B mean that the bit has 9,000 lbf of pump-off force?

D. Explain how a bit rated at 1.0 sq in. TFA can have enough pressure drop to produce 4,000 lbf of pump-off force.

E. Initially (from the discussion in Problem 8.69A), it appeared that the mud motor was being operated 97% effectively. Now, with the benefit of the pump-off plot, determine how efficiently the motor was actually run.

F. The published literature for this particular mud motor tells us that the motor is rated at 2,540 ft-lbf maximum torque at 580-psi differential pressure. Determine the bit torque in this example at an applied WOB of 24,000 lbf.

8.70. You are drilling with a 12-in. PDM (Fig. 8.101B) with a circulating rate of 1,000 gal/min. The bit torque changes from 4,200 to 6,100 ft-lbf. What is the real WOB if you are drilling with 35,000 lbf? You have 4,000 ft

**TABLE 8.43—DEFLECTIONS MEASURED  
IN TESTING A MUD MOTOR—PROBLEM 8.74**

Bending Plane	Test 1				Test 2				Loading
	1	2	3	4	1	2	3	4	
XX	0.315	0.444	0.452	0.324	0.320	0.455	0.456	0.324	its own weight
	0.331	0.466	0.475	0.340	0.336	0.477	0.478	0.339	101 lbf at L
	0.347	0.448	0.498	0.357	0.351	0.498	0.499	0.355	202 lbf at L
	0.362	0.510	0.519	0.372	0.366	0.520	0.521	0.370	303 lbf at L
YY	0.340	0.478	0.485	0.348	0.340	0.478	0.485	0.348	its own weight
	0.354	0.497	0.505	0.363	0.355	0.498	0.506	0.364	101 lbf at L
	0.369	0.517	0.525	0.378	0.369	0.518	0.526	0.378	202 lbf at L
	0.383	0.538	0.547	0.393	0.383	0.539	0.547	0.393	303 lbf at L

\* Turbine was rotated 90° and then leveled before the two tests were repeated.

of 6½-in. drillpipe (24.7 lbf/ft) and 45 joints of 10-in.-OD by 3-in.-ID steel drill collars. *Answer.* Assuming a bit with zero pumpoff force, the real WOB is 35,660 lbf.

8.71. Develop the strategy and economics for kicking off your wells for Problem 8.12. Will you jet, use a turbine, or use a PDM? Where will you kick off? Describe in detail the BHA you will use to kick off each well. Give a procedure for your kick-off, supplying details on whether you will use MWD as a steering tool or simply use single shots. Give estimated tool-fall headings and expected reverse torque. Note: You will have to research the current costs of the motors, MWD, steering, and single-shot tools to determine the best economics.

8.72. Derive the axial moment of inertia and the polar moment of inertia for a square drill collar. *Answer.*  $J = (L^4/6) - (\pi d^4/32)$ .

8.73. Derive the axial moment of inertia and polar moment of inertia for a hexagonal kelly.

8.74. Fig. 8.166 shows deflections measured in testing a mud motor. Calculate the equivalent stiffness, using the following information and Table 8.43.

Weight of turbine in air = 2,980 lbm

Diameter = 7.05 in.

Outside radius = 3.525 in.

Circumference =  $\pi D = 22.148228$  in.

$\pi/4$  or 90° rotation is 5.5370570 in. of circumference for a solid circle  $I = \pi r^4/4 = \pi(3.53 \text{ in.})^4/4 = 121.26 \text{ in}^4$ .

Structural steel,  $E = 30 \times 10^6$  psi.

*Answer.*  $2.1707 \times 10^9$ .

8.75. Determine the air weight and the weight for the following drillstring in a 16.2-lbm/gal mud.

Drillpipe: 2,520 ft of 5-in. Grade S135

Drillpipe: 6,520 ft of 5-in. Grade E

Heavy-weight

drillpipe: 850 ft of 5-in. Range II

Drill collar: 620 ft of 6½-in. (H90 6½-in. tool joints)

Drill collar: 500 ft of 8 in. (H90 6½-in. tool joints)

Stabilizers: Four 5.5 ft stainless steel  
8.23-in. OD by 2¼-in. ID

Bit: 12¼-in. Series 5-2-4

8.76. Determine the static drag of the drillstring and BHA of Problem 8.75, assuming drag coefficients of 0.15, 0.18, and 0.22, where the wellbore is at a constant 30°

**TABLE 8.44—FORCES  
FOR PROBLEM 8.85**

Depth (ft)	Hole Diameter (in.)	Force (lbf)
0 to 4,000	26	–2,500 to –3,600
4,000 to 6,500	26	–5,000 to –6,500
6,500 to 8,500	17½	–3,500 to –5,000
8,500 to 14,500	17½	–2,000 to –25,000
14,500 to 18,000	17½	–4,000 to –7,000
18,000 to 22,000	8½	–1,000 to 2,000

**TABLE 8.45—COORDINATES  
FOR PROBLEM 8.86**

Well 12A	Sec. 12	1,320 FNL and 3,960 FEL
Well 13A	Sec. 11	200 FWL and 2,640 FSL
Well 14A	Sec. 11	500 FWL and 1,000 FNL
Well 15A	Sec. 1	440 FNL and 440 FEL
Well 16A	Sec. 2	2,640 FWL and 2,640 FSL
Well 17A	Sec. 12	400 FSL and 800 FWL
Well 18A	Sec. 12	3,960 FNL and 600 FEL
Well 19A	Sec. 1	1,320 FSL and 3,690 FEL
Well 20A	Sec. 11	1,320 FSL and 100 FEL
Well 21A	Sec. 2	2,640 FSL and 300 FSL

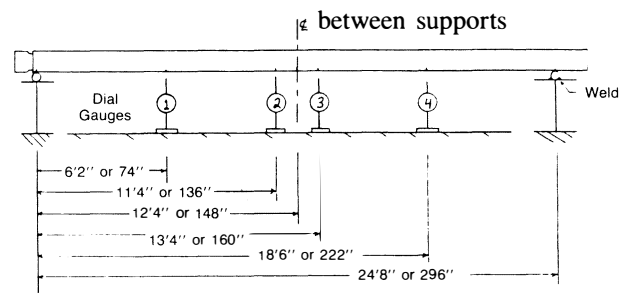


**Fig. 8.166—Deflections measured in testing a mud motor—Problem 8.74.**

inclination. The well was drilled with a slant-hole drilling rig. Mud weight is 12.8 lbm/gal. (Assume the load is equally distributed along each tool joint.)

8.77. You are drilling with a slick BHA at 1,650 ft where the inclination is at a constant  $8^\circ$  and the mud weight is 10.2 lbm/gal. The wellbore diameter is  $12\frac{1}{4}$  in. and you have thirty-six  $8\frac{1}{4}$ -in.-OD by  $2\frac{1}{16}$ -in.-ID aluminum drill collars. If the formation force at this depth is 745 lbf, will the bit build or drop again with WOB's of 20,000, 30,000, and 45,000 lbf? At what WOB will it hold angle?

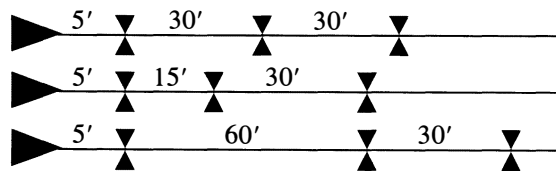
8.78 You are drilling at 7,450 ft with a  $9\frac{7}{8}$ -in. bit. The inclination was built to  $15^\circ$ . If the formation force that is causing the bit to build angle is 385 lbf, where should the stabilizer be placed (assuming one stabilizer) to drill with 45,000 lbf and to maintain a 100-lbf bit side force? Assume  $7\frac{3}{4}$ -in.-OD by  $2\frac{1}{16}$ -in.-ID steel drill collars. The stabilizer is  $\frac{1}{32}$  in. under gauge. Mud weight is 9.8 lbm/gal.

8.79. What will be the side force at the bit in the solution of Problem 8.78 if a second stabilizer is used (if it is  $\frac{1}{32}$ -in. under gauge and 344 ft above the first stabilizer)? All other parameters are the same.

8.80. It is desired to drill a high-angle directional well to obtain a horizontal departure of 8,500 ft at a TVD of 5,500 ft. You have a slant-hole rig that can start at  $20^\circ$  inclination. If you need 2,500 lbf of bit side force to achieve a build of  $2^\circ/100$  ft or 4,500 lbf of bit side force to achieve  $3.5^\circ/100$  ft, can you use a single-stabilizer BHA and drill with WOB's between 15,000 and 30,000 lbf to achieve your build? Would it be better to use a two-stabilizer building assembly? What would be an appropriate WOB? The hole size is  $14\frac{3}{4}$  in. throughout the build portion; the mud weight is 10.5 lbm/gal, and you will use six  $9\frac{1}{2}$ -in.-OD  $\times 2\frac{1}{16}$ -in.-ID drill collars for the first two stands and twelve 8-in.-OD  $\times 2\frac{1}{16}$ -in.-ID drill collars for the remainder of the BHA.

8.81. Using the same method as was used to derive the one- and two-stabilizer BHA side forces, derive the equations necessary to calculate the tangency point and side force for a three-stabilizer BHA.

8.82. For the following three BHA's, determine the side forces at the bit with WOB's of 10,000 and 20,000 lbf, inclinations of  $10^\circ$  and  $30^\circ$ , a  $9\frac{7}{8}$ -in. bit,  $7\frac{3}{4}$ -in.-OD  $\times 2\frac{1}{16}$ -in.-ID drill collar, and a 9.0-lbm/gal mud. All stabilizers are  $\frac{1}{32}$ -in. under gauge.



**Answer.** For a BHA with an inclination of  $10^\circ$ , WOB of 10,000 lbf, and length of 609.6 in., the side force is 237 lbf. For a BHA with an inclination of  $10^\circ$ , WOB of 20,000, and length of 603.7 in., the side force is 250 lbf. For a BHA with an inclination of  $30^\circ$ , a WOB of 10,000 lbf, and length of 466.7 in., the side force is 723 lbf. For a BHA with an inclination of  $30^\circ$ , WOB of 20,000, and length of 463.4, the side force is 741 lbf.

8.83. Design all the BHA's to drill your directional wells for Problem 8.12. State collar sizes, exact placement of stabilizers, number of drill collars, and your estimate of the operating conditions—i.e., WOB and rotary speed.

8.84. Determine the bit-walking tendency for the following situations, and give reasons for your decision.

A. Slick assembly, 10,000-lbf WOB, 60-rpm speed,  $9\frac{7}{8}$ -in. Series 1-1-5 bit,  $5^\circ$  inclination, drilling gumbo shale. Hole is slightly overgauge (size is 12 to 13 in.).

B. Single-stabilizer building assembly (Fig. 8.136, No. 9), 35,000-lbf WOB, 110-rpm speed,  $17\frac{1}{2}$ -in. Series 5-1-4 bit,  $20^\circ$  inclination, drilling soft sandstones and shales at 60 to 300 ft/hr. Hole is washing out (size is about 20 in.).

C. 70-ft building assembly (Fig. 8.136, No. 5), 30,000-lbf WOB, 90-rpm speed,  $12\frac{1}{4}$ -in. BHD bit,  $15^\circ$  inclination, drilling sandstones at 60 ft/hr and shales at 25 ft/hr. The hole is elliptical.

D. Holding assembly (Fig. 8.138, No. 4), 45,000-lbf WOB, 75-rpm speed,  $12\frac{1}{4}$ -in. Series 5-2-4 bit,  $42^\circ$  inclination, drilling siltstone and limestones at 12 ft/hr. The hole is gauge.

E. Dropping assembly (Fig. 8.142, No. 2), 3,500-lbf WOB, 60-rpm speed,  $8\frac{1}{2}$ -in. Series 6-1-7 bit,  $22^\circ$  inclination, drilling limestone and dolomite at 6 ft/hr. The hole is gauge.

8.85. You are planning to drill a 22,000-ft exploration well, starting with a 26-in. hole to 4,000 ft, followed by  $17\frac{1}{2}$ -in. hole to 14,500 ft,  $12\frac{1}{4}$ -in. hole to 18,500 ft, and  $8\frac{1}{2}$ -in. hole to 22,000 ft. The well will be a deep test (Fig. 8.156A, 300 ft north of Well A). Design the drillstring, BHA's, bits, and operating conditions for the well to total depth, and give reasons for your selections. You must have the side forces listed in Table 8.44 to offset the formation forces to maintain less than  $0.5^\circ/1,000$  ft to 4,000 ft and  $1^\circ/1,000$  ft to 22,000 ft.

8.86. Calculate the dip at each surface location for the coordinates cited in Table 8.45 (see Fig. 8.155), and estimate where the bottomhole location would be if a well were drilled at each location.

8.87. You have been asked to develop a drilling plan to hit Target C in Fig. 8.156B. The top of the target is 14,000 ft TVD, and total depth is 15,100 ft TVD. Hole and casing sizes should be the same as those in Example 8.33. State where the surface location should be, determine the best trajectory plan to hit the target, and explain your strategy. Design the BHA's to accomplish your plan.

8.88. You are drilling ahead at 3,450 ft. A drilling break was experienced at 3,400 ft, after which the penetration rate increased to 75 ft/hr at a rotary speed of 70 rpm. Offset core information shows a formation bedding dip of  $15.0^\circ$  and an angle of internal friction of  $29.0^\circ$ . The current bit is a new milltooth with an individual wedge angle of  $40^\circ$ . The cohesive strength of the core was found to follow the variable cohesive strength equation,

$$\tau(p_i) = A - B[\cos 2(\alpha - p_i)]^n,$$

where  $A$  and  $B$  are empirical constants,  $n$  is a rock parameter constant, and  $\alpha$  is the orientation angle between the bedding planes where the cohesive strength is a minimum. Tests show  $A=6,035$ ,  $B=2,035$ ,  $\alpha=30^\circ$ , and  $n=6$ . Determine whether the tendency is to drill up dip

or down dip. *Answer.* A chip should form on the up dip side of the hole, and the hole should deviate upward.

8.89. Refer to Fig. 8.160. Note that over the range of  $\alpha_{dh}$  from  $0^\circ$  to  $30^\circ$ , the values of  $(F_2 - F_1)/F_{\min}$  for the  $60^\circ$  wedge are zero. This indicates that symmetrical chips should be formed and a bit with a  $60^\circ$  tooth should alleviate the natural hole deviation problem. What can be said about the  $70^\circ$  wedge curve?

8.90. Refer to Problem 8.88. Plot strength variance  $(F_2 - F_1)/F_{\min}$  for formation dips from  $0^\circ$  to  $90^\circ$ .

## References

- Craig, J.T. Jr. and Randall, B.V.: "Directional Survey Calculation," *Pet. Eng.* (March 1976).
- Walstrom, J.E., Harvey, R.P., and Eddy, H.D.: "A Comparison of Various Directional Survey Models and an Approach To Model Error Analysis," *J. Pet. Tech.* (Aug. 1972) 935-43.
- Wilson, G.J.: "An Improved Method for Computing Directional Survey," *J. Pet. Tech.* (Aug. 1968) 871-76; *Trans.*, AIME, **243**.
- Taylor, H.L. and Mason, C.M.: "A Systematic Approach To Well Surveying Calculations," *Soc. Pet. Eng. J.* (Dec. 1972) 474-88.
- Millheim, K.K., Gubler, F.H., and Zaremba, H.B.: "Evaluating and Planning Directional Wells Utilizing Post Analysis Techniques and Three Dimensional Bottomhole Assembly Program," paper SPE 8339 presented at the 1979 SPE Annual Technical Conference and Exhibition, Las Vegas, Sept. 23-26.
- Lubinski, A.: "How Severe Is That Dogleg?" *World Oil* (Feb. 1, 1957) 95-104.
- "Ragland Diagram," *Drilling Data Handbook*, Editions Technip (Paris) (1978) 334, 338.
- Eickelberg, D. *et al.*: "Controlled Directional Drilling Instruments and Tools," paper presented at the 9th International Symposium of the firms Baker Oil Tools GmbH, Christensen Diamond Products GmbH, and Vetco Inspection GmbH (1982).
- Gearhart, M., Zierner, K.H., and Knight, O.M.: "Mud Pulse MWD Systems Report," *J. Pet. Tech.* (Dec. 1981) 2301-06.
- Uttecht, G.W. and DeWardt, J.P.: "Survey Accuracy is Improved by a New, Small OD Gyro," *World Oil* (March 1983) 61-66.
- Wolff, C.J.M. and DeWardt, J.P.: "Borehole Position Uncertainty—Analysis of Measuring Methods and Derivation of Systematic Error Model," *J. Pet. Tech.* (Dec. 1981) 2339-50.
- Cagle, *et al.*: "Casing Sidetracks Made Easy," *Pet. Eng.* (Sept. 1976).
- Jürgens, R.: "Down-Hole Motors—Technological Status and Development Trends," paper presented at the 7th International Symposium of the firms Baker Oil Tools GmbH, Christensen Diamond Products GmbH, and Vetco Inspection GmbH, Celle, FDR (Sept. 8, 1978).
- Warren, T.M.: "Factors Affecting Torque for a Roller Cone Bit," *J. Pet. Tech.* (Sept. 1984) 1500-08.
- Winters, W. and Warren, T.M.: "Variations in Hydraulic Lift With Diamond Bits," paper SPE 10960 presented at the 1982 SPE Annual Technical Conference and Exhibition, New Orleans, Sept. 26-29.
- Winters, W. and Warren, T.M.: "Determining the True Weight-on-Bit for Diamond Bits," paper SPE 11950 presented at the 1983 SPE Annual Technical Conference and Exhibition, San Francisco, Oct. 5-8.
- Feenstra, R. and Kamp, W.A.: "A Technique for Continuously Controlled Directional Drilling," paper presented at the 1984 Drilling Technology Conference of the International Association of Oilwell Drilling Contractors, March 19-21.
- Lubinski, A. and Woods, H.B.: "How to Determine Best Hole and Drill Collar Size," *Oil and Gas J.* (June 7, 1954) 104-05.
- Millheim, K.K.: "Directional Drilling," *Oil and Gas J.* (eight-part series) beginning Nov. 6, 1978 and ending Feb. 12, 1979.
- Jiazhi, B.: "Bottomhole Assembly Problems Solved by Beam-Column Theory," paper SPE 10561 presented at the 1982 SPE International Meeting on Petroleum Engineering, Beijing, March 19-22.
- Timoshenko, S.: *Theory of Elastic Stability*, McGraw-Hill Book Co. Inc., New York City (1936).
- Walker, H.B.: "Downhole Assembly Design Increases ROP," *World Oil* (June 1977) 59-65.
- Millheim, K.K. and Apostol, M.C.: "The Effect of Bottomhole Assembly Dynamics on the Trajectory of a Bit," *J. Pet. Tech.* (Dec. 1981) 2323-38.
- Lubinski, A. and Woods, H.B.: "Factors Affecting the Angle of Inclination and Dog-legging in Rotary Boreholes," *Drill. and Prod. Prac.*, API (1953) 222-42.
- Rollins, H.M.: "Are  $3^\circ$  and  $5^\circ$  Straight Holes Worth Their Cost?" *Oil and Gas J.* (Nov. 1959) 163-64, 167-68, 171.
- Murphey, C.E. and Cheatham, J.B. Jr.: "Hole Deviation and Drill String Behavior," *Soc. Pet. Eng. J.* (March 1966) 44-53; *Trans.*, AIME, **237**.
- Knapp, S.R.: "New Bit Concept Helps Control Hole Deviation," *World Oil* (1965) 113-16.
- Sultanov, R. and Shandalov, G.: "Effects of Geological Conditions on Well Deviation," (in Russian), *Izv. Vyssh. Ucheb. Zaved. Geol. Razved* (1961) **3**, 106.
- Smith, M.B. and Cheatham, J.B.: "Deviation Forces Arising From Single Bit Tooth Indentation of an Anisotropic Porous Medium," *Trans.*, ASME, Series 399 (1977) 363-66.
- McLamore, R.T.: "The Role of Rock Strength Anisotropy in Natural Hole Deviation," *J. Pet. Tech.* (Nov. 1971) 1313-21; *Trans.*, AIME, **251**.
- Bradley, W.B.: "Deviation Forces From the Wedge of Penetration Failure of Anisotropic Rock," *J. Eng. Ind.* (Nov. 1973) 1093-99.

## Nomenclature

- $A$  = area  
 $A_{\text{corr}}$  = intercardinal correction  
 $A_i$  = internal drillpipe area  
 $A_s$  = cross-sectional area of steel in drillpipe  
 $B_c$  = buoyancy correction factor  
 $\Delta c$  = actual compass deflection  
 $d_b$  = bit diameter  
 $d_r$  = rotor diameter  
 $D$  = depth  
 $\Delta D$  = depth increment  
 $D_M$  = total measured depth  
 $D_{MN}$  = new measured depth  
 $D_s$  = stake direction  
 $D_{\text{tar}}$  = total measured depth to target  
 $D_x$  = depth of wedge penetration  
 $D_2$  = TVD at end of the buildup section  
 $e$  = rotor eccentricity  
 $E$  = Young's modulus  
 $E_h$  = hydraulic efficiency  
 $E_M$  = mechanical efficiency  
 $E_R$  = Earth's spin vector  
 $F$  = force  
 $F_c$  = correction factor  
 $F_d$  = ratio of drillpipe OD/ID  
 $F_B$  = side force at bit  
 $F_R$  = factor of the straight line section vs. section ratios  
 $G$  = shear modulus  
 $G$  = resultant bit curvature  
 $h$  = height of vane  
 $H_M$  = magnetic field  
 $\Delta H_M$  = strength of the magnetic error field  
 $i$  = angle of index change  
 $i_s$  = index setting  
 $I$  = axial moment of inertia  
 $J$  = moment of inertia  
 $\ell$  = clearance between bit and drill collar



$L$  = north/south coordinate  
 $\Delta L$  = change in drillpipe length  
 $L_c$  = course length between measured surveys  
 $L_r$  = rotor lead  
 $L_s$  = stator lead  
 $L_{Dc}$  = length of arc section  
 $L_T$  = tangency length  
 $M$  = torque generated at the bit  
 $M_b$  = bending moment  
 $n$  = number of lobes or teeth on stator  
 $n_r$  = number of lobes or teeth on rotor  
 $n_s$  = number of stages  
 $N_b$  = bit speed  
 $\Delta p$  = pressure drop  
 $p_b$  = axial or compressive load on bit  
 $\Delta p_b$  = pressure drop across the bit  
 $p_{do}$  = off-bottom standpipe pressures  
 $\Delta p_i$  = change in internal drillpipe pressure  
 $p_{ob}$  = drilled-off standpipe pressure  
 $P_r$  = rotor pitch  
 $P_s$  = stator pitch  
 $q$  = circulation rate  
 $Q$  = specific displacement  
 $r_c$  = radius of curvature  
 $s_c$  = east/west coordinate  
 $s_{DC}$  = arc length  
 $T_e$  = horizontal component of Earth's spin rate  
 $W_b$  = weight on bit  
 $\Delta W_b$  = change in weight on bit  
 $W_c$  = weight of the collars  
 $W_m$  = mud weight  
 $x$  = departure

$\alpha_{dh}$  = bedding dip angle relative to bottom of hole  
 $\alpha_q$  = inclination angle buildup  
 $\alpha_N$  = new inclination angle  
 $\beta$  = exit blade angle  
 $\beta$  = overall angle change  
 $\gamma$  = tool-face angle  
 $\delta$  = dogleg severity  
 $\epsilon$  = azimuth  
 $\Delta\epsilon$  = change in azimuth  
 $\eta$  = efficiency  
 $\theta$  = maximum inclination angle  
 $\mu$  = Poisson's ratio  
 $\tau_\rho$  = shear strength of the anisotropic rock along the plane of failure  
 $\phi$  = angle of internal friction of the anisotropic rock  
 $\Omega$  = included wedge half-angle

### SI Metric Conversion Factors

ft	× 3.048*	E-01	= m
ft-lbf	× 1.355 818	E-03	= kJ
gal	× 3.785 412	E-03	= m <sup>3</sup>
hp	× 7.460 43	E-01	= kW
in.	× 2.54*	E+00	= cm
lbf	× 4.448 222	E+00	= N
lbf/ft	× 1.459 390	E+01	= N/m
lbf/sq ft	× 4.788 026	E-02	= kPa
lbm/cu ft	× 1.601 846	E+01	= kg/m <sup>3</sup>
lbm/gal	× 1.198 264	E+02	= kg/m <sup>3</sup>
psi	× 6.894 757	E+00	= kPa
sq in.	× 6.451 6*	E+00	= cm <sup>2</sup>

\*Conversion factor is exact.